

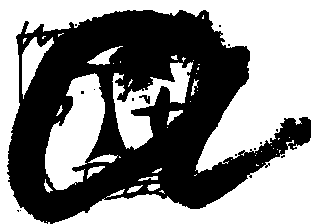
Lucas Montero de Espinosa Meléndez

Plant Oils As Renewable Precursors Of  
Thermosetting And Flame Retardant Polymers

PhD THESIS

Supervised by Dr. Virginia Cádiz Deleito and Dr. Joan  
Carles Ronda Bargalló

Departament de Química Analítica i Química Orgànica



UNIVERSITAT ROVIRA I VIRGILI

Tarragona  
2009

UNIVERSITAT ROVIRA I VIRGILI  
PLANT OILS AS RENEWABLE PRECURSORS OF THERMOSETTING AND FLAME RETARDANT POLYMERS  
Lucas Montero de Espinosa Meléndez  
ISBN:978-84-692-9759-9/DL:T-205-2010



Departament de Química Analítica  
i Química Orgànica  
c/ Marcel·li Domingo, s/n  
Campus Sescelades  
43007, Tarragona  
Telf. 977 559 769  
Fax. 977 558 446

Virginia Cádiz Deleito, catedrática, y Joan Carles Ronda Bargalló, profesor titular, ambos del Departamento de Química Analítica y Química Orgánica de la Universidad Rovira i Virgili,

#### CERTIFICAMOS:

Que el presente trabajo, titulado “Plant oils as renewable precursors of thermosetting and flame retardant polymers”, que presenta Lucas Montero de Espinosa Meléndez para la obtención del título de Doctor, ha sido realizado bajo nuestra dirección en el Departamento de Química Analítica y Química Orgánica de esta universidad y que cumple los requisitos para poder optar a la Mención Europea.

Tarragona, 6 de octubre de 2009

Dra. Virginia Cádiz Deleito

Dr. Joan Carles Ronda

UNIVERSITAT ROVIRA I VIRGILI  
PLANT OILS AS RENEWABLE PRECURSORS OF THERMOSETTING AND FLAME RETARDANT POLYMERS  
Lucas Montero de Espinosa Meléndez  
ISBN:978-84-692-9759-9/DL:T-205-2010

UNIVERSITAT ROVIRA I VIRGILI  
PLANT OILS AS RENEWABLE PRECURSORS OF THERMOSETTING AND FLAME RETARDANT POLYMERS  
Lucas Montero de Espinosa Meléndez  
ISBN:978-84-692-9759-9/DL:T-205-2010

UNIVERSITAT ROVIRA I VIRGILI  
PLANT OILS AS RENEWABLE PRECURSORS OF THERMOSETTING AND FLAME RETARDANT POLYMERS  
Lucas Montero de Espinosa Meléndez  
ISBN:978-84-692-9759-9/DL:T-205-2010

En primer lugar, quiero agradecer a Virginia y a Joan Carles que me dieran la posibilidad de hacer la tesis y de conocer Tarragona, donde he pasado algunos de los mejores años de mi vida.

También quiero agradecer a Marina su ayuda y comentarios durante el desarrollo de este trabajo, a Mike for receiving me in his group and counting on me for the next years y a José por ayudarme a encontrar un lugar donde hacer la tesis.

Gracias a Pagi por diseñar la cubierta de esta tesis. No dudé ni un momento en pedirte a ti.

De las personas que he conocido durante estos años me llevo muchos recuerdos, de Andy e Ixchel me quedan música y cocina, del núcleo duro, cafés y puerto, de Robert, unas cuantas técnicas y palas a última hora. Me veo con David partiendo la pana en la calle Sierpes, congelado en el Cavall Bernat con Jaime y escalando con Ciril en La Mussara. Recuerdo muchas paellas y muchas noches en el Déjà Vu, y a Aitor detrás de todas ellas. Recuerdo muchos jueves con Elena, Sergio, Cati, Gerald, Mihai, y con todos ellos muchas noches de Sala Zero. A Cristina en El Soportal, a Patricia muerta de risa, a Marisa y su pastel de papas. Me llevo comidas en casa de Simona, conversaciones con Vanessa y la compañía de los incondicionales del plafón. Me llevo la impaciencia adictiva de Hatice, el Rakı de Osman, el Glühwine con Thao y la expresividad de Manuela. Recuerdo Heavy Metal. Recuerdo a Quique, en todos los congresos, en Valero, en la calle Van Dyck, con Mayra, detrás de la red de Volley, a sus gatos. Recuerdo a Cristina, siempre, aquí y allá. Recuerdo a Ana, desde el primer verano, hasta la última copa. Recuerdo a Marta y recuerdo su enorme compañía.

Esta tesis es para mi familia. Tiene su origen y sentido en ellos.

UNIVERSITAT ROVIRA I VIRGILI  
PLANT OILS AS RENEWABLE PRECURSORS OF THERMOSETTING AND FLAME RETARDANT POLYMERS  
Lucas Montero de Espinosa Meléndez  
ISBN:978-84-692-9759-9/DL:T-205-2010





El Roto

UNIVERSITAT ROVIRA I VIRGILI  
PLANT OILS AS RENEWABLE PRECURSORS OF THERMOSETTING AND FLAME RETARDANT POLYMERS  
Lucas Montero de Espinosa Meléndez  
ISBN:978-84-692-9759-9/DL:T-205-2010

## Table of Contents

General introduction	1
Plant oils in the context of sustainable development	1
Plant oils in polymer chemistry	2
Structure and reactivity of plant oils	3
Objectives and summary	9
First part	13
The chemistry of singlet oxygen	15
Introduction	15
Singlet oxygen generation	15
The <i>ene</i> reaction of singlet oxygen with alkenes	17
Chapter one	19
A New Enone-Containing Triglyceride Derivative as Precursor of Thermosets from Renewable Resources	21
Quinoline-Containing Networks from Enone and Aldehyde Triglyceride Derivatives	35
Chapter two	57
A New Route to Acrylated Oils. Cross-linking and Properties of Acrylated Triglycerides from High Oleic Sunflower Oil	59
Second part	77
Flame retardant materials	79
Introduction	79
Mechanism of action	80
Classification	81
Phosphorus-based flame retardants	82

Polymer flammability tests. Limiting Oxygen Index (LOI)	84
ADMET polymerization	89
Background	89
ADMET polymerization	91
Chapter three	95
A Straightforward Strategy for the Efficient Synthesis of Acrylate and Phosphine Oxide-Containing Vegetable Oils and their Cross-linked Materials	97
Chapter four	119
Fatty Acid Derived Phosphorus-Containing Polyesters via Acyclic Diene Metathesis (ADMET) Polymerization	121
Phosphorus-Containing Renewable Polyester-Polyols via ADMET Polymerization. Synthesis, Functionalization and Radical Cross-Linking	143
General conclusions	169
Apendixes	171
Apendix A. List of abbreviations	171
Apendix B. List of publications	173
Apendix C. Stages and meeting contributions	175

## GENERAL INTRODUCTION

### Plant oils in the context of sustainable development

The concept of sustainable development appeared in 1987 after the Brundtland commission<sup>1</sup> as the main goal to be achieved in response to the accelerated deterioration of the environment. It was defined as the social and economic advance to assure human beings a healthy and productive life, but one that do not compromise the ability of future generations to meet their own needs.<sup>2</sup> Although the availability of energy was admitted to be key for the future development, the necessity of a steady transition to a broader and more sustainable mix of energy sources was pointed out as a major objective. Sustainable development was further addressed in the United Nations Conference on Environment and Development (UNCED), held in 1992 in Rio de Janeiro.<sup>3</sup> Among other documents that resulted from the Earth summit, Agenda 21<sup>4</sup> was launched as a wide-ranging blueprint for action to achieve sustainable development worldwide. Within the means of implementation, the role of sciences “in supporting the prudent management of the environment and development for the daily survival and future development of humanity” was established. It was pointed out that “scientific knowledge should be applied to articulate and support the goals of sustainable development” and that it was “necessary to build up scientific capacity and strengthen such capacity in all countries for the generation and application of the results of scientific research and development concerning sustainable development” (Agenda 21, Chapter 35). In relation to chemical sciences, the Environmental Protection Agency coined a new term in 1998 that collected the ideals of sustainability applied to chemistry: *green chemistry*, also called sustainable chemistry. It was formally delineated with the aim of preventing pollution through better process design rather than by managing emissions and waste. Green chemistry is based on a set of 12 principles<sup>5</sup> that provide a jumping-off point for all chemists and chemical engineers to use classical chemistry to design chemical products and processes that have little or no impact on the environment.

In 2002, the Johannesburg summit<sup>6</sup> aimed to assess progress toward attaining the goals of Agenda 21, strengthening commitment of parties to the program and setting priorities for further action. But more than anything else, the summit was a message to the world to stop talking about what needs to be done and to get on with

implementation.<sup>7</sup> Important contributions have been made towards these objectives, being some of the most relevant the use of renewable raw materials, direct oxidations using oxygen, improved separations technology, and all forms of catalysis. However, progress toward sustainable chemistry has to increase drastically to meet the challenges of this century.<sup>8</sup>

Although there are few examples of green processes that have had an industry wide impact, the increasing application of the principles of green chemistry to individual products and processes at lab scale has led to the appearance of a new branch of chemistry, which is now consolidated. The fully application of the twelve principles in the development of new chemical processes or in the modification of the existing ones is not viable in most cases; however, if part of these principles can be accomplished, the objective of sustainable development will be closer.

The use of raw materials and feedstocks that are renewable rather than depleting, as written in the fourth principle, is crucial both from environmental and economic reasons. Petrochemicals are the main feedstock for the chemical industry, but they are subjected to price variations due to its scarcity and non-renewable nature. Nowadays, renewable raw materials make up an approximate 10-12% of the feedstocks used by the chemical industry and it is expected to increase up to 25% in 2020. Oils and fats constitute the most important renewable raw materials for the chemical industry, followed by carbohydrates and other renewables such as proteins and protein surfactants.<sup>8,9</sup>

## **Plant oils in polymer chemistry**

The application of plant oils and their derivatives in polymer chemistry has become an important research area in constant growth. The versatile chemistry that can be applied to triglyceride oils has led to a wide variety of polymeric structures from linear, processible polymers<sup>10</sup> to cross-linked systems with applications as resins and coatings among others.<sup>11</sup> Due to the presence of fatty acid chains within the polymeric structure, these polymers present improved physical properties such as higher flexibility, adhesion and resistance to water and chemicals.<sup>11</sup> Although to date plant oils have been widely used in polymer science, their potential for the development of new monomers and polymeric structures has not yet been fully exploited. Regarding the future developments in this area, the study of well defined polymers for specialty applications,

obtained by controlled/living polymerization techniques will improve the application possibilities.<sup>10</sup> Furthermore, it is expected that fatty diacids as well as  $\omega$ -amino fatty acids, and  $\omega$ -hydroxy fatty acids derived from plant oils, will be available and may substitute during the next few years the respective petrochemical monomers for the production of polyamides, polyurethanes, and polyesters. Moreover, linear  $\omega$ -unsaturated fatty acids of different chain length will be available, being interesting monomers for copolymerization with alkenes.<sup>9</sup>

## Structure and reactivity of plant oils

Plant oils are mainly constituted by triglycerides, which are the product of esterification between a molecule of glycerol and three fatty acids (Figure 1). They are liquid at ambient temperature and insoluble in water. Fatty acids are an approximate 95 % of the total weight of a triglyceride molecule and their length varies from 12 to 22 carbon atoms. Common fatty acids can be completely saturated but they can also present several double bonds. Besides, there is a number of naturally occurring fatty acids containing other functional groups such as hydroxyls or epoxides. The most common fatty acids are shown in figure 2. Each plant oil is composed by a characteristic fatty acid distribution that determines its physical and chemical properties (Table 1).

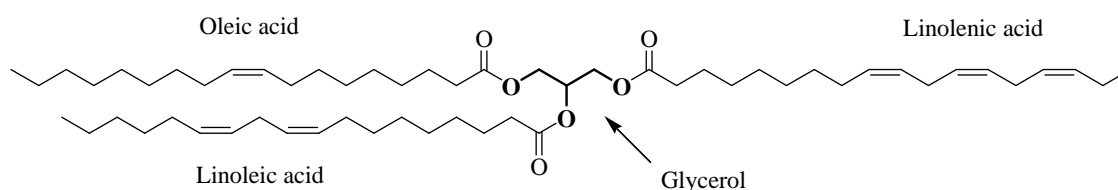


**Figure 1.** General structure of triglycerides. In this example, with oleic, linoleic and linolenic acids.

Triglycerides can be polymerized directly using its intrinsic reactivity but they can also be chemically modified in order to increase their reactivity towards polymerization. The first approach consists of the direct polymerization of the internal double bonds of the fatty acid chains of different plant oils. This process can be carried out *via* radical, cationic or thermal polymerization.<sup>12</sup> In this way, castor oil can also be

directly cross-linked by reaction of the hydroxyl groups of ricinoleic acid with diisocyanates or dicarboxilates to obtain elastomers and thermosetting materials.

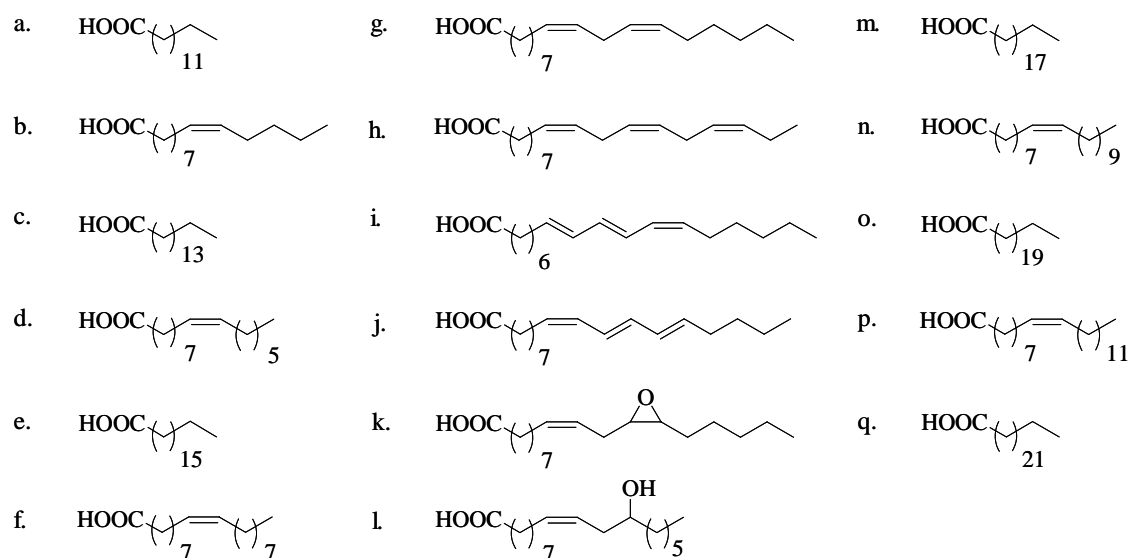


**Figure 2.** Structure of some common fatty acids. Mistiric (a), myristoleic (b), palmitic (c), palmitoleic (d), stearic (e), oleic (f), linoleic (g), linolenic (h), calendic (i),  $\alpha$ -eleostearic (j), vernolic (k), ricinoleic (l), arachidonic (m), gadoleic (n), behenic (o), erucic (p), lignoceric (q).

Although straightforward, the direct polymerization of triglycerides do not provide polymeric materials with the mechanical and thermal properties required for some applications. Moreover, low crosslinking degrees are usually obtained which are accompanied by high soluble fractions.<sup>13</sup> For these reasons, the second approach, that is, the chemical modification of the triglyceride is preferred, enabling the synthesis of designed monomers in the way to target polymeric materials.

The chemical transformation of triglycerides affords a wide variety of monomers for the synthesis of linear<sup>10</sup>, hyperbranched<sup>14</sup>, or cross-linked structures<sup>10,11</sup>. The modification of triglycerides is performed using the reactivity of the functional groups in their structure. For the synthesis of cross-linked structures, the epoxidation of the C-C double bonds is one of the most important functionalization reactions, that can be achieved by environmentally friendly procedures such as catalyzed chemical oxidation with hydrogen peroxide<sup>15,16</sup> or by enzymatic oxidation.<sup>17</sup> The opening of the epoxide ring is a versatile reaction that leads to numerous products,<sup>18</sup> some of which are represented in figure 3.



**Table 1** Fatty acids percentage distribution in different plant oil. **C:** number of carbon atoms.  
**DB:** number of double bonds.

Fatty acid	C:DB	Canola	Corn	Cotton seed	Linseed	Olive	Palm	Soybean	Sunflower	High oleic
Misticric	14:0	0.1	0.1	0.7	0.0	0.0	1.0	0.1	0.0	0.0
Myristoleic	14:1	0.0	0.0	0.0	0.0	0.0	0.0	0.0	0.0	0.0
Palmitic	16:0	4.1	10.9	21.6	5.5	13.7	44.4	11.0	6.1	6.4
Palmitoleic	16:1	0.3	0.2	0.6	0.0	1.2	0.2	0.1	0.0	0.1
Margaric	17:0	0.1	0.1	0.1	0.0	0.0	0.1	0.0	0.0	0.0
Margaroleic	17:1	0.0	0.0	0.1	0.0	0.0	0.0	0.0	0.0	0.0
Stearic	18:0	1.8	2.0	2.6	3.5	2.5	4.1	4.0	3.9	3.1
Oleic	18:1	60.9	25.4	18.6	19.1	71.1	39.3	23.4	42.6	82.6
Linoleic	18:2	21.0	59.6	54.4	15.3	10.0	10.0	53.2	46.4	2.3
Linolenic	18:3	8.8	1.2	0.7	56.6	0.6	0.4	7.8	1.0	3.7
Arachidonic	20:0	0.7	0.4	0.3	0.0	0.9	0.3	0.3	0.0	0.2
Gadoleic	20:1	1.0	0.0	0.0	0.0	0.0	0.0	0.0	0.0	0.4
Eicosadienoic	20:2	0.0	0.0	0.0	0.0	0.0	0.0	0.0	0.0	0.0
Behenic	22:0	0.3	0.1	0.2	0.0	0.0	0.1	0.1	0.0	0.3
Erucic	22:1	0.7	0.0	0.0	0.0	0.0	0.0	0.0	0.0	0.1
Lignoceric	24:0	0.2	0.0	0.0	0.0	0.0	0.0	0.0	0.0	0.0
DB/Triglyceride		3.9	4.5	3.9	6.6	2.8	1.8	4.6	0.0	3.0

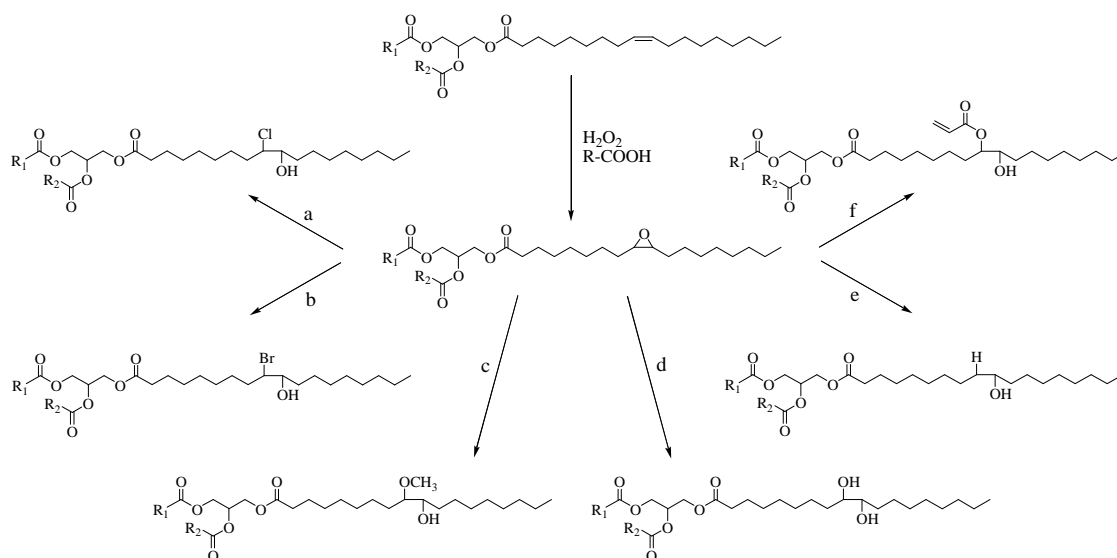


**Figure 3.** Ring opening products of epoxidized triglycerides with HCl (a), HBr (b), MeOH/H<sup>+</sup> (c), H<sub>2</sub>O/H<sup>+</sup> (d), catalytic hydrogenation (e) and acryloyl chloride (f).

Recent publications report the use of polyols derived from epoxidized plant oils for the preparation of polyurethanes,<sup>19</sup> polyurethane dispersions,<sup>20</sup> polyurethane foams,<sup>21</sup> polyurethane IPNs<sup>22</sup> and hybrid latexes prepared from waterborne PU and acrylic MMA/BA copolymers.<sup>23</sup> Direct polymerization of epoxidized plant oils and fatty acids has also been reported with diamines,<sup>24</sup> anhydrides<sup>25</sup> or by cationic polymerization in the synthesis of linseed oil-POSS hybrid materials<sup>26</sup>.

As mentioned above, some plant oils present functional groups in their structure. Castor oil has lately found applications in the synthesis of hyperbranched polyurethanes<sup>27</sup>, in the synthesis of biodegradable plastic foams by curing with maleic anhydride<sup>28</sup> and in the preparation of UV-curable thiol-ene formulations.<sup>29</sup> An interesting castor oil derivative is 10-undecenoic acid, which is produced by cracking of castor oil under pressure. It is one of the oldest renewable building blocks, being used in the industry as a Nylon 11 precursor. It has been recently used for the synthesis of a variety of  $\alpha,\omega$ -dienes as interesting monomers for acyclic diene metathesis (ADMET) polymerization.<sup>14</sup> The dehydration of castor oil followed by crosslinking with bismaleimides *via* Diels-Alder reaction has been also recently reported<sup>30</sup>.

Another recent examples of fatty acid and plant oil-based polymers include the synthesis of polyols through Pd catalyzed cyclotrimerization of fatty acid derivatives for polyurethane synthesis,<sup>31</sup> the synthesis of isocyanate-containing triglycerides,<sup>32</sup> the preparation of thermosets from soybean oil and *p*-dinitrosobenzene *via* an *ene* reaction,<sup>33</sup> the development of a linseed oil-based thermoset *via* ROMP,<sup>34</sup> the cationic polymerization of soybean oil in supercritical CO<sub>2</sub><sup>35</sup> and the synthesis of soybean-based silicon-containing thermosets by cationic polymerization.<sup>36</sup>

---

<sup>1</sup> The Brundtland Commission, formally the World Commission on Environment and Development (WCED). Convened by the United Nations in 1983.

<sup>2</sup> G. Brundtland, *Our Common Future*, Oxford University Press, Oxford, 1987.

<sup>3</sup> Report of the United Nations Conference on Environment and Development, Rio de Janeiro, 1992; <http://www.un.org/esa/sustdev>.

<sup>4</sup> Report of the United Nations Conference on Environment and Development in June 1992 in Rio de Janeiro—Documents—Agenda 21.

<sup>5</sup> Anastas, P. T.; Warner, J. C. *Green Chemistry: Theory and Practice*, Oxford University Press, Oxford, 1998, p. 11.

- 
- <sup>6</sup> The World Summit on Sustainable Development, WSSD or Earth Summit 2002. Held in Johannesburg in 2002. *Johannesburg Declaration on Sustainable Development* in <http://www.un-documents.net/jburgdec.htm>.
- <sup>7</sup> Ritter, S. K. *C&EN* 2002, 80 19-23.
- <sup>8</sup> Eissen, M.; Metzger, J. O.; Schmidt, E.; Schneidewind, U. *Angew Chem Int Ed* 2002, 41, 414-436.
- <sup>9</sup> Metzger, J. O. *Eur J Lipid Sci Technol* 2009, 111, 865–876.
- <sup>10</sup> Meier, M. A. R.; Metzger, J. O.; Schubert, U. S. *Chem Soc Rev* 2007, 36, 1788–1802.
- <sup>11</sup> Güner, F. S.; Yağcı, Y.; Erciyas, A. T. *Prog Polym Sci* 2006, 31, 633-670.
- <sup>12</sup> Sharma, V.; Kundu P. P. *Prog Polym Sci* 2006, 31, 983–1008.
- <sup>13</sup> a) Sharma, V.; Banait J. S.; Larock, R. C.; Kundu, P. P. *Express Polym Lett* 2008, 2, 265-276, b) Andjelkovic, D. D.; Larock, R. C. *Biomacromolecules* 2006, 7, 927-936, c) Li, F.; Marks, D. W.; Larock, R. C.; Otaigbe, J. U. *Polymer* 2000, 41, 7925-7939, d) Li, F.; Larock, R. C. *Biomacromolecules* 2003, 4, 1018-1025.
- <sup>14</sup> Meier, M. A. R. *Macromol Chem Phys* 2009, 210, 1073–1079.
- <sup>15</sup> Lane, B. S.; Burgess, K. *Chem Rev* 2003, 103, 2457-2474.
- <sup>16</sup> Grigoropoulou, G.; Clark, J. H.; Elings, J. A. *Green Chem* 2003, 5, 1-7.
- <sup>17</sup> Uyama, H.; Kuwabara, M.; Tsujimoto, T.; Kobayashi, S. *Biomacromolecules* 2003, 4, 211-215.
- <sup>18</sup> a) Esen, H.; Küseföglu, S.H.; *J Appl Polym Sci* 2003, 89, 3882-3888, b) Petrović, Z. S.; Guo, A.; Zhang, W. *J Polym Sci: Part A: Polym Chem* 2000, 38, 4062–4069, c) Behera, D.; Banthia, A. K. *J App Polym Sci*, 2008, 109, 2583–2590.
- <sup>19</sup> a) Hojabri, L.; Kong, X.; Narine S. S. *Biomacromolecules* 2009, 10, 884–891, b) Wang, C. S.; Yang, L. T.; Ni, B. L.; Shi, G. *J Appl Polym Sci* 2009, 114, 125–131, c) Zhao, H. P.; Zhang, J. F.; Sun, X. S.; Hua1, D. H. *J Appl Polym Sci* 2008, 110, 647–656, d) Kong, X.; Yue, J.; Narine, S. S. *Biomacromolecules* 2007, 8, 3584-3589, e) Kong, X.; Narine, S. S. *Biomacromolecules* 2007, 8, 2203–2209.
- <sup>20</sup> Lu, Y.; Larock, R. C. *Biomacromolecules* 2008, 9, 3332–3340.
- <sup>21</sup> a) Tu, Y. C.; Fan, H.; Suppes, G. J.; Hsieh, F. H. *J Appl Polym Sci*, 2009, 114, 2577–2583 b) Campanella, A.; Bonnaillie, L. M.; Wool, R. P. *J Appl Polym Sci* 2009, 112, 2567–2578.
- <sup>22</sup> a) Kong, X.; Narine, S. S. *Biomacromolecules* 2008, 9, 2221–2229, b) Kong, X.; Narine, S. S. *Biomacromolecules* 2008, 9, 1424–1433.
- <sup>23</sup> Lu, Y.; Larock, R. C. *Biomacromolecules* 2007, 8, 3108-3114.
- <sup>24</sup> Earls, J. D.; White, J. E.; López, L. C.; Lysenko, Z.; Dettloff, M. L.; Null, M. J. *Polymer* 2007, 48, 712-719.
- <sup>25</sup> Tanrattanakul, V.; Saithai, P. *J Appl Polym Sci* 2009, 114, 3057–3067.

- 
- <sup>26</sup> Lligadas, G.; Ronda, J. C.; Galià, M. Cádiz, V. *Biomacromolecules*, 2006, 7, 3521–3526.
- <sup>27</sup> Karak, N.; Rana, S.; Cho, J. W. *J Appl Polym Sci* 2009, 112, 736–743.
- <sup>28</sup> Wang, H. J.; Rong, M. Z.; Zhang, M. Q.; Hu, J.; Chen, H. W.; Czigány, T. *Biomacromolecules* 2008, 9, 615–623.
- <sup>29</sup> Black, M.; Rawlins, J. W. *Eur Polym J* 2009 45, 1433–1441.
- <sup>30</sup> Hirayama, K. I.; Irie, T.; Teramoto, N.; Shibata, M. *J Appl Polym Sci* 2009, 114, 1033–1039.
- <sup>31</sup> Lligadas, G.; Ronda, J. C.; Galià, M. Cádiz, V. *Biomacromolecules* 2007, 8, 1858–1864.
- <sup>32</sup> Çaylı, G.; Küsefoğlu, S. *J Appl Polym Sci* 2008, 109, 2948–2955.
- <sup>33</sup> Mutlu, H.; Küsefoğlu, S. H. *J Appl Polym Sci* 2009, 113, 1925–1934.
- <sup>34</sup> Henna, P.; Larock, R. C. *J Appl Polym Sci* 2009, 112, 1788–1797.
- <sup>35</sup> Liu, Z.; Sharma, B. K.; Erhan, S. Z. *Biomacromolecules* 2007, 8, 233–239.
- <sup>36</sup> Sacristán, M.; Ronda, J. C.; Galià, M.; Cádiz, V. *Biomacromolecules* 2009, 10, 2678–2685.

## OBJECTIVES

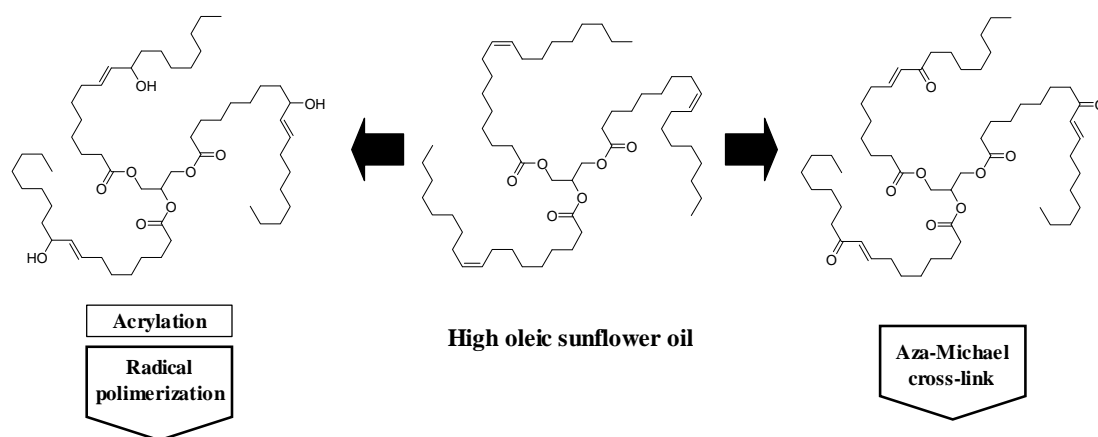
As explained in the introduction, the use of renewable feedstocks, such as vegetable oils, for the development of polymers is a crucial step towards sustainability. The general objective of this thesis is the investigation of new approaches for the synthesis of plant oil-derived polymeric materials.

The first objective consist of the development of new synthetic pathways for the synthesis of thermosetting materials using high oleic sunflower oil as starting material. High oleic sunflower oil is obtained from modified sunflowers.<sup>1</sup> It contains a minimum of 80 % of oleic acid (monounsaturated) that makes it specially attractive for certain synthetic applications.

The second main objective is the synthesis of phosphorus-containing plant oil monomers for the synthesis of *reactive* phosphorus-containing flame retardant materials.

## SUMMARY

The first part of this thesis (chapters one and two) is focused on the modification of commercial high oleic sunflower oil for the synthesis of two triglyceride-monomers. Both monomers were synthesized through the singlet oxygen photoperoxidation of high oleic sunflower oil. Further dehydration or reduction led to a  $\alpha,\beta$ -unsaturated ketone-containing derivative and an allylic hydroxyl-containing derivative.

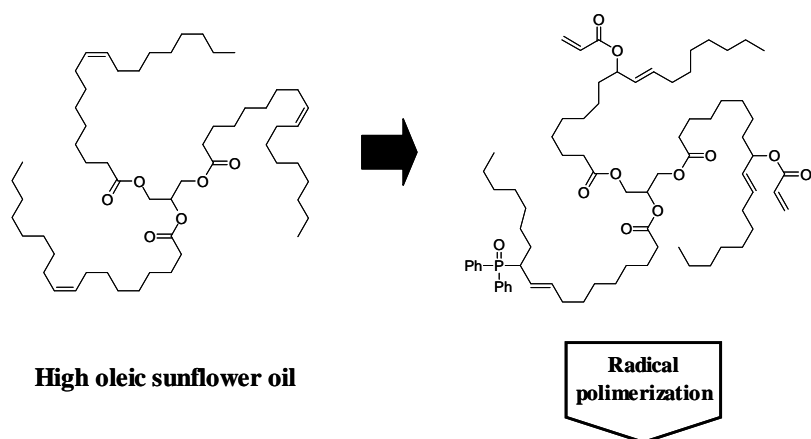


- Chapter one contains the work developed on the cross-link of the enone derivative with an aromatic diamine *via* aza-Michael addition reaction. First, the reactivity of the curing system is presented and compared with a conventional epoxy-diamine system. Secondly, a thorough study of the secondary reactions taking place, in relation with the reaction conditions, enabled the development of new quinoline-containing triglyceride-based thermosets.

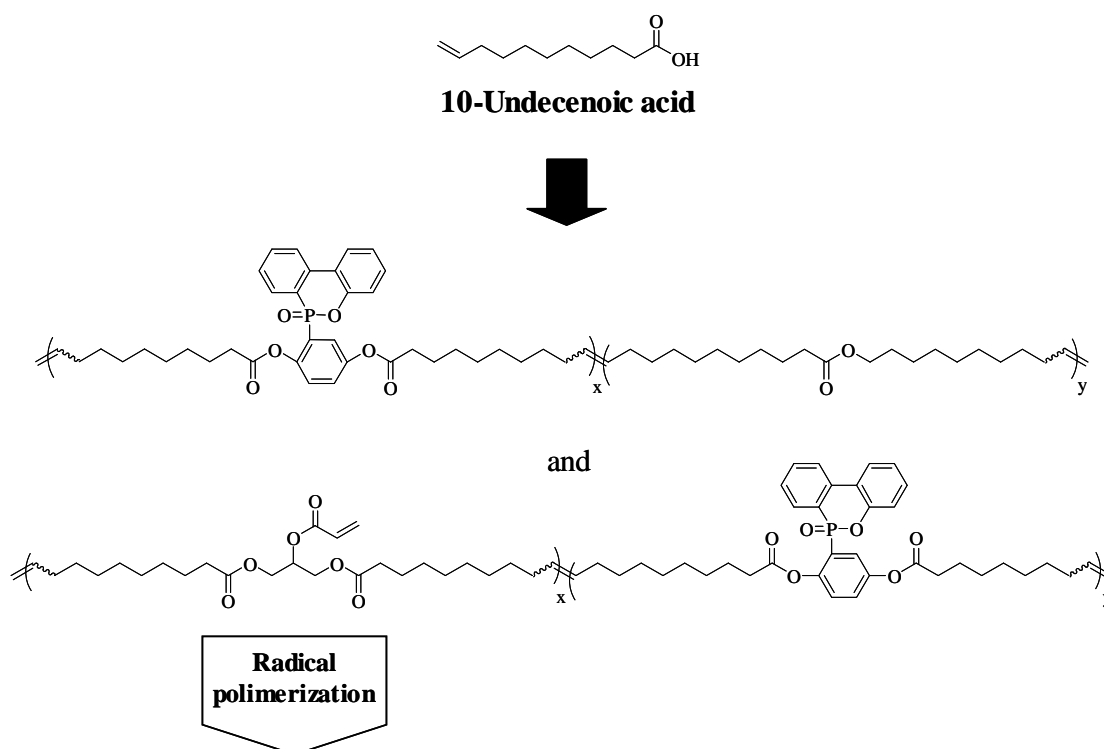
- Chapter two contains the cross-link of the allylic hydroxyl derivative through acrylation and subsequent radical polymerization. The study of the effect of an increase of cross-link density on the material properties was carried out by using different amounts of pentaerythritol tetraacrylate as cross-linking agent. Moreover, a complete hydrogenation of the internal double bonds of the monomer was carried out to study the effect of unsaturations on the cross-linked polymer properties.

The second part of this thesis (chapters three and four) is focused on the development of phosphorus-containing plant oil-based materials with flame retardant properties. High oleic sunflower oil and 10-undecenoic acid (derived from castor oil cracking) were used as starting reagents.

- Chapter three contains the synthesis of flame retardant thermosets from high oleic sunflower oil. The previously mentioned allylic hydroxyl derivative was partially modified by introducing different amounts of tertiary phosphine oxide groups *via* formation of allyl phosphinite and [2,3]-sigmatropic rearrangement. The remaining hydroxyls were acrylated and the subsequent radical polymerization afforded a family of thermosets with improved fire resistance.



• Chapter four contains the synthesis of linear and cross-linked castor oil-derived phosphorus-based flame retardants. In the first section, a series of flame retardant linear polyesters with different phosphorus contents were synthesized *via* ADMET polymerization. The effect of the polymerization temperature on the molecular weight and thermal properties is also reported. In the second section, hydroxyl-containing linear polyesters with different phosphorus contents were synthesized *via* ADMET polymerization. The acrylation of the backbone hydroxyl groups followed by radical polymerization afforded a family of flame retardant thermosets.



<sup>1</sup> Fick, G. N. (Breckenridge, MN) *Sunflower products and methods for their production* US Patent 4627192, 1986.





## FIRST PART

---

In the first part of this thesis, the *ene* reaction of singlet oxygen with the internal double bonds of high oleic sunflower oil has been applied as a general first functionalization step for the development of plant oil-based thermosets. The photoperoxidation of high oleic sunflower oil has been used for the synthesis of two different triglyceride derivatives. Chapter one describes the synthesis of thermosets from a triglyceride derivative containing  $\alpha,\beta$ -unsaturated groups via aza-Michael reaction. Chapter two contains the synthesis of thermosets from a hydroxyl-containing triglyceride derivative via acrylation and radical polymerization.

---



## THE CHEMISTRY OF SINGLET OXYGEN

### Introduction

For more than 70 years, researchers in several areas of science have been intrigued by the physical and chemical properties of the lowest excited states of molecular oxygen. With two singlet states lying close above its triplet ground state (Figure 1), the  $O_2$  molecule possesses a very unique configuration, which gives rise to a very rich and easily accessible chemistry, and also to a number of important photophysical interactions. In particular, photosensitized reactions of the first excited state  $O_2(^1\Delta_g)$ , play a key role in many natural photochemical and photobiological processes, such as photodegradation and aging processes including even photocarcinogenesis. Reactions of  $O_2(^1\Delta_g)$  are associated with significant applications in several fields, including organic synthesis, purification of water, bleaching processes, and, most importantly, the photodynamic therapy of cancer, which has now obtained regulatory approval in most countries for the treatment of several types of tumors.

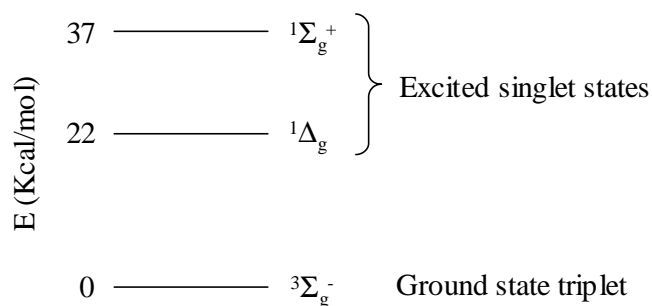
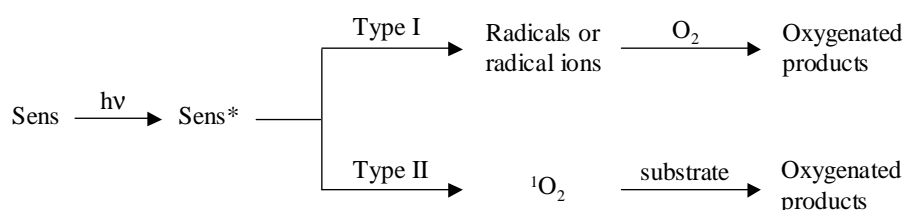


**Figure 1.** Ground state and excited states of molecular oxygen.

### Singlet oxygen generation

Singlet oxygen is the lowest excited state of the dioxygen molecule. The most common means of singlet oxygen generation is photosensitization or, more precisely, energy transfer to  $O_2$  from an excited state of a sensitizer, which is formed by the absorption of light in a specific wavelength region (Scheme1). A photosensitizer is irradiated to its singlet excited state, followed by conversion (called intersystem crossing) to its triplet

excited state. The triplet excited sensitizer may undergo radical reactions (type I process) or produce singlet oxygen (type II process). Ideal sensitizer properties and experimental conditions that favor the singlet oxygen (type II) pathway include (i) a low sensitizer and  $O_2$  concentration, (ii) a high intersystem crossing yield of the sensitizer, (iii) a low chemical reactivity of the sensitizer triplet state, and (iv) a small singlet-triplet splitting of the sensitizer. However, competition between type I and II photooxidation chemistry is inevitable upon the formation of an excited sensitizer in the presence of  $^3O_2$ .<sup>1</sup> Other experimental parameters influencing the singlet oxygen photosensitized generation are the solvent polarity, the temperature or the pressure.<sup>2</sup>



**Scheme 1.** Substrate photosensitized oxidation through type I and type II mechanisms.

Figure 2 shows some examples of the great synthetic utility of singlet oxygen for generating oxygenated hydrocarbons, such as endoperoxides from [2 + 4] cycloadditions, dioxetanes from [2 + 2] cycloadditions, sulfoxides from sulfide oxidations, phosphine oxides from phosphine oxidations, and hydroperoxides from phenol oxidations and “ene” reactions.

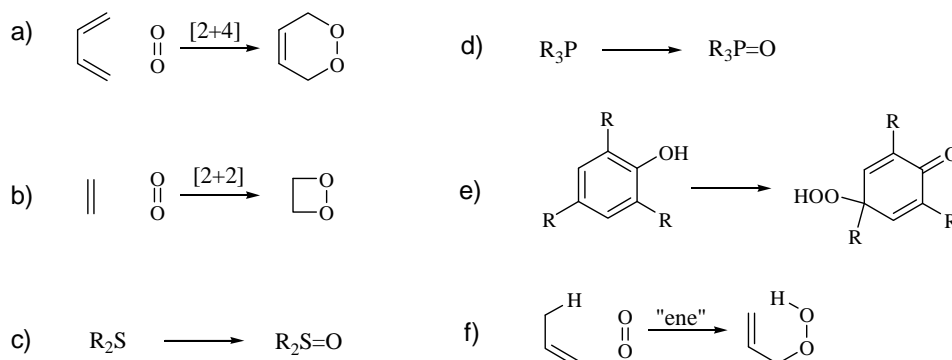
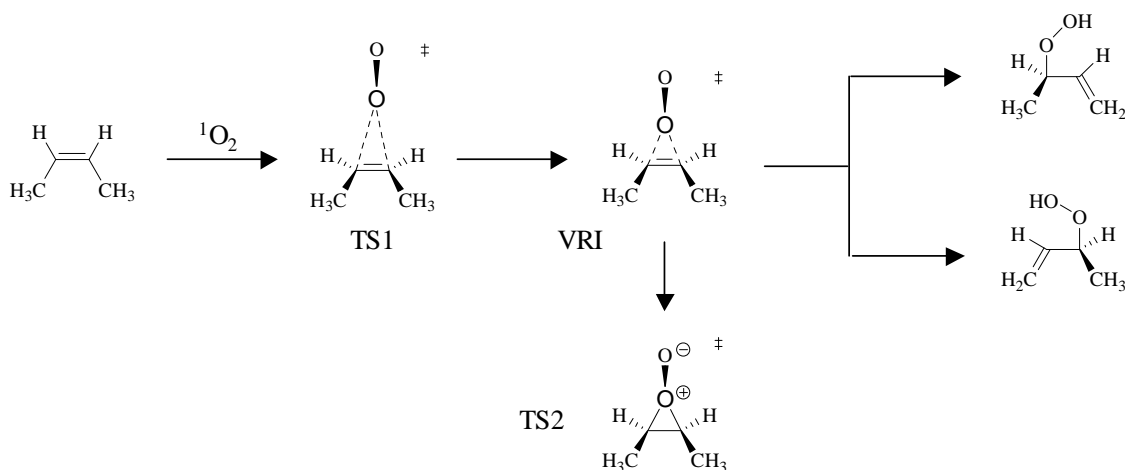


**Figure 2.** synthesis of a) endoperoxides, b) dioxetanes, c) sulfoxides, d) phosphine oxides, and e) and f) hydroperoxides with singlet oxygen.

## The *ene* reaction of singlet oxygen with alkenes

Singlet oxygen reacts with alkenes through an *ene* reaction to form allylic hydroperoxides. This reaction was first described in 1945 by Schenck<sup>3</sup> but it was not until 2003 that its mechanism was elucidated by combination of computational and experimental investigations on the reaction between  $^1\text{O}_2$  and *cis*-2-butene.<sup>4</sup> It is now accepted that the *ene* reaction contains a valley-ridge inflection (VRI) between two transition states (TS1 and TS2) which are connected sequentially. The pathway bifurcates at the VRI point prior to TS2 to give the allylic hydroperoxide products (Scheme 2).



**Scheme 2.** Mechanism of the *ene* reaction between singlet oxygen and *cis*-2-butene.

A biological example of the  $^1\text{O}_2$  “ene” reaction is in lipid peroxidation processes, where a shift in the double bond takes place. As an example, figure 3 shows the products of hydroperoxidation of linoleoyl groups at the 9', 10', 12', and 13' positions.

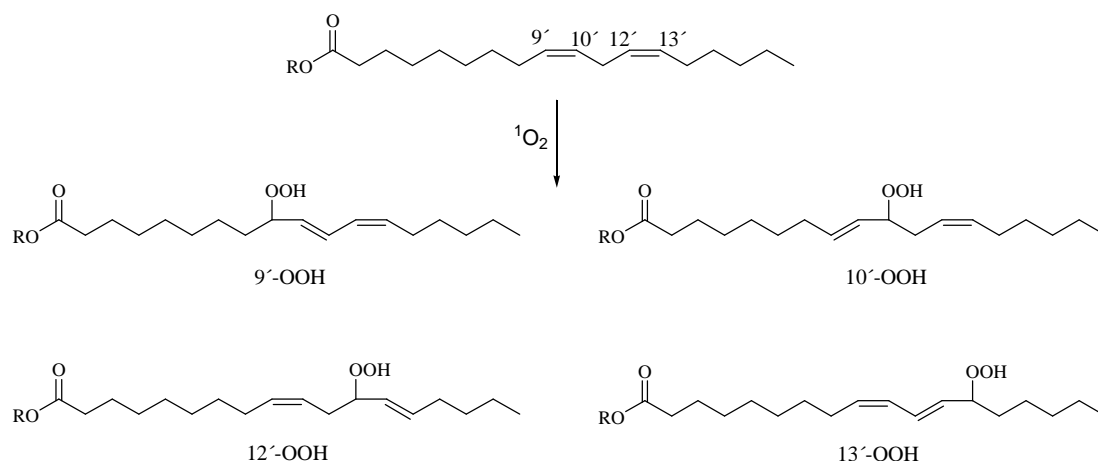


**Figure 3.** Products of the *ene* reaction of an ester of linoleic acid with singlet oxygen.

The *ene* reaction of singlet oxygen with the internal double bonds of high oleic sunflower oil has been applied in this work as a general first step for the development of plant oil-based thermosets. The photoperoxidation of high oleic sunflower oil affords a triglyceride derivative with allylic hydroperoxides. Dehydration or reduction of the hydroperoxides can afford a triglyceride containing  $\alpha,\beta$ -unsaturated groups or allylic hydroxyls that have been used as new monomers in the synthesis of plant oil-based thermosets.

<sup>1</sup> Greer, A. *Acc Chem Res* 2006, 39, 797-804.

<sup>2</sup> Schweitzer, C.; Schmidt, R. *Chem Rev*, 2003, 103, 1685-1758.

<sup>3</sup> Schenck, G. O. *Naturwissenschaften* 1948, 35, 28-29.

<sup>4</sup> Singleton, D. A.; Hang, C.; Szymanski, M. J.; Meyer, M. P.; Leach, A. G.; Kuwata, K. T.; Chen, J. S.; Greer, A.; Foote, C. S.; Houk, K. N. *J Am Chem Soc* 2003, 125, 1319-1328.

## **Chapter 1**

- 1. A New Enone-Containing Triglyceride Derivative as Precursor of Thermosets from Renewable Resources**
- 2. Quinoline-Containing Networks from Enone and Aldehyde Triglyceride Derivatives**





# A New Enone-Containing Triglyceride Derivative as Precursor of Thermosets from Renewable Resources

Lucas Montero de Espinosa, Juan C. Ronda, Marina Galia, Virginia Cádiz

Department of Analytical and Organic Chemistry, Rovira i Virgili University, Campus  
Sescelades, Marcel·lí Domingo s/n, 43007 Tarragona, Spain.

**ABSTRACT.** A novel triglyceride containing  $\alpha,\beta$ -unsaturated ketone was prepared through photoperoxidation from high oleic sunflower oil by two steps one pot environmentally friendly procedure. This new enone-containing triglyceride was crosslinked with diaminodiphenylmethane (DDM) via aza-Michael addition. A kinetic study of the reaction of *p*-toluidine with either enone-containing methyl oleate or epoxidized methyl oleate, as model compounds, allowed to establish the higher reactivity of the former, thus confirming this curing system as an alternative to amine-cured epoxidized vegetable oils. The thermal properties of thermosets from enone and epoxy-containing triglycerides with DDM have been evaluated.

**Keywords:** triglyceride, crosslinking, renewable resources, aza-Michael

## INTRODUCTION

The development of environmentally compatible polymers is one of the current challenges in polymer chemistry. The scarcity of non renewable resources encouraged the scientific community to develop and commercialize new biobased products that can alleviate the wide-spread dependence on fossil fuels and, enhance security, the environment and the economy.<sup>1</sup> Natural oils are considered to be the most important class of renewable sources.<sup>2</sup> The main component of the triglyceride vegetable oils are saturated and unsaturated fatty acids. Although they have double bonds which can be used as reactive sites in coatings, for obtaining high performance polymeric materials the introduction of more reactive functional groups, such as hydroxyl, epoxy or carboxyl groups, is much more suitable.<sup>3,4</sup> Various chemical pathways for functionalizing triglycerides and fatty acids have been studied.<sup>5</sup> Epoxidation is one of the most important functionalization reactions of the C-C double bonds, that can be achieved by environmentally friendly procedures such as catalyzed chemical oxidation

with hydrogen peroxide<sup>6,7</sup> or by enzymatic oxidation.<sup>8</sup> The opening of the epoxide ring is a versatile reaction that leads to numerous products.<sup>4,9,10</sup> Thus, epoxidized vegetable oils are extremely promising as inexpensive renewable materials for industrial applications<sup>11</sup> because they share many of the characteristics of conventional epoxy thermosets. In this way, naturally occurring epoxy oil, as vernonia seed oil or epoxidized vegetable oils from soybean, linseed or castor oils have been cured cationically<sup>12</sup> or with conventional hardeners as diamines or dianhydrides.<sup>13-16</sup>

The challenge to progressively replace fossil feedstocks by materials arising from plant-derived renewable sources implies not only the development of new original reactions and catalysts but also the application of well established reactions to the production of new tailor made compounds capable to produce competitive performance materials.

In this communication we report the synthesis of a new highly reactive triglyceride derivative with  $\alpha,\beta$ -unsaturated carbonyl groups. This enone-containing triglyceride is obtained by an environmentally friendly chemical procedure from high oleic sunflower oil and it could be an interesting alternative to epoxidized vegetable oils to produce thermosets by crosslinking with conventional aromatic diamines. Amine-cured  $\omega$ -epoxy fatty acid triglycerides have been shown to yield robust networks with good adhesive characteristics similar to those of conventional thermosets based on diglycidylether of Bisphenol A.<sup>13</sup> However, epoxidized fatty oils such as epoxidized linseed and soybean oils, which contain oxirane groups that are hindered at both carbons, react sluggishly with nucleophilic curing agents.<sup>17</sup> On the other hand, the Michael addition reaction is a valuable tool in the synthesis of polymeric networks.<sup>18</sup> The aza-Michael reaction, a variation in which an amine acts as the nucleophile, has been used in the synthesis of improved bismaleimide networks,<sup>19</sup> but this reaction has not been applied to the synthesis of crosslinked polymers derived from vegetable oils.

In this work the high reactivity of the enone groups has been proved. By means of a <sup>1</sup>H NMR kinetic experiment, the reactivity of *p*-toluidine with either enone or epoxy functions in fatty acid derivatives as model compounds has been studied. The crosslinking of the enone- and epoxy-containing triglycerides with diaminodiphenylmethane was followed by FTIR spectroscopy and the thermal properties of the final materials were evaluated.

## EXPERIMENTAL PART

### Materials

High oleic sunflower oil (minimum 80% oleic acid) was kindly supplied by Borges<sup>®</sup>. Methyl oleate (Alfa Aesar), *meso*-tetraphenylporphyrin (TPP) (Aldrich), borontrifluoride monoethanolamine complex (BF<sub>3</sub>·MEA) (Aldrich), *p*-toluidine (Aldrich), diaminodiphenylmethane (DDM) (Aldrich), triethylamine (Scharlau), acetic anhydride (Scharlau) and hydrogen peroxide 50% (w/v) (Scharlau), were used as received. Toluene was dried over sodium/benzophenone and dichloromethane from P<sub>2</sub>O<sub>5</sub>, both distilled immediately before use. Epoxidized methyl oleate (EMO),<sup>20</sup> and the mixture of methyl-9-oxo-10-octadecenoate and methyl-10-oxo-8-octadecenoate<sup>21</sup> were synthesized as previously reported. Tetrakis(diperoxotungsto)phosphate was synthesized following a published procedure.<sup>22</sup> TLC plates were developed by spraying with sulphuric acid/anisaldehyde ethanol solution and heating at 200 °C.

**Photoperoxydation of high oleic sunflower oil.** In a 450mL standard immersion-well photochemical reactor with a 400W high pressure sodium vapour lamp, high oleic sunflower oil (70 g, 79.1 mmol), TPP (0.02 g, mol) and dichloromethane (400mL) were introduced. Cold water was circulated through the lamp jacket, while a gentle stream of oxygen was bubbled through the stirred reaction mixture. After a few minutes, the lamp was turned on and the reaction was monitored by TLC (hexane/ethyl acetate, 5:1). After 4 h of irradiation the total disappearance of isolated double bonds and formation of the intermediate allylic hydroperoxides was observed. The lamp was turned off and the reactor was placed into a water bath. Acetic anhydride (24.60 mL, 260.9 mmol) and triethylamine (18.20 mL, 130.4 mmol) were added with stirring at room temperature. After 30 min TLC (hexane/ethyl acetate, 5:1) confirmed the formation of the enone and the complete disappearance of the hydroperoxide. The solvent was then eliminated at reduced pressure. The reaction mixture was diluted with ethyl acetate (500 mL) and washed successively with water, saturated NaHCO<sub>3</sub>, HCl (10% v/v) and saturated NaCl. After drying over MgSO<sub>4</sub> and concentrating under reduced pressure, the product was obtained as a triglyceride mixture with 2.3  $\alpha,\beta$ -unsaturated ketones per molecule (determined by <sup>1</sup>H NMR spectroscopy). Further purification was achieved by crystallization, at 5°C, from hexane (200 mL) obtaining a product with 2.6  $\alpha,\beta$ -unsaturated ketones per molecule (determined by <sup>1</sup>H NMR) with 76% yield.

FTIR: 1740  $\text{cm}^{-1}$  (ester C=O, st), 1696  $\text{cm}^{-1}$  (C=O,s-cis, st), 1673  $\text{cm}^{-1}$  (C=O, s-trans, st), 1629  $\text{cm}^{-1}$  (C=C, st), 1162  $\text{cm}^{-1}$  (C-O, st).

$^1\text{H}$  NMR ( $\text{CDCl}_3$ , TMS,  $\delta$  ppm): 6.78-6.70 (3H, m, H-11), 5.99 (3H, dd,  $J_{10-11}$  = 16 Hz,  $J_{10-12}$  = 1.6 Hz, H-10), 5.22-5.16 (1H, m, H-19), 4.24-4.20 (2H, m, H-20), 4.06 (2H, dd,  $J_{20-20}$  = 11.6 Hz,  $J_{20-19}$  = 6.0 Hz, H-20), 2.44 (6H, t,  $J_{2-3}$  = 7.2 Hz, H-8), 2.25-2.21 (6H, m, H-2), 2.15-2.09 (6H, m,  $J_{12-11}$   $\cong$   $J_{12-13}$  = 7.3 Hz, H-12), 1.58-1.43 (12H, m, H-3 H-7), 1.43-1.30 (6H, m, H-13), 1.30-1.10 (42H, m, aliphatic chain), 0.83-0.76 (9H, m, H-18).

$^{13}\text{C}$  NMR ( $\text{CDCl}_3$ , TMS,  $\delta$  ppm): 200.76 (C-9), 200.65 (C-9'), 173.21-172.66 (C-1 C-1'), 147.33, 146.86 (C-11), 130.42-130.30 (C-10), 68.94-68.89 (C-19), 62.05 (C-20), 40.12-39.94 (C-8), 34.11-33.89 (C-2), 32.47-32.35 (C-12), 31.95-31.76 (C-16), 29.72-28.79 (C-Al), 28.13-27.92 (C-13), 24.86-24.67 (C-3), 24.29-24.15 (C-7), 22.72-22.64 (C-17), 14.15-14.10 (C-18).

**Synthesis of epoxidized high oleic sunflower oil.** A 250 mL round-bottomed flask fitted with a reflux condenser was charged with high oleic sunflower oil (50 g), tetrakis(diperoxotungsto)phosphate (0.84 g, 0.38 mmol), 1,2-dichloroethane (50 mL) and  $\text{H}_2\text{O}_2$  16% (50 mL). The mixture was heated to 70 °C and stirred vigorously until TLC (hexane/ethyl acetate, 9:1) showed completion of the reaction (5 h). The reaction mixture was diluted with water (100 mL) and the resulting two phases were separated. The organic layer was washed with 50 mL of water and dried over  $\text{MgSO}_4$ . The product was concentrated under reduced pressure and purified by crystallization at -25 °C from acetone. An epoxidized high oleic sunflower oil containing 2.7 epoxy groups per molecule (determined by  $^1\text{H}$  NMR) was obtained with 92% yield.

FTIR: 1733  $\text{cm}^{-1}$  (ester C=O, st), 1171  $\text{cm}^{-1}$  (C-O, st), 844  $\text{cm}^{-1}$  (ring, st).

$^1\text{H}$  NMR ( $\text{CDCl}_3$ , TMS,  $\delta$  ppm): 5.26-5.22 (1H, m, -CH(O)-), 4.27 (2H, dd,  $J_1$  = 12 Hz,  $J_2$  = 4 Hz, -CH<sub>2</sub>-O), 4.12 (2H, dd,  $J_1$  = 11.6 Hz,  $J_2$  = 5.6 Hz, -CH<sub>2</sub>-O), 2.91-2.86 (5.3 H, m, -CH(O)- epoxide), 2.29 (6H, t,  $J$  = 7.2 Hz, -CH<sub>2</sub>-CO), 1.65-1.15 (78H, m, aliphatic chain), 0.86 (9H, t,  $J$  = 6.8 Hz, -CH<sub>3</sub>).

$^{13}\text{C}$  NMR ( $\text{CDCl}_3$ , TMS,  $\delta$  ppm): 173.22, (COOR), 172.82 (C' OOR), 68.93 (-CH(O)-), 62.13 (-CH<sub>2</sub>-O), 57.23-57.17 (-CH(O)-, epoxide), 34.18-34.02 (-CH<sub>2</sub>-CO), 31.98-29.01 (C-Al), 27.89-27.86 (-CH<sub>2</sub>-CH(O)-), 26.68-26.65 (C-Al), 24.86-24.83 (-CH<sub>2</sub>-CH<sub>2</sub>-CO), 22.73(Al), 14.17 (-CH<sub>3</sub>).

### **Kinetic Measurements**

Kinetic experiments were carried out by  $^1\text{H}$  NMR using rubber septa sealed NMR tubes. The precise amounts of a 1M solution of epoxidized methyl oleate or the methyl-oxo-octadecenoate mixture and 0.5M solution of *p*-toluidine in dry deuterated toluene were introduced using general vacuum-line techniques. The reaction was monitored at 80 °C. In the case of the epoxidized methyl oleate an experiment using 4% mol of  $\text{BF}_3\cdot\text{MEA}$  as catalyst was also carried out.

### **Curing reactions**

The curing reactions were carried out as follows. The enone-containing triglyceride and the DDM were melted and then mixed. The resulting liquid was put into a previously heated (60 °C) mold. The mixture was heated at 90 °C for 12h and post-cured at 120 °C for 6h. In the case of the epoxidized high oleic sunflower oil, the procedure was similar. The epoxy-containing triglyceride and DDM were melted, mixed and placed into a mold at 120 °C for 6h. The material was post-cured at 140 °C for 2h. In the catalyzed curing reaction,  $\text{BF}_3\cdot\text{MEA}$  (4% mol) was added to the mixture just before putting it into the mold.

### **Instrumentation**

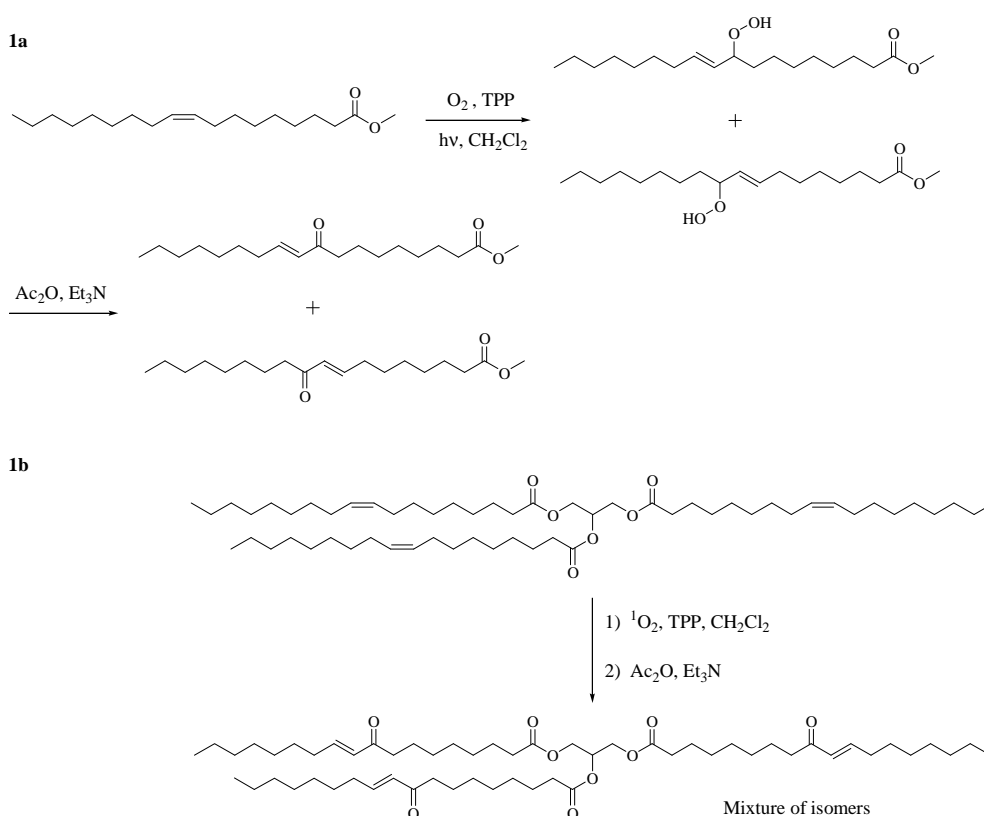
$^1\text{H}$  NMR 400 MHz and  $^{13}\text{C}$  NMR 100.6 MHz NMR spectra were obtained using a Varian Gemini 400 spectrometer with Fourier transform,  $\text{CDCl}_3$  as solvent and TMS as internal standard. The crosslinking process at 90°C was monitored with a FTIR-680PLUS spectrophotometer with a resolution of 4  $\text{cm}^{-1}$  in the transmittance mode. An attenuated-total-reflection accessory with thermal control and a diamond crystal was used to determine FTIR/ATR spectra.

Calorimetric studies were carried out on a Mettler DSC821e thermal analyzer using  $\text{N}_2$  as a purge gas (20 ml/min) at scan rates between 5 and 20°C/min and dynamic mechanical thermal analysis (DMTA) apparatus (TA DMA 2928). The thermal transitions were studied in the -80-120°C range at a heating rate of 10°C/min and at a fixed frequency of 1 Hz.

Thermal stability studies were carried out on a Mettler TGA/SDTA851e/LF/1100 with  $\text{N}_2$  as a purge gas, in the 30-800°C at scan rates of 10°C/min.

## RESULTS AND DISCUSSION

As mentioned in the introduction the synthesis of the new enone containing-triglyceride derivative was carried out by an environmentally friendly chemical procedure from high oleic sunflower oil. For this purpose we used the singlet oxygen “ene” reaction which is one of the highly investigated processes in organic chemistry to functionalize the allylic C-H bonds of unsaturated compounds. This reaction was discovered in 1948 by Schenck,<sup>23</sup> who demonstrated that allylic hydroperoxides are handily prepared by reaction of alkenes with photochemically generated singlet oxygen. The mechanism of this reaction has been widely studied and it is actually well established.<sup>24</sup> For synthetic applications, the unsaturated substrate can be photooxygenated “in situ” with singlet



**Scheme 1.** Synthesis of 1a) enone-containing fatty acid derivative and 1b) enone-containing triglyceride derivative.

oxygen generated by means of a high pressure sodium-vapor lamp and TPP as sensitizer in an oxygen saturated medium, to give a mixture of isomeric allylic hydroperoxides (scheme 1a). This reaction has been used to oxidize the allylic position of fatty acids and their derivatives<sup>24-26</sup> such the methyl oleate. The mild conditions utilized and the use of oxygen, as the only reagent, makes this process particularly favorable from both an economical and ecological viewpoint.

The allylic hydroperoxides can undergo a number of different transformations.<sup>27</sup> One of the most interesting reactions is the conversion of these hydroperoxides into a regioisomeric mixture of enones (scheme 1a),<sup>28,29</sup> that can be carried out in the presence of acetic anhydride and pyridine or tertiary amines. This reaction has been scarcely used with fatty acids and their derivatives.<sup>21</sup> The application of this reaction to unsaturated triglycerides, not explored up to date, affords to a multifunctional reactive compound useful to obtain thermosetting materials from renewable resources. Thus, the photooxidation and further dehydration of samples of high oleic sunflower oil (scheme 1b) led to the quantitative double bond transformation, according to <sup>1</sup>H NMR measurements.

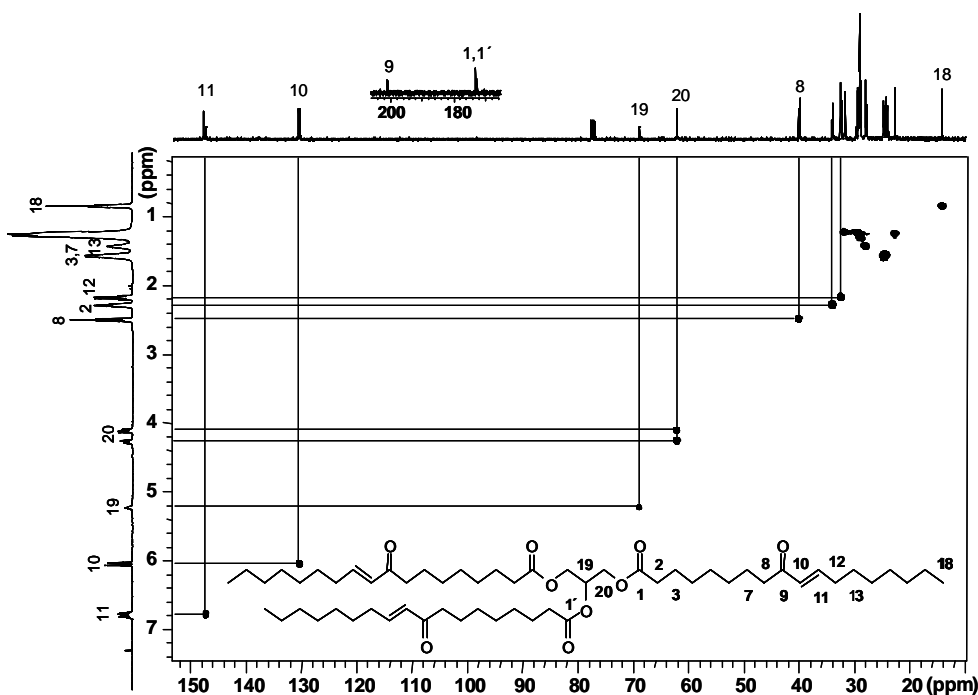


**Figure 1.** <sup>1</sup>H, <sup>13</sup>C, and HSQC NMR spectra of the enone-containing triglyceride.

The obtained product was purified by crystallization in hexane at 5° C to remove some triglyceride fractions rich in saturated fatty acids. In this way, a product

containing 2.6 enone groups per triglyceride was obtained with a yield of 76%. Fig 1 depicts the  $^1\text{H}$ ,  $^{13}\text{C}$  and HSQC NMR spectra with all the assignments.

To compare the reactivity of aromatic amines with either enone or epoxy functions in triglycerides, a  $^1\text{H}$  NMR kinetic experiment using the enone or the epoxy methyl oleate derivatives, as monofunctional model compounds, was carried out. In this way, the same amounts of 1M solution of epoxidized methyl oleate or the methyl-oxo-octadecenoate mixture, were mixed with a 0.5M solution of *p*-toluidine in sealed NMR tubes (molar ratio 2:1). The reaction was monitored at 80 °C through the disappearance of the characteristic multiplet epoxy signal at 2.68 ppm or the double bond doublet signal at 5.96 ppm corresponding to the methine directly attached to the carbonylic group. We used as internal reference the signal at 3.40 ppm corresponding to the methyl in the ester group. Fig. 2 shows the conversion of the enone and epoxy groups versus time. As can be seen, the enone groups react much faster with *p*-toluidine than epoxy groups do. Moreover, the analysis of the aromatic region (doublet at 6.39 ppm) allowed

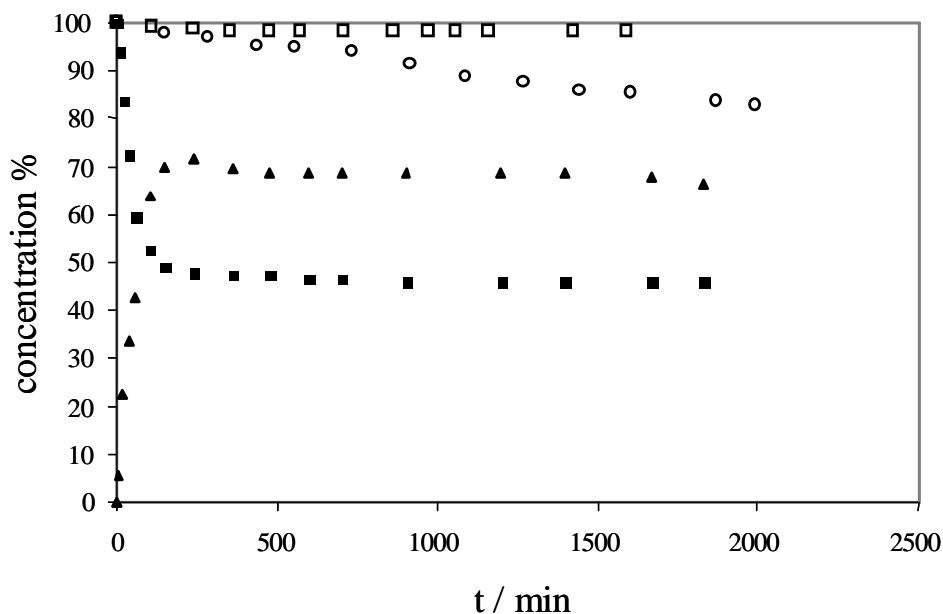


**Figure 2.** kinetic  $^1\text{H}$  NMR experiment. Conversion versus time of a) EMO (□); b) EMO with 4% mol  $\text{BF}_3\text{-MEA}$  (○) and c) mixture of methyl-9-oxo-10-octadecenoate and methyl-10-oxo-8-octadecenoate (■) when reacted with *p*-toluidine; d) secondary amine in reaction c) (▲).

to follow the formation of the secondary amine which is depicted also in Fig. 2 for the case of enone derivative. The reaction between amine and enone groups occurs very



fastly reaching a *plateau* after 4h. Taking into account the molar ratio used and the observed conversion we can conclude that only the secondary amine is formed and other by-products are negligible. This could be confirmed in an experiment in which the methyl-oxo-octadecenoate mixture, was mixed with a 1M solution of *p*-toluidine in sealed NMR tube (molar ratio 1:1). The reaction was monitored at 80 °C by  $^1\text{H}$  NMR until the enone groups completely reacted. As can be seen in Fig. 3 only signals corresponding to the secondary amine derivative could be observed.

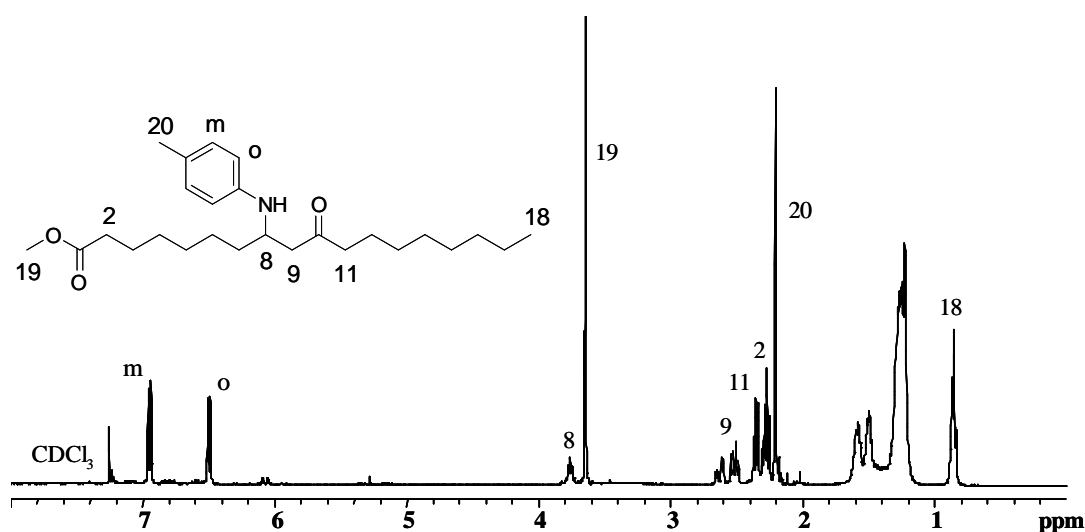


**Figure 3.**  $^1\text{H}$  NMR spectrum of the product from the reaction between methyl-oxo-decenoate and *p*-toluidine in a 1:1 molar ratio.

Because of the scarce reactivity observed in the case of epoxy derivative the reaction was investigated using  $\text{BF}_3\cdot\text{MEA}$  as catalyst. In this case, as can be seen in Fig. 2, the reaction was accelerated but did not reach the high reactivity observed in the enone derivative.

The curing reaction of enone-containing triglyceride with DDM was monitored by FTIR-ATR spectroscopy. Both compounds were mixed in a amine/enone 1:1 molar ratio and heated at 90°C during 5h. This technique allowed us to follow the evolution of the groups involved in the process by means of the variations in the corresponding absorptions. Fig. 4 shows FTIR spectra of the pure triglyceride derivative (a), the mixture with DDM at  $t=0$  min (b) and the mixture after 60 min (c). In the spectrum b) typical primary amine bands at  $3372\text{ cm}^{-1}$  and  $3460\text{ cm}^{-1}$ , conjugated ketone carbonyl group at  $1696\text{ cm}^{-1}$  (*s-cis*) and  $1673\text{ cm}^{-1}$  (*s-trans*) and double bonds stretching at  $1629$

$\text{cm}^{-1}$  corresponding to both aromatic amine and enone, can be observed. In the spectrum c) only a band at  $3385 \text{ cm}^{-1}$  corresponding to secondary amine appears. Moreover, there is a shift of ketone carbonyl band to higher wavenumbers because of the disappearance of the conjugated double bond. This saturated ketone band overlaps to carbonyl ester group at  $1741 \text{ cm}^{-1}$ . Therefore, we confirmed the reaction of the primary amine with the enone groups in the triglyceride.

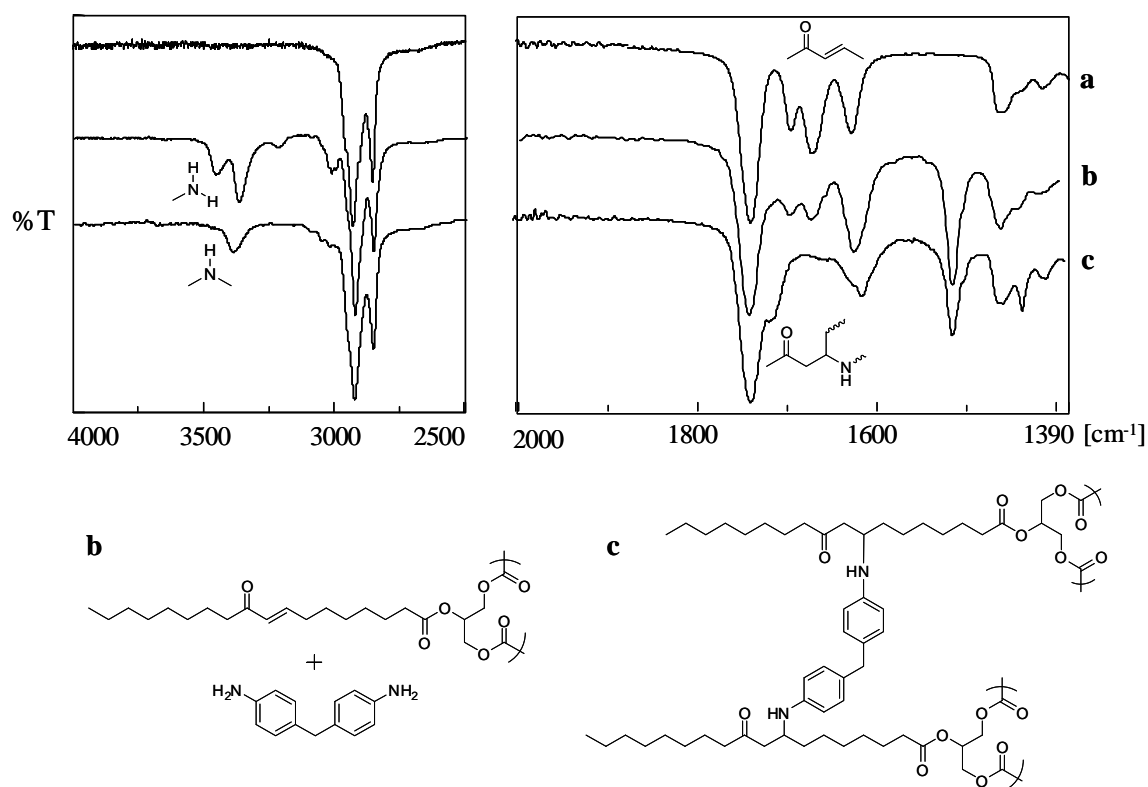


**Figure 4.** FTIR-ATR spectrum of the enone-containing triglyceride (a) and the initial (b) and final (c) FTIR spectra of the crosslinking reaction.

A similar curing reaction of epoxidized high oleic sunflower oil with DDM was monitored by FTIR-ATR spectroscopy. Both compounds were mixed in a amine/epoxy group 1:1 molar ratio and heated at  $90^\circ\text{C}$ . After 5h no reaction was observed remaining in the spectrum the corresponding absorptions due to the primary amine. Moreover no hydroxyl absorption was observed. After this reaction the resulting compound was soluble indicating the no formation of the network. Thus,  $\text{BF}_3 \cdot \text{MEA}$  (4% molar) was added as catalyst to the mixture at  $90^\circ\text{C}$ . In this case, the ring opening polymerization with DDM took place (primary amine absorptions diminish) but

homopolymerization of epoxidized triglyceride was favoured. This fact was confirmed by comparison of the spectra of this curing mixture and that of epoxidized triglyceride only with the Lewis acid catalyst. Both of them show a broad band at  $1050\text{ cm}^{-1}$  corresponding to ether bond in the resulting polyether.

Finally, the thermal properties of these polymeric networks were evaluated by DSC and DMTA. Dynamic DSC experiments allowed us to select the appropriate curing cycles. Thus, the curing was performed at the onset temperature of the curing exotherm in the plot and the post-curing at the maximum of this exotherm. In this way, the enone-containing triglyceride was cured for 12h at  $90^{\circ}\text{C}$  and post-cured for 5h at  $120^{\circ}\text{C}$  and the epoxidized triglyceride/ $\text{BF}_3\cdot\text{MEA}$  was cured for 6h at  $120^{\circ}\text{C}$  and post-cured for 2h at  $140^{\circ}\text{C}$ . DSC traces after these curing cycles show  $T_g$ 's at  $-10^{\circ}\text{C}$  and  $-7^{\circ}\text{C}$  respectively and no residual curing enthalpy was observed.

The dynamic mechanical behavior of the crosslinked materials was obtained as a function of the temperature beginning in the glassy state of each composition to the rubbery plateau of each material (Fig. 5). The crosslinking density of a polymer can be estimated from the plateau of the elastic modulus in the rubbery state.<sup>30</sup> However, this theory is strictly valid only for lightly crosslinked materials, and is therefore used only to make qualitative comparisons of the level of crosslinking among the various polymers. Figure 5 depicts the storage modulus and the  $\tan \delta$  of both samples. As can be observed,  $T_g$  values are  $16^{\circ}\text{C}$  for the enone derivative and  $19^{\circ}\text{C}$  for the epoxy derivative from the  $\tan \delta$  curves according to the elastomeric nature of these materials. Moreover, from storage modulus in the rubbery state and from the height of the  $\tan \delta$  peak, it can be inferred that crosslinking density is higher in the case of the enone derivative. Moreover, the  $\tan \delta$  peak width at half-height is broader, in the case of enone derivative, what is associated with the increasing number of branching modes and a wider distribution of structures. This could be due to a more complex crosslinking mechanism, than the single aza-Michael reaction. Further studies are now in progress and will be presented in a forthcoming paper.

The thermal stability was evaluated by TGA under nitrogen atmosphere. In both cases the thermogravimetric plots show that the materials have good thermal stability with 5% of weight loss about  $330^{\circ}\text{C}$  for the material cured via Aza-Michael and  $370^{\circ}\text{C}$  for the material cured by catalyzed oxirane ring opening. The shapes of the first

derivative TGA plots show that the degradations take place in broad temperature ranges in both cases.

## CONCLUSIONS

The “ene” reaction has been successfully applied to obtain  $\alpha,\beta$ -unsaturated ketone-containing triglycerides using a two steps one pot environmentally friendly procedure. This new enone-containing triglyceride derivative has shown high reactivity towards amines providing a promising route to obtain polymeric networks under mild conditions and without the aid of a catalyst.

The authors express their thanks to CICYT (Comisión Interministerial de Ciencia y Tecnología) (MAT2005-01593) for financial support for this work.

## REFERENCES

- <sup>1</sup> Bozell, J.J.; Patel, M. Eds., Feedstocks for the Future: Renewable for the Production of Chemicals and Materials; ACS Symposium Series 921; American Chemical Society: Washington, DC, 2006
- <sup>2</sup> Biermann, U.; Friedt, W.; Lang, S.; Lühs, W.; Machmüller, G.; Metzger, J. O.; Klaas, M. R.; Schäfer, H. J.; Schneider, M. P. *Angew Chem Int Ed* 2000, 39, 2206-2224.
- <sup>3</sup> Güner, F. S.; Yagci, Y.; Erciyas, A. T. *Prog Polym Sci* 2006, 31, 633-670.
- <sup>4</sup> Meier, M. A. R.; Metzger, J. O.; Schubert, U. S. *Chem Soc Rev* 2007, 36, 1788-1802.
- <sup>5</sup> Khot, S. N.; LaScala, J. J.; Can, E. S.; Morye, S. G.; Williams, I.; Palmese, G. R. S.; Küseföglu, H.; Wool, R. P. *J Appl Polym Sci* 2001, 82, 703-723.
- <sup>6</sup> Lane, B. S.; Burgess, K. *Chem Rev* 2003, 103, 2457-2474.
- <sup>7</sup> Grigoropoulou, G.; Clark, J. H.; Elings, J. A. *Green Chem.* 2003, 5, 1-7.
- <sup>8</sup> Uyama, H.; Kuwabara, M.; Tsujimoto, T.; Kobayashi, S. *Biomacromolecules*, 2003, 4, 211-215.
- <sup>9</sup> Esen, H.; Küseföglu, S.H.; *J Appl Polym Sci* 2003, 89, 3882-3888.
- <sup>10</sup> Guo, A.; Javni, I.; Petrovic, Z.S. *J Appl Polym Sci* 2000, 77, 467-473.
- <sup>11</sup> Kaplan, D.L. *Biopolymers from Renewable Resources*, Springer: Berlin 1998, p. 267.
- <sup>12</sup> Park, S-J.; Jin, F-L.; Lee, J-R. *Macromol Rapid Commun* 2004, 25, 724-727.
- <sup>13</sup> Earls, J.D.; White, J.E.; López, L.C.; Lysenko, Z.; Dettloff, M.L.; Null, M.J. *Polymer*, 2007, 48, 712-719.

- 
- <sup>14</sup> Miyagawa, H.; Misra, M.; Drzal, L. T.; Mohanty, A. K. *Polym Eng Sci* 2005, 487-495.
- <sup>15</sup> Miyagawa, H.; Mohanty, A.K.; Misra, M.; Drzal, L.T. *Macromol Mater Eng* 2004, 289, 636-641.
- <sup>16</sup> Ahmad, S.; Naqvi, F.; Sharmin, E.; Verma, K. L. *Prog Org Coat* 2006, 55, 268-275.
- <sup>17</sup> Corley, L. S. U.S. Patent 4,962,179, 1990.
- <sup>18</sup> Mather, B.D.; Viswanathan, K.; Miller, K. M.; Long, T.E. *Prog Polym Sci* 2006, 31, 487-531.
- <sup>19</sup> Wu, C.S.; Liu, Y.L.; Chiu, Y.S. *Polymer* 2002, 43, 1773-1779.
- <sup>20</sup> Bunker, S. P.; Wool, R.P. *J. Polym. Sci: Part A: Polym. Chem.* 2002, 40, 451-458.
- <sup>21</sup> Mihelich, E.D.; Eickhoff, D.J. *J Org Chem* 1983, 48, 4135-4137.
- <sup>22</sup> Venturello, C.; D'Aloisio, R. *J Org Chem* 1988, 53, 1553-1557.
- <sup>23</sup> Schenck, G.O. *Naturwissenschaften* 1948, 35, 28-29.
- <sup>24</sup> Greer, A. *Acc. Chem. Res.* 2006, 39, 797-804.
- <sup>25</sup> Hui, S-P.; Yoshimura, T.; Murai, T.; Chiba, H.; Kurosawa, T. *Anal Sci* 2000, 16, 1023-1028.
- <sup>26</sup> Samadi, A.; Martinez, L. A.; Miranda, M. A.; Morera, I. M. *Photochem Photobiol* 2001, 73, 359-365.
- <sup>27</sup> Frimer, A. A. *Chem Rev* 1979, 79, 359-387.
- <sup>28</sup> Kornblum, N.; DeLaMare, H.E. *J Am Chem Soc* 1951, 73, 880-881.
- <sup>29</sup> Ohloff, G. *Pure Appl Chem* 1975, 43, 481-502.
- <sup>30</sup> Tobolsky, A. V.; Carlson, D.W.; Indictor, N. J. *J Polym Sci* 1961, 54, 175-192.



# Quinoline-Containing Networks from Enone and Aldehyde Triglyceride Derivatives

Lucas Montero de Espinosa, Juan C. Ronda, Marina Galia, Virginia Cádiz

Department of Analytical and Organic Chemistry, Rovira i Virgili University, Campus Sescelades, Marcel·lí Domingo s/n, 43007 Tarragona, Spain.

**ABSTRACT.** The crosslinking reaction of a triglyceride derivative containing  $\alpha,\beta$ -unsaturated ketones with diaminodiphenylmethane via aza-Michael addition has been extensively studied. First, a model study with monofunctional compounds showed that the conjugated addition product undergoes a series of transformations leading to formation of a substituted quinoline. The proposed reaction pathway is presented as a variation of the Skraup-Doebner-Von Miller quinoline synthesis. The presence of quinolines as crosslinking points in the cured materials has been proved by means of different characterization techniques and the properties derived from this aromatization process have been described. This new crosslinking approach has been successfully applied to an aldehyde-containing triglyceride to obtain high performance thermosets.

**Keywords:** triglyceride, crosslinking, renewable resources, aza-Michael, aromatization.

## INTRODUCTION

The utilization of fossil fuels for the manufacture of plastics accounts for about 7% of the worldwide use of oil and gas, which will arguably be depleted within the next 100 years.<sup>1</sup> In these next decades of increasing oil prices, global warming, and other environmental concerns, a change from fossil feedstocks to renewable resources is important for sustainable development into the future.<sup>2</sup> Among the renewable raw materials, natural oils are the most widely used renewable resource for the chemical and polymer industries.<sup>3</sup> The main component of the triglyceride vegetable oils are saturated and unsaturated fatty acids. Although they have double bonds which can be used as reactive sites in coatings, for obtaining high performance polymeric materials the introduction of more reactive functional groups, such as hydroxyl, epoxy or carboxyl groups, is much more suitable.<sup>4,5</sup> Various chemical pathways for functionalizing

triglycerides and fatty acids have been studied.<sup>6</sup> Epoxidation is one of the most important functionalization reactions of the C-C double bonds, that can be achieved by environmentally friendly procedures such as catalyzed chemical oxidation with hydrogen peroxide<sup>7,8</sup> or by enzymatic oxidation.<sup>9</sup> The opening of the epoxide ring is a versatile reaction that leads to numerous products.<sup>4,10,11</sup> Thus, epoxidized vegetable oils are extremely promising as inexpensive renewable materials for industrial applications<sup>12</sup> because they share many of the characteristics of conventional epoxy thermosets. In this way, naturally occurring epoxy oil, as vernonia seed oil or epoxidized vegetable oils from soybean, linseed or castor oils have been cured cationically<sup>13</sup> or with conventional hardeners as diamines or dianhydrides.<sup>14-18</sup>

Recently, in a previous communication we reported the synthesis of a new highly reactive triglyceride derivative with  $\alpha,\beta$ -unsaturated carbonyl groups.<sup>19</sup> This enone-containing triglyceride obtained by an environmentally friendly chemical procedure from high oleic sunflower oil resulted an interesting alternative to epoxidized vegetable oils to produce thermosets by crosslinking with conventional aromatic diamines. The Michael addition reaction came out as a valuable tool in the synthesis of polymeric networks.<sup>20</sup> The aza-Michael reaction, a variation in which an amine acts as the nucleophile, had been used in the synthesis of improved bismaleimide networks,<sup>21</sup> but this reaction had not been applied to the synthesis of crosslinked polymers derived from vegetable oils. In the aza-Michael reaction with the enone-containing triglyceride derivative we observed the existence of secondary reactions during the crosslinking process at high temperatures, reactions that can take place not only in this case, but also in any other curing process in which an aza-Michael addition is involved. Thus, this work is focused on the study of the nature of these secondary reactions and their extent, as they can have a great influence in the properties of the obtained thermosets. The reactions were followed by NMR, UV and fluorescence spectroscopy, showing that at high temperatures aromatic moieties are formed in the network. This finding is relevant to enhance the material properties. Usually, materials from oils are incapable of displaying the necessary rigidity and strength required for structural applications, and so modification or copolymerization with aromatic components are required to overcome this drawback.<sup>22</sup> Finally, the evaluation of thermal properties of the final material could be related to the presence of the aromatic structures.



## EXPERIMENTAL

### Materials.

High oleic sunflower oil (minimum 80% oleic acid) was kindly supplied by Borges<sup>®</sup>, BF<sub>3</sub>·MEA (Aldrich), Decanal (Aldrich), HClO<sub>4</sub> (60%, Probus), NaIO<sub>4</sub> (Fluka), NaHCO<sub>3</sub> (Scharlab) and MgSO<sub>4</sub> (Scharlab) were used as received. *p*-Toluidine (Aldrich) was recrystallized from heptane. Hexane, ethyl acetate, tetrahydrofuran, dichloromethane and 1,4-dioxane were purchased to Scharlab and used directly. Silica for column chromatography was purchased to SDS (60 A. C. C. 40-63 μm) and Silica gel TLC aluminium sheets to Merck (60, F<sub>254</sub>). The mixture of methyl-9-oxo-10-octadecenoate and methyl-10-oxo-8-octadecenoate (**4**),<sup>23</sup> glyceryl tris(9-oxo-10-octadecenoate) and glyceryl tris(10-oxo-8-octadecenoate) mixture (**1**)<sup>19</sup> and epoxidized high oleic sunflower oil (**15**)<sup>19</sup> were synthesized as previously reported. TLC plates were developed with an UV lamp (254 nm) or by spraying with sulphuric acid/anisaldehyde ethanol solution and heating at 200 °C.

**Reaction between *p*-toluidine and methyl-9-oxo-10-octadecenoate/methyl-10-oxo-8-octadecenoate mixture.** The α,β-unsaturated ketone (300.0 mg, 0.96 mmol), *p*-toluidine (103.5 mg, 0.96 mmol) and BF<sub>3</sub>·MEA (3.3 mg, 0.03 mmol) were mixed in a 10 mL round bottomed flask under argon. The stirred reaction mixture was heated at 90 °C for 30 minutes, at 110 °C for 2h and finally at 140 °C for 2h more. 100 mg samples were taken at the end of each reaction step and analysed by <sup>1</sup>H-NMR spectroscopy.

**Quinoline (**11**) synthesis from decanal and *p*-toluidine.** Decanal (200 mg, 1.28 mmol), *p*-toluidine (137 mg, 1.28 mmol) and BF<sub>3</sub>·MEA (4.3 mg, 0.038 mmol) were mixed in a 10 mL round bottomed flask under argon. The stirred reaction mixture was heated at 50 °C for 4h and then the temperature was raised to 140 °C and maintained for 12h. The final mixture was analysed by <sup>1</sup>H-NMR spectroscopy. Quinoline **11** was isolated by column chromatography using hexane/ethyl acetate 150/1 with 38 % yield. FTIR (cm<sup>-1</sup>): 3060 (C-H, Ar), 3016 (C-H, Ar), 2921 (C-H), 2850 (C-H), 1602 (C=C), 1562 (C=C), 1493 (C=C), 1460 (CH<sub>2</sub> and CH<sub>3</sub>), 823 (C-H, Ar).

<sup>1</sup>H NMR (CDCl<sub>3</sub>, TMS, δ in ppm) (assignments of quinoline ring according to IUPAC nomenclature): 7.90 (d, *J* = 8.50 Hz, 1H, C<sub>8</sub>-H), 7.74 (s, 1H, C<sub>4</sub>-H), 7.46 (s, 1H, C<sub>5</sub>-H), 7.43 (dd, *J* = 8.58, 1.92 Hz, 1H, C<sub>7</sub>-H), 2.96-2.92 (m, 2H, Ar-CH<sub>2</sub>), 2.77-2.73 (m, 2H,

Ar-CH<sub>2</sub>), 2.49 (s, 3H, Ar-CH<sub>3</sub>), 1.81-1.74 (m, 2H, Ar-CH<sub>2</sub>-CH<sub>2</sub>), 1.71-1.63 (m, 2H, Ar-CH<sub>2</sub>-CH<sub>2</sub>), 1.50-1.22 (m, 24H), 0.93-0.84 (m, 6H, CH<sub>3</sub>).

<sup>13</sup>C NMR (CDCl<sub>3</sub>, TMS, δ in ppm) (assignments of quinoline ring according to IUPAC nomenclature): 161.50 (C<sub>Ar2</sub>), 145.25 (quaternary), 135.31 (quaternary), 134.41 (C<sub>Ar4</sub>), 134.22 (quaternary), 130.70 (C<sub>Ar7</sub>), 128.31 (C<sub>Ar8</sub>), 127.41 (quaternary), 125.93 (C<sub>Ar5</sub>), 36.12 (Ar-CH<sub>2</sub>), 32.60 (Ar-CH<sub>2</sub>), 32.10 (CH<sub>2</sub>-CH<sub>2</sub>-CH<sub>3</sub>), 32.07 (CH<sub>2</sub>-CH<sub>2</sub>-CH<sub>3</sub>), 30.77 (CH<sub>2</sub>), 30.17 (CH<sub>2</sub>), 30.07 (CH<sub>2</sub>), 29.80 (CH<sub>2</sub>), 29.78 (CH<sub>2</sub>), 29.68 (CH<sub>2</sub>), 29.54 (CH<sub>2</sub>), 29.47 (CH<sub>2</sub>), 22.88 (CH<sub>2</sub>-CH<sub>3</sub>), 21.69 (Ar-CH<sub>3</sub>), 14.32 (CH<sub>3</sub>).

**Synthesis of *vic*-diol-containing triglyceride (16).** Epoxidized high oleic sunflower oil (5g, 5.3 mmol) was dissolved in 400 mL of THF in a 1L round bottomed flask which was placed in a water bath at 20 °C. A mixture of water (80 mL) and 60 % HClO<sub>4</sub> (2.4 mL) was added dropwise under vigorous stirring. The reaction was kept for 12 h and then reaction mixture was extracted with dichloromethane and washed with water. The organic layer was dried over MgSO<sub>4</sub> and the solvent was removed at reduced pressure. **16** was obtained with 96 % yield after crystallization from hexane. The product has an average of 2.5 diol groups per triglyceride (by <sup>1</sup>H NMR spectroscopy).

FTIR (cm<sup>-1</sup>): 3540 (O-H), 1742 (C=O), 1142 (C-O).

<sup>1</sup>H NMR (CDCl<sub>3</sub>, TMS, δ in ppm): 5.28-5.20 (m, CH-OCO), 4.28 (dd, *J* = 12.0, 4.0 Hz, CH<sub>2</sub>-OCO), 4.12 (dd, *J* = 12.0, 6.0 Hz, CH<sub>2</sub>-OCO), 3.38-3.32 (m, CH-OH), 2.45-2.80 (broad, OH), 2.29 (t, *J* = 7.4 Hz, CH<sub>2</sub>-CO), 1.65-1.52 (m, CH<sub>2</sub>-CH<sub>2</sub>-CO), 1.52-1.20 (m, CH<sub>2</sub>-CHOH and CH<sub>2</sub>), 0.85 (t, *J* = 6.8 Hz, CH<sub>3</sub>).

<sup>13</sup>C NMR (CDCl<sub>3</sub>, TMS, δ in ppm): 173.55 (COOR), 173.12 (COOR), 74.70 (CH-OH), 74.63 (CH-OH), 69.07 (CH-OCO), 62.31 (CH<sub>2</sub>-OCO), 34.40 (CH<sub>2</sub>-CO), 34.23 (CH<sub>2</sub>-CO), 33.80 (CH<sub>2</sub>-CHOH), 32.07 (CH<sub>2</sub>-CH<sub>2</sub>-CH<sub>3</sub>), 29.91-29.14 (CH<sub>2</sub>), 25.91 (CH<sub>2</sub>-CH<sub>2</sub>-CHOH), 25.01 (CH<sub>2</sub>-CH<sub>2</sub>-CO), 22.87 (CH<sub>2</sub>-CH<sub>3</sub>), 14.31 (CH<sub>3</sub>).

**Synthesis of aldehyde-containing triglyceride (17).** **16** (5.2 g, 5.3 mmol) and NaIO<sub>4</sub> (3.11 g, 14.5 mmol) were placed in a 100 mL round bottomed flask and 50 mL of a 9/1 mixture of 1,4-dioxane/water were added. The reaction mixture was stirred vigorously at room temperature for 1 h and then it was diluted with 20 mL of dichloromethane and washed twice with NaHCO<sub>3</sub> and water. The pale brown oily product was connected to a high vacuum pump equipped with a liquid nitrogen trap to remove nonanal. The product was obtained quantitatively with an average of 2.5 aldehyde groups per triglyceride (by <sup>1</sup>H NMR spectroscopy).

FTIR ( $\text{cm}^{-1}$ ): 2719 (C-H, aldehyde), 1735 (C=O, ester), 1721 (C=O, aldehyde), 1162 (C-O), 1096 (C-O).

$^1\text{H}$  NMR ( $\text{CDCl}_3$ , TMS,  $\delta$  in ppm): 9.71 (t,  $J = 1.77$  Hz, CHO), 5.24-5.18 (m, CH-OCO), 4.25 (dd,  $J = 11.90, 4.28$  Hz,  $\text{CH}_2\text{-OCO}$ ), 4.09 (dd,  $J = 11.91, 5.96$  Hz,  $\text{CH}_2\text{-OCO}$ ), 2.38 (t,  $J = 7.36$  Hz,  $\text{CH}_2\text{-CHO}$ ), 2.27 (dt,  $J = 7.61$  Hz,  $\text{CH}_2\text{-COOR}$ ), 1.64-1.50 (m,  $\text{CH}_2\text{-CH}_2\text{COOR}$  and  $\text{CH}_2\text{-CH}_2\text{CHO}$ ), 1.34-1.16 (m,  $\text{CH}_2$ ), 0.83 (t,  $J = 6.83$  Hz,  $\text{CH}_3$ ).

$^{13}\text{C}$  NMR ( $\text{CDCl}_3$ , TMS,  $\delta$  in ppm): 202.96 (CHO), 173.25 (COOR), 172.85 (COOR), 68.99 (CH-OCO), 62.19 ( $\text{CH}_2\text{-OCO}$ ), 43.92 ( $\text{CH}_2\text{-CHO}$ ), 34.18 ( $\text{CH}_2\text{-COOR}$ ), 34.02 ( $\text{CH}_2\text{-COOR}$ ), 32.01 ( $\text{CH}_2\text{-CH}_2\text{-CH}_3$ ), 29.79-28.89 ( $\text{CH}_2$ ), 24.80 ( $\text{CH}_2\text{-CH}_2\text{-COOR}$ ), 22.79 ( $\text{CH}_2\text{-CH}_3$ ), 22.05 ( $\text{CH}_2\text{-CH}_2\text{-CHO}$ ), 14.24 ( $\text{CH}_3$ ).

**Curing reactions and extraction of soluble parts.** For the **1**/DDM curing system (samples I and II), **1** and DDM were dissolved in dichloromethane and placed inside a petri dish. The mixture was heated at 50 °C for 30 min to remove the solvent and then sample I was heated 4h at 90 °C and sample II, 4h at 90 °C and 12h at 120 °C. For the **1**/DDM/ $\text{BF}_3\cdot\text{MEA}$  curing system (samples III-V), **1**, DDM and  $\text{BF}_3\cdot\text{MEA}$  (3% mol related to ketone groups) were dissolved in dichloromethane and the solution was put inside a petri dish and heated at 50 °C for 30 min to remove the solvent. For each sample, the corresponding curing program was then applied. Sample III (90 °C / 4h), sample IV (90 °C / 4h and 120 °C / 12h) and sample V (90 °C / 4h and 140 °C / 12h). For the **17**/DDM/ $\text{BF}_3\cdot\text{MEA}$  curing system (samples VI-VIII), **17** and DDM (see Table 1 for proportions in each sample) were dissolved in THF separately.  $\text{BF}_3\cdot\text{MEA}$  (3% mol related to aldehyde groups) was added to the DDM solution and then both solutions were mixed. The mixture was quickly placed into a petri dish and maintained at 40 °C for 2h to eliminate all the solvent. The same curing program was applied for the three samples: 4h at 90 °C and 12h at 140 °C. All samples were subjected to soxhlet extraction with previously distilled dichloromethane to determine their soluble fractions. 0.5g of each sample (previously grinded) were extracted with 125 mL of dichlorometane.

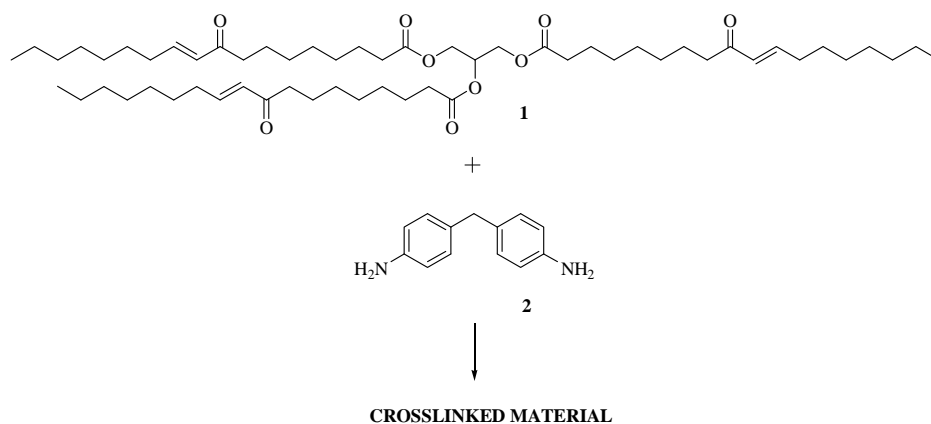
**Characterization.**  $^1\text{H}$  NMR 400 MHz and  $^{13}\text{C}$  NMR 100.6 MHz NMR spectra were obtained using a Varian Gemini 400 spectrometer with Fourier transform.  $\text{CDCl}_3$  was used as solvent and TMS as internal reference. The IR analyses were performed on a FTIR-680PLUS spectrophotometer with a resolution of 2  $\text{cm}^{-1}$  in the transmittance mode. An attenuated-total-reflection accessory with thermal control and a diamond

crystal was used to determine FTIR/ATR spectra. Dynamic mechanical thermal analysis (DMTA) was performed using a TA DMA 2928 in the controlled force-Tension Film mode with a preload force of 0.1 N, an amplitude of 10  $\mu\text{m}$  and at a fixed frequency of 1 Hz, in the  $-100$  to  $200$   $^{\circ}\text{C}$  range and at a heating rate of  $3$   $^{\circ}\text{C}/\text{min}$ . Rectangular samples with dimensions  $10 \times 5 \times 0.2$   $\text{mm}^3$  were used. Thermal stability studies were carried out on a Mettler TGA/SDTA851e/LF/1100 with  $\text{N}_2$  as purge gas. The studies were performed in the  $30$ - $800$   $^{\circ}\text{C}$  temperature range at a scan rate of  $10^{\circ}\text{C}/\text{min}$ . The UV-vis data were acquired and monitored by a Hewlett-Packard 8452A spectrophotometer using the HP89531A software. The spectra were recorded from  $190$  to  $800$  nm in  $4$  nm steps. The spectrofluorimetric data were acquired on an Aminco–Bowman Series 2 Luminescence spectrometer (SLM Aminco, Rochester, NY, USA) equipped with a  $150\text{W}$  continuous xenon lamp and a PMT detector. For UV-vis and fluorescence measurements,  $20$   $\mu\text{m}$  thick films supported on a quartz plate were used. For the preparation of the films, the dichloromethane or THF solutions employed for the curing reactions were cast over the quartz plate.

## RESULTS AND DISCUSSION

As mentioned in the introduction we synthesized a new enone containing-triglyceride derivative (**1**) by an environmentally friendly chemical procedure from high oleic sunflower oil using the singlet oxygen “ene” reaction. A mixture of allylic hydroperoxides was obtained and further transformed in a regioisomeric mixture of enones in the presence of acetic anhydride and pyridine or tertiary amines.<sup>19</sup> We proved the high efficiency of the aza-Michael crosslinking reaction between **1** and diaminodiphenylmethane (**2**) (Scheme 1) in a  $^1\text{H-NMR}$  kinetic experiment using model compounds. However, while conversion of the  $\alpha,\beta$ -unsaturated ketone was uniform throughout the experiment until total consumption, it could be observed that formation of the aza-Michael adduct reached a point from which no further growing was observed. This fact, together with a slight decrease of the aza-Michael product concentration at long reaction times, made us think about the possibility of a secondary reaction taking place in which the aza-Michael product was involved. Moreover, the dynamomechanical analysis of the crosslinked material gave a very broad tan delta peak, indicating low structural homogeneity and therefore supporting the theory of the

existence of minor secondary reactions during the crosslinking process.<sup>19</sup> We could also observed that at higher temperatures the extent of these secondary reactions increases, leading to an unexpectedly harder material.

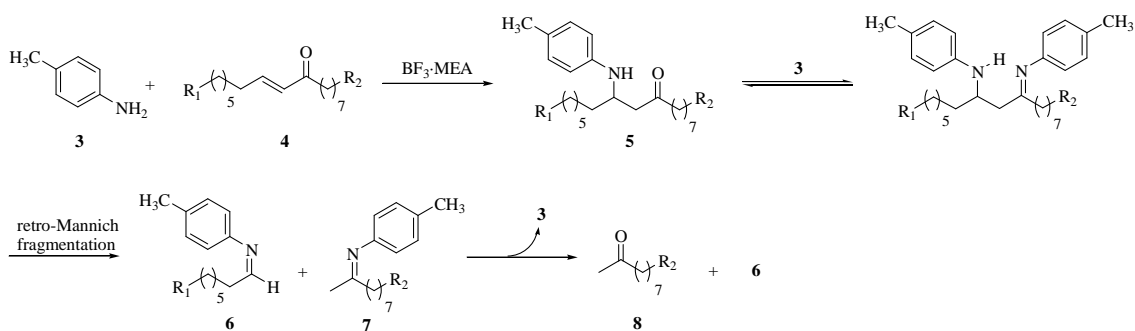


**Scheme 1.** aza-Michael crosslinking reaction between **1** and DDM (**2**).

Our first aim is to understand and establish the reactions taking place in the crosslinking reaction after the aza-Michael adduct is formed. As the reaction of **1** and **2** leads to an insoluble crosslinked material (Scheme 1), the accurate analysis of the chemical reactions involved in the process can not be performed. For this reason, *p*-toluidine (**3**) and a methyl oleate derived enone (**4**) were used as model compounds and a <sup>1</sup>H-NMR analysis was carried out.

As commented, high temperatures and long reaction times are important factors in the development of side reactions, for this reason, we tested the effect of adding a Lewis acid catalyst (BF<sub>3</sub>·MEA) to the reaction between **3** and **4** in an attempt to reduce the reaction time. The conversion of the reactants was accelerated and the <sup>1</sup>H-NMR signals corresponding to the secondary products were even increased. The chromatographic isolation of the side products revealed the presence, among other complex structures, of a methyl ketone. This finding can only be explained by a Lewis acid catalyzed retro-Mannich type fragmentation of the aza-Michael adduct,<sup>24</sup> that would lead to the formation of a methyl ketone (**8**) and an aldimine (**6**) (Scheme 2).

During the crosslinking reaction of **1** and **2**, the fragmentation of the aza-Michael adduct would mean the breakage of the forming network and a deterioration of the mechanical properties. However, while the non-catalyzed crosslinking reaction at 90 °C (sample I, Table 1) gave a material with a T<sub>g</sub> of -8 °C (maximum of the tan delta



**Scheme 2.** Lewis acid catalyzed retro-Mannich type fragmentation of the aza-Michael adduct and formation of a methyl ketone (**8**) and an aldimine (**6**).

peak) and a soluble fraction of 25.6 %, the material obtained at 120 °C (sample II, Table 1) gave a  $T_g$  of 16 °C, a soluble fraction of 20.3 % and a higher crosslinking density (by DMTA). From this data, it can be inferred that not only the retro-Mannich fragmentation is taking place, but also further reactions leading to crosslinked networks. As these chemical processes could be generalized to any other curing processes in which an aza-Michael addition is involved, it is important to determine their nature and the effect of the reaction conditions.

For this purpose, **3** and **4** were reacted again in presence of 3% (mol) of  $BF_3 \cdot MEA$ . In this model reaction no solvent was added to better reproduce the crosslinking reaction

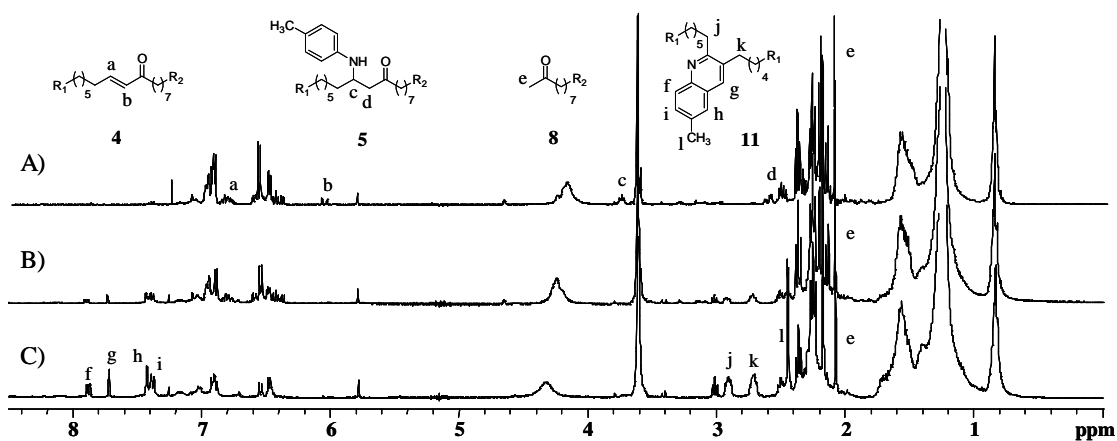
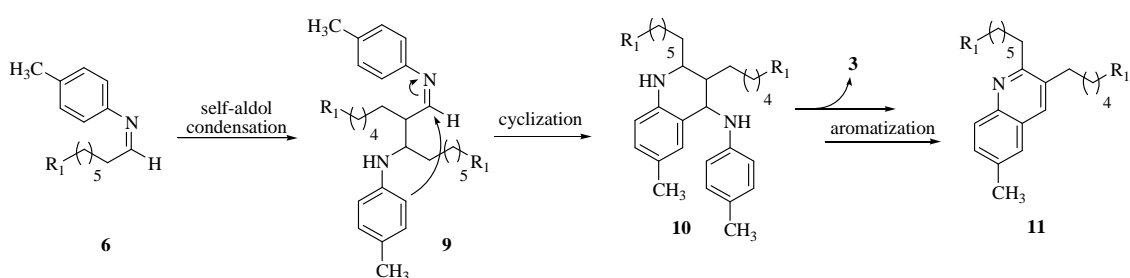


**Figure 1.**  $^1H$ -NMR spectra of reaction **3** + **4** in presence of 3% mol of  $BF_3 \cdot MEA$  after heating. A) At 90 °C for 30 minutes. B) After raising the temperature to 110 °C for 2h. C) When the reaction mixture was heated 2h at 140 °C.

conditions. To determine the effect of the temperature on the formed products, the mixture was first heated at 90 °C for 30 minutes, then at 110 °C for 2h and finally at 140 °C for 2h more. The progress of the reaction was followed by <sup>1</sup>H-NMR spectroscopy (Fig 1).

After heating the mixture at 90 °C for 30 minutes, the signals **c** and **d** of the aza-Michael product (**5**) can be observed together with a decreasing in the intensity of the conjugated ketone (**4**) double bond signals (**a** and **b**) (Fig 1A). However, a singlet (**e**) at 2.07 ppm appears which belongs to a methyl ketone, presumably formed in the expected retro-Mannich type fragmentation (Scheme 2). This fragmentation, which proceeds through a BF<sub>3</sub>·MEA catalyzed condensation of a molecule of *p*-toluidine and the aza-Michael adduct, produces two new species, an aldimine (**6**) and a ketimine (**7**). While the ketimine can be hydrolyzed under the reaction conditions to the observed methyl ketone (**8**) and *p*-toluidine, the aldimine **6** is more reactive and prone to undergo self-aldol condensation<sup>25</sup> (Scheme 3).



**Scheme 3.** Proposed self-aldol condensation of the aldimine **6** and further cyclization and aromatisation to give quinoline **11**.

When the temperature was raised to 110 °C and kept for 2h, the starting enone and the intermediate aza-Michael adduct signals disappeared almost completely (Fig. 1B). The singlet of the methyl ketone (**e**) remained unaltered ruling out the self-aldol condensation in the reaction conditions and new signals appeared in the aromatic region which could be attributed to further reactions involving the aldimine **6**.

Finally, the reaction mixture was heated 2h at 140 °C. The methyl ketone still remained unaltered, but in this case, the new aromatic signals were clearly observed (Fig. 1C). As mentioned above, the aldimine **6** can undergo a BF<sub>3</sub>·MEA self-aldol condensation to yield **9**, which, in the reaction conditions, can undergo a cyclization reaction to give the dihydroquinoline **10**. The subsequent elimination of a molecule of *p*-toluidine,<sup>25</sup>

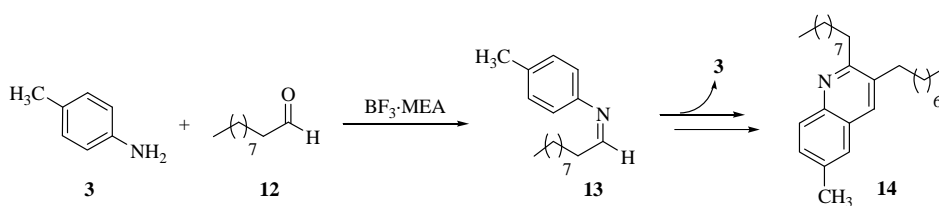
followed by aromatization through hydrogen transfer to Schiff bases present in the mixture, can give the quinoline **11** (Scheme 3).

Thus summarizing, the reaction pathway proposed involves several reactions: aza-Michael addition, retro-Mannich type fragmentation, self-condensation of the aldimine fragment and its cyclization followed by deamination and aromatization. The fact that the methyl ketone remains unaltered throughout all the reaction steps suggests that the retro-Mannich fragmentation is irreversible and that the methyl ketone is not involved in further steps of the reaction.

Studies on the Skraup-Doebner-Von Miller reaction by Denmark et al.<sup>26</sup> allowed them to establish a complex mechanism for the condensation of aniline derivatives with 3-disubstituted  $\alpha,\beta$ -unsaturated ketones to form quinolines. It consists of a conjugated addition followed by a fragmentation to the corresponding imine and ketone and a recombination of both fragments to form an anil that leads to the final quinoline product. The initial conjugated addition and subsequent fragmentation are in accordance to our results. However, the presence of the ketone **8** at the end of the reaction rules out condensation with the aldimine **6**. Instead of this, the aldimine **6** undergoes aldol-self condensation leading to the final quinoline product as described above. The difference may relay on the Michael acceptor used. In our study, the  $\alpha,\beta$ -unsaturated ketone is 3-monosubstituted and thus, fragmentation of the aza-Michael adduct yields an aldimine and a ketimine instead of two ketimines. The higher reactivity of the aldimine compared to the ketimine justifies the self-aldol condensation of the former instead of the cross condensation.

The synthesis of quinolines through reaction of “in situ” generated alkylimines was described by Tanaka et al.<sup>27</sup> Therefore, to further confirm the propensity of the intermediate aldimine to give self-aldol condensation and to produce the final quinoline, decanal (**12**) was taken as a model compound. **12** was reacted with *p*-toluidine in presence of  $\text{BF}_3 \cdot \text{MEA}$  (3% mol) at 50 °C to allow formation of the aldimine **13** and then at 140 °C to favour the cyclization and aromatization reactions (Scheme 4). The  $^1\text{H-NMR}$  spectrum of the final reaction mixture (Fig. 2A) revealed the formation of the expected quinoline **14** (Fig. 2B), which was obtained with 38 % yield after column chromatography.





**Scheme 4.** Reaction of decanal with *p*-toluidine in presence of  $\text{BF}_3 \cdot \text{MEA}$  (3% mol) to give aldimine **13** and further cyclization and aromatization to quinoline **14**.

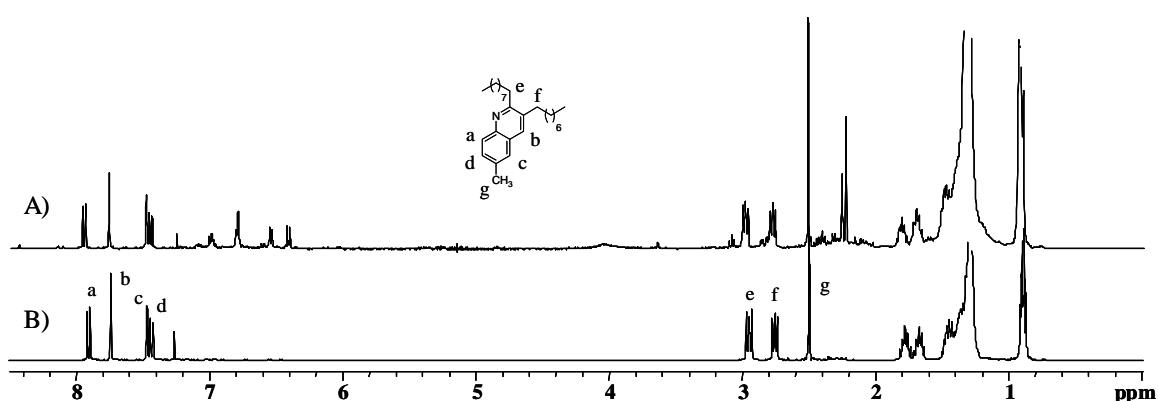


**Figure 2.**  $^1\text{H-NMR}$  spectra of: A) Final reaction mixture of **12** + **3** in presence of  $\text{BF}_3 \cdot \text{MEA}$ . B) pure quinoline **14**.

These results confirm the proposed mechanism and can help to explain the crosslinking-temperature dependent properties found in the materials obtained when triglyceride derivative **1** reacts with DDM. Moreover, since most plant-oil derived materials can be considered as elastomers due to their high content in long alkyl chains, the formation of quinolines as crosslinking points would lead to a marked improvement in their thermal and mechanical properties. Thus, the study of the properties derived from this aromatization process is of great interest.

We started by studying the effect of the crosslinking temperature on the properties of the materials obtained by reaction of **1** and DDM in presence of 3% mol of  $\text{BF}_3 \cdot \text{MEA}$ . For this purpose, equal amounts of the three-component mixture were put on three different petri dishes. The first dish (sample III) was heated at 90 °C for 4h, the second dish (sample IV) was heated 4h at 90 °C and 12h at 120 °C and the third dish (sample V) was heated 4h at 90 °C and 12h at 140 °C.

The expected chemical changes in this curing system include the Aza-Michael reaction of an aromatic amine with an enone system and the appearance of a new

aromatic structure. Thus, UV-vis and fluorescence spectroscopies can be useful techniques to monitor the crosslinking process. For this purpose, the measurements were performed with a 20  $\mu\text{m}$  thick films supported on a quartz plate. Figure 3A) shows the normalized UV-vis spectra as a function of cure temperature for **1/2**/ $\text{BF}_3$ -MEA system. Although the spectral regions of several species overlap, there is a clear change in the spectra of cure temperatures over 90  $^\circ\text{C}$  with the appearance of a new absorption peak at longer wavelengths (ca. 370 nm). As previously mentioned, the aromatization process proceeds at high temperatures. Since the quinoline structure has a higher conjugation degree than the initial species and possess a donor heteroatom, the observed red shift confirms their presence, which is maximized at 140  $^\circ\text{C}$ .

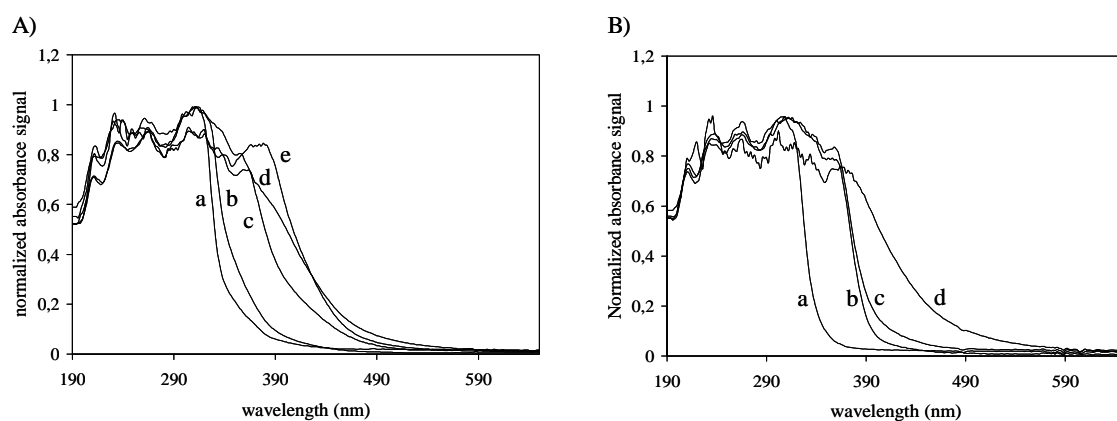


**Figure 3.** Normalized UV-vis spectra as a function of cure temperature of : A) **1/2**/ $\text{BF}_3$ -MEA system (a: initial mixture; b: 90 $^\circ\text{C}$ ; c: 110 $^\circ\text{C}$ ; d: 120 $^\circ\text{C}$  ; e: 140 $^\circ\text{C}$ ) and B) **17/2**/ $\text{BF}_3$ -MEA system (a: initial mixture; b: 90 $^\circ\text{C}$ ; c: 110 $^\circ\text{C}$ ; d: 140 $^\circ\text{C}$ ).

The crosslinking reaction could also be monitored following the changes in the fluorescence spectra. Figures 4A) and 4B) depict the fluorescence emission spectra of the **1/2**/ $\text{BF}_3$ -MEA system as a function of the cure temperature with excitation wavelengths at 255 and 325 nm. The excitation wavelengths were chosen as the ones giving the maxima of emission in a 2D excitation-emission spectrum of the initial mixture. By using a constant excitation wavelength throughout the curing process, the changes in the emission spectra can be related to the species involved in the process. In figure 4A), as the temperature is raised to 90  $^\circ\text{C}$ , part of the fluorescence of the initial mixture occurring at short wavelengths disappears as a result of the reaction between **1** and **2** and the subsequent fragmentation. When the sample is heated at 120  $^\circ\text{C}$  and

finally at 140 °C, the fluorescence intensity at longer wavelengths is increased due to the developing aromatization process. In figure 4B), a clear shift of the fluorescence spectra towards longer wavelengths is observed as the cure temperature is increased. These findings are in accordance with the development of an aromatic system with a higher conjugation degree.

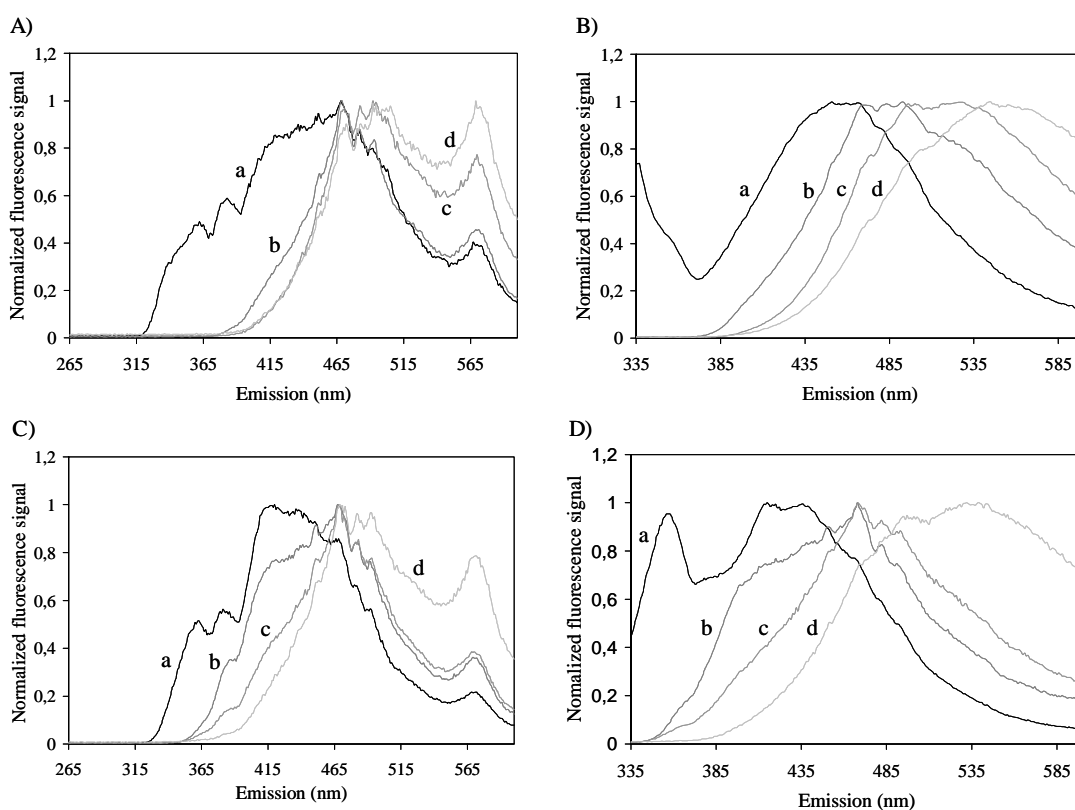


**Figure 4.** Normalized fluorescence emission spectra as a function of the cure temperature of **1/2/BF<sub>3</sub>·MEA** system with excitation wavelengths at A) 255 nm and B) 325 nm (a: initial mixture; b: 90°C; c: 120°C; d: 140°C ) and **17/2/BF<sub>3</sub>·MEA** system with excitation wavelengths at C) 255 nm and D) 325 nm (a: initial mixture; b: 60°C; c: 90°C; d: 140°C).

As already explained, an increase of the crosslinking temperature should promote the formation of quinolines through the proposed mechanism. In this way, while sample III was expected to only suffer retro-Mannich type fragmentation, the crosslinking temperature used for sample V should allow quinoline formation. An increase in the aromatic content of the polymeric network would increase the rigidity and thus the glass transition temperature ( $T_g$ ) should increase from sample III to sample

V. The dynamomechanical analysis of samples III, IV and V is shown in figure 5 and data is collected in table 1.

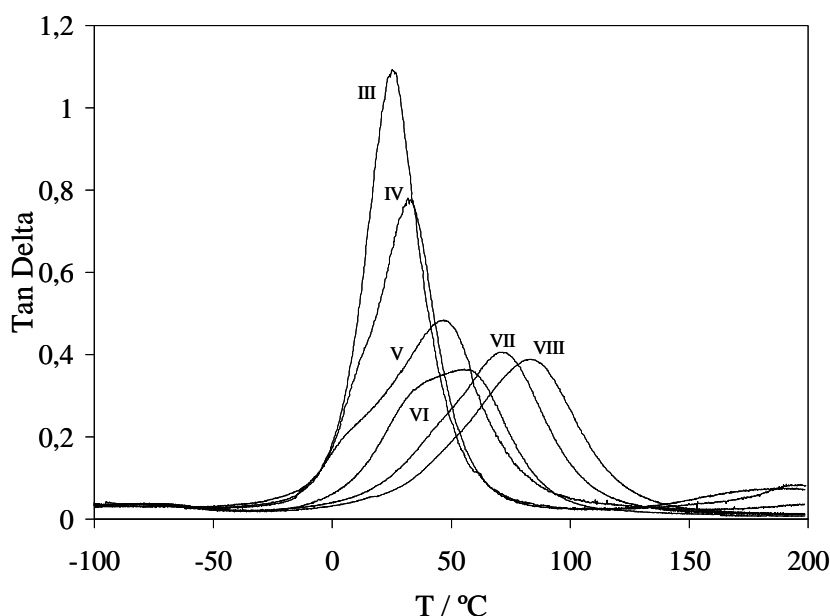


**Figure 5.** Tan  $\delta$  plots as a function of temperature for the cured samples III-VIII.

**Table 1.** Soluble fractions, Tgs and TGA data of the Cured Samples I-VIII.

Sample	Curing system (molar ratio)	catalyst	Soluble part (%) <sup>a</sup>	T <sub>g</sub> (°C) <sup>b</sup>	TGA (N <sub>2</sub> )		
					T <sub>5% loss</sub> (°C)	T <sub>max</sub> (°C) <sup>c</sup>	Char <sub>800°C</sub> (%)
I	<b>1</b> / DDM (1 / 1.25)	-	25.6	-8	283	466	9.4
II	<b>1</b> / DDM (1 / 1.25)	-	20.3	16	320	466	11.7
III	<b>1</b> / DDM (1 / 1.25)	BF <sub>3</sub> ·MEA	20.5	27	275	466	9.7
IV	<b>1</b> / DDM (1 / 1.25)	BF <sub>3</sub> ·MEA	18.2	34	304	472	11.1
V	<b>1</b> / DDM (1 / 1.25)	BF <sub>3</sub> ·MEA	13.0	48	324	468	13.9
VI	<b>17</b> / DDM (1 / 0.75)	BF <sub>3</sub> ·MEA	7.0	57	339	414 / 467	16.1
VII	<b>17</b> / DDM (1 / 1)	BF <sub>3</sub> ·MEA	6.4	73	331	413 / 468	16.3
VIII	<b>17</b> / DDM (1 / 1.25)	BF <sub>3</sub> ·MEA	9.9	84	321	413 / 468	16.1

<sup>a</sup> 12h soxhlet extraction of 0.5g with 125 mL of DCM . <sup>b</sup> Maximum of the Tan delta peak. <sup>c</sup> Temperature of the maximum weight loss rate.

As expected, the  $T_g$  (maximum of the tan delta peak) increases from sample III (27 °C) to sample V (48 °C). Interestingly, the height of the tan delta peak decreases from sample III to sample V indicating an increase in the crosslinking density despite the initial retro-Mannich fragmentation. However, the tan delta peak width at half-height increases, what is associated with a increasing number of branching modes and a wider distribution of structures, showing a lower structural homogeneity, that should be caused by the mentioned fragmentation. It was explained above that aromatization of the dihydroquinoline **10** can be accomplished through hydrogenation of Schiff bases present in the reaction media. The amines formed this way are still crosslinking points and thus, no cleavage of the network is produced. Moreover, Tanaka et al.<sup>27</sup> demonstrated that aromatization of the intermediate hydroquinoline is promoted in air atmosphere. For this reason, despite the initial fragmentation, the crosslinking density increases together with the structural diversity.

Soxhlet extraction with dichloromethane (Table 1) gave the higher soluble fraction for sample III (20.5 %) and the lower for sample V (13.0 %). The fact that the soluble part is lower for the higher crosslinking temperature also supports the proposed crosslinking mechanism taking place after the initial fragmentation. However, the samples undergo some weight loss during the crosslinking reaction due to evaporation of the free aliphatic methyl ketones released in the retro-Mannich fragmentation. Samples III, IV and V lost 11, 15 and 15 % of its total weight respectively, but anyway, these slight differences do not justify the differences in soluble parts.

Another evidence of the increase in the aromatic content can be found in the thermogravimetric analysis (TGA) under  $N_2$  of samples III-V (Fig 6). As aromatic moieties are known to promote char formation during the combustion process, the analysis of the char yield at 800 °C (Table 1) can provide valuable information. Sample III has a 9.7 % char yield due to the presence of DDM as one of the main components. The char yield increases to 11.1 % for sample IV as the quinolines start forming and finally, for sample V, the char yield obtained is 13.9 %. This increase in the char yield can be attributed to the aromatization process. In these TGA plots can also be observed that the temperature of 5% loss increases from sample III to sample V according to the higher content in aromatic structures and high crosslinking density of the sample V.

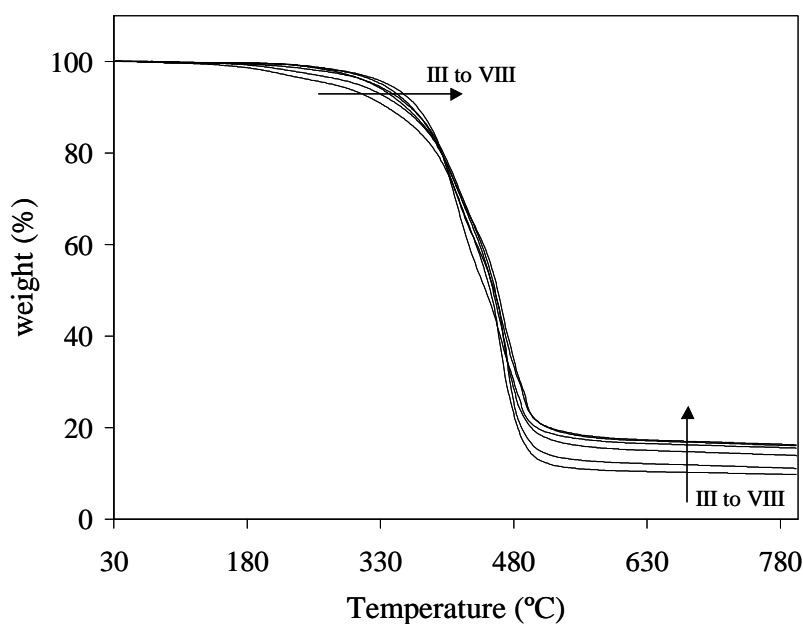
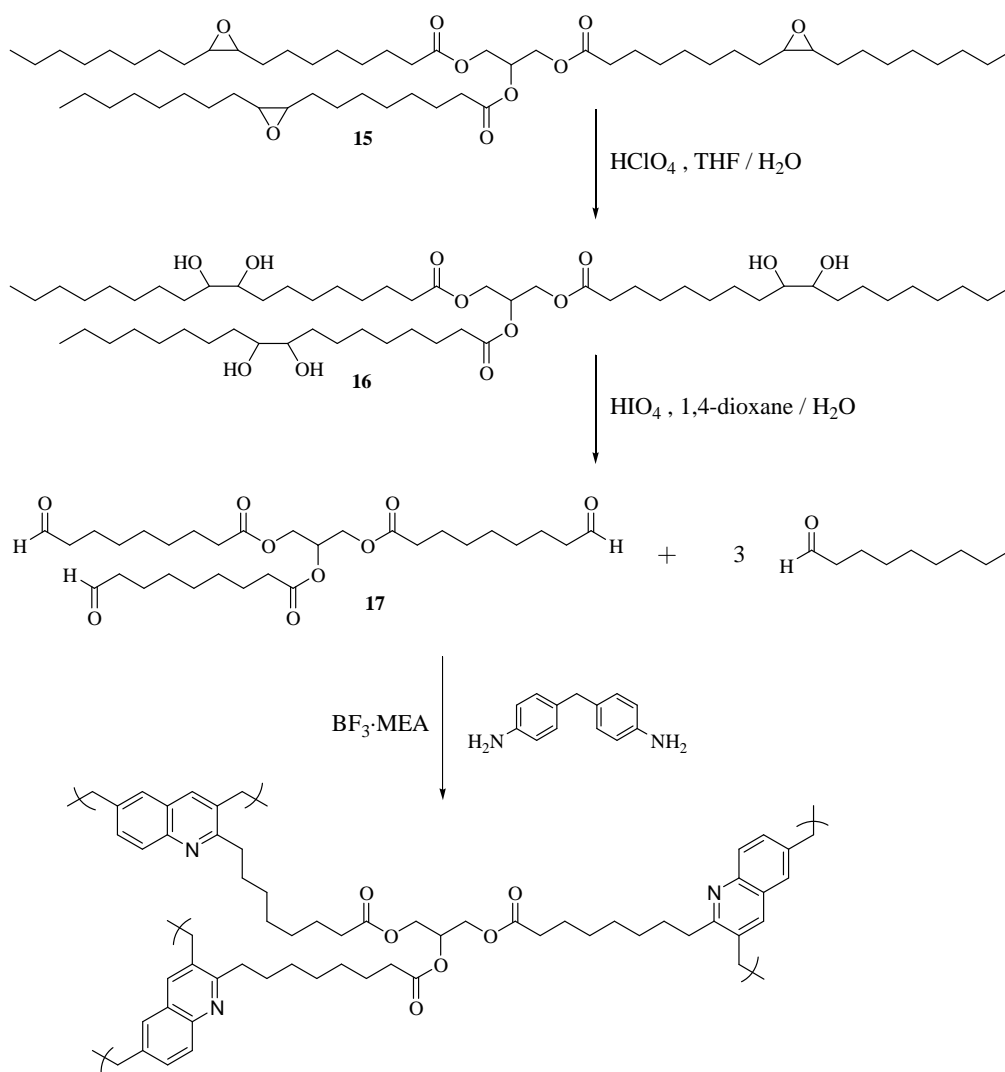


**Figure 6.** TGA plots under nitrogen for the cured samples III-VIII.

Based on the information obtained with the model reactions and the study and interpretation of the properties of these materials, it seems shown that quinoline structures are formed as crosslinking points and that the temperature plays a key role on the aromatization process. However, the retro-Mannich fragmentation of the former intermediate aza-Michael adduct causes the presence of long aliphatic methyl ketones that can move freely acting as plastizicers. As starting triglyceride derivative **1** is a statistical mixture of positional isomers, the retro-Mannich fragmentation also leads to aliphatic methyl ketones which are not linked to the polymeric network. To overcome this problem and improve the thermal and mechanical properties of the final materials, a new strategy was used. Taking into account the high reactivity of aldimine **13** towards quinoline formation, we decided to prepare a triglyceride derivative containing aldehyde groups. The reaction of this new derivative with DDM in presence of  $\text{BF}_3 \cdot \text{MEA}$  should give an intermediate aldimine which, at high temperature, would lead to quinoline formation (see scheme 4). In this way, we should be able to obtain a crosslinked polymer with higher content of quinolines as crosslinking points.

For the preparation of the aldehyde-containing triglyceride, epoxidized high oleic sunflower oil **15** was used as starting material (Scheme 5).



**Scheme 5.** Synthesis of the aldehyde-containing triglyceride (**17**) and  $\text{BF}_3 \cdot \text{MEA}$  catalysed crosslinking with DDM.

The epoxide groups were hydrolyzed in presence of perchloric acid to give the triglyceride **16** with 2.5 diol groups (determined by  $^1\text{H-NMR}$  spectroscopy). The oxidative cleavage of the 1,2-diols was performed with sodium periodate to obtain a mixture of aldehyde-containing triglyceride **17** and nonanal. The later was removed by applying high vacuum to the stirred mixture at  $80\text{ }^\circ\text{C}$  and **17** was obtained as a slightly yellow oil with 2.5 aldehyde groups per triglyceride (determined by  $^1\text{H-NMR}$  spectroscopy).

In the model reaction of *p*-toluidine and decanal (see scheme 4), the formation of the quinoline structure requires two molecules of aldehyde for one of amine. However, a second amine molecule is needed as catalyst. Normally, a little excess of amine over

the 2/1 ratio could be enough, but in the case of crosslinking reactions, where reactants diffusion is limited, a higher amount of amine may be needed. For this reason, three different **17/2** ratios were used for the crosslinking reactions to determine the optimum proportion depending on the properties of the final materials. Since the reaction between **2** and **17** proceeds very fast, to properly homogenize the curing mixture, both components were dissolved in THF separately.  $\text{BF}_3\cdot\text{MEA}$  was added to the DDM solution and then both solutions were mixed. The mixture was placed in a petri dish and maintained at 40 °C for 2h to eliminate all the solvent. The temperature was raised to 90 °C for 4h and finally the sample was heated at 140 °C for 12h to promote the cyclization and aromatization reactions. In this way, three samples were prepared with **17/2** ratios of 1/0.75 (sample VI), 1/1 (sample VII) and 1/1.25 (sample VIII) with 3% mol of  $\text{BF}_3\cdot\text{MEA}$  (related to aldehyde groups).

The crosslinking of **17/2**/ $\text{BF}_3\cdot\text{MEA}$  system was monitored by UV-vis and fluorescence spectroscopy. The measurements were performed with a 20  $\mu\text{m}$  thick film supported on a quartz plate and to minimize DDM absorption interferences, the **17/2** ratio used was 1/0.75. Figure 3B) shows the UV-vis spectra as a function of cure temperature in which the development of the absorption bands is similar to that of the **1/2**/ $\text{BF}_3\cdot\text{MEA}$  system. The appearance of an absorption band around 370 nm at high temperatures can be related with the presence of quinolines. The fluorescence emission spectra as a function of the cure temperature with excitation wavelengths at 255 and 325 nm are depicted in figure 4C) and 4D) respectively. The spectra are similar to those of the **1/2**/ $\text{BF}_3\cdot\text{MEA}$  system and therefore the same conclusions can be extracted. The bathochromic shift observed in both spectra supports the formation of quinolines.

The analysis of the tan delta peaks of samples VI-VIII shows as the main difference with respect to sample V a shoulder around 10 °C due to the fragmentation products, that act as plastizicers in sample V. On the other hand, the tan delta peaks of samples VI-VIII are narrower, indicating a higher structural homogeneity. As the initial content of **2** is increased, the maxima of the tan delta peak shift to higher temperatures due to the higher aromatic content, reaching a  $T_g$  of 84 °C for sample VIII. However, the peak height is similar for the three samples, indicating that a similar crosslinking density is achieved even when the amount of amine groups is increased. The diffusion of amines in the curing mixture is a limiting factor, but adding an excess does not seem to solve the problem provided that more amine groups will remain unreacted though quinoline formation might be favoured. To further confirm this fact, the soluble



fractions of samples VI-VIII were analysed by  $^1\text{H-NMR}$ . While DDM was found to be one of the main components of the soluble fraction of sample V, it was not found in the soluble part of samples VI and VII. It is also worth to mention the low soluble fraction weight percentages found in samples VI-VIII when compared to those of samples III-V. Fig. 6 depicts the thermal stability of samples VI-VIII showing similar behavior to that of samples III-V. Char yields are found around 16 %, slightly over sample V (14 %) due to the higher aromatic content.

## CONCLUSIONS

The crosslinking reaction of **1** and DDM is a complex process which depends on the reaction conditions. First the aza-Michael adduct is formed. However, high temperatures and the presence of  $\text{BF}_3\cdot\text{MEA}$  promote a retro-Mannich type fragmentation followed by self-aldol condensation, cyclization and aromatization reactions. As a result, quinoline structures are formed as crosslinking points into the polymeric network. Based on these findings, a triglyceride functionalized with aldehyde groups has been reacted with DDM as an improved approach to quinoline-containing materials. The properties observed in the cured materials support the proposed crosslinking process. While common plant oils derived materials do not have the necessary rigidity and strength required for structural applications, the obtained materials present improved properties and could be considered as high performance thermosets.

The authors express their thanks to MICINN (Ministerio de Ciencia e Innovación) (MAT2008-01412) for financial support for this work.

## REFERENCES

- 
- <sup>1</sup> Williams, C.K.; Hillmyer, M.A. *Polym Rev* 2008, 48, 1-10.
  - <sup>2</sup> Bozell, J.J.; Patel, M. Eds., *Feedstocks for the Future: Renewable for the Production of Chemicals and Materials*; ACS Symposium Series 921; American Chemical Society: Washington, DC, 2006.

- 
- <sup>3</sup> Biermann, U.; Friedt, W.; Lang, S.; Lühs, W.; Machmüller, G.; Metzger, J. O.; Klaas, M. R.; Schäfer, H. J.; Schneider, M. P. *Angew Chem Int Ed* 2000, 39, 2206-2224.
- <sup>4</sup> Güner, F. S.; Yagci, Y.; Erciyas, A. T. *Prog Polym Sci* 2006, 31, 633-670.
- <sup>5</sup> Meier, M. A. R.; Metzger, J. O.; Schubert, U. S. *Chem Soc Rev* 2007, 36, 1788-1802.
- <sup>6</sup> Khot, S. N.; LaScala, J. J.; Can, E. S.; Morye, S. G.; Williams, I.; Palmese, G. R. S.; Küsefoglu, H.; Wool, R. P. *J Appl Polym Sci* 2001, 82, 703-723.
- <sup>7</sup> Lane, B. S.; Burgess, K. *Chem Rev* 2003, 103, 2457-2474.
- <sup>8</sup> Grigoropoulou, G.; Clark, J. H.; Elings, J. A. *Green Chem.* 2003, 5, 1-7.
- <sup>9</sup> Uyama, H.; Kuwabara, M.; Tsujimoto, T.; Kobayashi, S. *Biomacromolecules*, 2003, 4, 211-215.
- <sup>10</sup> Esen, H.; Küsefoglu, S.H.; *J Appl Polym Sci* 2003, 89, 3882-3888.
- <sup>11</sup> Guo, A.; Javni, I.; Petrovic, Z.S. *J Appl Polym Sci* 2000, 77, 467-473.
- <sup>12</sup> Kaplan, D.L. *Biopolymers from Renewable Resources*, Springer: Berlin 1998, p. 267.
- <sup>13</sup> Park, S-J.; Jin, F-L.; Lee, J-R. *Macromol Rapid Commun* 2004, 25, 724-727.
- <sup>14</sup> Earls, J.D.; White, J.E.; López, L.C.; Lysenko, Z.; Dettloff, M.L.; Null, M.J. *Polymer*, 2007, 48, 712-719.
- <sup>15</sup> Miyagawa, H.; Misra, M.; Drzal, L. T.; Mohanty, A. K. *Polym Eng Sci* 2005, 487-495.
- <sup>16</sup> Miyagawa, H.; Mohanty, A.K.; Misra, M.; Drzal, L.T. *Macromol Mater Eng* 2004, 289, 636-641.
- <sup>17</sup> Ahmad, S.; Naqvi, F.; Sharmin, E.; Verma, K. L. *Prog Org Coat* 2006, 55, 268-275.
- <sup>18</sup> Lligadas G; Ronda, J. C.; Galià, M.; Cádiz, V. J. *Polym Sci: Part A: Polym Chem.* 2006, 44, 6717-6727.
- <sup>19</sup> Montero de Espinosa, L.; Ronda, J. C.; Galià, M.; Cádiz, V. J. *Polym Sci: Part A: Polym Chem.* 2008, 46, 6843-6850.
- <sup>20</sup> Mather, B.D.; Viswanathan, K.; Miller, K. M.; Long, T.E. *Prog Polym Sci* 2006, 31, 487-531.
- <sup>21</sup> Wu, C.S.; Liu, Y.L.; Chiu, Y.S. *Polymer* 2002, 43, 1773-1779.
- <sup>22</sup> Lu, Y.; Larock, R.C. *ChemSusChem* 2009, 2, 136-147.

<sup>23</sup> Mihelich, E.D.; Eickhoff, D.J. *J Org Chem* 1983, 48, 4135-4137.

<sup>24</sup> Lim, S-G.; Jun C-H. *Bull. Korean Chem Soc* 2004, 25, 1623.

<sup>25</sup> Lauer, R.W. *Chem Rev* 1963, 63, 489-510.

<sup>26</sup> Denmark, S.E.; Venkatraman, S. *J Org Chem* 2006, 71, 1668-1676.

<sup>27</sup> Tanaka, S-Y.; Yasuda, M.; Baba, A. *J Org Chem* 2006, 71, 800-803.



## **Chapter 2**

### **1. A New Route to Acrylated Oils. Cross-linking and Properties of Acrylated Triglycerides from High Oleic Sunflower Oil**



# A New Route To Acrylated Oils. Crosslinking And Properties Of Acrylated Triglycerides From High Oleic Sunflower Oil

Lucas Montero de Espinosa, Juan C. Ronda, Marina Galilà, Virginia Cádiz

Department of Analytical and Organic Chemistry, Rovira i Virgili University, Campus Sescelades, Marcel·lí Domingo s/n, 43007 Tarragona, Spain.

**ABSTRACT.** Triglycerides with acrylate functionality were prepared from a new route that involves the singlet oxygen photooxygenation of high oleic sunflower oil and further reduction of the resulting hydroperoxide derivatives to a mixture of secondary allylic alcohols. These unsaturated alcohols can be further reduced to saturated alcohols. These two new hydroxyl-containing triglycerides were acrylated and radically crosslinked in presence of different amounts of pentaerythritol tetraacrylate. The crosslinking reactions were followed by FTIR spectroscopy and the thermal properties of the final materials were evaluated.

**Keywords:** triglyceride, acrylate, crosslinking, renewable resources.

## INTRODUCTION

The replacement of petroleum-based raw materials by renewable resources constitutes a major contemporary challenge in terms of both economical and environmental aspects.<sup>1</sup> Because of the wide variety of possibilities for chemical transformations, universal availability, and low price, oils, and fats of vegetable and animal origin are preferred by the chemical industry as alternative. Natural vegetable oils are considered to be one of the most important class of renewable sources.<sup>2</sup> The main component of the triglyceride vegetable oils are saturated and unsaturated fatty acids. Although they have double bonds which can be used as reactive sites in coatings, for obtaining high performance polymeric materials the introduction of more reactive functional groups, such as hydroxyl, epoxy or carboxyl groups, is much more suitable. Various chemical pathways for functionalizing triglycerides and fatty acids have been studied<sup>3-5</sup> including acrylation, maleinization, epoxidation (either chemical<sup>6-8</sup> or enzymatic<sup>9,10</sup>), hydroxymethylation<sup>11</sup>, esterification, and halogenation. Acrylated triglycerides are usually low viscosity monomeric liquids that can be free radically polymerized and can be copolymerized easily with other commercial comonomers due to the high reactivity

of the acrylate group.<sup>12</sup> The special properties<sup>13</sup> of these chemically modified triglycerides offer a widespread field of applications and so they are excellent candidates for use as thermosetting liquid molding resins in techniques such as vacuum assisted resin transfer molding,<sup>5</sup> composite fabrication processes<sup>14</sup> or pressure-sensitive adhesives.<sup>15</sup>

The traditional method used to obtain acrylated oils is to convert the triglyceride double bonds first to an epoxide and then open the epoxy groups with acrylic acid to yield hydroxy acrylated oils.<sup>16-18</sup> Alternatively acrylated groups can be introduced directly to the unsaturated fatty oil groups through a bromonium cyclic intermediate.<sup>19</sup> In this case a vic-bromoacrylate ester is obtained which not only is able to polymerize through the reactive acrylate, but also the presence of bromine imparts considerable flame resistance to the product polymer.

The direct acrylation by esterification of hydroxyl groups in the fatty oil is a scarcely described pathway as there are not many hydroxy-containing natural oils. The remarkable exceptions are castor oil and lesquerella oil which has been used to prepare the corresponding acrylate derivatives.<sup>20,21</sup>

In this work we report the synthesis of a new general and environmentally friendly route to introduce acrylate groups in unsaturated vegetable oils. The key step of this approach is the singlet oxygen “ene” reaction which has been used to oxidize the allylic position of fatty acids and their derivatives<sup>22-24</sup> such the methyl oleate. The mild conditions utilized and the use of oxygen, as the only reagent, makes this process particularly favorable from both an economical and ecological viewpoint. The allylic hydroperoxides can undergo a number of different transformations.<sup>25</sup> One of these reactions is the conversion of these hydroperoxides into a regioisomeric mixture of enones,<sup>26,27</sup>. The application of this reaction to unsaturated triglycerides, allowed us to obtain thermosetting materials by Aza-Michael crosslinking reaction with amines.<sup>28</sup>

Another interesting transformation of allylic hydroperoxides is their reduction to the corresponding hydroxylic compounds. Thus, this work involves a three-step synthetic pathway that firstly uses the singlet oxygen photooxygenation of high oleic sunflower oil to lead to a mixture of allylic hydroperoxides, which secondly can be reduced to a mixture of secondary allylic alcohols. The new hydroxyl-containing triglyceride was acrylated and radically crosslinked in presence of different amounts of pentaerythritol tetraacrylate. Alternatively, the unsaturated alcohols can be further reduced to saturated alcohols which can be also acrylated and crosslinked. The



crosslinking reactions were followed by FTIR spectroscopy and the thermal properties of the final materials were evaluated.

## EXPERIMENTAL PART

### Materials

High oleic sunflower oil (minimum 80% oleic acid) (SO) was kindly supplied by Borges<sup>®</sup>. *Meso*-tetraphenylporphyrin (TPP) (Aldrich), sodium borohydride (Scharlab), NH<sub>4</sub>Cl (Scharlab), Pt/C (5% Pt) (Aldrich), dicumyl peroxide (DCP) (Aldrich), methanol (Scharlab) and ethyl acetate (Scharlab) were used as received. Triethylamine (Aldrich) was dried by distillation over CaH<sub>2</sub> and acryloyl chloride (Aldrich) was distilled before use. Dichloromethane was dried over P<sub>2</sub>O<sub>5</sub> and distilled immediately before use. Pentaerythritol tetraacrylate (PETA) (Aldrich) was dissolved in ethyl ether and washed with an aqueous solution of NaOH (5%) before use to remove the stabiliser. TLC plates were developed by spraying with sulphuric acid/anisaldehyde ethanol solution and heating at 200 °C.

**Synthesis of hydroxyl sunflower oil (HSO) (Scheme 1a).** In a 450mL standard immersion-well photochemical reactor with a 400W high pressure sodium vapour lamp, high oleic sunflower oil (SO) (70 g, 79.1 mmol), TPP (0.02 g) and dichloromethane (400mL) were introduced. Cold water was circulated through the lamp jacket, while a gentle stream of oxygen was bubbled through the stirred reaction mixture. After a few minutes, the lamp was turned on and the reaction was monitored by TLC (hexane/ ethyl acetate, 5:1). After 4 h of irradiation the total disappearance of isolated double bonds and formation of the intermediate allylic hydroperoxides was observed. The lamp was turned off and the solvent was removed under reduced pressure. The reaction mixture was diluted with 200 mL of methanol and transferred to a 500 mL round bottomed flask which was cooled to 0 °C. NaBH<sub>4</sub> (3.8 g, 0.1 mol) was then added slowly with moderate stirring controlling that the temperature of the reaction mixture did not exceed 0 °C. The reduction was followed by TLC (hexane/ ethyl acetate, 2:1) until completion and then the reaction was quenched carefully with 10% NH<sub>4</sub>Cl solution. The pH was adjusted to around 6 and the product was extracted with dichloromethane and washed twice with brine. The organic phase was dried over MgSO<sub>4</sub> and the solvent was eliminated under reduced pressure obtaining a oil with 98% yield and a number of hydroxyl groups per triglyceride of 2.6 (calculated by <sup>1</sup>H-NMR spectroscopy).

FTIR: 3390  $\text{cm}^{-1}$  (OH, stretching), 1739  $\text{cm}^{-1}$  (ester C=O, stretching), 1675  $\text{cm}^{-1}$  (double bond, stretching) and 967  $\text{cm}^{-1}$  (double bond, bending).

$^1\text{H}$  NMR ( $\text{CDCl}_3$ , TMS,  $\delta$  in ppm): 5.62-5.53 (3H, m,  $\text{CH}=\text{CH}-\text{CHOH}$ ), 5.40 (3H, ddd,  $J = 15.28, 6.94, 1.02$  Hz,  $\text{CH}=\text{CH}-\text{CHOH}$ ), 5.26-5.20 (1H, m, CH-O), 4.26 (2H, dd,  $J_1 = 11.87$  Hz,  $J_2 = 4.21$  Hz,  $\text{CH}_2-\text{O}$ ), 4.11 (2H, dd,  $J_1 = 11.94$  Hz,  $J_2 = 5.94$  Hz,  $\text{CH}_2-\text{O}$ ), 3.98 (3H, q,  $J = 6.65$  Hz, CH-OH), 2.28 (6H, t,  $J = 7.26$  Hz,  $\text{CO}-\text{CH}_2-$ ), 1.98 (6H, m,  $J = 6.88$  Hz,  $\text{CH}_2-\text{CH}=\text{CH}$ ), 1.94-1.78 (broad m, -OH), 1.63-1.52 (6H, m,  $\text{CH}_2-\text{CH}_2\text{CO}$ ), 1.52-1.39 (6H, m,  $\text{CH}_2-\text{CHOH}$ ), 1.39-1.15 (54 H, m, aliphatic), 0.84 (9H, t,  $J = 6.58$  Hz,  $\text{CH}_3$ ).

$^{13}\text{C}$  NMR ( $\text{CDCl}_3$ , TMS,  $\delta$  in ppm): 173.34-172.88 (COOR), 133.38-133.12 ( $\text{CH}=\text{CH}-\text{CHOH}$ ), 132.06-131.66 ( $\text{CH}=\text{CH}-\text{CHOH}$ ), 73.11 (CH-OH), 68.90 (CH-O), 62.15 ( $\text{CH}_2-\text{O}$ ), 37.40-37.34 ( $\text{CH}_2-\text{CHOH}$ ), 34.22-34.03 ( $\text{CH}_2-\text{COOR}$ ), 32.27-32.16 ( $\text{CH}_2-\text{CH}=\text{CH}$ ), 31.95-31.91 ( $\text{CH}_2-\text{CH}_2-\text{CH}_3$ ), 29.65-28.80 (aliphatic), 25.59-25.51 ( $\text{CH}_2-\text{CH}_2\text{CHOH}$ ), 24.91-24.81 ( $\text{CH}_2-\text{CH}_2\text{COOR}$ ), 22.74-22.73 ( $\text{CH}_2-\text{CH}_3$ ), 14.20 ( $\text{CH}_3$ ).

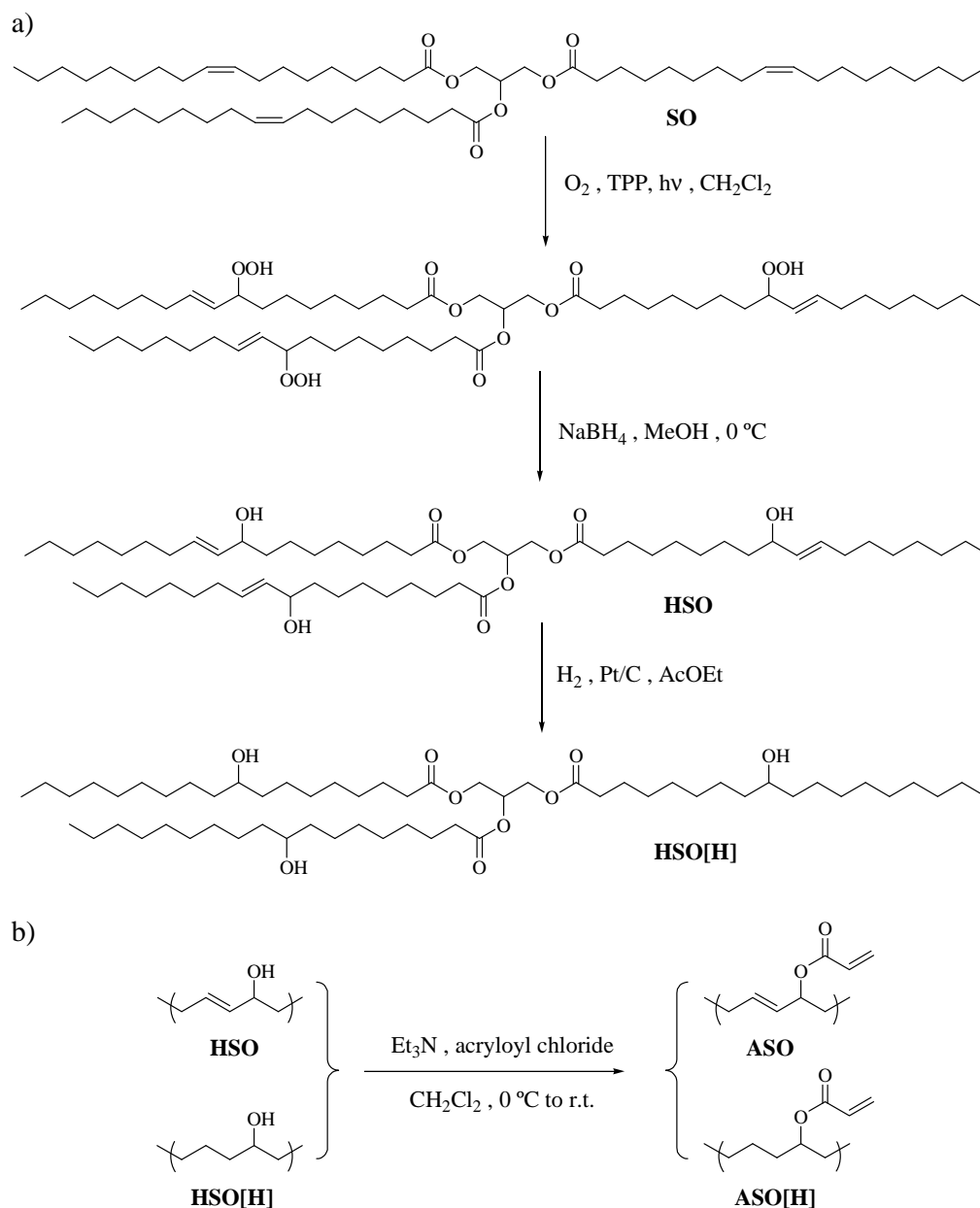
**Synthesis of hydrogenated hydroxyl sunflower oil. (HSO[H]) (Scheme 1a).** A 100 mL round-bottomed flask was charged with HSO (10 g, 0.01 mol), Pt/C (5% Pt) (0.3 g) and ethyl acetate (20 mL). A continuous flow of hydrogen was bubbled through the solution while stirring at room temperature until TLC (hexane/ethyl acetate, 2:1) showed completion of the reduction (3h). The catalyst was removed by filtration and the solvent was eliminated under reduced pressure obtaining a white solid with quantitative yield and an average of 2.6 hydroxyl groups per triglyceride (calculated by  $^1\text{H}$ -NMR spectroscopy).

FTIR: 3383  $\text{cm}^{-1}$  (OH, stretching), 1736  $\text{cm}^{-1}$  (ester C=O, stretching).

$^1\text{H}$  NMR ( $\text{CDCl}_3$ , TMS,  $\delta$  in ppm): 5.27-5.20 (1H, m, CH-O), 4.27 (2H, dd,  $J_1 = 11.97$  Hz,  $J_2 = 3.85$  Hz,  $\text{CH}_2-\text{O}$ ), 4.12 (2H, dd,  $J_1 = 11.88$  Hz,  $J_2 = 5.93$  Hz,  $\text{CH}_2-\text{O}$ ), 3.59-3.50 (3H, m, CH-OH), 2.29 (6H, t,  $J = 7.46$  Hz,  $\text{CO}-\text{CH}_2-$ ), 2.03-1.69 (broad m, OH), 1.69-1.50 (6H, m,  $\text{CH}_2-\text{CH}_2\text{CO}$ ), 1.50-1.34 (12H, m,  $\text{CH}_2-\text{CHOH}$ ), 1.34-1.15 (66 H, m, aliphatic), 0.86 (9H, t,  $J = 6.76$  Hz,  $\text{CH}_3$ ).

$^{13}\text{C}$  NMR ( $\text{CDCl}_3$ , TMS,  $\delta$  in ppm): 173.46-173.04 (COOR), 72.09-72.06 (CH-OH), 68.99 (CH-O), 62.24 ( $\text{CH}_2-\text{O}$ ), 37.67-37.57 ( $\text{CH}_2-\text{CHOH}$ ), 34.33-34.17 ( $\text{CH}_2-\text{COOR}$ ),

32.08-32.05 ( $\text{CH}_2\text{-CH}_2\text{-CH}_3$ ), 29.89-29.14 (aliphatic), 25.84-25.75 ( $\text{CH}_2\text{-CH}_2\text{CHOH}$ ),  
 25.00-24.97 ( $\text{CH}_2\text{-CH}_2\text{COOR}$ ), 22.84 ( $\text{CH}_2\text{-CH}_3$ ), 14.293 ( $\text{CH}_3$ ).



Please note that a mixture of isomers is obtained in each step of the synthesis. They are omitted for simplicity.

### Scheme 1

**Synthesis of acrylated sunflower oil (ASO) (Scheme 1b).** A 100 mL round-bottomed flask with a magnetic stirrer and under inert atmosphere was charged with HSO (10 g, 0.01 mol) and dichloromethane (50 mL). The solution was cooled to 0 °C and acryloyl

chloride (3.3 mL, 0.04 mol) followed by triethylamine (11.3 mL, 0.08 mol) were added carefully. The resulting mixture was allowed to reach room temperature and was stirred for one additional hour. The solvent was removed at reduced pressure and the resulting oil was eluted with ethyl acetate through a short celite column. The dichloromethane solution of the resulting product was washed twice with brine, dried over  $\text{MgSO}_4$  and concentrated to dryness to obtain ASO in 89% yield. The number of acrylate groups per triglyceride was found to be 2.5 by  $^1\text{H-NMR}$  spectroscopy.

FTIR:  $1740\text{ cm}^{-1}$  (ester  $\text{C}=\text{O}$ , stretching),  $1720\text{ cm}^{-1}$  (acrylate  $\text{C}=\text{O}$ , stretching),  $1675\text{ cm}^{-1}$  (double bond, stretching)  $1630$  and  $1618\text{ cm}^{-1}$  (acrylate double bond, stretching),  $1400$ ,  $1294$ ,  $1266$  and  $1042\text{ cm}^{-1}$  ( $\text{CH}$  and  $\text{CH}_2$  in-plane deformations) and  $985$ ,  $960$  and  $810\text{ cm}^{-1}$  ( $\text{CH}$  and  $\text{CH}_2$  out-of-plane deformations) and  $1187\text{ cm}^{-1}$  ( $\text{C-O}$ , stretching).

$^1\text{H NMR}$  ( $\text{CDCl}_3$ , TMS,  $\delta$  in ppm): 6.36 (3H, dd,  $J_1 = 17.32\text{ Hz}$ ,  $J_2 = 1.50\text{ Hz}$ ,  $\text{CO-CH}=\text{CH}_2$ ), 6.08 (3H, dd,  $J_1 = 17.32$ ,  $J_c = 10.38\text{ Hz}$ ,  $\text{CO-CH}=\text{CH}_2$ ), 5.77 (3H, dd,  $J_c = 10.39$ ,  $J_g = 1.51\text{ Hz}$ ,  $\text{CO-CH}=\text{CH}_2$ ), 5.73-5.63 (3H, m,  $\text{CH}=\text{CH-CHOH}$ ), 5.40-5.33 (3H, m,  $\text{CH}=\text{CH-CHOH}$ ), 5.27-5.20 (4H, m,  $\text{CH-OH}$  and  $\text{CH-O}$ ), 4.27 (2H, dd,  $J_1 = 11.88$ ,  $J_2 = 4.26\text{ Hz}$ ,  $\text{CH}_2\text{-O}$ ), 4.11 (2H, dd,  $J_1 = 11.94$ ,  $J_2 = 5.84\text{ Hz}$ ,  $\text{CH}_2\text{-O}$ ), 2.28 (6H, t,  $J = 7.71\text{ Hz}$ ,  $\text{CO-CH}_2\text{-}$ ), 1.99 (5H, dd,  $J_1 = 14.16$ ,  $J_2 = 7.12\text{ Hz}$ ,  $\text{CH}_2\text{-CH}=\text{CH}$ ), 1.71-1.47 (12H, m,  $\text{CH}_2\text{-CHOH}$  and  $\text{CH}_2\text{-CH}_2\text{CO}$ ), 1.39-1.16 (54 H, m, aliphatic), 0.85 (9H, t,  $J = 6.85\text{ Hz}$ ,  $\text{CH}_3$ ).

$^{13}\text{C NMR}$  ( $\text{CDCl}_3$ , TMS,  $\delta$  in ppm): 173.36-172.93 ( $\text{COOR}$ , triacylglyceride), 165.72 ( $\text{COOR}$ , acrylate), 134.82-134.37 ( $\text{CH}=\text{CH-CHO}$ ), 130.43 ( $\text{COCH}=\text{CH}_2$ ), 129.15 ( $\text{COCH}=\text{CH}_2$ ), 128.51-128.23  $\text{CH}=\text{CH-CHOH}$ , 75.34 ( $\text{CH-O}$ ), 68.99 ( $\text{CH-O}$ ), 62.21 ( $\text{CH}_2\text{-O}$ ), 34.68-34.66 ( $\text{CH}_2\text{-CHO}$ ), 34.27-34.11 ( $\text{CH}_2\text{-COOR}$ ), 32.35-32.27 ( $\text{CH}_2\text{-CH}=\text{CH}$ ), 31.99-31.96 ( $\text{CH}_2\text{-CH}_2\text{-CH}_3$ ), 29.85-28.79 (aliphatic), 25.34-25.30 ( $\text{CH}_2\text{-CH}_2\text{CHO}$ ), 24.92-24.88 ( $\text{CH}_2\text{-CH}_2\text{COOR}$ ), 22.81 ( $\text{CH}_2\text{-CH}_3$ ), 14.274 ( $\text{CH}_3$ ).

**Synthesis of acrylated hydrogenated sunflower oil (ASO[H]) (Scheme 1b).** By similar way as described above, ASO[H] was obtained in 91% yield. The number of acrylate groups per triglyceride was found to be 2.5 by  $^1\text{H-NMR}$  spectroscopy

FTIR:  $1742\text{ cm}^{-1}$  (ester  $\text{C}=\text{O}$ , stretching),  $1721\text{ cm}^{-1}$  (acrylate  $\text{C}=\text{O}$ , stretching),  $1630$  and  $1618\text{ cm}^{-1}$  (acrylate double bond, stretching),  $1400$ ,  $1294$ ,  $1266$  and  $1042\text{ cm}^{-1}$  ( $\text{CH}$

and CH<sub>2</sub> in-plane deformations) and 985, 960 and 810 cm<sup>-1</sup> (CH and CH<sub>2</sub> out-of-plane deformations) and 1187 cm<sup>-1</sup> (C-O, stretching).

<sup>1</sup>H NMR (CDCl<sub>3</sub>, TMS, δ in ppm): 6.32 (3H, dd, <sup>3</sup>J<sub>t</sub> = 17.32 Hz, <sup>2</sup>J<sub>g</sub> = 1.36 Hz, CO-CH=CH<sub>2</sub>), 6.05 (3H, dd, <sup>3</sup>J<sub>t</sub> = 17.31 Hz, <sup>3</sup>J<sub>c</sub> = 10.37 Hz, CO-CH=CH<sub>2</sub>), 5.74 (3H, dd, <sup>3</sup>J<sub>c</sub> = 10.38 Hz, <sup>2</sup>J<sub>g</sub> = 1.15 Hz, CO-CH=CH<sub>2</sub>), 5.23-5.16 (1H, m, CH-O), 4.88 (3H, m, J = 6.67 Hz, CH-O-), 4.23 (2H, dd, J<sub>1</sub> = 11.89 Hz, J<sub>2</sub> = 4.12 Hz, CH<sub>2</sub>-O), 4.08 (2H, dd, J<sub>1</sub> = 11.92 Hz, J<sub>2</sub> = 5.88 Hz, CH<sub>2</sub>-O), 2.24 (6H, t, J = 7.31 Hz, CO-CH<sub>2</sub>-), 1.60-1.40 (18H, m, CH<sub>2</sub>-CHOH and CH<sub>2</sub>-CH<sub>2</sub>CO), 1.40-1.08 (66 H, m, aliphatic), 0.81 (9H, t, J = 6.63 Hz, CH<sub>3</sub>).

<sup>13</sup>C NMR (CDCl<sub>3</sub>, TMS, δ in ppm): 173.31-172.90 (COOR, triacylglyceride), 166.13 (COOR, acrylate), 130.26 (COCH=CH<sub>2</sub>), 129.06 (COCH=CH<sub>2</sub>), 74.63-74.60 (CH-O), 68.92 (CH-O), 62.14 (CH<sub>2</sub>-O), 34.22 (CH<sub>2</sub>-COOR), 34.04, 32.00-31.95 (CH<sub>2</sub>-CH<sub>2</sub>-CH<sub>3</sub>), 31.92, 29.78-29.08 (aliphatic), 25.35 (CH<sub>2</sub>-CH<sub>2</sub>CHO), 24.92-24.85 (CH<sub>2</sub>-CH<sub>2</sub>COOR), 22.77-22.74 (CH<sub>2</sub>-CH<sub>3</sub>), 14.20 (CH<sub>3</sub>).

### Curing reactions and solubility tests.

The curing reactions were carried out as follows. ASO or ASO[H] were deoxygenated using vacuum-argon cycles to prevent oxygen free radical inhibition processes. Then they were mixed with the desired amount of deoxygenated PETA. Dicumyl peroxide (1.5% w/w) was added with effective stirring and the mixture was heated to 50°C. The resulting homogeneous mixture was put in a previously heated (80 °C) mold (100 x 6.5 x 3 mm<sup>3</sup>). The temperature was increased from 80 °C to 110 °C at a heating rate of 2 °C/min and then the temperature was increased rapidly to 130 °C and maintained for 2h. 0.5 g of finely ground sample was extracted by refluxing in 50 mL of distilled THF during 12 h to determine the amount of soluble material.

### Instrumentation

<sup>1</sup>H NMR 400 MHz and <sup>13</sup>C NMR 100.6 MHz NMR spectra were obtained using a Varian Gemini 400 spectrometer with Fourier transform, using CDCl<sub>3</sub> as solvent and TMS as internal standard. The IR analyses were performed on a FTIR-680PLUS spectrophotometer with a resolution of 4 cm<sup>-1</sup> in the transmittance mode. An attenuated-total-reflection accessory with thermal control and a diamond crystal was used to determine FTIR/ATR spectra.

Calorimetric studies were carried out on a Mettler DSC821e thermal analyzer using N<sub>2</sub> as a purge gas (20 mL/min) at a scan rate of 10°C/min. Dynamic mechanical

thermal analysis (DMTA) was performed using a TA DMA 2928 in three-point bending geometry at a fixed frequency of 1 Hz in the  $-100$  to  $200$  °C range and at a heating rate of  $3$  °C/min. The dimensions of the samples were  $15 \times 8 \times 2.5$  mm<sup>3</sup>. Thermal stability studies were carried out on a Mettler TGA/SDTA851e/LF/1100 with N<sub>2</sub> as purge gas. The studies were performed in the  $30$ - $800$  °C temperature range at a scan rate of  $10$ °C/min.

## RESULTS AND DISCUSSION

As mentioned in the introduction the synthesis of a new secondary alcohol containing-triglyceride derivative was carried out by an environmentally friendly chemical procedure from high oleic sunflower oil. For this purpose we used the singlet oxygen “ene” reaction which is one of the highly investigated processes in organic chemistry to functionalize the allylic C-H bonds of unsaturated compounds. Alkenes can be photochemically oxidized in situ with singlet oxygen generated with a high pressure sodium-vapor lamp and TPP as sensitizer in an oxygen saturated medium. In this way a mixture of isomeric allylic hydroperoxides (scheme 1a) is obtained. The mechanism of this reaction has been widely studied and it is actually well established.<sup>22</sup> These hydroperoxides are effectively reduced using triphenylphosphine,<sup>29,2</sup> but they can also be reduced with many other common reducing agents, such as sodium borohydride.<sup>30</sup> Thus, the photooxidation and further reduction using sodium borohydride of samples of high oleic sunflower oil give a quantitative transformation to the corresponding allylic alcohol HSO (Scheme 1a). <sup>1</sup>H NMR spectroscopy showed the complete disappearance of the signal at  $5.3$  ppm corresponding to the SO double bonds and the appearance of three new multiplets at  $5.6$ ,  $5.4$  and  $4.0$  ppm corresponding to the protons Ha, Hb and Hc of the allylic alcohol moiety. (Figure 1a). In this way, a product containing  $2.6$  hydroxyl groups per triglyceride (determined by <sup>1</sup>H NMR) was obtained with a yield of  $98\%$ .

The resulting allylic alcohol triglyceride derivatives were further transformed to the saturated analogues by hydrogenation at room temperature using  $5\%$  charcoal supported platinum as catalyst (Scheme 1a). Under these conditions complete reduction of the double bonds was achieved after  $3$ h leading to HSO[H] in quantitative yield. The <sup>1</sup>H NMR spectrum of this product, depicted in Fig. 1b, shows the complete disappearance of the signals corresponding to the double bond and the shielding of the

methine proton linked to the hydroxylic group, which appears at 3.5 ppm. No signals attributable to by-products were detected. It must be noted that this same product could be obtained in one step by direct hydrogenation of the mixture of allylic hydroperoxides.<sup>31</sup>

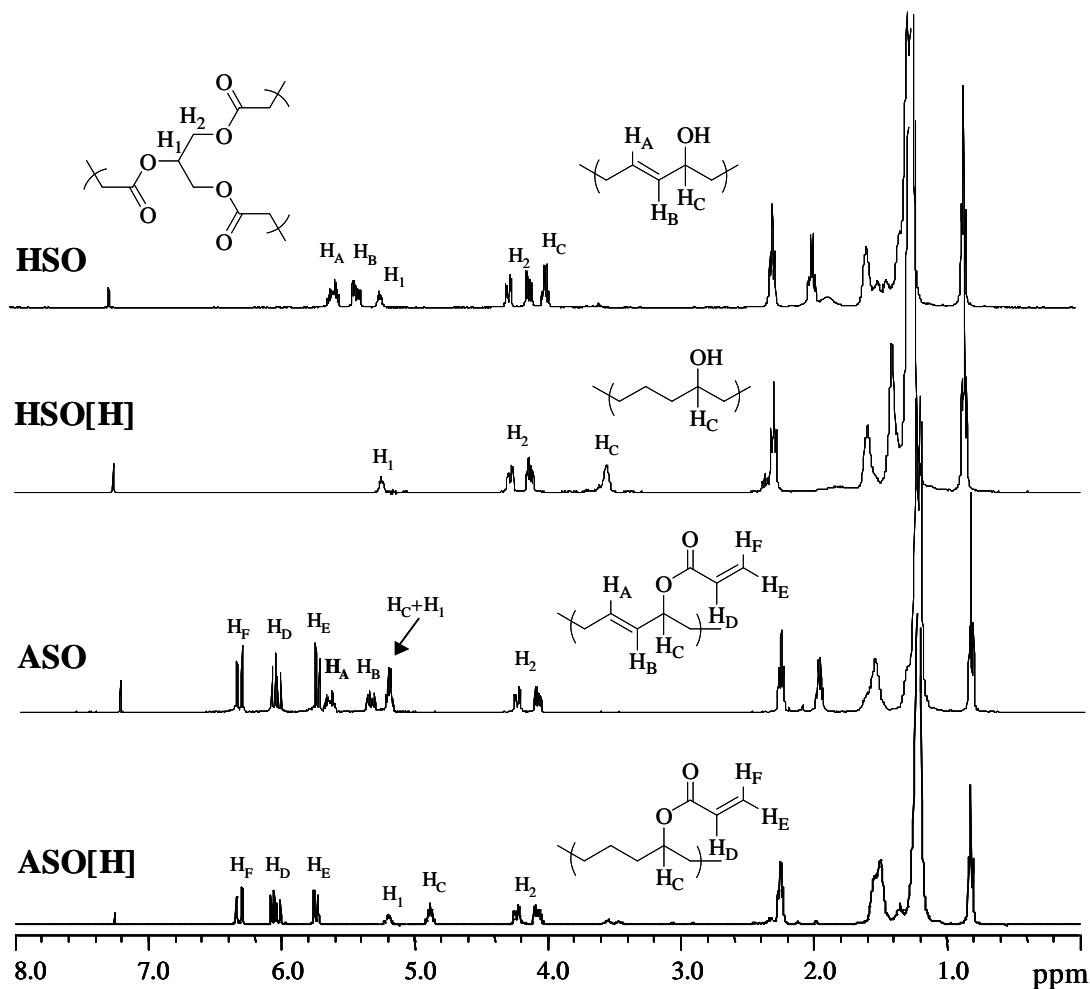


**Figure 1.** <sup>1</sup>H NMR spectra of a) HSO, b) HSO[H], c) ASO and d) ASO[H] recorded in CDCl<sub>3</sub>.

The saturated and unsaturated secondary alcohol triglycerides, HSO and HSO[H], were acrylated with acryloyl chloride, in presence of triethylamine, following a conventional procedure (Scheme 1b).<sup>32</sup> In this way, after a workup to remove the amine salts, yellowish liquids were obtained in about 90% yields. The characterization of the resulting acrylic products, ASO and ASO[H] was carried out by <sup>1</sup>H (Fig. 1c and 1d), <sup>13</sup>C NMR and FTIR/ATR spectroscopy. The <sup>1</sup>H NMR spectra confirm the introduction of the acrylic moieties by the typical set of signals at 6.3, 6.1 and 5.7 ppm. and allow to determine its content in 2.5 acrylate groups per triglyceride. Moreover, total absence of remaining hydroxylic alcohols and other secondary products is

observed and therefore these acrylated triglyceride were used without further purification.

ASO and ASO[H] were crosslinked in absence and in presence of 5,10, 15 and 20% (w/w) of PETA, using 1.5 % (w/w) of DCP as radical initiator. DSC experiments were performed with ASO and ASO[H] to determine the appropriate crosslinking conditions. Figure 2 (a) and (b) shows the DSC traces of ASO and ASO[H] respectively with different PETA concentrations. The DSC traces of ASO and ASO[H] in absence of radical initiator are also shown. As can be seen, dicumyl peroxide lowers the curing exotherm of ASO and ASO[H], but in both cases, still remains a little residual exotherm

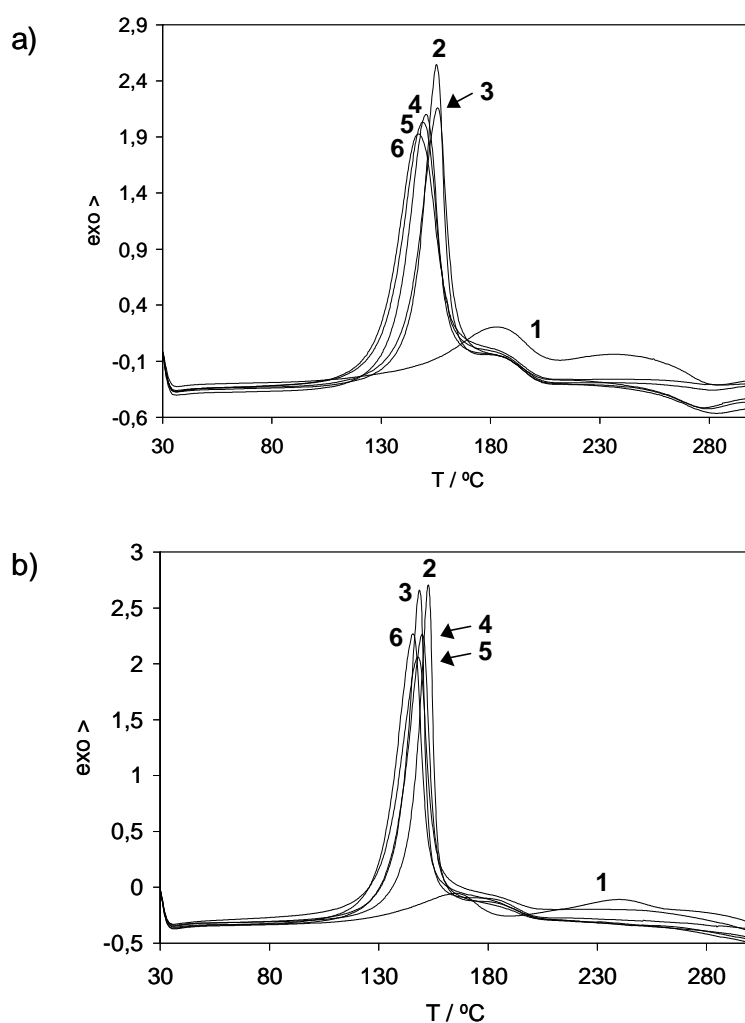


**Figure 2.** Curing DSC plots of a) ASO and b) ASO[H]. 1) without initiator, 2) 1.5% of DCP, 3) 5%PETA and 1.5% DCP, 4) 10%PETA and 1.5% DCP, 5) 15%PETA and 1.5% DCP, 6) 20%PETA and 1.5% DCP.



centred at 180 °C that can be attributed to the thermal polymerization of the non reacted acrylates. In general, it was observed that the increase of PETA content lead to a slightly shift of the curing exotherms to lower temperatures. According to these data the curing was performed at 130 °C for 2h.

The crosslinking process of two representative samples was also followed by FTIR/ATR spectroscopy. Figure 3 (a) and (b) shows the initial and final IR spectra of the ASO or ASO[H]/10% PETA/1.5% DCP curing systems. The total disappearance of the acrylate double bond bands at ca., 1630 and 1618  $\text{cm}^{-1}$  (stretching vibration), 1400, 1294, 1266 and 1042  $\text{cm}^{-1}$  (CH and  $\text{CH}_2$  in-plane deformations) and 985, 960 and 810  $\text{cm}^{-1}$  (CH and  $\text{CH}_2$  out-of-plane deformations) confirms the completion of the crosslinking in both cases.<sup>33,34</sup>

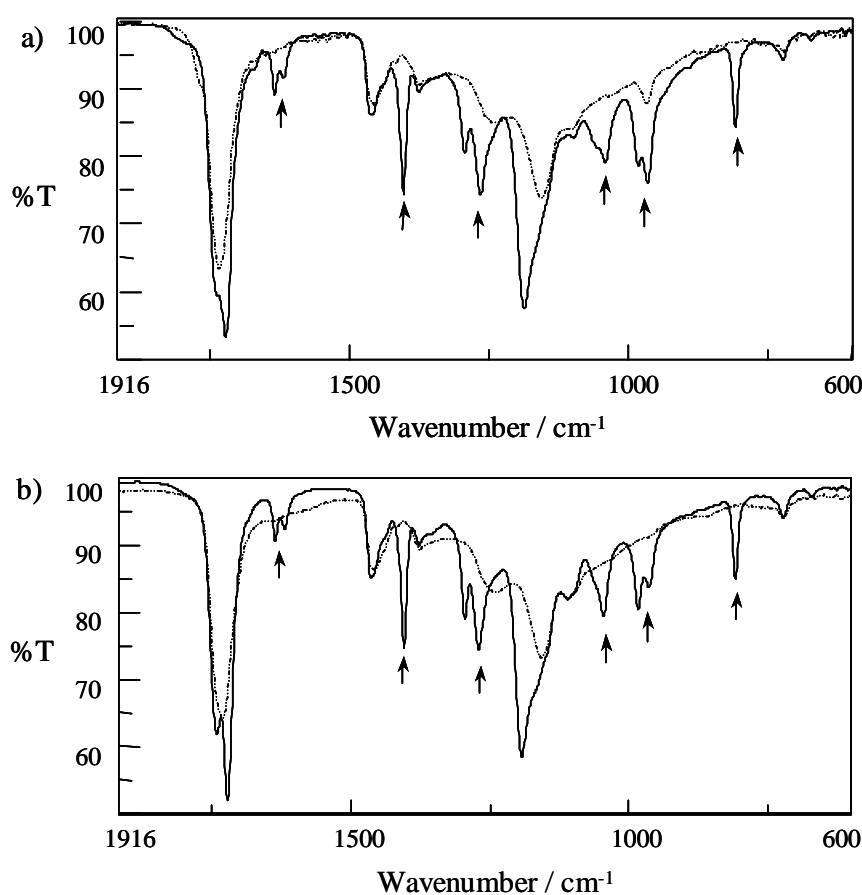


**Figure 3.** FTIR-ATR spectra of mixtures of a) ASO and b) ASO[H] with 10% of PETA and 1.5% of DCP before heating (plain line) and after heating at 130°C for 2h (dashed line).

The extent of the crosslinking reactions was investigated by extracting the soluble part of the cured samples. Table 1 shows the weight percentages of the soluble

fractions for each system. These low values indicate the formation of crosslinked structures due to the reaction of the acrylated groups, in agreement with the IR data. Moreover, as PETA content increases a higher crosslinking degree structure should be obtained which is in accordance with the lower values of soluble fractions calculated. It must be pointed out that even at high PETA concentrations soluble fractions are observed. This is related to the small fraction of rich-saturated chains in the starting oil.

**Table 1:** Soluble fractions, Tg's and thermogravimetric data of the cured ASO/PETA and ASO[H]/PETA systems.

Triglyceride	PETA (%) <sup>a</sup>	Soluble fraction (%) <sup>b</sup>	Tg (°C) <sup>c</sup>	TGA (N <sub>2</sub> )		
				T <sub>5% loss</sub> (°C)	T <sub>max</sub> (°C) <sup>d</sup>	Yield <sub>800°C</sub> (%)
ASO	0	7.5	17	303	431	3.3
ASO	5	2.7	25	305	431 / 455	3.3
ASO	10	0.7	31	308	429 / 461	3.4
ASO	15	0.4	27	307	434 / 462	3.2
ASO	20	0.4	28	312	467	3.3
ASO[H]	0	8.2	-2	334	356 / 421	3.7
ASO[H]	5	3.5	4	333	356 / 421	3.4
ASO[H]	10	1.1	1	332	353 / 418 / 458	3.7
ASO[H]	15	1.0	8	333	353 / 420 / 458	3.9
ASO[H]	20	0.8	11	334	350 / 420 / 462	4.2

<sup>a</sup> Weight / weight percentages. <sup>b</sup> In THF. <sup>c</sup> Maximum of the Tan delta peak. <sup>d</sup> Temperature of the maximum weight loss rate.

The dynamic mechanical behavior of the crosslinked materials was obtained as a function of the temperature beginning in the glassy state of each composition to the rubbery plateau of each material. The crosslinking density of a polymer can be estimated from the plateau of the elastic modulus in the rubbery state.<sup>35</sup> However, this theory is strictly valid only for lightly crosslinked materials, and is therefore used only to make qualitative comparisons of the level of crosslinking among the various polymers. The DMA behaviour of these polymers was similar to that of other thermosetting polymers.<sup>36</sup> Fig. 4 shows the dynamic mechanical analysis of the ASO

and ASO[H] systems. The  $\tan \delta$  peaks of both systems show the typical behaviour of triglyceride based thermosets elastomers. This behaviour is described as a combination of two factors, crosslinking density and plasticization.<sup>5,18</sup> As the amount of tetrafunctional acrylate (PETA) increases the overall crosslinking increases broadening  $\tan \delta$  peaks and decreasing their height. The other factor, plasticization is due to the presence of saturated fatty acid in the triglyceride that remain unreacted acting as plastizicers. So, these saturated chains introduce free volume and enable the network to

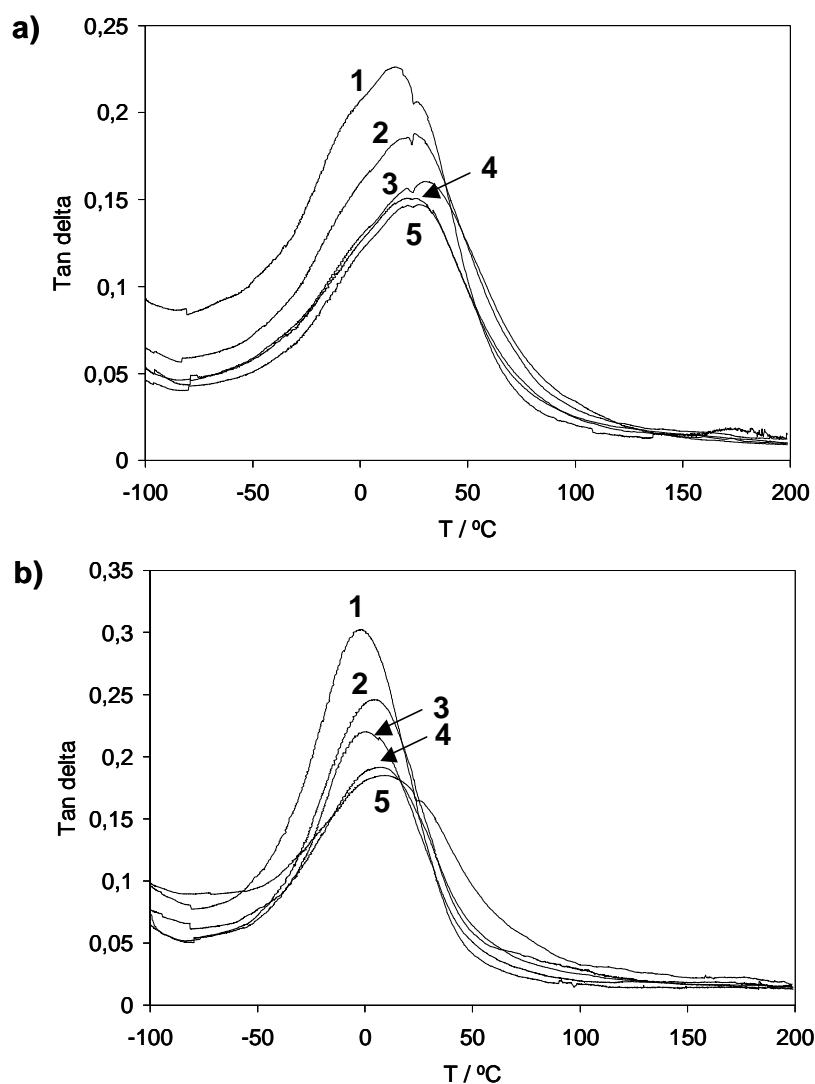


**Figure 4:**  $\tan \delta$  plots as a function of temperature for the systems cured with 1.5% of DCP at 130°C. a) ASO and b) ASO[H]. 1) without PETA, 2) 5%PETA, 3) 10%PETA, 4) 15%PETA, and 5) 20%PETA.

deform more easily. As it is well known the addition of small amounts of plasticizers to polymers drastically broadens the transition from glassy to rubbery state<sup>37</sup>. The  $T_g$  values estimated as the maximum of the  $\tan \delta$  peak are collected in Table 1 and show a slight increase with the PETA content indicating a higher crosslinking density. Moreover the height of the  $\tan \delta$  peak also decreases when PETA content increases. Because  $\tan \delta$  is the ratio of viscous component to elastic component, it can be assumed that the decreasing height is associated with lower segmental mobility and fewer relaxing species, and is therefore indicative that networks with higher PETA content show lower flexibility. The analysis of the width of the  $\alpha$ -relaxation peak allow estimate the network structural homogeneity. For the ASO systems (Fig. 4a) we can observe that the peak width at half height of all samples does not broaden with the PETA content indicating the absence of triglyceride-rich and PETA-rich regions in these systems. In the case of ASO[H] systems shown in Fig. 4b) the  $\tan \delta$  peaks are less broad than those of the ASO systems. As ASO[H] was synthesized from ASO and no purification was carried out, the amount of saturated alkyl chains acting as plasticizers must be the same in both cases. However, according with the width of the  $\alpha$ -relaxation peak, the ASO[H]/PETA curing systems seem to have a higher structural homogeneity. A possible explanation of this fact may relay on the absence of double bonds in ASO[H], that could allow the long alkyl chains to arrange in a more homogeneous way during the crosslinking process. Moreover, the width of the  $\tan \delta$  peaks is not appreciably affected by the increase of PETA except in the case of the highest content (20% PETA). Also, the general tendency of the  $\tan \delta$  maximums is towards higher temperatures as the PETA content increases, and a decrease of the height of  $\tan \delta$  peak is observed as the crosslinking density increases.

The  $T_g$ s calculated for the ASO[H] systems (Table 1) are around 15-20 °C above those of the ASO systems. The presence of double bonds contributes to increase the rigidity of the polymers network thus increasing the  $T_g$  values of the ASO/PETA materials. These materials can be considered elastomers as the  $T_g$  values are basically below the ambient temperature. All the cured samples show high toughness and good transparency.

To determine the thermal stability of the polymers, thermogravimetric analyses were carried out under nitrogen atmosphere. The TGA curves and their derivatives for ASO and ASO[H] systems are represented in Figures 5 and 6 respectively, and the temperatures of 5% weight loss, the temperature of the maximum weight loss rate and

the residue at 800°C are collected in Table 1. In both systems, it can be observed that the higher PETA content the higher thermal stability. The char yield at 800 °C was around 3.5% for all the samples.

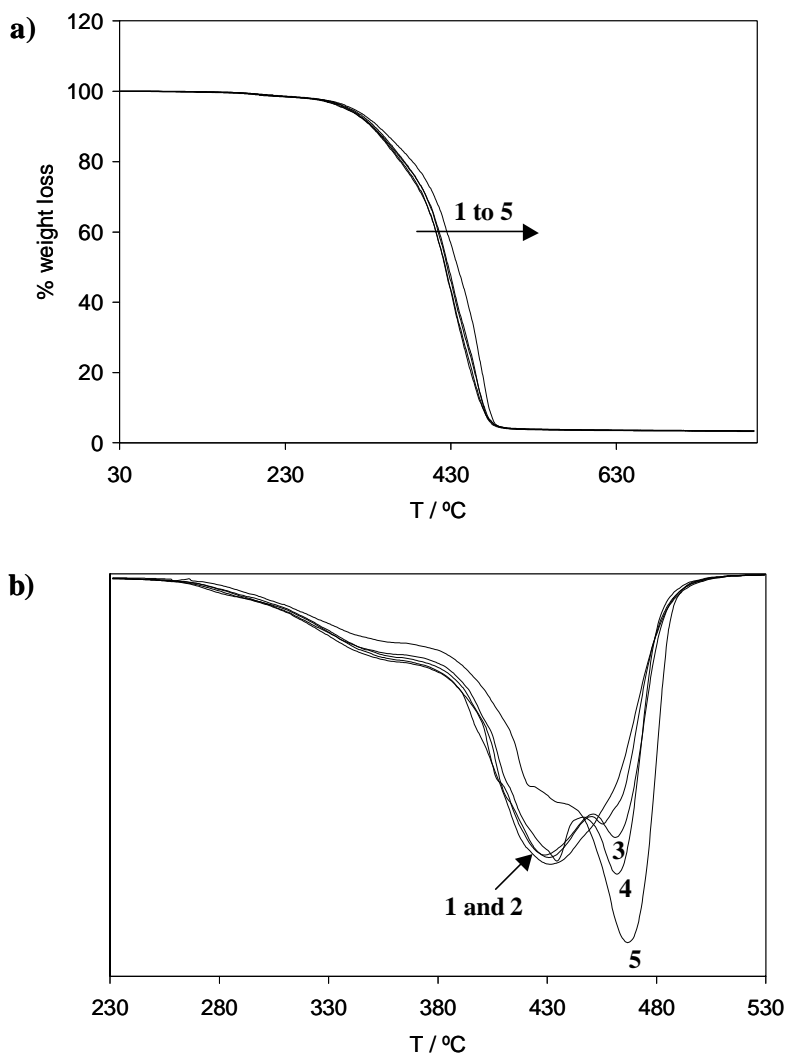


**Figure 5:** a) TGA plots and b) first derivative curves of ASO based systems cured with 1.5% DCP 1) without PETA, 2) 5% PETA, 3) 10% PETA, 4) 15% PETA and 5) 20% PETA.

The ASO[H]/PETA polymers show higher thermal stability in the initial stages of degradation with temperatures of 5% weight loss around 30 °C over those of the ASO/PETA polymers (see Table 1). This has to be attributed to the double bonds present in ASO, which favours the formation of allylic radicals and the thermal degradation process. Three maximum weight loss rate are observed in both cases in the derivative curves indicating the existence of several processes. The weight loss rate decreases as the PETA content increases for the two first steps while opposite is true for

the higher temperature step. These complex degradations can be related to different factors. Firstly, the different crosslinking density that increases with PETA content. Secondly, the different ability of saturated and unsaturated secondary esters to thermal  $\beta$ -elimination and finally the stability of neopentilic moieties.

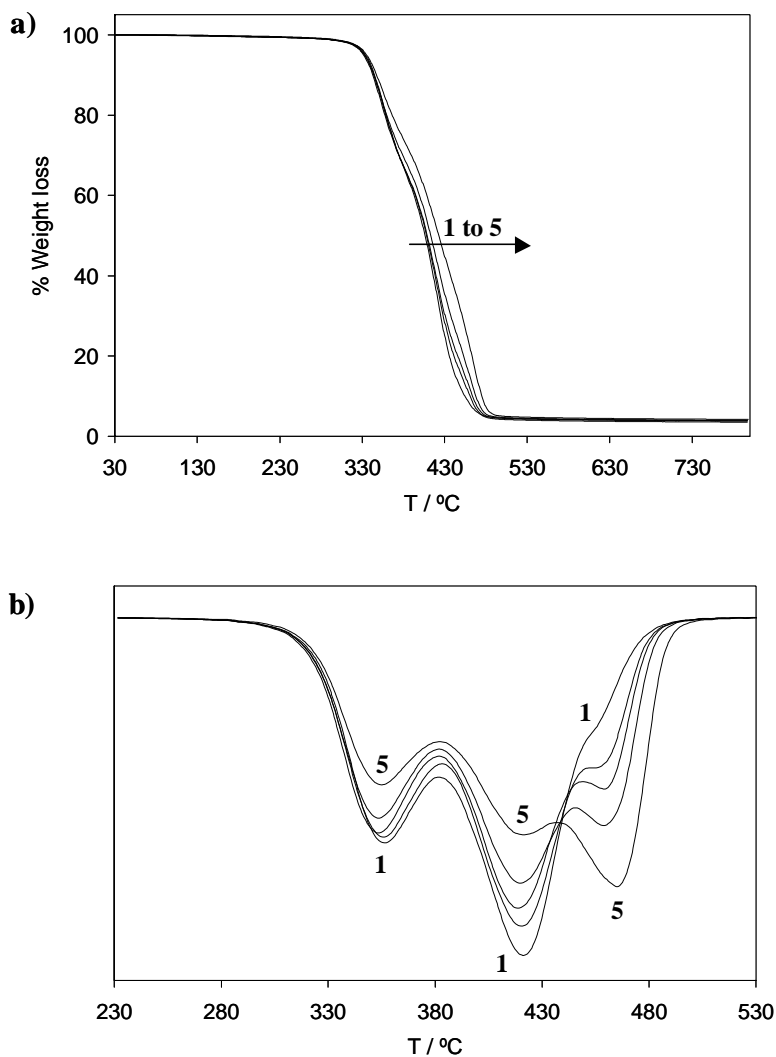


**Figure 6:** a) TGA plots and b) first derivative curves of ASO[H] based systems cured with 1.5% DCP 1) without PETA, 2) 5% PETA, 3) 10% PETA, 4) 15% PETA and 5) 20% PETA.

## CONCLUSIONS

Acrylated triglycerides were obtained by a new route that involves the singlet oxygen photooxygenation and further reduction of the resulting hydroperoxides derivatives to a mixture of secondary allylic alcohols. These unsaturated alcohols can be further reduced

to saturated alcohols. These two new hydroxyl-containing triglycerides were easily acrylated. These acrylate-containing triglyceride derivatives have shown high reactivity to radical polymerisation in presence of different amounts of pentaerythritol tetraacrylate providing a promising route to obtain polymeric networks. These materials show properties and characteristics as good as other acrylated triglyceride-based thermosets reported.

The authors express their thanks to CICYT (Comisión Interministerial de Ciencia y Tecnología) (MAT2005-01593) for financial support for this work.

## REFERENCES

- <sup>1</sup> Bozell, J.J.; Patel, M. Eds., Feedstocks for the Future: Renewable for the Production of Chemicals and Materials; ACS Symposium Series 921; American Chemical Society: Washington, DC, 2006
- <sup>2</sup> Biermann, U.; Friedt, W.; Lang, S.; Lühs, W.; Machmüller, G.; Metzger, J. O.; Klaas, M. R.; Schäfer, H. J.; Schneider, M. P. *Angew Chem Int Ed* 2000, 39, 2206-2224.
- <sup>3</sup> Güner, F. S.; Yagci, Y.; Erciyas, A. T. *Prog Polym Sci* 2006, 31, 633-670.
- <sup>4</sup> Meier, M. A. R.; Metzger, J. O.; Schubert, U. S. *Chem Soc Rev* 2007, 36, 1788-1802.
- <sup>5</sup> Khot, S. N. ; LaScala, J. J.; Can, E. S.; Morye, S. G.; Williams, I.; Palmese, G. R. S.; Küseföglu, H.; Wool, R. P. *J Appl Polym Sci* 2001, 82, 703-723.
- <sup>6</sup> Lane, B. S.; Burgess, K. *Chem Rev* 2003, 103, 2457-2474.
- <sup>7</sup> Grigoropoulou, G.; Clark, J. H.; Elings, J. A. *Green Chem.* 2003, 5, 1-7.
- <sup>8</sup> Park, S.-J.; Jin, F.-L.; Lee, J.-R. *Macromol Rapid Commun* 2004, 25, 724-727.
- <sup>9</sup> Rüschen, Klaas M. and Warwel S., *J Am Oil Chem Soc* 1996, 73, 1453-1457
- <sup>10</sup> Vlcek T. and Petrovic Z. S. *J Am Oil Chem Soc* 2006, 83, 247-252
- <sup>11</sup> Eren, T.; Küseföglu, S. H.; *J Appl Polym Sci* 2004, 91, 4037-4046.
- <sup>12</sup> Sharma, V.; Kundu, P. P. *Prog Polym Sci* 2006, 31, 983-1008.
- <sup>13</sup> La Scala, J.; Wool, R.P. *J apl. Polym Sci* 2005, 95, 774-783.
- <sup>14</sup> Williams, G.I.; Wool, R.P. *Appl Compos Mater* 2000, 7, 421-432
- <sup>15</sup> Bunker, S.P.; Wool, R.P. *J Polym Sci: Part A: Polym Chem* 2002, 40, 451-458.
- <sup>16</sup> Wool, R.P.; Küseföglu, S. H.; Palmese, G.; Khot, S.; Zhao, R. U.S. Patent 6, 121, 398, 2000.
- <sup>17</sup> Guo, A.; Cho, Y; Petrovic, Z. S. *J Polym Sci: Part A: Polym Chem* 2000, 38, 3900-3910.
- <sup>18</sup> La Scala, J.; Wool, R.P. *Polymer* 2005, 46, 61-69.
- <sup>19</sup> Eren, T.; Küseföglu, S. H.; *J Appl Polym Sci* 2004, 91, 2700-2710.

- 
- <sup>20</sup> Pelletier, H.; Gandini, A. *Eur J Lipid Sci Technol* 2006, 108, 411-420.
- <sup>21</sup> Thames, S.F.; Haibin, Y.; Schuman, T.P.; Min, D.W. *Prog Org Coat*, 1996, 28, 299-305
- <sup>22</sup> Greer, A. *Acc Chem Res.* 2006, 39, 797-804.
- <sup>23</sup> Hui, S-P.; Yoshimura, T.; Murai, T.; Chiba, H.; Kurosawa, T. *Anal Sci* 2000, 16, 1023-1028.
- <sup>24</sup> Samadi, A.; Martinez, L. A.; Miranda, M. A.; Morera, I. M. *Photochem Photobiol* 2001, 73, 359-365.
- <sup>25</sup> Frimer, A. A. *Chem Rev* 1979, 79, 359-387.
- <sup>26</sup> Kornblum, N.; DeLaMare, H.E. *J Am Chem Soc* 1951, 73, 880-881.
- <sup>27</sup> Ohloff, G. *Pure Appl Chem* 1975, 43, 481-502.
- <sup>28</sup> Montero de Espinosa, L.; Ronda, J. C.; Galià, M.; Cádiz, V. *J Polym Sci Part A: Polym Chem* 2008, 46, 6843-6850.
- <sup>29</sup> Hiatt, R.; Smythe, J.; McColeman, C. *Can J Chem*, 1971, 49, 1707-1711.
- <sup>30</sup> Thomas, M. J.; Pryor, W. A. *Lipids* 1979, 15, 544-548.
- <sup>31</sup> Coleman, J.E.; Swern, D *J Am Oil Chem Soc* 1955, 32, 221-224.
- <sup>32</sup> Reddy M. V. R., Yucel A. J., Ramachandran P. V. *J. Org. Chem.* 2001, 66, 2512-2514.
- <sup>33</sup> Roeges, N.P.G. *A Guide to the Complete Interpretation of Infrared Spectra of Organic Structures.* John Wiley & Sons Ltd, Chichester, 1994.
- <sup>34</sup> Pelletier, H.; Belgacem, N.; Gandini, A. *J Appl Polym Sci* 2006, 99, 3218-3221.
- <sup>35</sup> Tobolsky AV, Carlson DW, Indictor NJ. *J Polym Sci* 1961, 54,175-192.
- <sup>36</sup> Malik, M.;Choudhary, V.; Varma IK. *Rev Macromol Chem Phys* 2000, C40, 139-165.
- <sup>37</sup> Nielsen, L.E.; Landel, R.F. *Mechanical Properties of Polymers and Composites;* Marcel Dekker Ed. New York 1994.



## SECOND PART

---

The second part of this thesis is focused on the development of plant oil-based flame retardant polymers. Chapter three describes the synthesis of phosphine oxide-containing thermosets from high oleic sunflower oil. In chapter four, acyclic diene metathesis polymerization has been used as a way to linear and cross-linked phosphorus containing renewable polymers.

---



## FLAME RETARDANT MATERIALS

### Introduction

Every day in Europe there are about 12 fire victims and 120 people severely injured. The total economic damage is estimated at about 25 billion € per year. When it comes to global statistics, fires kill an average of over 37.000 persons per year in the 31 (2.3 billion inhabitants) countries covered by CTIF (International Association of Fire and Rescue Services).<sup>1</sup> About 80 % of all fire deaths occur in residential buildings, where fires can develop rapidly and violently due to the presence of upholstered furniture, varied electrical and electronic equipment (made mainly of plastics) and many other consumer goods.

A recent study by the US National Institute for Science and Technology (NIST)<sup>2</sup> confirms that the increasing fire load of consumer products and home decorations is effectively making home fires increasingly dangerous. The heat released in such fires results within minutes in “flashover”, that is the fire gas and smoke in a room reaches temperatures such that all combustible materials in the room will ignite (around 600°C), so that death of room occupants is inevitable. The risk of fire can be reduced by:<sup>3</sup>

- The use of non-combustible materials or materials less likely to ignite and propagate a fire.
- The treatment of potentially flammable materials to inhibit ignition and spread of fire.
- Designing and constructing buildings that are safer.
- Using "fire stop" sealings to help confine a fire to one area or compartment.
- Using smoke detectors, fire alarms and sprinkler systems.
- By educating people, at all levels, of the importance of fire safety.

In order to fulfil these requirements, flame retardants (FRs) are thus increasingly critical to slow fire spread and development.

Concerning the toxicity of FRs, many studies have been carried out<sup>3</sup> and show that modern flame retardants, when appropriately applied, can be used in consumer products without significant risk to human health or the environment. As concluded by the DPI report<sup>4</sup> in 1999, “the major hazards of most fires arise from the existence of the fire, not from the materials burned and there is no evidence that flame retardants

contribute to the direct human health risks arising from toxic gas effects” and “information available suggests that the benefits of many flame retardants in reducing the risk from fire outweigh the risks to human health”.

## Mechanism of action

To better understand the role of flame retardants it is first necessary to understand the combustion process of polymeric materials; a process that takes place in the condensed phase, in the gas phase and in the interphase between both. In the first stage of the combustion cycle, an external source of heat causes the thermal degradation of the material. Due to scission of the chemical bonds, volatile residues are released to the surrounding air (gas phase) forming a flammable mixture that leads to combustion in the moment that its ignition temperature is reached. If the exothermic combustion reactions taking place produce the required thermal energy to maintain the thermal degradation of the material, the combustion cycle proceeds (Fig. 1).

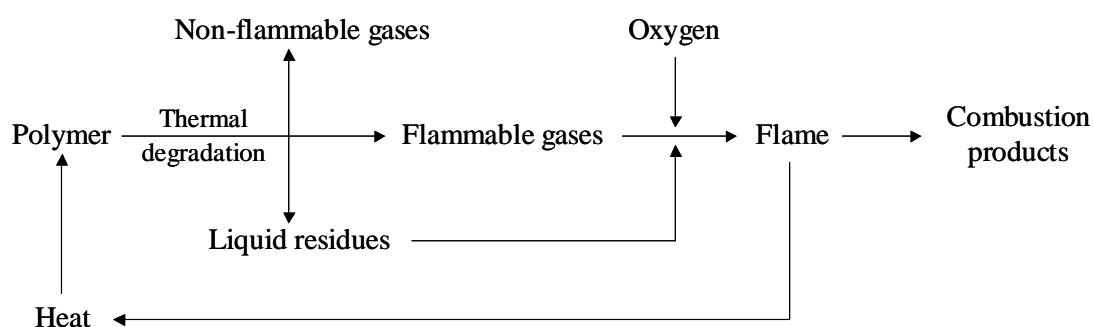
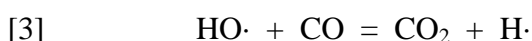


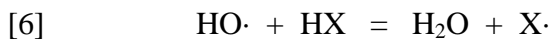
**Figure 1.** Combustion cycle of polymeric materials

Flame retardants are compounds that reduce the chances of a fire starting by providing increased resistance to ignition. Even if ignition does occur, flame retardants will act to delay the spread of flame, providing extra time in the early stages when the fire can be extinguished or an escape can be made. They can be added to or applied as a treatment to materials such as plastics, textiles, foams or timber (Additives). Alternatively they can be used during the production process as a chemical modification of some plastic materials (Reactives). Flame retardants can perform their activity in the condensed phase, in the gas phase or in both depending on their composition.<sup>5</sup>

- The gas-phase activity of flame retardants is based on its interference in the reactions that maintain the combustion cycle. The combustion of polymeric materials produces species capable of reaction with atmospheric oxygen. As a result, the propagation of combustion occurs through the following branching reactions.



The main exothermic reaction is [3] and provides the most energy to maintain the flame. Halogenated flame retardants release hydrogen halides during combustion (reaction [4]), which effectively interfere with these branching reactions acting as flame inhibitors (reactions [5] and [6]).



- The condensed-phase mechanism implies a chemical interaction between the flame retardant and the polymer through two main modes of interaction: dehydration and cross-linking. Both contribute to formation of char, a solid residue that protects the polymer by isolating the non-burned surface from the heat source and preventing the volatile species to reach the flame and feed it.

## Classification

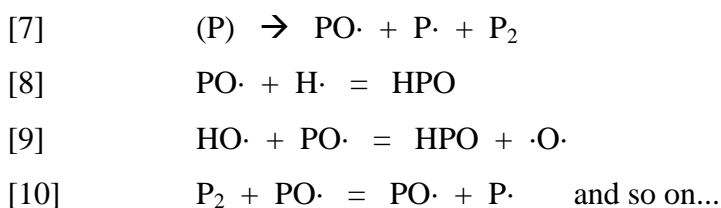
As already mentioned, flame retardants are usually classified in two main categories, namely additives and reactives.<sup>6</sup> Additives are added mechanically to manufactured polymers, while reactives are introduced during the synthesis of polymers and thus they are chemically bound to their structure. Additives are cost effective and more widely applicable than reactives; however, high loads are usually needed to reach good flame retardancy (10-40 % w/w) that modify the physical and mechanical properties of the parent polymer. Furthermore, since additives are mechanically blended with the

polymer, migration can take place at long usage times. On the other hand, the synthesis of intrinsic flame retardant polymers through the design of flame retardant monomers or the chemical modification of existing polymers, enables a better control of the final polymer properties. Moreover, low levels of modification have comparable effects to those achieved with relatively high loadings of FR additives and the migration problems associated with additives are avoided.<sup>7</sup>

Flame retardants can also be roughly classified in two groups: halogenated FRs and non-halogenated FRs. This classification obeys the nowadays concerns about environment and health protection. Halogenated FRs are the most widely applied. Very low amounts are needed to infer good flame retardancy to polymers, they are cheap and versatile. However, during combustion, toxic decomposition products like dibenzodioxines and halogenated dibenzofuranes and corrosive gases like hydrogen halides are evolved. Some of these products are non-easily degradable and accumulate in the environment being classified as persistent organic pollutants (POPs). Non-halogenated flame retardants stand as the alternative to overcome these drawbacks. There is an immense range of different non-halogenated flame retardant products such as inorganic chemicals (metal hydroxides, antimony oxides or stannates) and FRs based on heteroatoms like phosphorus, nitrogen, silicon and boron.<sup>7</sup> Among them, phosphorus-based FRs have been extensively studied and proven to act efficiently in the condensed phase. Moreover, a number of studies describe their action also in the gas phase.

### **Phosphorus-based flame retardants**

The use of phosphorus compounds to infer flame retardant properties to polymeric material is well established.<sup>8</sup> Phosphorus-based FRs can be inorganic, organic, or elemental (red phosphorus), can be active in the gas phase or in the condensed phase, and sometimes may operate simultaneously in both phases. Phosphine oxides<sup>9</sup> and phosphonates<sup>10,11</sup> have been proven to act in the gas phase through the formation of PO· radicals (reactions [7] to [10]), and PO<sub>2</sub>·, HOPO·, and HOPO<sub>2</sub>· radicals respectively, which terminate the highly active flame-propagation radicals (HO· and H·). These radicals are formed after the decomposition of the parent compound and therefore, the flame inhibition does not depend on the form of the parent compound, provided that the parent breaks down in the flame.<sup>10</sup>



In the condensed phase mechanism, the phosphorus FR is thermally decomposed giving phosphoric acid, which is further dehydrated to polyphosphoric acid. Polyphosphoric acid promotes condensation and dehydration reactions in the surface of the polymer giving rise to unsaturated carbonous species that make up a residue that protects the polymer surface from further degradation (Fig. 2).

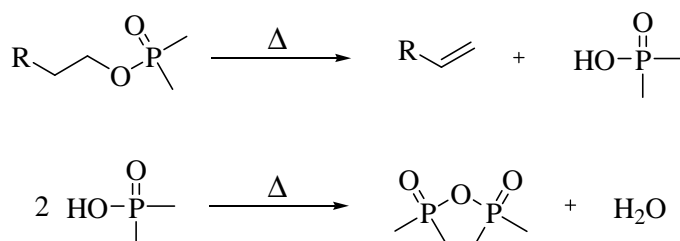


**Figure 2.** condensed phase mechanism of phosphorus-based FRs.

The carbonization process takes place through several stages.<sup>12</sup> During the process, in addition to polyphosphoric acid being formed, also reducing compounds such as phosphites can be present. They reduce carbon oxidation in favor of char.<sup>13</sup> Phosphate, phosphonate and phosphinate based FRs have been the most widely used; The P-O bond has a quite high thermal stability (heat of dissociation about 85 Kcal/mol); however, it presents general poor hydrolytic stability<sup>14,15</sup> that limits the range of application of the final polymeric materials. On the other hand, phosphine oxides present a P-C bond, which has a lower reactivity, being more stable and having a higher hydrolytic stability. Moreover, it also has a quite high thermal stability (heat of dissociation about 65 Kcal/mol).<sup>15,16</sup>

As commented above, the disadvantages of additives make the reactive approach a more suitable way to flame retardant polymeric materials. In this way, increasing research is now being directed at the synthesis of phosphorus-based FR polymers. Some recently published examples include polyphosphonates<sup>17</sup>, phosphonate-based

polyurethanes,<sup>18</sup> epoxy resins,<sup>19</sup> poly(ether-ester)s<sup>20</sup> and polymethacrylates,<sup>21</sup> phosphate containing nylon<sup>22</sup>, silk<sup>23</sup> and polyacrylates,<sup>24</sup> modification of cotton fabric with phosphoric acid,<sup>25</sup> phosphine oxide-based epoxy resins<sup>26</sup> polybenzoxazines,<sup>27</sup> polyethers,<sup>28</sup> poly(ether-ester)s<sup>29</sup> and poly(ether-ketone)s,<sup>30</sup> DOPO-containing epoxy resins,<sup>31,26d</sup> polybenzoxazines,<sup>32</sup> polyesters,<sup>33</sup> polyethers<sup>28</sup> and poly(ether-ester)s.<sup>29a</sup> Other examples are ionomer polyesters,<sup>34</sup> polyphosphorinanes,<sup>35</sup> and advances in flame retardant polystyrene, HIPS, ABS and polystyrene foams.<sup>36</sup>

### **Polymer flammability tests. Limiting Oxygen Index (LOI)**

Various organizations throughout the world create fire standards. These include both national and international organizations, being the American Society for Testing and Materials (ASTM), Underwriters Laboratories (UL) and the International Organization for Standardization (ISO) some of the most important. All of these organizations create various types of fire standards-mainly guidance documents and test methods addressing most of the major fire properties.<sup>37</sup>

All the standards of polymer combustibility can be subdivided into five major types: ignitability tests, flame spread tests, oxygen index, heat release tests and smoke tests. In this thesis, the combustibility measurements have been carried out using the Limiting Oxygen Index (LOI).

The LOI test is a widely used research and quality control tool for determining the relative flammability of polymeric materials. A numerical index, the 'LOI', is defined as the minimum concentration of oxygen in a flowing oxygen/nitrogen mixture, required to just support candle-like downward burning of a vertically mounted test specimen. Hence, higher LOI values represent better flame retardancy. This test method is generally reproducible to an accuracy of + 0.5% and although originally designed for testing of plastics, the method has been used extensively for evaluating the relative flammability of rubbers, textiles, paper, coatings and other materials.

LOI tests can be conducted in accordance with international standards including ASTM D2863 and ISO 4589-2.



- 
- <sup>1</sup> [www.ctif.org](http://www.ctif.org), CTIF 9<sup>th</sup> Annual Report, June 2003  
[http://www.vfdb.de/feuerwehr/index/vfdbproducts/stres\\_ctif/stresctif\\_ger/textvorlagen/CTIF\\_Report9\\_2003.pdf](http://www.vfdb.de/feuerwehr/index/vfdbproducts/stres_ctif/stresctif_ger/textvorlagen/CTIF_Report9_2003.pdf).
- <sup>2</sup> <http://smokealarm.nist.gov> Full study report: NIST July 2004 study, Bukowski, R.W. et al. "Performance of Home Smoke Alarms, Analysis of the Response of Several Available Technologies in Residential Fire Settings" NIST Technical Note 1455 (396 pages)  
<http://smokealarm.nist.gov/HSAT.pdf>.
- <sup>3</sup> European Flame Retardants Association (EFRA) <http://www.flameretardants.eu/content>.
- <sup>4</sup> Stevens, G. C.; Mann, A. H. "Risks and benefits in the use of flame retardants in consumer products". A report for the UK Department of Trade and Industry, January 1999, DTI References URN 98/1026.
- <sup>5</sup> Lewin M.; Weil, E. D. In *Fire Retardant Materials*; Horrocks, A. R. and Price, D., Eds.; CRC Press, 2001; 31-68.
- <sup>6</sup> Ebdon, J. R.; Jones, M. S. In *Concise Polymeric Materials Encyclopedia*; Salamone, J. C., Ed.; CRC Press, 1996; 2397-2411.
- <sup>7</sup> Lu, S. Y.; Hamerton, I. *Prog Polym Sci* 2002, 27, 1661-1712.
- <sup>8</sup> Ebdon, J. R.; Price, D.; Hunt, B. J.; Joseph, P.; Gao, F.; Milnes, G. J.; Cunliffe, L. K. *Polym Degrad Stab* 2000, 69, 267-277.
- <sup>9</sup> Shmakov, A. G.; Shvartsberg, V. M.; Korobeinichev, O. P.; Beach, M. W.; Hub, T. I.; Morgan, T. A. *Mendeleev Commun* 2007, 17, 186-187.
- <sup>10</sup> Macdonald, M. A.; Gouldin, F. C.; Fisher, E. M. *Comb Flame* 2001, 125, 668-683.
- <sup>11</sup> Jayaweera, T. M.; Melius, C. F.; Pitz, W. J.; Westbrook, C. K.; Korobeinichev, O. P.; Shvartsberg, V. M.; Shmakov, A. G.; Rybitskaya, I. V.; Curran, H. J. *Comb Flame* 2005, 140, 103-115.
- <sup>12</sup> Delobel, R.; Le Bras, M.; Ouassou, N.; Descressain, R. *Polym Degrad Stab* 1990, 30, 41-56.
- <sup>13</sup> Hörold, S. *Polym Degrad Stab* 1999, 64, 427-431.
- <sup>14</sup> Beach, M. W.; Rondan, N. G.; Froese, R. D.; Gerhart, B. B.; Green, J. G.; Stobby, B. G.; Shmakov, A. G.; Shvartsberg, V. M.; Korobeinichev, O. P. *Polym Degrad Stab* 2008, 93, 1664-1673.
- <sup>15</sup> Quin, L. D. *A guide to organophosphorus chemistry*, John Wiley & Sons, 2000.
- <sup>16</sup> Morgan, P. W.; Herr, B. C. *J Am Chem Soc* 1952, 74, 4526-4529.
- <sup>17</sup> Ranganathan, T.; Zilberman, J.; Farris, R. J.; Coughlin, E. B.; Emrick, T. *Macromolecules* 2006, 39, 5974-5975.
- <sup>18</sup> Chen, H.; Luo, Y.; Chai, C.; Wang, J.; Li, J.; Xia, M. *J Appl Polym Sci* 2008, 110, 3107-3115.

- 
- <sup>19</sup> Seibold, S.; Schäfer, A.; Lohstroh, W.; Walter, O.; Döring, M. *J Appl Polym Sci* 2008, 108, 264–271.
- <sup>20</sup> Canadell, J.; Mantecón, A.; Cádiz, V. *J Polym Sci Part A: Polym Chem* 2007, 45, 1980–1992.
- <sup>21</sup> a) Youssef, B.; Lecamp, L.; El Khatib, W.; Bunel, C.; Mortaigne, B. *Macromol Chem Phys* 2003, 204, 1842–1850, b) Edizer, S.; Sahin, G.; Avci, D. *J Polym Sci Part A: Polym Chem* 2009, 47, 5737–5746
- <sup>22</sup> Yang, H.; Yang, C. Q.; He, Q. *Polym Deg Stab* 2009, 94, 1023–1031.
- <sup>23</sup> Guan, J.; Yang, C. Q.; Chen, G. *Polym Deg Stab* 2009, 94, 450–455.
- <sup>24</sup> Xing, W. Y.; Hua, Y.; Song, L.; Chen, X. L.; Zhang, P.; Ni, J. X. *Polym Deg Stab* 2009, 94, 1176–1182.
- <sup>25</sup> Cireli, A.; Onar, N.; Ebeoglugil, M. F.; Kayatekin, I.; Kutlu, B.; Culha, O.; Celik, E. *J Appl Polym Sci* 2007, 105, 3747–3756.
- <sup>26</sup> a) Spontón, M.; Ronda, J. C.; Galià, M.; Cádiz, V. *J Polym Sci Part A: Polym Chem* 2007, 45, 2142–2151, b) Ren, H.; Sun, J.; Zhao, Q. Zhiqi, C.; Ling, Q.; Zhou, Q. *J Appl Polym Sci* 2009, 112, 761–768, c) Seibold, S.; Schäfer, A.; Lohstroh, W.; Walter, O.; Döring, M. *J Appl Polym Sci* 2008, 108, 264–271, d) Lligadas, G.; Ronda, J. C.; Galià, M.; Cádiz, V. *J Polym Sci Part A: Polym Chem* 2006, 44, 6717–6727.
- <sup>27</sup> Spontón, M.; Ronda, J. C.; Galià, M.; Cádiz, V. *Polym Deg Stab* 2009, 94, 145–150.
- <sup>28</sup> Hoffmann, T.; Pospiech, D.; Häußler, L.; Komber, H.; Voigt, D.; Harnisch, C.; Kollann, C.; Ciesielski, M.; Döring, M.; Graterol, R. P.; Sandler, J.; Altstädt, V. *Macromol Chem Phys* 2005, 206, 423–431.
- <sup>29</sup> a) Canadell, J.; Mantecón, A.; Cádiz, V. *J Polym Sci Part A: Polym Chem*, 2007, 45, 1980–1992, b) Canadell, J.; Hunt, B. J.; Cook, A. G.; Mantecón, A.; Cádiz, V. *J Polym Sci Part A: Polym Chem* 2006, 44, 6728–6737.
- <sup>30</sup> Chen, X. T.; Sun, H.; Tang, X. D.; Wang, C. Y. *J Appl Polym Sci* 2008, 110, 1304–1309.
- <sup>31</sup> a) Seibold, S.; Schäfer, A.; Lohstroh, W.; Walter, O.; Döring, M. *J Appl Polym Sci* 2008, 108, 264–271, b) Lligadas, G.; Ronda, J. C.; Galià, M.; Cádiz, V. *J Polym Sci Part A: Polym Chem* 2006, 44, 5630–5644.
- <sup>32</sup> a) Hwang, H. J.; Lin, C. Y.; Wang, C. S. *J Appl Polym Sci* 2008, 110, 2413–2423, b) Spontón, M.; Lligadas, G.; Ronda, J. C.; Galià, M.; Cádiz, V. *Polym Degrad Stab* 2009, doi:10.1016/j.polymdegradstab.2009.06.020.
- <sup>33</sup> Yang, S. C.; Kim, J. P. *J Appl Polym Sci* 2007, 106, 2870–2874, b) Yang, S. C.; Kim, J. P. *J Appl Polym Sci* 2008, 108, 2297–2300, c) Zhao, C. S.; Chen, L.; Wang, Y. Z. *J Polym Sci Part A: Polym Chem* 2008, 46, 5752–5759.
- <sup>34</sup> Ge, X. G.; Wang, C.; Hu, Z.; Xiang, X.; Wang, J. S.; Wang, D. Y.; Liu, C. P.; Wang, Y. Z. *J Polym Sci Part A: Polym Chem* 2008, 46, 2994–3006.

- <sup>35</sup> Negrell-Guirao, C.; Boutevin, B. *Macromolecules* 2009, 42, 2446-2454.
- <sup>36</sup> Levchik, S. V.; Weil, E. D. *Polym Int* 2008, 57, 431-448.
- <sup>37</sup> Lomakin, S. M.; Zaikov, G. E. *Modern Polymer Flame Retardancy*, VSP, 2003, 8-28



## ADMET POLYMERIZATION

### Background

In the last years, olefin metathesis has become one of the most powerful synthetic methods.<sup>1</sup> Although double-bond scrambling reactions were initially reported in the mid-1950s,<sup>2</sup> and Banks and Bailey from Philips Petroleum conducted the first research on olefin metathesis and its industrial application in 1964,<sup>3</sup> it was not until 1967 that Calderon and co-workers recognized that both ring-opening polymerization and the disproportionation of acyclic olefins were the same reaction. They coined the term “olefin metathesis” (from greek, changing or exchanging positions).<sup>4</sup> As shown in figure 1, this transformation has a variety of applications. The illustrated examples include ring-opening metathesis (ROM), ring-closing metathesis (RCM), ring-opening metathesis polymerization (ROMP), acyclic diene metathesis polymerization (ADMET), and cross-metathesis (CM). These reactions have enabled the synthesis of an impressively wide range of unsaturated molecules which were challenging or even impossible to prepare by any other means.

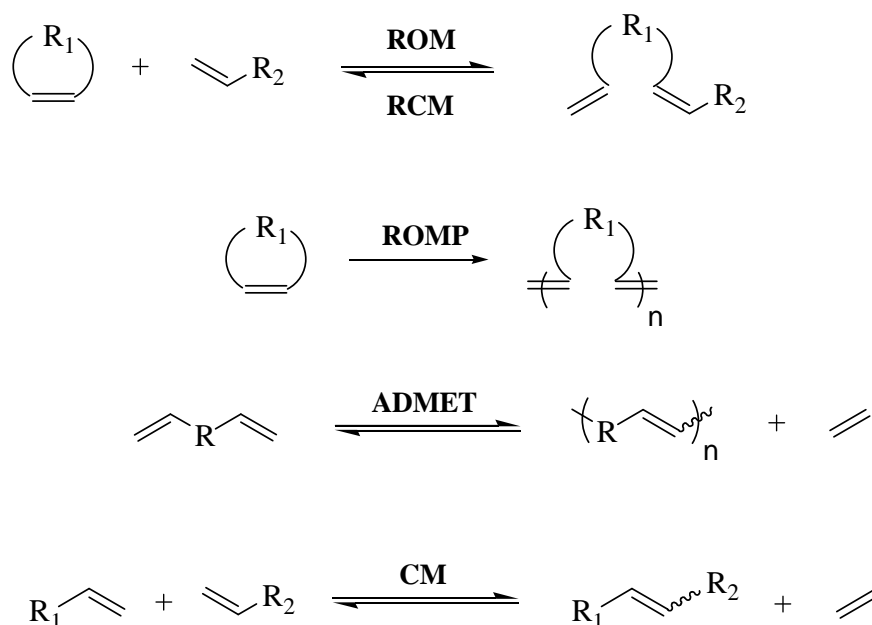
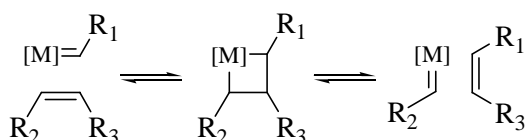


**Figure 1.** Various metathesis reactions.

From the mid-1950s to the early 1980s, all olefin metathesis was accomplished with poorly defined, multicomponent homogeneous and heterogeneous catalyst systems. These systems consisted of transition metal salts combined with main group alkylating agents or deposited on solid supports. The utility of these catalysts, however, was limited by the harsh conditions and strong Lewis acids that they required and that made them incompatible with most functional groups.<sup>5</sup> Extensive work was done to overcome these problems and to better understand this transformation. The mechanism of the reaction remained unknown until 1970, when Chauvin proposed that the key step in the reaction involves the formation of a metallocyclobutane ring intermediate from a metal carbene and an alkene (Scheme 1).<sup>6</sup>



**Scheme 1.** Mechanism proposed by Chauvin and Herisson.

The discovery of the mechanism of olefin metathesis eventually led to the rational design of progressively more advanced, well-defined catalyst systems. A significant breakthrough occurred in 1990 with Schrock's discovery of the well-defined, single-site tungsten and molybdenum alkylidene catalysts.<sup>7</sup> However, these early transition metal based complexes are highly oxophilic, making them susceptible to air and moisture poisoning if they are not employed under rigorously dry, oxygen-free conditions. They are also relatively intolerant to many functional groups, such as alcohols, aldehydes, and carboxylic acids. These factors limited the use of early transition metal-based catalyst for the metathesis of certain functionalized olefins, and thus, the key to improved functional group tolerance in olefin metathesis was the development of catalysts reacting preferentially with olefins in the presence of heteroatomic functionalities. Among the transition metal metathesis catalysts, ruthenium reacts preferentially with carbon-carbon double bonds over most other species, which makes these catalysts unusually stable toward alcohols, amides, aldehydes, and carboxylic acids.

The first well defined ruthenium based metathesis catalyst (**1**, figure 2), developed by Grubbs in the early 1990s, permitted the application of the olefin

metathesis reactions in presence of a wide variety of functional groups.<sup>8,9</sup> The metathesis activity as well as the functional group tolerance of these catalysts was further improved by the substitution of one of the trialkyl phosphine ligands by a N-heterocyclic carbene (NHC),<sup>10</sup> leading to the second generation Grubbs catalysts (**2** and **3** are shown as representative examples in figure 2).<sup>11</sup> Thus, with the introduction of highly active and robust metathesis catalysts, the number of polymeric structures available through the design of new monomers has ever since increased.

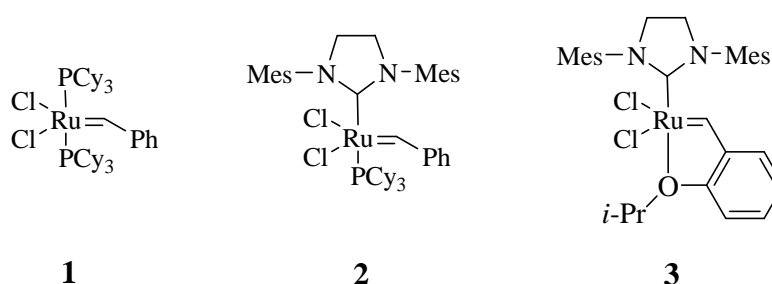


**Figure 2.** Grubbs 1<sup>st</sup> generation, Grubbs 2<sup>nd</sup> generation and Hoveyda-Grubbs 2<sup>nd</sup> generation metathesis catalysts

## ADMET polymerization

Acyclic diene metathesis (ADMET) polymerization is performed on  $\alpha,\omega$ -dienes to produce well-defined strictly linear polymers with unsaturated polyethylene backbones, as shown in figure 1. This step-growth polymerization is a thermally neutral process driven by the release of a small molecule condensate, ethylene. The development of the robust ruthenium metathesis catalysts greatly increased the versatility of this polymerization reaction to a point that “with few exceptions, if the diene monomer can be made, then a polymer can be produced by ADMET”, as affirmed by Wagener *et al.*<sup>12</sup>

The mechanism of the ADMET polymerization cycle (Figure 3) has been well documented where coordination of the olefin, followed by formation of a metalacyclobutane intermediate (**4**), and productive cleavage leads to the formation of the metathesis active alkylidene complex (**5**). Subsequent reaction with the double bond of a diene produce the metalacyclobutane ring (**6**) that leads to polymer formation. The continuation of the cycle proceeds by the coordination of another diene or growing polymer, productive cleavage, and the release of ethylene.

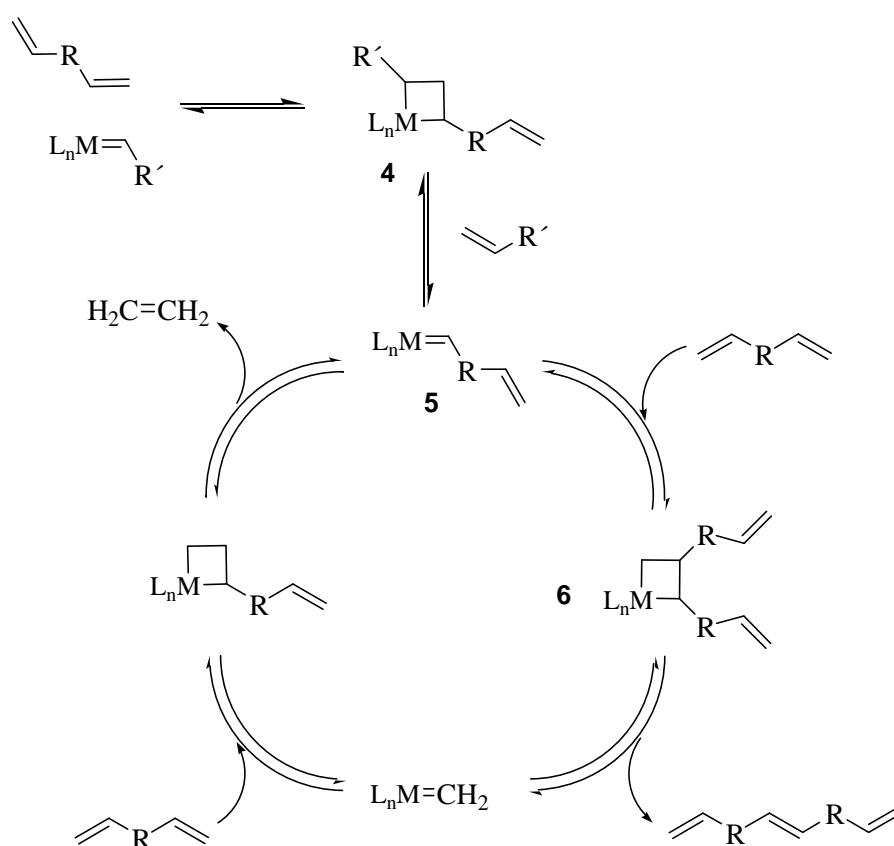


**Figure 3.** Mechanism of ADMET polymerisation.

It has been proven that ADMET polymerization can be carried out with heteroatom-containing monomers if the number of carbon atoms between an active olefin group and the functional group containing the heteroatom is high enough. This way, a potential coordination of the catalyst to the non-bonded electron pairs of the heteroatom is minimized, a phenomenon that has been called the negative neighboring group effect (NNGE).<sup>13</sup> Figure 4 shows some examples of polymers synthesized *via* ADMET containing different functional groups.<sup>12</sup>

Some examples of the versatility of ADMET polymerization found in recent literature include the ADMET polymerisation of glucose<sup>14</sup> and aminoacid-derived monomers,<sup>15</sup> the synthesis of fluorophore-containing organosilicon polymers,<sup>16</sup> carbosilane-based polymers,<sup>17</sup> telechelic elastomers containing silacyclobutane end groups,<sup>18</sup> halogen-<sup>19</sup> or nitro<sup>20</sup>-containing polymers, carbazol-,<sup>21</sup> thiophene-,<sup>22</sup> and diketopiperazine<sup>23</sup>-based polymers, polyamides,<sup>24</sup> polyesters,<sup>25</sup> polyacetals,<sup>26</sup> and even



oligomers of a transition metal-based monomer with phosphine ligands<sup>27</sup> and a monomer containing a dimeric transition metal (Mo) complex.<sup>28</sup>

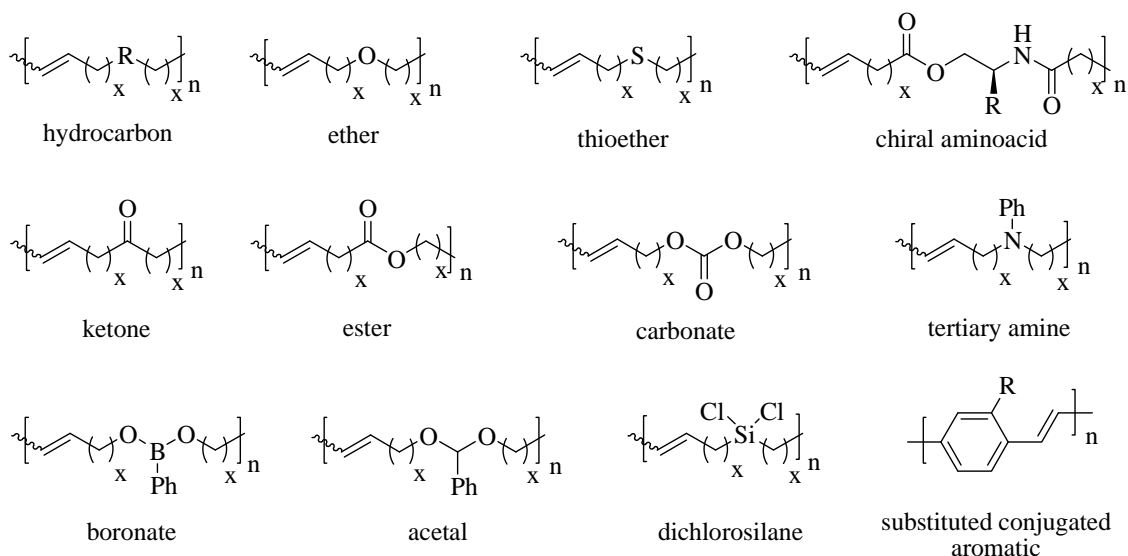


**Figure 4.** ADMET polymers with different functional groups

<sup>1</sup> a) Fürstner, A. *Angew Chem* 2000, 39, 3012-3043, b) Nicolaou, K. C.; Bulger, P. G.; Sarlah, D. *Angew Chem Int Ed* 2005, 44, 4490-4527.

<sup>2</sup> a) Eleuterio, H. S. *Olefin metathesis: chance favors those minds that are best prepared*. *J Mol Catal* 1991, 65, 55-61, b) Anderson, A. W.; Merckling, N. G. Polymeric bicyclo[2.2.1]hept-2-ene. U.S. Patent 2,721,189, 1955; *Chem. Abstr.* 1956, 50, 3008.

<sup>3</sup> Banks, R.L.; Bailey, G.C. *Ind Eng Chem Prod Res Develop* 1964, 3, 170.

<sup>4</sup> a) Calderon, N.; Ofstead, E. A.; Judy, W. A. *J. Polym Sci Pol Chem* 1967, 5, 2209, b) Calderon, N.; Chen, H. Y.; Scott, K. W. *Tetrahedron Lett.* 1967, 3327.

<sup>5</sup> Trnka T. M.; Grubbs R. H. *Acc Chem Res* 2001, 34, 18-29.

<sup>6</sup> Herisson, J. L.; Chauvin, Y. *Makromolekulare Chemie* 1971, 141, 161.

<sup>7</sup> Schrock, R. R. *Tetrahedron* 1999, 55, 8141-8153.

<sup>8</sup> Schwab, P.; France, M. B.; Ziller, J. W.; Grubbs, R. H. *Angew Chem Int Ed* 1995, 34, 2039-2041.

<sup>9</sup> Schwab, P.; Grubbs, R. H.; Ziller J. W. *J Am Chem Soc* 1996, 118, 100-110.

<sup>10</sup> Weskamp, T.; Schattenmann, W. C.; Spiegler, M.; Herrmann, W. A. *Angew Chem Int Ed* 1998, 37, 2490-2493.

- 
- <sup>11</sup> Scholl, M.; Ding, S.; Lee, C. W.; Grubbs, R. H. *Org Lett* 1999, 1, 953-956.
- <sup>12</sup> Schwendeman, J. E.; Church, A. C.; Wagener, K. B. *Adv Synth Catal* 2002, 344, 597-613.
- <sup>13</sup> Wagener, K. B.; Brzezinska, K.; Anderson, J. D.; Younkin, T. R.; Steppe, K.; DeBoer, W. *Macromolecules* 1997, 30, 7363-7369, b) Patton, J. T.; Boncella, J. M.; Wagener, K. B. *Macromolecules* 1992, 25, 3862, c) Wagener, K. B.; Smith, D. W. *Macromolecules* 1991, 24, 6073-6078.
- <sup>14</sup> Fokou, P. A.; Meier, M. A. R. *J Am Chem Soc* 2009, 131, 1664-1665.
- <sup>15</sup> Leonard, J. K.; Hopkins, T. E.; Chaffin, K.; Wagener, K. B. *Macromol Chem Phys* 2008, 209, 1485-1494.
- <sup>16</sup> Rathore, J. S.; Interrante, L. V. *Macromolecules* 2009, 42, 4614-4621.
- <sup>17</sup> Matloka, P. P.; Kean, Z.; Greenfield, M.; Wagener, K. B. *J Polym Sci: Part A: Polym Chem* 2008, 46, 3992-4011.
- <sup>18</sup> Delgado, P. A.; Zuluaga, F.; Matloka, P. P.; Wagener, K. B. *J Polym Sci: Part A: Polym Chem* 2009, 47, 5180-5183.
- <sup>19</sup> a) Boz, E.; Wagener, K. B.; Ghosal, A.; Fu, R.; Alamo, R. G. *Macromolecules* 2006, 39, 4437-4447, b) Boz, E.; Nemeth, A. J.; Wagener, K. B.; Jeon, K.; Smith, R.; Nazirov, F.; Bockstaller, M. R.; Alamo, R. G. *Macromolecules* 2008, 41, 1647-1653.
- <sup>20</sup> Walba, D. M.; Yang, H.; Keller, P.; Zhu, C.; Shao, R.; Coleman, D. A.; Jones, C. D.; Clark, *Macromol. Rapid Commun.* 2009, 30, N. A. DOI: 10.1002/marc.200900249.
- <sup>21</sup> Yamamoto, N.; Ito, R.; Geerts, Y.; Nomura, K. *Macromolecules* 2009, 42, 5104-5111.
- <sup>22</sup> Qin, Y.; Hillmyer, M. A. *Macromolecules* 2009, 42, 6429-6432.
- <sup>23</sup> Terada, K.; Berda, E. B.; Wagener, K. B.; Sanda, F.; Masuda, T. *Macromolecules* 2008, 41, 6041-6046.
- <sup>24</sup> Mutlu, H.; Meier, M. A. R. *Macromol Chem Phys* 2009, 210, 1019-1025.
- <sup>25</sup> Berda, E. B.; Wagener, K. B. *Macromol Chem Phys* 2008, 209, 1601-1611.
- <sup>26</sup> Wolfe, P. S.; Wagener, K. B. *Macromol Rapid Commun* 1998, 19, 305-308.
- <sup>27</sup> Shultz, G. V.; Zakharov, L. N.; Tyler, D. R. *Macromolecules* 2008, 41, 5555-5558.
- <sup>28</sup> Shultz, G. V.; Zemke, J. M.; Tyler, D. R. *Macromolecules* 2009 DOI: 10.1021/ma9013252

## **Chapter 3**

### **1. A Straightforward Strategy for the Efficient Synthesis of Acrylate and Phosphine Oxide-Containing Vegetable Oils and their Cross-linked Materials**



# A Straightforward Strategy for the Efficient Synthesis of Acrylate and Phosphine Oxide-Containing Vegetable Oils and their Cross-linked Materials

Lucas Montero de Espinosa, Juan C. Ronda, Marina Galià, Virginia Cádiz

Department of Analytical and Organic Chemistry, Rovira i Virgili University, Campus Sescelades, Marcel·lí Domingo s/n, 43007 Tarragona, Spain.

**ABSTRACT.** Phosphorus-containing triglycerides were prepared from a new route that involves the singlet oxygen photooxygenation of high oleic sunflower oil and further reduction of the resulting hydroperoxide derivatives to a mixture of secondary allylic alcohols. These allylic alcohols in presence of chlorodiphenylphosphine give allylic phosphinites capable to undergo a [2,3]-sigmatropic rearrangement leading to tertiary phosphine oxides directly linked to triglyceride in a one pot two step reaction. The obtained phosphorus-containing triglycerides with different hydroxyl content were activated to polymerisation by acrylation and these acrylate triglycerides were radically crosslinked in presence of different amounts of pentaerythritol tetraacrylate. The thermal, dynamic-mechanical, and flame retardancy properties of the final materials were evaluated. Thermal and thermooxidative degradation was studied by gas chromatography/mass spectrometry,  $^{31}\text{P}$  HR-MAS NMR spectroscopy, and scanning electron microscopy.

**Keywords:** triglyceride, phosphorus-containing, acrylate, crosslinking, renewable resources.

## INTRODUCTION

The exhaustion forecasts of petroleum reserves have lead the chemical industry to search for alternative feedstocks that can provide raw materials for the development of polymeric materials.<sup>1</sup> Plant oils, which can be found all around the world, are an attractive alternative to petroleum derivatives as precursors of polymeric materials.<sup>2</sup> Soybean oil, sunflower oil or linseed oil contain internal double bonds and have been used directly to obtain polymeric resins by cationic copolymerization with styrene and divinylbenzene.<sup>3</sup> However, the reactivity of these internal double bonds is limited. For

this reason, much work has been done on the functionalization of triglycerides to obtain useful monomers for the development of polymeric materials.<sup>4,5</sup> The epoxidation of natural oils and subsequent ring opening with acrylic acid has been well studied giving rise to different derivatives as acrylate epoxydized soybean oil (AESO),<sup>6</sup> which is commercially available. These monomers, that can be polymerized either radically or photochemically,<sup>7</sup> have been used in the development of resins. The properties of these materials, that can be conveniently modified by copolymerization with styrene or by variation of the monomer functionality<sup>8</sup> are comparable to those of conventional polymers and composites.<sup>9,10</sup> Recently, we described a new environmentally friendly route to obtain acrylate tryglicerides by photoperoxidation of high oleic sunflower oil and further reduction of the resulting hydroperoxide to allylic alcohols capable to be acrylated.<sup>11</sup>

Among all the desirable properties thermosets and elastomers should have, flame retardancy is one of the most important concerning the security of the final users of these materials. There are two ways to achieve flame retardancy in polymers. The first one is to incorporate flame retardants to manufactured polymers as additives, which is the most economical and straightforward way to infer flame retardancy. However, high amounts of the flame retardant component must be added to be effective and problems like incompatibility, migration and reduction of the mechanical properties of the base polymer make this approach unattractive. The second approach to flame retardancy is the design of new intrinsically flame retardant polymers. This reactive approach avoids the problems that can be found in additive flame retardants and permits the preparation of polymers with specific properties through the design of flame retardant monomers.

In this way, we are working on the development of flame retardant thermosets based on phosphorus-containing vegetable oils.<sup>12,13</sup> There are few examples on the modification of plant oils to infer flame retardant properties. Küseföglu and Eren<sup>14</sup> reported the bromoacrylation of soybean and high oleic sunflower oil to afford a new monomer that was used in the preparation of flame retardant thermosets. Halogenated flame retardants present advantages as the high efficiency, even in very small amounts, or the low cost. However, they have clear disadvantages as the generation of toxic and corrosive gases during the combustion process. Efforts have been made in the development of halogen-free flame retardants such as those containing P, N, Si and B, which are known to inhibit or retard the fire spreading by acting in the condensed phase, in the gaseous phase or in both. Among them, phosphorus is known to act in the

condensed phase promoting char formation and thus preventing air to reach the material surface and diffusion of gaseous products into the flame.<sup>15</sup> There is a wide range of phosphorus containing flame retardants since phosphorus can exist in several oxidation states. Phosphate, phosphonate and phosphinate based reactive flame retardants have been widely used.<sup>15-19</sup> They have proved to generate very efficiently the char residue, but also there are evidences of their action in the gas phase.<sup>16-18</sup> However, the P-O bond has a general poor hydrolytic and thermal stability<sup>20</sup> that limits the range of application of the final polymeric materials. The tertiary phosphine oxides have also been used as reactive flame retardants.<sup>19,21,22</sup> They have P-C bonds that confer a higher thermal and hydrolytic stability to the polymers.<sup>23</sup>

Among the different possible ways of preparing tertiary phosphine oxides-containing triglycerides, we chose the simple and straightforward [2,3]-sigmatropic rearrangement of allylic phosphinites.<sup>24</sup> Thus, in this work we describe the synthesis of phosphorus-containing triglycerides from a new route that involves the singlet oxygen photooxygenation of high oleic sunflower oil and further reduction of the resulting hydroperoxide derivatives to a mixture of secondary allylic alcohols that are suitable precursors of the allylic phosphinites. The obtained phosphorus-containing triglycerides with different hydroxyl content were activated to polymerisation by acrylation and these acrylate triglycerides were radically crosslinked in presence of different amounts of pentaerythritol tetraacrylate. Following this strategy, a range of phosphorus-containing triglycerides has been prepared from high oleic sunflower oil and their thermal and flame retardance properties (LOI) have been investigated.

## EXPERIMENTAL

### Materials

High oleic sunflower oil (SO) (minimum 80% oleic acid) was kindly supplied by Borges<sup>®</sup>. *Meso*-tetraphenylporphyrin (TPP) (Aldrich), *N,N'*-dimethylaminopyridine (Aldrich), chlorodiphenylphosphine (Aldrich), dicumyl peroxide (DCP) (Aldrich), ethylacetate (Scharlab), celite 535 (Fluka) and MgSO<sub>4</sub> (Scharlab) were used as received. Triethylamine (Aldrich) was dried by distillation over CaH<sub>2</sub> and acryloyl chloride (Aldrich) was distilled before use. Dichloromethane was dried over P<sub>2</sub>O<sub>5</sub> and distilled immediately before use. Toluene was distilled over sodium/benzophenone immediately before use. Pentaerythritol tetraacrylate (PETA) (Aldrich) was dissolved in ethyl ether

and washed with an aqueous solution of NaOH (5%) before use to remove the stabiliser. Hydroxyl sunflower oil (HSO) was synthesized as previously described.<sup>11</sup> TLC plates were developed by spraying with sulphuric acid/anisaldehyde ethanol solution and heating at 200 °C.

**Synthesis of Phosphorus-containing Sunflower Oil (P-SO) (Scheme 1).** 10 g (0.01 mol) of HSO and the desired amount of N,N'-dimethylaminopyridine: 0.76 g (0.006 mol), 1.51 g (0.012 mol) or 2.27 g (0.018 mol) were placed in a 500 mL round bottomed flask and degassed applying vacuum for 10 minutes. 250 mL of dry toluene were added under argon atmosphere and the mixture was stirred. The required amount of chlorodiphenylphosphine: 1.32 g (0.006 mol), 2.65 g (0.012 mol) or 3.97 g (0.018 mol) was added and the mixture was stirred for 1 hour at room temperature. The mixture was then heated to reflux for 12 h. The reaction was allowed to cool down and toluene was removed under reduced pressure. The reaction mixture was dissolved in 100 mL of dichlorometane and washed with 10% HCl, brine and water. The organic layer was dried over MgSO<sub>4</sub> and the solvent was removed under reduced pressure. P-SO was obtained as an oily product with 90% yield.

FTIR: 3396 cm<sup>-1</sup>, 3054 cm<sup>-1</sup> (Aromatic, stretching), 1734 cm<sup>-1</sup> (ester C=O, stretching), 1436 cm<sup>-1</sup>, (P-C<sub>Ar</sub>, stretching), 1116 cm<sup>-1</sup> (P=O, stretching), 748 and 696 cm<sup>-1</sup> (Aromatic, out-of-plane deformation).

<sup>1</sup>H NMR (CDCl<sub>3</sub>, TMS, δ in ppm): 7.82-7.67 (m, *o*-Ar), 7.50-7.36 (m, *m*-Ar, *p*-Ar), 5.63-5.54 (m, CH=CH-CHOH), 5.41 (dd, *J* = 15.6, 7.2 Hz, CH=CH-CHOH), 5.32-5.19 (m, -CH=CH- and CH-O), 4.31-4.22 (m, CH<sub>2</sub>-O), 4.16-4.08 (m, CH<sub>2</sub>-O), 3.99 (q, *J* = 6.7 Hz, CH-OH), 2.94-2.84 (m, CH-P), 2.33-2.20 (m, CO-CH<sub>2</sub>-), 1.98 (q, *J* = 6.67 Hz, CH<sub>2</sub>-CH=CH-CHOH), 1.93-1.81 (m, CH<sub>2</sub>-CH=CH-CHP), 1.66-1.41 (m, CH<sub>2</sub>-CH-P and CH<sub>2</sub>-CH<sub>2</sub>-CO), 1.47-0.91 (m, aliphatic), 0.89-0.78 (m, CH<sub>3</sub>).

<sup>13</sup>C NMR (CDCl<sub>3</sub>, TMS, δ in ppm): 173.36-172.95 (COOR, ester), 137.27-136.87 (CH=CH-CHP), 133.41-133.13 (CH=CH-CHOH), 132.52-132.12 (CH=CH-CHOH), 132.12-131.17 (Ar), 128.72-128.23 (*m*-Ar or *p*-Ar), 124.15-123.87 (CH=CH-CHP), 73.17 (CH-OCO, acrylate), 68.95 (CH-OCO, glyceryl), 62.18 (CH<sub>2</sub>-OCO, glyceryl), 43.93 (d, *J* = 70.42 Hz, CH-P) out-of-plane deformation, 37.44 (CH<sub>2</sub>-CHOH), 34.22-34.08 (CH<sub>2</sub>-CO), 32.69 (CH<sub>2</sub>-CH=CH-CHP), 32.31-32.19 (CH<sub>2</sub>-CH=CH-CHOH), 31.98-31.84 (CH<sub>2</sub>-CH<sub>2</sub>-CH<sub>3</sub>), 29.80-28.82 (aliphatic), 27.75-27.62 (CH<sub>2</sub>-CH<sub>2</sub>CHP),



27.09 (CH<sub>2</sub>-CHP), 25.79-25.55 (CH<sub>2</sub>-CH<sub>2</sub>CHO), 24.92 (CH<sub>2</sub>-CH<sub>2</sub>COOR), 22.76 (CH<sub>2</sub>-CH<sub>3</sub>), 14.20 (CH<sub>3</sub>).

<sup>31</sup>P NMR (CDCl<sub>3</sub>, H<sub>3</sub>PO<sub>4</sub>, δ in ppm): 34.30, 34.25.

### Synthesis of Phosphorus-containing Acrylate Sunflower Oil (P-ASO) (Scheme 1).

A 100 mL round-bottomed flask was charged with P-SO (10 g), dichloromethane (50 mL) and a magnetic stirrer under inert atmosphere. The solution was cooled to 0 °C. Acryloyl chloride: 3.3 mL (0.041 mol), 2.36 mL (0.029 mol), 1.62 mL (0.020 mol) or 1.07 mL (0.013 mol) followed by triethylamine: 11.3 mL (0.081), 8.1 mL (0.058 mol), 5.6 mL (0.040 mol) or 3.7 mL (0.026) were carefully added with immediate formation of a white precipitate. The resulting mixture was allowed to reach room temperature and was stirred for 1h more. The solvent was eliminated at reduced pressure. Then 5 mL of ethyl acetate were added. The solution was filtered through a short pad of celite and ethyl acetate was passed to recover the entire product. The solvent was removed at reduced pressure and then the oily product was dissolved in dichloromethane and washed twice with brine. The organic layer was dried over MgSO<sub>4</sub> and the solvent was removed under reduced pressure to obtain P-ASO. The number of acrylate groups per triglyceride in the three derivatives was found to be 1.6, 1.4 and 1.0 per triglyceride by <sup>1</sup>H-NMR spectroscopy (calculated by the integration of methine linked to P). No further purification was carried out. Yields 83-88%.

FTIR: 1740 cm<sup>-1</sup> (ester C=O, stretching), 1722 cm<sup>-1</sup> (acrylate C=O, stretching), 1636 and 1618 cm<sup>-1</sup> (double bond, stretching), 1403 cm<sup>-1</sup> (double bond, in-plane deformation), 1187 cm<sup>-1</sup> (C-O, st.), 809 cm<sup>-1</sup> (double bond, out-of-plane deformation).

<sup>1</sup>H NMR (CDCl<sub>3</sub>, TMS, δ in ppm): 7.83-7.67 (m, *o*-Ar), 7.52-7.35 (m, *m*-Ar, *p*-Ar), 6.36 (dd, *J* = 17.32, 1.27 Hz, CO-CH=CH<sub>2</sub>), 6.09 (dd, *J* = 17.31, 10.40 Hz, CO-CH=CH<sub>2</sub>), 5.78 (dd, *J* = 10.38, 1.45 Hz, CO-CH=CH<sub>2</sub>), 5.72-5.64 (m, CH=CH-CHOH), 5.37 (ddd, *J* = 15.32, 7.46, 1.58 Hz, CH=CH-CHOH), 5.30-5.20 (m, -CH=CH-CHP and CH-O), 4.27 (dd, *J* = 11.77, 3.75 Hz, CH<sub>2</sub>-O), 4.15-4.07 (m, CH<sub>2</sub>-O), 2.94-2.84 (m, CH-P), 2.33-2.20 (m, CO-CH<sub>2</sub>), 1.99 (q, *J* = 7.05 Hz, CH<sub>2</sub>-CH=CH-CHOH), 1.93-1.79 (m, CH<sub>2</sub>-CH=CH-CHP), 1.70-1.47 (m, CH<sub>2</sub>-CH-P, CH<sub>2</sub>-CHOH and CH<sub>2</sub>-CH<sub>2</sub>-CO), 1.45-0.98 (m, aliphatic), 0.90-0.78 (CH<sub>3</sub>).

<sup>13</sup>C NMR (CDCl<sub>3</sub>, TMS, δ in ppm): 173.09-172.64 (COOR), 165.45 (COOR, acrylate), 136.97-136.58 (CH=CH-CHP), 134.55-134.17 (CH=CH-CHO), 131.45-130.98 (Ar),

130.21 (CO-CH=CH<sub>2</sub>), 128.94 (CO-CH=CH<sub>2</sub>), 128.54-128.04 (*m*-Ar or *p*-Ar), 128.33-128.08 (CH=CH-CHO), 124.13-123.87 (CH=CH-CHP), 75.10 (CH-OCO, acrylate), 68.82 (CH-OCO, glyceryl), 61.99 (CH<sub>2</sub>-O, glyceryl), 43.83 (d, *J* = 69.38 Hz, CH-P), 34.47 (CH<sub>2</sub>-CHO), 34.04-33.81 (CH<sub>2</sub>-COOR), 32.51-32.45 (CH<sub>2</sub>-CH=CH-CHP), 32.14-32.05 (CH<sub>2</sub>-CH=CH-CHO), 31.86-31.67 (CH<sub>2</sub>-CH<sub>2</sub>-CH<sub>3</sub>), 29.63-28.55 (aliphatic), 27.60-27.33 (CH<sub>2</sub>-CH<sub>2</sub>-CHP), 27.01 (CH<sub>2</sub>-CHP), 25.12-25.07 (CH<sub>2</sub>-CH<sub>2</sub>CHO), 24.77-24.62 (CH<sub>2</sub>-CH<sub>2</sub>COOR), 22.63-22.55 (CH<sub>2</sub>-CH<sub>3</sub>), 14.09-14.05 (CH<sub>3</sub>).

<sup>31</sup>P NMR (CDCl<sub>3</sub>, H<sub>3</sub>PO<sub>4</sub>, δ in ppm): 34.26, 34.20.

### Curing reactions and solubility tests.

The curing reactions were carried out as follows. Each triglyceride derivative, ASO and P-ASOs was deoxygenated using vacuum-argon cycles to prevent oxygen free radical inhibition processes. Then they were mixed with the desired amount of deoxygenated PETA. Dicumyl peroxide (1.5% w/w) was added with effective stirring and the mixture was heated to 50°C. The resulting homogeneous mixture was put in a previously heated (80 °C) mold (100 x 6 x 4 mm<sup>3</sup>). The temperature was increased from 80 °C to 110 °C at a heating rate of 1° C/min and then the temperature was increased rapidly to 130 °C and maintained for 2h.

The soluble part of the cured samples was extracted by refluxing 0.5 g. of each sample (thoroughly triturated) in 50 mL of distilled THF during 12 h.

### Instrumentation

<sup>1</sup>H NMR 400 MHz, <sup>13</sup>C NMR 100.6 MHz and <sup>31</sup>P 161.9 MHz NMR spectra were obtained using a Varian Gemini 400 spectrometer with Fourier transform, CDCl<sub>3</sub> as solvent and TMS as internal standard. <sup>1</sup>H and <sup>31</sup>P HR-MAS spectra were recorded on a Bruker Avance III 500 spectrometer operating at a proton frequency of 500.13 MHz. The instrument was equipped with a 4-mm triple resonance (<sup>1</sup>H, <sup>13</sup>C, <sup>31</sup>P) gradient HR-MAS probe. A Bruker Cooling Unit (BCU-Xtreme) was used to keep the sample temperature at 27°C. Samples conveniently prepared with CDCl<sub>3</sub> were spun at 6 kHz in order to keep the rotation side bands out of the spectral region of interest. One-dimensional (1D) <sup>1</sup>H spectra were acquired in 1 min and 16 scans with a 1.0-s relaxation delay. The IR analyses were performed on a FTIR-680PLUS spectrophotometer with a resolution of 4 cm<sup>-1</sup> in the transmittance mode. An attenuated-

total-reflection accessory with thermal control and a diamond crystal was used to determine FTIR/ATR spectra.

Calorimetric studies were carried out on a Mettler DSC821e thermal analyzer using N<sub>2</sub> as a purge gas (20 mL/min) at a scan rate of 10°C/min in the 30-300°C temperature range. Dynamic mechanical thermal analysis (DMTA) was performed using a TA DMA 2928 in three-point bending geometry at a fixed frequency of 1 Hz in the -100 to 200 °C range and at a heating rate of 3 °C/min. The dimensions of the samples were 15 x 6 x 4 mm<sup>3</sup>.

Thermal stability studies were carried out on a Mettler TGA/SDTA851e/LF/1100 with N<sub>2</sub> as purge gas. The studies were performed in the 30-800 °C temperature range at a scan rate of 10°C/min.

The limiting oxygen index (LOI) (ASTM D 2863) is the minimum concentration of oxygen determined in a flowing mixture of oxygen and nitrogen that will just support the flaming combustion of materials. LOI values were measured on a Stanton Redcroft instrument provided with an oxygen analyser. The dimensions of the polymer plaques were 100 x 6 x 4 mm<sup>3</sup>.

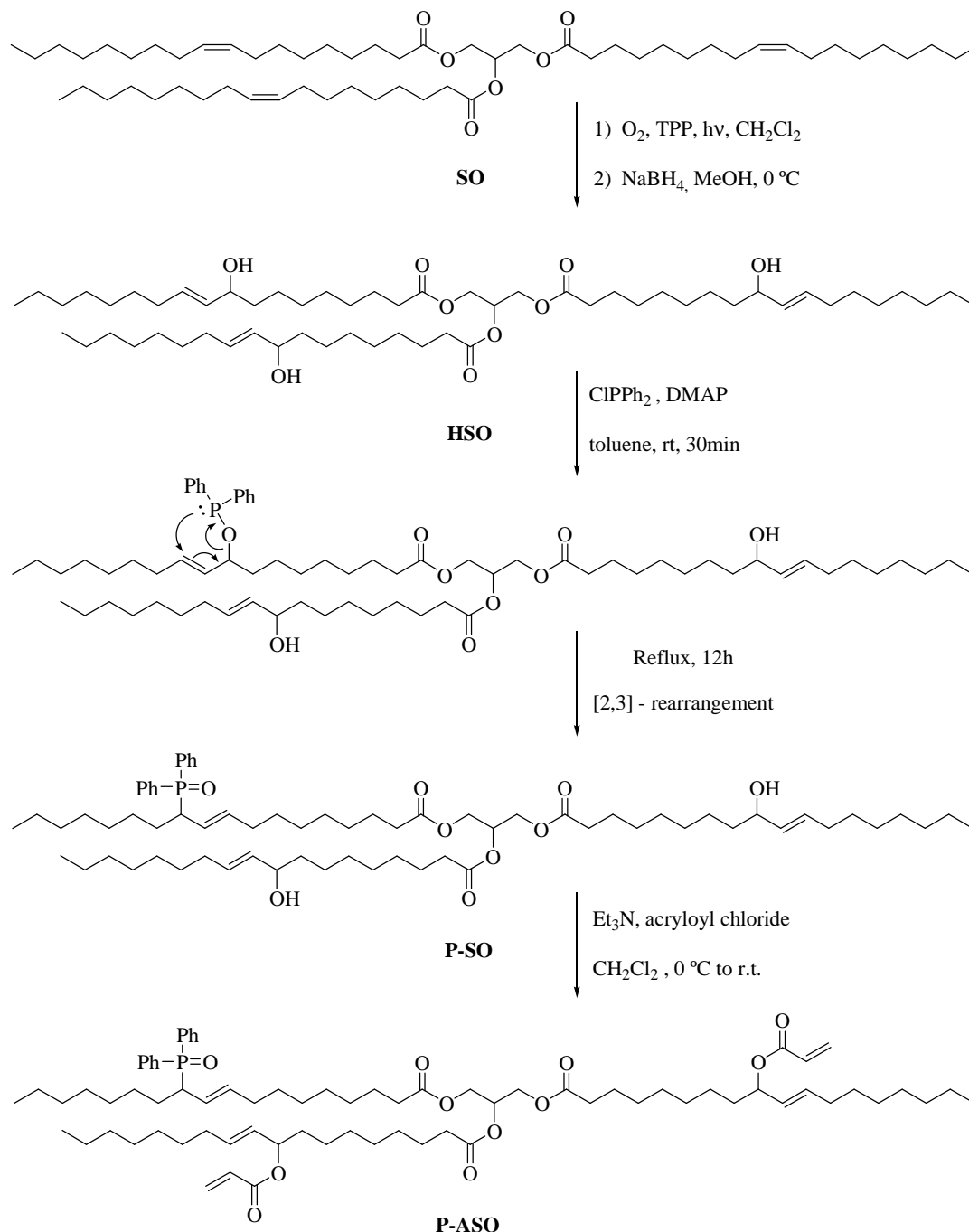
Degradation studies were carried out in a Carbolite TZF 12/38/400 oven connected to a condenser cooled by liquid nitrogen. GC-MS measurements were carried out using an HP 6890 gas chromatograph with an Ultra 2 capillary column (crosslinked 5 % PH ME siloxane) and an HP 5973 mass detector.

Scanning electron microscopy (SEM) was performed on a JEOL JSM 6400 scanning electron microscope, at an activation voltage of 10 kV. For the atomic mapping, an Oxford INCA Energy Dispersive X-Ray Micro Analyzer was used.

## RESULTS AND DISCUSSION

In the synthesis of phosphorus-containing triglycerides (Scheme 1) we used as starting compound a secondary alcohol containing-triglyceride derivative (HSO) which was synthesized through photoperoxidation with singlet oxygen and further reduction of high oleic sunflower oil (SO).<sup>11</sup> The allylic hydroxyls of HSO were reacted with chlorodiphenylphosphine (CDPP), in presence of DMAP as base, to obtain the intermediate allylic phosphinites. When heated to 120 °C, these allylic phosphinites undergo a [2,3] sigmatropic rearrangement to give a tertiary phosphine oxide with new P-C bonds that link the phosphorus directly to the fatty acid chains (P-SO). To the best

of our knowledge, this thermal rearrangement (Arbuzov-type rearrangement) of allylic diphenylphosphinites has not been applied to a triglyceride derivative, as a very efficient procedure to obtain allylic phosphine oxides.



**Scheme 1.** Synthesis of hydroxyl functionalized triglycerides (HSO), phosphorus-containing derivatives (P-SO) and acrylated phosphorus-containing derivatives (P-ASO).

This phosphorus-containing triglyceride was obtained with high purity after work-up of the reaction and no further purification was carried out. Taking into account that the average number of allylic hydroxyls per triglyceride in the starting material is 2.5 (measured by  $^1\text{H-NMR}$ ), we could react it with different amounts of CDPP in order to obtain a set of triglyceride derivatives with different phosphorus content. The remaining hydroxyl groups were esterified with acryloyl chloride in presence of triethylamine to obtain P-ASOs, thus introducing the necessary reactive sites for further crosslinking.

NMR spectroscopy allowed us to follow each step of the synthesis. Figure 1a) shows the  $^1\text{H-NMR}$  spectrum of the starting triglyceride HSO where the three multiplets at 5.6, 5.4 and 4.0 ppm corresponding to the protons  $\text{H}_\text{A}$ ,  $\text{H}_\text{B}$  and  $\text{H}_\text{C}$  of the allylic alcohol moiety can be seen. The  $^1\text{H NMR}$  spectrum of the P-SO, depicted in Fig. 1b), shows the partial disappearance of the signals corresponding to the double bond ( $\text{H}_\text{A}$  and  $\text{H}_\text{B}$ ) of HSO and the appearance of new double bond signals ( $\text{H}_\text{D}$  and  $\text{H}_\text{E}$ ) corresponding to the allylic tertiary phosphine oxide in P-SO. Moreover, there is a decreasing in the intensity of the signal belonging to the methine proton linked to the hydroxylic group ( $\text{H}_\text{C}$ ) at 4.0 ppm, and a multiplet of new appearance due to the methine

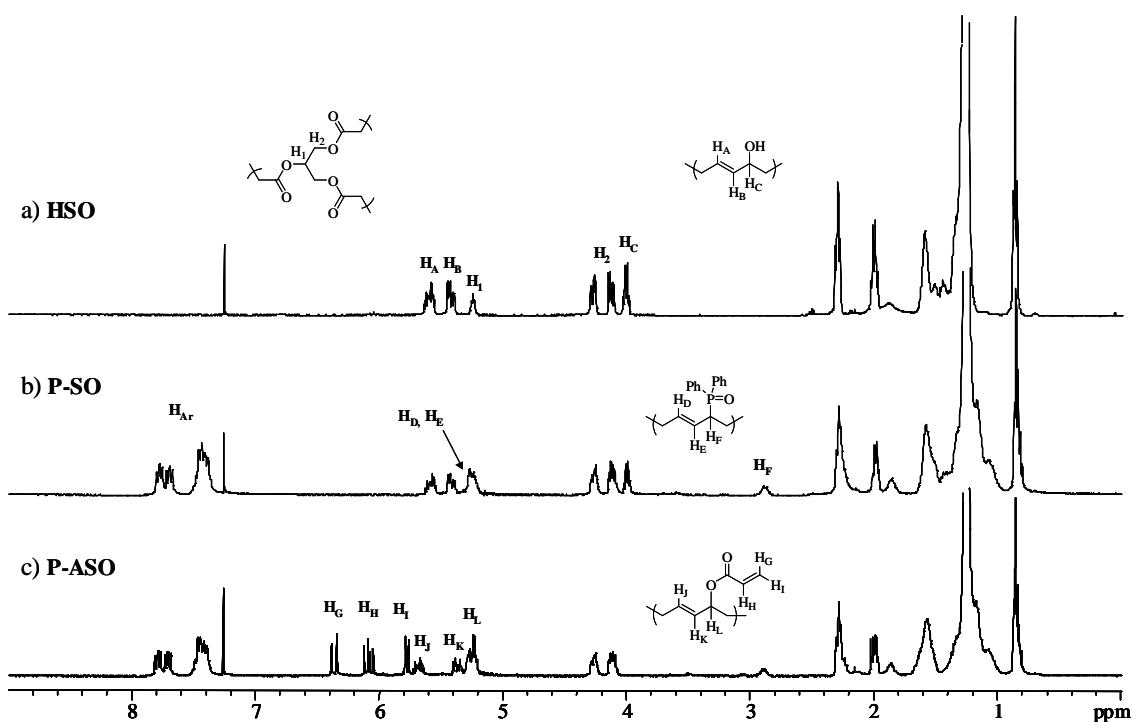


**Figure 1.**  $^1\text{H NMR}$  spectra of a) HSO, b) P-SO and c) P-ASO recorded in  $\text{CDCl}_3$ .

linked to the phosphorus ( $H_F$ ) centered at 2.8 ppm. Fig 1c) shows the  $^1H$  NMR spectrum of P-ASO which confirms the complete introduction of the acrylic moieties by the typical set of vinyl signals at 6.3, 6.1 and 5.7 ppm ( $H_G$ ,  $H_H$  and  $H_I$  respectively), the disappearance of the signal  $H_C$  of proton methine linked to OH and the presence of the signal  $H_L$  of proton methine linked to O-CO-CH=CH<sub>2</sub>.

As the phosphorus content of the modified oil was increased, the number of free hydroxyl groups decreased. The problem associated with this fact is that few crosslinking reactive sites were available at high phosphorus contents. As the properties of the resulting materials are directly related to the crosslinking density, the use of a crosslinking agent is necessary to obtain highly crosslinked materials at high phosphorus contents. In a previous work we used pentaerythritol tetraacrylate (PETA) as crosslinking agent to improve the properties of two different acrylate high oleic sunflower oil derivatives.<sup>11</sup> We could determine that the addition of 5% w/w of PETA was enough to increase significantly the T<sub>g</sub> value and to decrease the soluble part until 2-3%. Thus, if we take as reference the 5% w/w of PETA added in the ASO crosslinking, the contents of PETA in the P-ASOs were increased to compensate the lower number of acrylate groups (Table 1). The phosphorus content in P-ASOs was determined by  $^1H$ -NMR spectroscopy. After crosslinking, the phosphorus content in the final materials was calculated regarding the amount of P-ASO and PETA added in each sample. In this way, four crosslinked materials were synthesized with 0.0 (ASO/PETA), 1.4, 2.0 and 2.8 % w/w of phosphorus content.

**Table 1.** Soluble fractions, T<sub>g</sub> values of the cured P-ASO/PETA systems.

Triglyceride	PETA (%) <sup>a</sup>	P content (%) <sup>a</sup>	Soluble Fraction (%) <sup>a,b</sup>	T <sub>g</sub> (°C) <sup>c</sup>
ASO	5	0.0	2.7	25
P-ASO-I	17	1.4	3.0	15
P-ASO-II	20	2.0	4.9	18
P-ASO-III	25	2.8	12.6	14

<sup>a</sup> Weight / weight percentages, <sup>b</sup> in THF, <sup>c</sup> maximum of the Tan  $\delta$  peak.

DSC experiments were carried out in order to establish the curing conditions. Figure 2 shows the DSC traces of the four curing systems. The 0% phosphorus sample

(curve a) exhibits a crosslinking exotherm centered at 153 °C with a little shoulder around 190 °C that can be attributed to the thermal crosslinking of the remaining unreacted acrylates.<sup>11</sup> However, the exotherms belonging to the phosphorus-containing curing systems show multiple exotherms. The P-ASO-I sample (curve b) presents a main exotherm at 158 °C with a shoulder at 142 °C. When the phosphorus content is increased to 2.0% in P-ASO-II (curve c), the intensities of both exotherms are reversed, the exotherm at 142 °C significantly increases and the other one, at 158 °C, becomes smaller. The P-ASO-III sample (curve d) gives two similar exotherms at 142 °C and 150 °C.

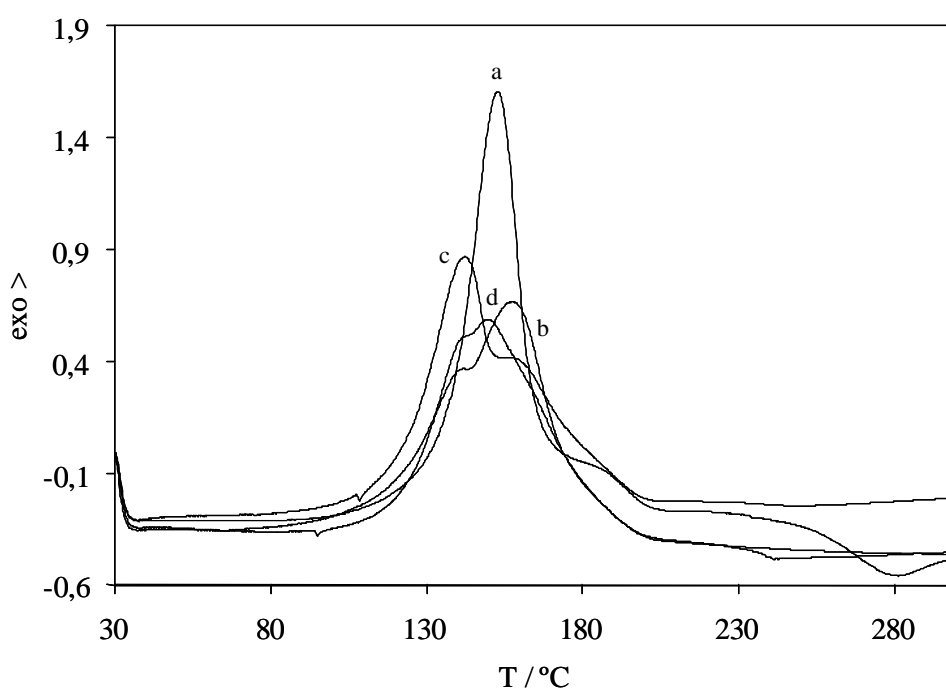


**Figure 2.** DSC plots of the curing systems a) ASO/PETA; b) P-ASO-I/PETA; c) P-ASO-II/PETA and d) P-ASO-III/PETA.

To better understand this behavior, DSC experiments of samples with different phosphorus and PETA contents were run. The results are shown in Figure 3. Firstly, the plot of the 0% phosphorus sample (ASO) gave, either in absence (Fig. 3a) or in presence (Fig. 3b) of PETA, only one sharp exotherm showing a similar reactivity between both acrylate groups. However, when P-ASO-I was run in absence of PETA (Fig. 3c) a broadening of the exotherm was observed. The addition of PETA to P-ASO-I caused the splitting of the exotherm in two peaks (Fig. 3d). Therefore, the presence of

phosphorus in any studied system produces either a broadening or even two maxima in the DSC curves, indicating that more than one process occurs. This fact is also observed in the case of P-ASO-II and P-ASO-III where the presence of PETA causes the same behavior (see curve c and d in Fig. 2).

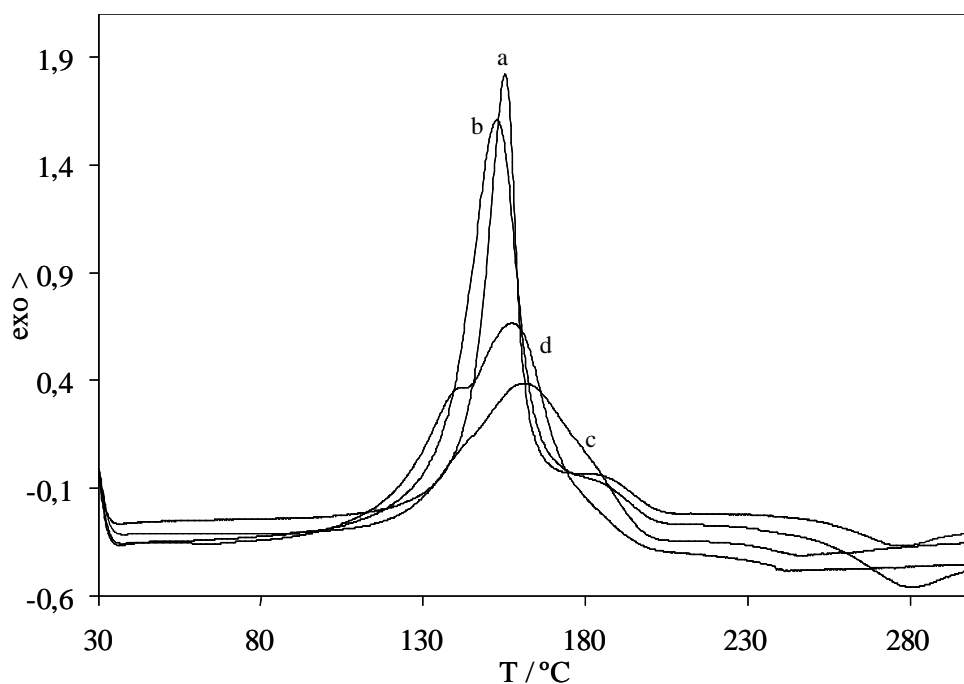


**Figure 3.** Curing DSC plots of a) ASO; b) ASO/PETA; c) P-ASO-I and d) P-ASO-I/PETA.

Taking the information from DSC curing, we applied the same curing program to all systems. The samples were heated in a mould from 80 °C to 110 °C at 1 °C/min and then at 130 °C for 2h. The temperature was raised at 1 °C/min to avoid bubbles formation during the first steps of the crosslinking. The curing was followed by FTIR-ATR spectroscopy. Figure 4 shows the initial and final spectra of the P-ASO-II curing system. The total disappearance of the acrylate double bond bands at ca., 1630 and 1620  $\text{cm}^{-1}$  (stretching vibration), 1405, 1292, 1261 and 1057  $\text{cm}^{-1}$  (CH and  $\text{CH}_2$  in-plane deformations) and 981, 967 and 806  $\text{cm}^{-1}$  (CH and  $\text{CH}_2$  out-of-plane deformations) confirms that the crosslinking reaction takes place.<sup>25,26</sup>

The extent of the crosslinking reactions was investigated by extracting the soluble part of the cured samples by refluxing in THF for 12h. Table 1 shows the weight



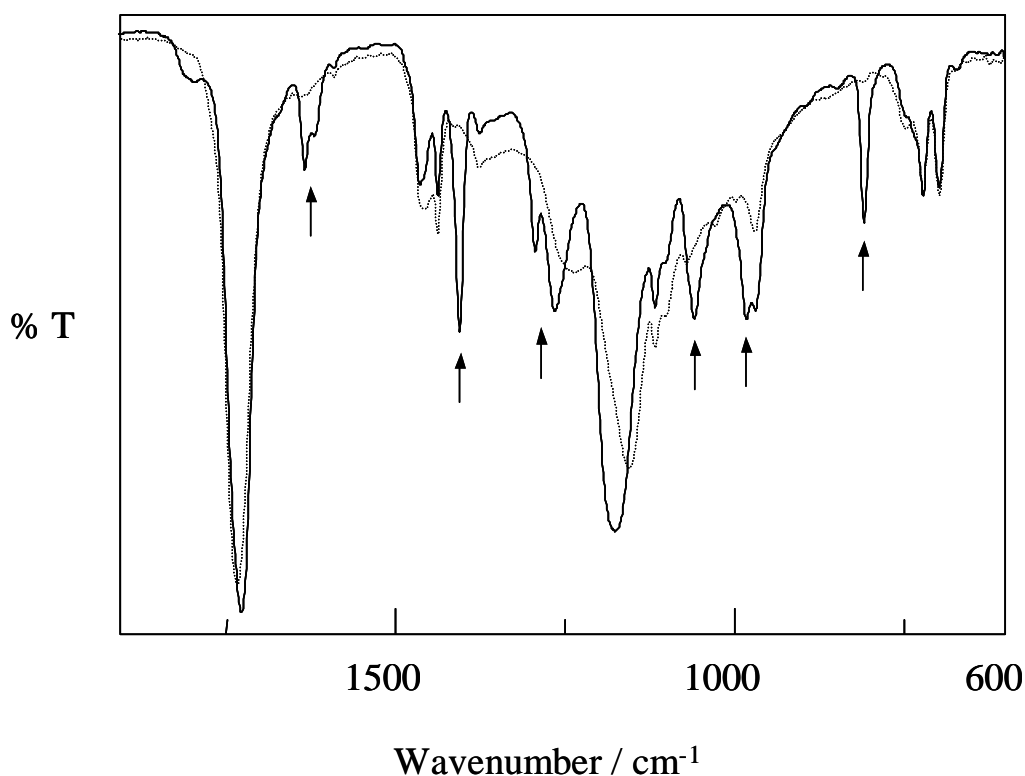


**Figure 4.** FTIR-ATR spectra of a mixture of P-ASO-I/ PETA before heating (plain line) and after curing (dashed line).

percentages of the soluble fractions for each system. These values indicate the formation of crosslinked structures due to the reaction of the acrylate groups, in agreement with the IR data. These values are the result of two opposite factors. First, an increase of the phosphorus content leads to a decrease of the acrylate functionality in the triglyceride and thus to a higher soluble fraction. On the other hand, as PETA content increases a higher crosslinking degree structure should be obtained with lower values of soluble fractions. However, this last factor seems not to be significant.

High Resolution MAS NMR spectroscopy was used as a useful tool to further study the extent of the crosslinking reaction in the resulting thermosets. Conventional solid NMR spectroscopy usually results in signal broadening due to the lack of molecular mobility. However, HR-MAS NMR spectroscopy reduces significantly this broadening by spinning the sample around an axis oriented at an angle  $\theta = 54.7^\circ$  with the direction of the magnetic field. The sample is spun at a rate larger than the anisotropic interactions causing them to be averaged to their isotropic value and therefore, resulting in signal narrowing. In order to obtain a good spectrum, a solvent

must be added that swells the polymer in some extent. However, the swelling is less effective in the sections of the polymer with a higher crosslinking density. As a result the crosslinking sites cannot be seen with the same resolution as the sections with higher mobility. Figure 5 depicts the  $^1\text{H}$  and  $^{31}\text{P}$  HR-MAS NMR spectra of P-ASO-III. This powerful technique makes possible to analyze in an accurate way the structural changes that took place during crosslinking. In the  $^1\text{H}$  NMR, spectrum not remaining acrylate signals are observed. Moreover, the internal double bonds of the triglyceride can still be observed indicating that these groups are less reactive than acrylate towards radical polymerisation and remain unreacted in the polymeric network. The  $^{31}\text{P}$  NMR spectrum shows a broad peak centred at 34 ppm showing that during crosslinking the phosphine oxide moiety remains unaltered.

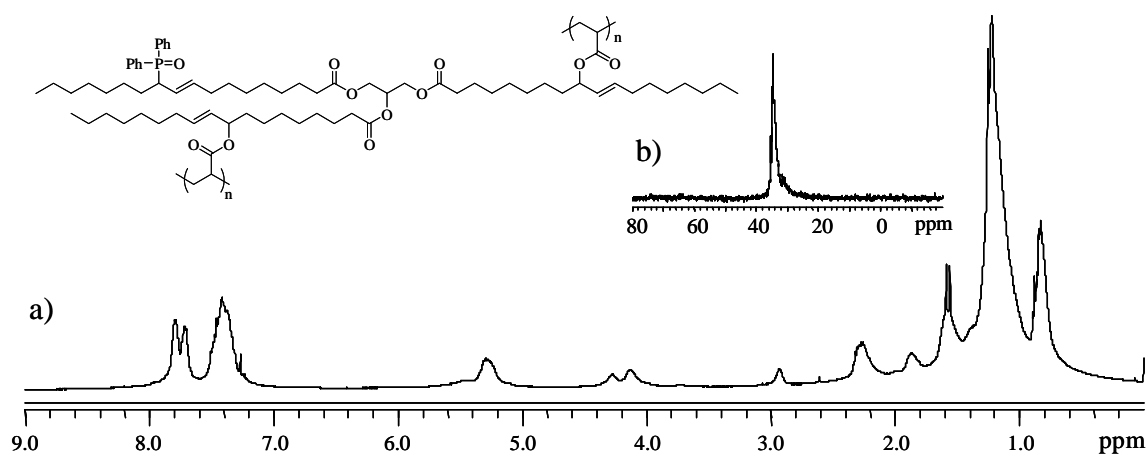


**Figure 5.**  $^1\text{H}$  (a) and  $^{31}\text{P}$  (b) hr-MAS NMR spectra of cured P-ASO-III.

The dynamic mechanical behavior of these polymers was similar to that of ASO systems<sup>11</sup> and other thermosetting polymers.<sup>27</sup> Figure 6 shows the DMA analysis of the P-ASO system. The Tgs were taken as the maximum of the Tan  $\delta$  peaks. The values, summarized in table 1, are similar for all the samples and were found around room temperature. The increase in the phosphorus content caused a slight decrease in the Tg value. As the phosphorus content is increased, the acrylate functionality in the triglycerides is decreased. Adding PETA as crosslinker increases the crosslinking density of the polymers, but does not avoid the increasing content of free fatty acid chains acting as plastizisers. As a consequence, the Tan  $\delta$  peak maxima shift to lower

temperatures. However, this effect is not so strong due to the increasing content of aromatic rings and strongly polar phosphoryl groups, that cause restriction in segmental mobility. The decreasing crosslinking density is in accordance with the height of the Tan  $\delta$  peaks, which increase with the phosphorus content indicating a lower rigidity of the polymeric network.

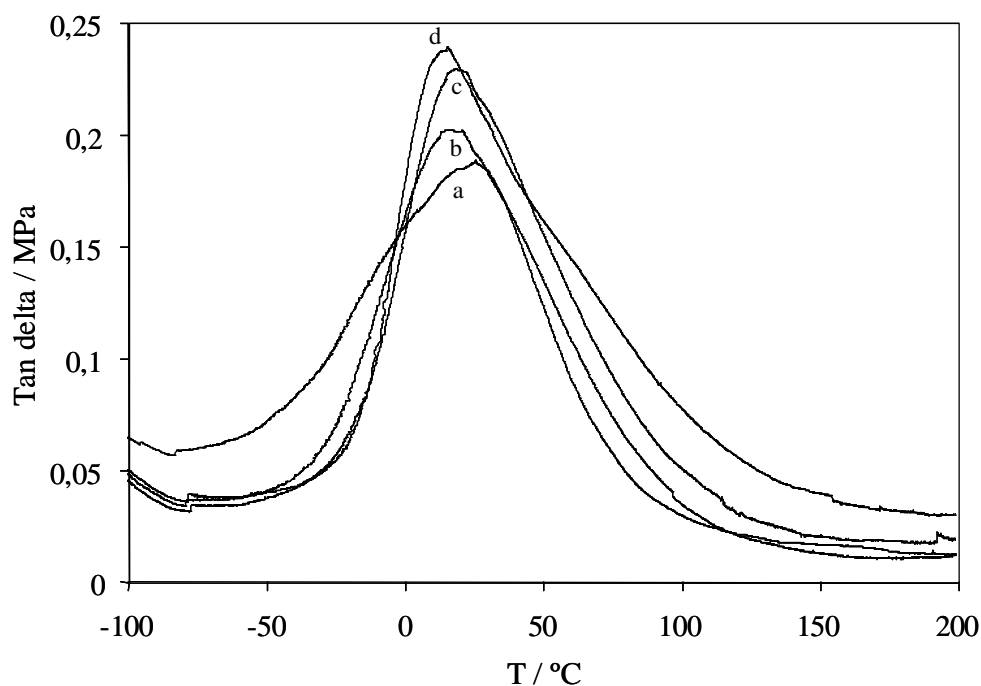


**Figure 6.** Tan delta plots as a function of temperature for the cured systems: a) ASO/PETA; b) P-ASO-I/PETA; c) P-ASO-II/PETA and d) P-ASO-III/PETA.

The thermal stability of these polymers was evaluated both under nitrogen and air atmosphere. The thermogravimetric plots are shown in figure 7 and 8 respectively and the temperature of 5% weight loss, the temperature of the maximum weight loss rate and the residue at 800°C are collected in Table 1. The temperatures of 5 % weight loss of all samples are in the 305-330 °C range under nitrogen and between 270-300 °C under air. The residues obtained at 800 °C range from 3 to 5 % under nitrogen and from 0 to 2 % under air atmosphere. This low residues could indicate that volatile phosphorus compounds are released upon heating. Thus, a gas-phase flame retardancy mechanism might be expected in combination with the condensed-phase mechanism.<sup>16-18</sup> The first derivative plots show that under nitrogen the degradation process consist of two main steps (Fig. 7b), while under air at least four maximum weight loss rates are involved

indicating the existence of more complex processes (Fig. 8b). Under air atmosphere and above 500 °C polymeric materials undergo a weight loss due to the char formed oxidized. It can be seen that the weight loss rate of the phosphorus-containing resins is significantly lower than that of the phosphorus-free resin in this thermo-oxidative degradation. In this retarded-degradation phenomenon, the phosphorus groups promote an insulating protective layer which prevents the combustible gases from transferring to the surface of the materials, increases the thermal stability at higher temperatures and improves the fire resistance.

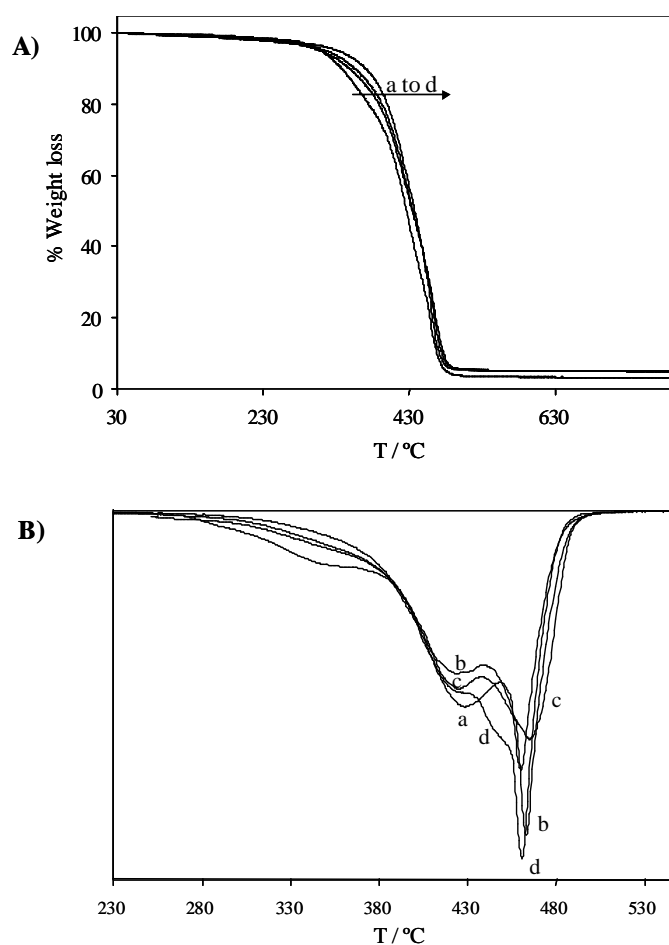


**Figure 7.** A) TGA plots under nitrogen and B) first derivative curves of the cured systems: a) ASO/PETA; b) P-ASO-I/PETA; c) P-ASO-II/PETA and d) P-ASO-III/PETA.

The flame retardancy of the resins was evaluated using the Limiting Oxygen Index value (LOI). The results are depicted in table 1. ASO resin gave a LOI of 19.6 which indicates that this material is not flame retardant. The addition of 1.4% of

phosphorus gave a LOI of 21.2 and the maximum content of phosphorus (2.8 %) gave a LOI of 22.4. These values show that this slight improvement on the flame retardant properties is related to the increase in the phosphorus content.

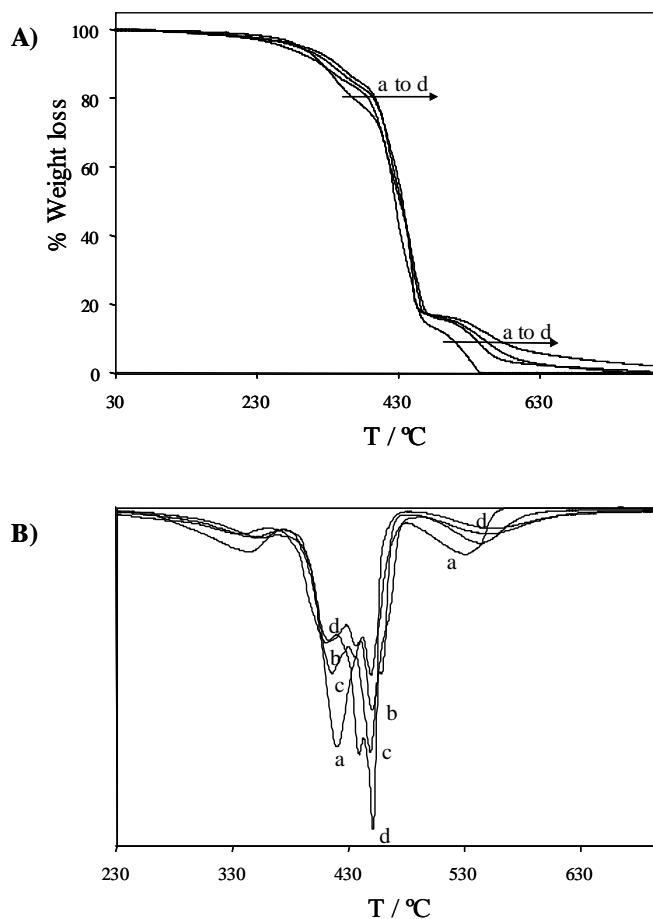


**Figure 8.** A) TGA plots under air and B) first derivative curves of the cured systems: a) ASO/PETA; b) P-ASO-I/PETA; c) P-ASO-II/PETA and d) P-ASO-III/PETA.

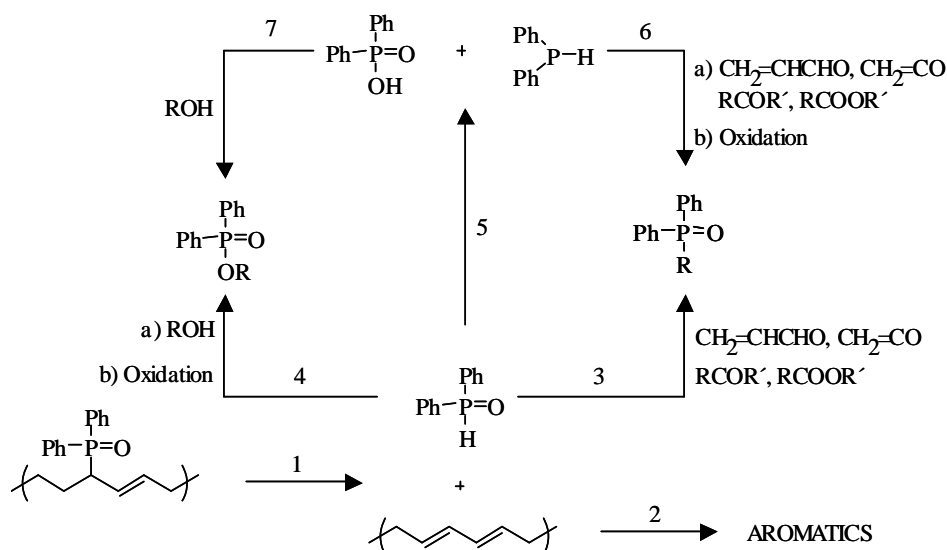
To further investigate the thermal degradation mechanism, samples of P-ASO-III were heated in an oven at different temperatures with air and nitrogen as purge gases. The degradation temperatures were selected from dynamic TGA data as the corresponding to weight loss rate maxima. Under nitrogen atmosphere the used temperatures were 350, 425 and 465°C and under air 340, 415 and 450 °C. In both atmospheres the heating time was 1h per each temperature. Volatile products were trapped at the liquid nitrogen temperature and subsequently analysed by GC/MS and  $^{31}\text{P}$ -NMR spectroscopy.

The thermal decomposition of plant oils has been widely reported in literature.<sup>28</sup> Considering the structure of P-ASOs, mainly composed by triglycerides, we can expect similar findings when analyzing the evolved gases. Thus, the main degradation products are long chain fatty acids (R-COOH), esters (R-COOR'), acrolein and substituted ketenes (R''-CH=C=O). Ketones (R-CO-R') and aldehydes (R-CHO) are secondly formed from fatty acids. These oxygenated hydrocarbons undergo decarbonylation giving hydrocarbon radicals (R and R') in the case of ketones and aldehydes while in the case of fatty acids and esters the products are alcohols (R-OH). Substituted ketenes decompose giving CH<sub>2</sub>=C=O and hydrocarbon radicals (R''). Moreover, the formation of alkanes and alkenes can be attributed to the generation of a RCOO· radical through triglyceride cleavage followed by decarboxylation. Unsaturated sites enhance the cleavage of the C-C bonds at allylic position and this cleavage is a dominant reaction. The formation of aromatics is supported by Diels-Alder ethylene addition of conjugate dienes.

Taking into account that P-ASOs are polyacrylates with ester function prone to suffer thermal C-O scission, the presence of secondary alcohols among the degradation products can be expected.<sup>29</sup>

On the other hand, the analysis of the evolved gases, in all fractions, shows the presence of several phosphorus aromatic compounds. In the degradation under nitrogen, diphenylphosphine oxide, methyldiphenyl phosphine oxide and methyl diphenylphosphinite could be detected. In the degradation under air, ethyldiphenyl phosphine oxide, *n*-propyldiphenyl phosphine oxide, *isopropyl* diphenylphosphine oxide, methyldiphenyl phosphine oxide and methyl diphenylphosphinite could be detected. The formation of these compounds could be explained through different chemical processes that involve some of the compounds evolved in the decomposition of triglyceride moieties. These reactions are summarized in Scheme 2. In reaction 1, P-C bond cleavage occurs due to the availability of a hydrogen in β position to the P atom in the starting tertiary phosphine oxide to give diphenylphosphine oxide and a conjugated diene.<sup>30</sup> This diene, as mentioned above, could react with alkenes (reaction 2) to form aromatic compounds which have been detected by GC-MS. Diphenylphosphine oxide is strongly nucleophilic due to P-H bond and can easily react with electrophile groups such as acrolein, ketene, ketones and esters, formed during the thermal decomposition (reaction 3). The products of these reactions would be tertiary

phosphine oxides, what was confirmed by the presence of typical signals in the tertiary phosphine oxides region in  $^{31}\text{P}$  NMR spectroscopy.



**Scheme 2.** Proposed thermal degradation pathways of P-ASO thermosets.

Diphenylphosphine oxide tautomer ( $\text{Ph}_2\text{P-OH}$ ) could undergo an esterification in the presence of different alcohols evolved in the thermal decomposition. The formed  $\text{Ph}_2\text{P-OR}$  can be oxidized to alkyl diphenyl phosphinites (reaction 4).

It is described that the secondary phosphine oxides can undergo a thermal disproportionation<sup>30</sup> to give a secondary phosphine and a phosphinic acid (reaction 5). As diphenylphosphine oxide, diphenylphosphine also shows high reactivity towards the electrophiles above mentioned (reaction 6) and can give the same tertiary phosphine oxides, after oxidation of the tertiary phosphine adducts, than reaction 3.

On the other hand, diphenyl phosphinic acid can be esterified with the different alcohols evolved in the thermal decomposition to give different alkyl diphenyl phosphinites (reaction 7).

The solid residues obtained after degradation under nitrogen and air were analyzed by  $^{31}\text{P}$  HR-MAS NMR spectroscopy. Any signal was observed in the spectrum of residue sample obtained under nitrogen. This fact is probably due to the availability of a hydrogen in  $\beta$  position to the P, in the starting tertiary phosphine oxide, that favors the cleavage of P-C bond and elimination of phosphorus-containing volatiles. However, in the spectrum of residue sample obtained under air a peak at 0 ppm ( $\text{H}_3\text{PO}_4$ ) was

observed. In this case the different evolved phosphorus species are oxidized to phosphoric acid. Looking the very low char yield obtained for P-ASO-III at 800 °C in TGA analysis under air, we can think that most of the phosphorus species are released to the gas phase instead of being oxydized and stay in the residue.

To better understand the role of phosphorus in the polymer flame retardancy, element mapping was performed with energy-dispersive X-ray spectroscopy (EDX) on the surface of a P-ASO-III sample after the LOI test (Fig 9). P mapping of the non-burned area showed a homogeneous distribution of this element, as can be observed in the micrograph (Fig. 9 b). The white points in the Fig. denote P rich zones. After burning, the presence of phosphorus in the char was confirmed by  $^{31}\text{P}$  MAS NMR spectroscopy which shows a broad peak at 0 ppm typical of phosphoric acid. Fig. 9 c) shows the P mapping of the burned zone of the P-ASO-III. The P distribution shows that the phosphorus density increased in the top burned surface and that a phosphorus-rich layer formed. When phosphorus compounds are heated they can form glass-like polyphosphoric acid, which protects the burning surface.

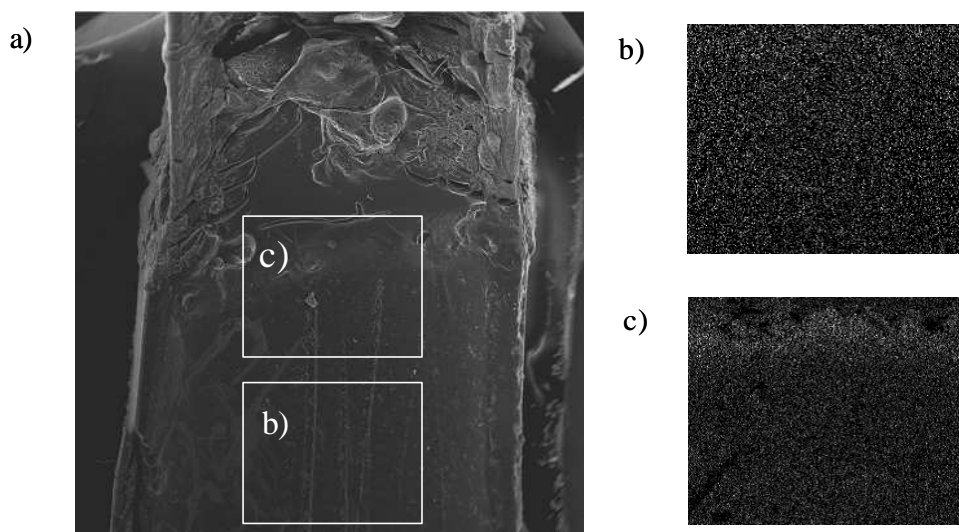


**Figure 9.** SEM (a) and SEM-EDX P-mapping micrographs of non-burned area (b) and burned area (c) of cured P-ASO-III.

## CONCLUSIONS

Phosphorus-containing triglycerides were prepared from a new route that involves the preparation of intermediate secondary allylic alcohol triglyceride. These allylic alcohols



in presence of chlorodiphenylphosphine give allylic phosphinites capable to undergo a [2,3]-sigmatropic rearrangement leading to tertiary phosphine oxides directly linked to triglyceride in a one pot two step reaction. The obtained phosphorus-containing triglycerides with different hydroxyl content were activated to polymerization by acrylation and these acrylate triglycerides were radically crosslinked in presence of different amounts of pentaerythritol tetraacrylate. The cured materials could be characterized by HR-MAS NMR spectroscopy. Final elastomeric materials with good thermal stabilities were obtained showing properties and characteristics as good as other acrylated triglyceride-based thermosets. The presence of phosphorus slightly increased the LOI values. Thermal degradation study showed that phosphorus-containing compounds are released upon heating acting through a gas phase mechanism. Moreover, by SEM and NMR it was possible to confirm the production of a char residue consistent with condensed-phase fire-retardant action.

This work is dedicated to the Professor Josep Font on occasion of his 70<sup>th</sup> birthday.

The authors express their thanks to CICYT (Comisión Interministerial de Ciencia y Tecnología) (MAT2008-01412) for financial support for this work.

## REFERENCES

- <sup>1</sup> Bozell, J.J.; Patel, M. Eds., *Feedstocks for the Future: Renewables for the Production of Chemicals and Materials*; ACS Symposium Series 921; American Chemical Society: Washington, DC, 2006.
- <sup>2</sup> Güner, F. S.; Yagcı, Y.; Erciyas, A. T. *Prog Polym Sci* 2006, 31, 633–670.
- <sup>3</sup> Lu, Y.; Larock, R. C. *Chem SusChem* 2009, 2, 136-147.
- <sup>4</sup> Sharma, V.; Kundu, P. P. *Prog Polym Sci* 2006, 31, 983-1008.
- <sup>5</sup> Sharma, V.; Kundu, P. P. *Prog Polym Sci* 2008, 33, 1199-1215.
- <sup>6</sup> La Scala, J.; Wool, R. P.; *Polymer* 2005, 46, 61-69.
- <sup>7</sup> Pelletier, H.; Belgacem, N.; Gandini, A. *J App Polym Sci* 2006, 99, 3218-3221.
- <sup>8</sup> Lu, J.; Wool, R. P. *J App Polym Sci* 2006, 99, 2481-2488.
- <sup>9</sup> Khot, S. N.; La Scala, J. J.; Can, E.; Morye, S. S.; Williams, G. I.; Palmese, G. R.; Kusefoglu, S. H.; Wool, R. P. *J App Polym Sci* 2001, 80, 703-723.
- <sup>10</sup> Lu, J.; Khot, S.; Wool, R. P. *Polymer* 2005, 46, 71-80.

- 
- <sup>11</sup> Montero de Espinosa, L.; Ronda, J. C.; Galià, M.; Cádiz V. *J Polym Sci Part A: Polym Chem* 2009, 47, 1159-1167.
- <sup>12</sup> Lligadas, G.; Ronda, J.C.; Galià, M.; Cádiz V. *J Polym Sci Part A: Polym Chem*, 2006, 44, 5630-5644.
- <sup>13</sup> Lligadas, G.; Ronda, J.C.; Galià, M.; Cádiz V. *J Polym Sci Part A: Polym Chem*, 2006, 44, 6717-6727.
- <sup>14</sup> Eren, T.; Küseföglu, S. H. *J. App Polym Sci* 2004, 91, 2700-2710.
- <sup>15</sup> Lu, S. Y.; Hamerton, I. *Prog Polym Sci* 2002, 27, 1661-1712.
- <sup>16</sup> Braun, U.; Balabanovich, A. I.; Schartel, B.; Knoll, U.; Artner, J.; Ciesielski, M.; Döring, M.; Perez, R.; Sandler, J. K. W.; Altstädt, V.; Hoffmann, T.; Pospiech, D. *Polymer* 2006, 47, 8495-8508.
- <sup>17</sup> Hergenrother, P. M.; Thompson, C. M.; Smith Jr, J. G.; Connella, J. W.; Hinkleya, J. A.; Lyonc, R. E.; Moulton, R. *Polymer* 2005, 46, 5012-5024.
- <sup>18</sup> Perez, R. M.; Sandler, J. K. W.; Altstädt, V.; Hoffmann, T.; Pospiech, D.; Artner, J.; Ciesielski, M.; Döring, M.; Balabanovich, A. I.; Knoll, U.; Braun, U.; Schartel, J. B. *J App Polym Sci* 2007, 105, 2744-2759.
- <sup>19</sup> Ebdon, J. R.; Price, D.; Hunt, B. J.; Joseph, P.; Gao, F.; Milnes, G. J.; Cunliffe, L. K. *Polym Deg Stab* 2000, 69, 267-277.
- <sup>20</sup> Beach, M. W.; Rondan, N. G.; Froese, R. D.; Gerhart, B. B.; Green, J. G.; Stobby, B. G.; Shmakov, A. G.; Shvartsberg, V. M.; Korobeinichev, O. P. *Polym Deg Stab* 2008, 93, 1664-1673.
- <sup>21</sup> Ribera, G; Mercado, L.A.; Galià, M.; Cádiz, V. *J App Polym Sci* 2006, 99, 1367-1373.
- <sup>22</sup> Spontón, M.; Ronda, J.C.; Galià, M.; Cádiz V. *J Polym Sci Part A: Polym Chem*, 2007, 45, 2142-2151.
- <sup>23</sup> Morgan, P. W.; Herr, B. C. *J Am Chem Soc* 1952, 74, 4526-4529.
- <sup>24</sup> Liron, F.; Knochel, P. *Chem Commun* 2004, 304-305.
- <sup>25</sup> Roeges, N.P.G. *A Guide to the Complete Interpretation of Infrared Spectra of Organic Structures*. John Wiley & Sons Ltd, Chichester, 1994.
- <sup>26</sup> Pelletier, H.; Belgacem, N.; Gandini, A. *J Appl Polym Sci* 2006, 99, 3218-3221.
- <sup>27</sup> Malik, M.; Choudhary, V.; Varma IK. *Rev Macromol Chem Phys* 2000, C40, 139-165.
- <sup>28</sup> Maher, K.D.; Bressler, D.C. *Bioresour Technol*, 2007, 98, 2351-2368 and references therein.
- <sup>29</sup> Haken, J.K.; Tan L. *J Polym Sci Part A: Polym Chem*, 1988, 26, 1315-1322.
- <sup>30</sup> Bailey, W.J.; Muir, W.M.; Marktscheffel, F. *J Org Chem*, 1962, 27, 4404-4408.

## **Chapter 4**

**1. Fatty Acid Derived Phosphorus-Containing Polyesters  
Via Acyclic Diene Metathesis (ADMET) Polymerization**

**2. Phosphorus-Containing Renewable Polyester-Polyols  
via ADMET Polymerization. Synthesis,  
Functionalization and Radical Cross-Linking**



# Fatty Acid Derived Phosphorus-Containing Polyesters via Acyclic Diene Metathesis (ADMET) Polymerization

Lucas Montero de Espinosa,<sup>1</sup> Juan C. Ronda,<sup>1</sup> Marina Galià,<sup>1</sup> Virginia Cádiz,<sup>1</sup> Michael A. R. Meier<sup>2</sup>

<sup>1</sup>Department of Analytical and Organic Chemistry, Rovira i Virgili University, Campus Sescelades, Marcel·lí Domingo s/n, 43007 Tarragona, Spain. <sup>2</sup>University of Applied Sciences Oldenburg / Ostfriesland / Wilhelmshaven, Constantiaplatz 4, 26723 Emden, Germany.

**ABSTRACT.** The acyclic diene metathesis (ADMET) polymerization of a phosphorus-containing  $\alpha,\omega$ -diene prepared with a plant oil derived building block is reported. Different ruthenium based metathesis catalysts and conditions were tested in order to optimize the ADMET polymerization of this new monomer. Undecylenyl undecenoate was used as comonomer in order to obtain polyesters with different phosphorus contents and to increase the renewable part of the final polymers. Copolymerization caused marked variations in the molecular weights leading to polyesters from 6 to 38 KDa. The effect of the ADMET polymerisation temperature in the thermal properties of the copolymers was studied and their thermal degradation and flame retardant properties were evaluated.

**Keywords:** polyester, renewable resources, ADMET, phosphorus-containing polymer, flame retardant.

## INTRODUCTION

Acyclic diene metathesis (ADMET) polymerization of  $\alpha,\omega$ -dienes has been shown to be an efficient tool for the synthesis of a wide variety of linear polymers and polymer architectures that are not available using other polymerization methods.<sup>1</sup> Essentially, ADMET is a step-growth polycondensation reaction in which two terminal olefins react to form a new internal carbon-carbon double bond and a molecule of ethylene. Since the metathesis reaction is an equilibrium, the ethylene must be removed by applying vacuum or a constant flow of an inert gas in order to shift the equilibrium towards the product. The first well defined ruthenium based metathesis catalyst, developed by

Grubbs in the early 1990s, permitted the application of the olefin metathesis reactions in presence of a wide variety of functional groups.<sup>2,3</sup> The metathesis activity as well as the functional group tolerance of these catalysts was further improved by the substitution of one of the trialkyl phosphine ligands by a N-heterocyclic carbene (NHC),<sup>4</sup> leading to the second generation Grubbs catalysts.<sup>5</sup> Thus, with the introduction of highly active and robust metathesis catalysts, the number of polymeric structures available through the design of new monomers has ever since increased.

It has been demonstrated that ADMET polymerization can proceed in the presence of heteroatoms, as long as the terminal olefins are far enough apart from them.<sup>6</sup> There are many examples of ADMET of heteroatom-containing  $\alpha,\omega$ -dienes in the literature, since the introduction of functionalities in the backbone of the polymers provides different properties and permits further modifications.<sup>1,7-9</sup>

One very desirable property for polymers is the flame retardancy.<sup>10</sup> Many kinds of flame retardants (FRs) have been tested to improve the flame resistance of polymers and have been applied to commercial products. Among them, halogenated FR are the most common. However, many kinds of halogenated FRs, especially brominated FRs., are restricted in many countries due to the formation of dioxins under combustion<sup>11</sup> Therefore much work has been done on the development of halogen-free FR polymers such as those containing phosphorus, which are known to promote the formation of a protecting char during combustion. This protecting layer isolates the material from the heat source and prevents the diffusion of gaseous products into the flame.<sup>12</sup> FR polymers can be prepared by blending with phosphorus FR and/or by polymerization of phosphorus-containing monomers. However, due to the problems associated with the blending method, the synthesis of inherent FR polymers is becoming more common.<sup>12</sup> Allcock *et al.*<sup>13,14</sup> prepared a series of substituted cyclic phosphazene-containing polymers with various pendant substituents on the phosphorus atoms using Grubbs 1<sup>st</sup> and 2<sup>nd</sup> generation catalysts. They could determine that the activity of the catalysts was affected by both electronic (preferential catalyst coordination to a functional group) and steric effects. To the best of our knowledge, this is the only example of the ADMET polymerization of a phosphorus-containing monomer.

Among the different commercially available polymers, polyesters are widely used for textile fibers, technical fibers, films, bottles or as a finish on high-quality wood products. The world demand of polyesters in 2008 was estimated to grow up to 50 million tons.<sup>15</sup> Furthermore, due to environmental concerns much work is devoted to the

industrial use of products from renewable resources. For this reason, renewable raw materials such as plant oils, polysaccharides, sugars and wood are widely used by the chemical industry for many purposes, and among them, plant oils and their derivatives have a large potential for the substitution of the currently used petrochemicals in the synthesis of polymeric materials.<sup>16-19</sup> Recent work has focused to the synthesis of monomers from plant oil derivatives for the development of linear,<sup>20,21</sup> branched,<sup>22</sup> as well as crosslinked<sup>23-25</sup> polymers.

In the present work, a phosphorus-containing monomer bearing two 10-undecenoic acid moieties has been homopolymerized and copolymerized with undecylenyl undecenoate *via* ADMET in absence of solvent. This procedure allowed us to synthesize a variety of polyesters with controlled phosphorus contents. All polymers were fully characterized and the thermal and flame retardant properties of these polyesters were studied.

## EXPERIMENTAL

### Instrumentation

<sup>1</sup>H NMR (400 MHz), <sup>13</sup>C NMR (100.6 MHz) and <sup>31</sup>P NMR (162 MHz) spectra were obtained in CDCl<sub>3</sub> using a Varian Gemini 400 spectrometer. Chemical shifts were reported relative to tetramethylsilane or phosphoric acid as internal standards. Calorimetric studies were carried out on a Mettler DSC822 differential scanning calorimeter using N<sub>2</sub> as a purge gas (20 mL/min) at a scan rate of 20°C/min. Thermal stability studies were carried out on a Mettler TGA/SDTA851e/LF/1100 with N<sub>2</sub> or synthetic air as purge gases. The studies were performed in the 30-800 °C temperature range at a heating rate of 10°C/min. Molecular weights were determined on a Shimadzu gel permeation chromatography (GPC) system equipped with a LC-20AD pump, RID-10A refractive index detector, SIL-20A autosampler, and a CTO-20A column oven set to 50 °C. A PLgel 5 μm Mixed-D column from Polymerlabs in THF at a flow rate of 1 mL/min was used. Linear poly(methyl methacrylate) standards (Polymer Standards Service PPS, Germany, Mp 102-981.000 Da) were used for calibration. GC-MS (EI) chromatograms were recorded using a VARIAN 3900 GC instrument with a capillary column FactorFour<sup>TM</sup> VF- 5ms (30 m x 0.25 mm x 0.25 mm, Varian) and a Saturn 2100T ion trap mass detector. Scans were performed from 40 to 650 m/z at rate of 1.0 scans x s<sup>-1</sup>. The oven temperature program was: initial temperature 95 °C, hold for 1

min, ramp at 15 °C x min<sup>-1</sup> to 200 °C, hold for 2 min, ramp at 15 °C x min<sup>-1</sup> to 325 °C, hold for 9 min. The injector transfer line temperature was set to 250 °C. Measurements were performed in the split-split mode (split ratio 50:1) using helium as carrier gas (flow rate 1.0 ml x min<sup>-1</sup>). Measurements were performed in the splitless and split-split mode (split ratio 50:1) using helium as the carrier gas (flow rate 1.0 mL/min). Thin layer chromatography (TLC) was performed on silica gel TLC-cards (layer thickness 0.20 mm, Fluka). Compounds were visualized by permanganate or iodine reagents. For column chromatography silica gel 60 (0.035-0.070 mm, Fluka) was used. Limiting oxygen index (LOI) values were measured on a Stanton Redcroft instrument provided with an oxygen analyser in vertical tests. The samples were impregnated on glass fibre plaques (50 x 10 x 1 mm<sup>3</sup>) using concentrated THF solutions of the polymers and. LOI values were taken as the average of three measurements.

## Materials

9,10-Dihydro-9-oxa-10-phosphaphenanthrene-10-oxide (DOPO) was kindly supplied by Aismalibar S.A., p-benzoquinone (Aldrich), 10-undecenoyl chloride (Fluka), 10-undecenoic acid (Fluka), 10-undecen-1-ol (Aldrich), 1,5,7-Triazabicyclo[4.4.0]dec-5-ene (TBD, Aldrich), ethyl vinyl ether (Aldrich), benzylidene-*bis*(tricyclohexylphosphine)dichlororuthenium (**C1**, Grubbs catalyst 1<sup>st</sup> generation, Aldrich), benzylidene[1,3-*bis*(2,4,6-trimethylphenyl)-2-imidazolidinylidene]dichloro(tricyclohexylphosphine)ruthenium (**C2**, Grubbs catalyst 2<sup>nd</sup> generation, Aldrich) and [1,3-*bis*-(2,4,6-trimethylphenyl)-2-imidazolidinylidene]dichloro(*o*-isopropoxyphenylmethylene)ruthenium (**C3**, Hoveyda-Grubbs catalyst 2<sup>nd</sup> generation, Aldrich) were used as received. 10-(2',5'-Dihydroxyphenyl)-9,10-dihydro-9-oxa-10-phosphaphenanthrene-10-oxide (DOPO-I) was synthesized in our laboratory according to the published procedure,<sup>26</sup> 10-(2',5'-Bis(10-undecenoyloxy) phenyl)-9,10-dihydro-9-oxa-10-phosphaphenanthrene-10-oxide (DOPO-II) was synthesized according to a previously published procedure.<sup>27</sup>

**Synthesis of DOPO-II (M1).** 5.0 g (15.4 mmol) of 10-(2',5'-dihydroxyphenyl)-9,10-dihydro-9-oxa-10-phosphaphenanthrene-10-oxide (DOPO-I), 4 mL of pyridine, and 125 mL of anhydrous dichloromethane were placed in a 250 mL round bottomed flask under dry argon atmosphere. To this solution, 6.5 g (32.0 mmol) of 10-undecenoyl chloride were added dropwise while stirring at room temperature for 15 min. The temperature



was raised to reflux temperature for 15 min. The progress of the reaction was monitored by thin layer chromatography using hexane/ethyl acetate (1:1) as eluent. After the reaction had finished, the crude was placed in a separation funnel and washed with water, 2 N HCl aqueous solution, a 5% NaHCO<sub>3</sub> solution and brine. DOPOII was obtained after drying the dichloromethane solution with anhydrous magnesium sulfate and eliminating the solvent at reduced pressure. The product was purified by recrystallization from hexane to give 9.5 g of DOPO-II (yield 94%) as a white crystalline solid (mp 63 °C).

Spectroscopic data for **M1** coincides with the previously described.<sup>27</sup>

**Synthesis of undec-10-enyl undec-10-enoate (M2).** To a solution of 10-undecenoic acid (46.5 g, 0.247 mol) and 10-undecen-1-ol (42.9 g, 0.247 mol) in toluene (200 mL) was added 1.95 mL (4.9 mmol) of titanium (IV) tert-butoxide. The reaction mixture was stirred magnetically and refluxed overnight in a Dean-Stark apparatus. At the end of reaction the mixture was cooled to ambient temperature, washed with acidic water, sodium carbonate solution, and water several times. After drying with anhydrous sodium sulfate, toluene was removed *in vacuo* and the residue was purified and separated by column chromatography with hexane–diethylether (8:2) as eluent. The product was obtained as a colorless liquid with a yield of 80g (96 %).

Spectroscopic data for **M2** coincides with the previously described.<sup>21</sup>

**ADMET polymerizations:** **M1** (0.3 g, 0.46 mmol), or **M2** (0.3 g, 0.89 mmol), or a mixture of both in the desired ratio (see Tables 2 and 3) and one of the metathesis catalysts (**C1-C3**, 1 % mol) were thoroughly mixed and placed in a 3 mL conical vial (Supelco) equipped with screw cap and septa. If required, the respective amount of end-capper (methyl 10-undecenoate) was added. The reaction mixture was stirred magnetically at 80 or 100 °C under a continuous flow of nitrogen. After 24 h reaction, the residue was dissolved in THF and the metathesis reaction was stopped by adding ethyl vinyl ether (500-fold excess to the catalyst) and stirring for 30 minutes at room temperature. **M1** homopolymers **P1** (at 80 °C) and **P'1** (at 100 °C) were precipitated as light brown sticky solids by slow addition in cold methanol and then in hexane. **M2** homopolymers **P11** (at 80 °C) and **P'11** (at 100 °C) were obtained as white solids by precipitation in cold methanol. **M1/M2** copolymers (**P2-P10** and **P'2-P'10**) were precipitated by slow addition in cold methanol and then in hexane.

Spectroscopic data for **P1**:

FTIR: 3066  $\text{cm}^{-1}$  (Ar C-H, stretching), 2920 and 2850 (C-H, stretching), 1764  $\text{cm}^{-1}$  (ester C=O, stretching), 1461  $\text{cm}^{-1}$  (C=C, stretching), 1238  $\text{cm}^{-1}$  (P=O, stretching), 1205  $\text{cm}^{-1}$  (C-O, stretching), 966  $\text{cm}^{-1}$  (C=C-H, out-of-plane deformation), 925  $\text{cm}^{-1}$  (P-O, stretching), 780, 757 and 714  $\text{cm}^{-1}$  (Ar).

$^1\text{H}$  NMR ( $\text{CDCl}_3$ , TMS, 400 MHz,  $\delta$  in ppm): 8.09-7.91 (3H, m, Ar), 7.71-7.63 (1H, m, Ar), 7.62-7.52 (1H, m, Ar), 7.45-7.33 (3H, m, Ar), 7.30-7.19 (2H, m, Ar), 7.18-7.10 (1H, m, Ar), 5.44-5.32 (2H, m,  $\text{CH}=\text{CH}$ ), 2.56 (2H, t,  $J = 7.42$  Hz,  $\text{COCH}_2$ ), 2.08-1.87 (4H, m,  $\text{CH}_2\text{-CH}=\text{CH}$ ), 1.81-1.60 (4H, m,  $\text{COCH}_2\text{-CH}_2$  and  $\text{COCH}_2$ ), 1.47-0.91 (22H, m,  $\text{COCH}_2\text{-CH}_2$  and aliphatic).

$^{13}\text{C}$  NMR ( $\text{CDCl}_3$ , TMS, 100.6 MHz,  $\delta$  in ppm, Scheme 1): 172.08 ( $\text{C}_{19}$ ), 171.03 ( $\text{C}_{29}$ ), 149.83 ( $\text{C}_5$ ), 149.42 (d,  $J = 8.45$  Hz,  $\text{C}_2$ ), 147.96 (d,  $J = 17.60$  Hz,  $\text{C}_{18}$ ), 135.25 (d,  $J = 6.14$  Hz,  $\text{C}_{12}$ ), 133.33 ( $\text{C}_9$ ), 131.00 ( $\text{C}_{11}$ ), 130.82 ( $\text{C}_{16}$ ), 130.50–130.43 ( $\text{C}_{28}$ ), 128.71 (d,  $J = 14.48$  Hz,  $\text{C}_{10}$ ), 128.38 ( $\text{C}_4$ ), 128.24 (d,  $J = 8.35$  Hz,  $\text{C}_2$ ), 124.92–124.76 ( $\text{C}_3$ ,  $\text{C}_{14}$ ,  $\text{C}_{15}$ ), 124.67 (d,  $J = 133.49$  Hz,  $\text{C}_7$ ), 123.31 (d,  $J = 10.66$  Hz,  $\text{C}_8$ ), 122.80 (d,  $J = 144.86$  Hz,  $\text{C}_1$ ), 121.24 (d,  $J = 11.17$  Hz,  $\text{C}_{13}$ ), 120.85 (d,  $J = 6.94$  Hz,  $\text{C}_{17}$ ), 34.39 ( $\text{C}_{30}$ ), 33.33 ( $\text{C}_{20}$ ), 32.76 ( $\text{C}_{27}$ ), 29.90-28.96 ( $\text{C}_{22}\text{-C}_{26}$ ), 27.38 ( $\text{C}_{27}$ ), 24.99 ( $\text{C}_{31}$ ), 24.19 ( $\text{C}_{21}$ ).

$^{31}\text{P}$  NMR ( $\text{CDCl}_3$ , 162 MHz,  $\delta$  in ppm): 18.09.

Spectroscopic data for **M1/M2** copolymers:

FTIR: 3066  $\text{cm}^{-1}$  (Ar C-H, stretching), 1764  $\text{cm}^{-1}$  (COOR, stretching), 1733  $\text{cm}^{-1}$  (COOR, stretching), 1461  $\text{cm}^{-1}$  (C=C, stretching), 1241  $\text{cm}^{-1}$  (C-O, stretching), 1238  $\text{cm}^{-1}$  (P=O, stretching), 1172  $\text{cm}^{-1}$  (C-O, stretching), 966  $\text{cm}^{-1}$  (C=C-H, out-of-plane deformation), 925  $\text{cm}^{-1}$  (P-O, stretching), 780, 757 and 714  $\text{cm}^{-1}$  (Ar).

$^1\text{H}$  NMR ( $\text{CDCl}_3$ , TMS, 400 MHz,  $\delta$  in ppm): 8.07-7.91 (m, Ar), 7.70-7.64 (m, Ar), 7.60-7.54 (m, Ar), 7.45-7.35 (m, Ar), 7.30-7.21 (m, Ar), 7.15-7.12 (m, Ar), 5.44-5.30 (m,  $\text{CH}=\text{CH}$ ), 4.03 (t,  $J = 6.73$  Hz,  $\text{COO-CH}_2$ ), 2.56 (t,  $J = 7.47$  Hz,  $\text{COCH}_2$ ), 2.27 (t,  $J = 7.53$  Hz,  $\text{CO-CH}_2$ ), 2.04-1.88 (m,  $\text{CH}_2\text{-CH}=\text{CH}$ ), 1.78-1.64 (m,  $\text{COCH}_2\text{-CH}_2$  and  $\text{COCH}_2$ ), 1.64-1.54 (m,  $\text{CH}_2\text{-CH}_2\text{COOCH}_2\text{-CH}_2$ ), 1.45-0.91 (m,  $\text{COCH}_2\text{-CH}_2$  and aliphatic).

$^{13}\text{C}$  NMR ( $\text{CDCl}_3$ , TMS, 100.6 MHz,  $\delta$  in ppm, Scheme 2): 174.12 (COOR,  $\text{C}_{29}$ ), 172.03 (COOR,  $\text{C}_{19}$ ), 170.98 ( $\text{C}'\text{OOR}$ ,  $\text{C}_{29}$ ), 149.79 ( $\text{C}_5$ ), 149.37 (d,  $J = 8.45$  Hz,  $\text{C}_2$ ),

147.94 (d,  $J = 16.90$  Hz, C<sub>18</sub>), 135.24 (d,  $J = 6.04$  Hz, C<sub>12</sub>), 133.27 (C<sub>9</sub>), 131.00 (C<sub>11</sub>), 130.80 (C<sub>16</sub>), 130.52–130.40 (C<sub>23</sub>), 128.68 (d,  $J = 14.99$  Hz, C<sub>10</sub>), 128.35 (C<sub>4</sub>), 128.23 (d,  $J = 8.45$  Hz, C<sub>2</sub>), 124.89–124.73 (C<sub>3</sub>, C<sub>14</sub>, C<sub>15</sub>), 124.70 (d,  $J = 133.69$  Hz, C<sub>7</sub>), 123.28 (d,  $J = 10.46$  Hz, C<sub>8</sub>), 122.80 (d,  $J = 150.39$  Hz, C<sub>1</sub>), 121.21 (d,  $J = 11.17$  Hz, C<sub>13</sub>), 120.84 (d,  $J = 6.14$  Hz, C<sub>17</sub>), 64.53 (C<sub>30</sub>), 34.53 (C<sub>28</sub>), 34.37 (C<sub>25</sub>), 33.33 (C<sub>20</sub>), 32.76 (C<sub>22</sub>), 29.90–28.78 (aliphatic), 27.36 (C<sub>22'</sub>), 26.07 (C<sub>31</sub>), 25.15 (C<sub>27</sub>), 24.99 (C<sub>26</sub>), 24.18 (C<sub>21</sub>).

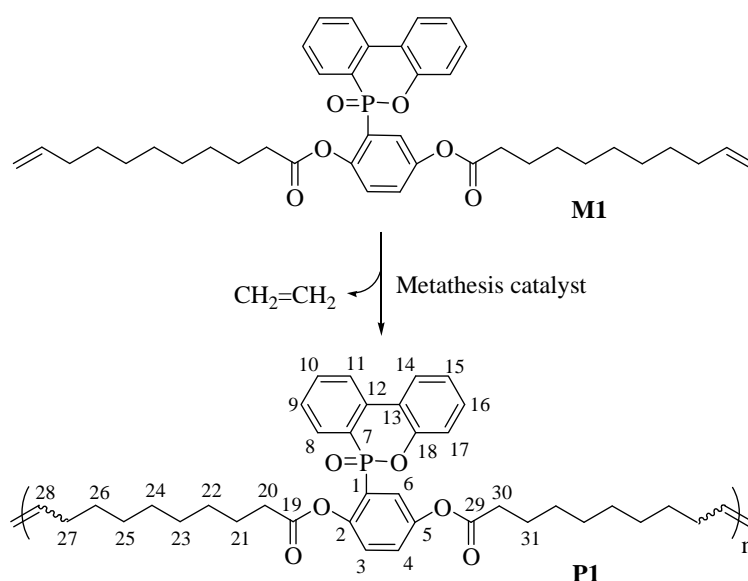
<sup>31</sup>P NMR (CDCl<sub>3</sub>, 162 MHz,  $\delta$  in ppm): 18.03.

Spectroscopic data for **P11** and **P'11** coincide with the previously described.<sup>21</sup>

## RESULTS AND DISCUSSION

The phosphorus-containing monomer DOPO II (**M1**, Scheme 1) was synthesized in two steps as previously reported.<sup>27</sup> Therefore, the nucleophilic DOPO was reacted with the electron deficient benzoquinone to give a diphenol which was then esterified with two molecules of 10-undecenoyl chloride. As already explained in the introduction, the activity of metathesis catalysts during ADMET polymerizations can be affected by the presence of heteroatoms or bulky substituents.<sup>6</sup> **M1** contains phosphorus and oxygen in a bulky aromatic core. However, the terminal double bonds of **M1** are nine carbons spaced from this core and the phosphorus of **M1** is non-coordinative. Therefore, we expected that this monomer might be polymerizable via ADMET. In order to confirm this expectation and to obtain some first insight into the behavior of different metathesis catalysts with **M1**, we studied the ADMET polymerization of **M1** using 1% mol first generation Grubbs (**C1**), second generation Grubbs (**C2**) and second generation Hoveyda-Grubbs (**C3**) catalysts. These ADMET reactions were run for 24 hours at 80 °C in absence of solvent and under a constant flow of nitrogen to remove the released ethylene more efficiently. When **M1** started melting (63 °C) the reaction proceeded very fast and the increase of the viscosity of the reaction mixture caused the non-homogeneous distribution of the catalyst in the melted monomer. For this reason, higher molecular weights were obtained when the monomer **M1** was thoroughly mixed with the metathesis catalysts in the solid state before the reactions were started. Adding a solvent (*o*-xylene) to increase the homogeneity of the reaction mixture did not give

better results. Moreover, the use of solvent was ruled out as it would favor the formation of cyclic oligomers due to statistics.



**Scheme 1.** Synthesis of phosphorus-containing polymer via ADMET polymerization.

The results of the ADMET polymerizations of **M1** are shown in Table 1. By GPC, a  $M_n$  of 21,300 Da was obtained when we used **C2** as catalyst. However, with **C1** and **C3**, molecular weights of only around 6000 Da were obtained together with poor monomer conversion. Furthermore, we observed that the obtained molecular weights decreased with higher or lower reaction temperatures and with lower amounts of catalyst. Therefore, we concluded that 1% of **C2** is best suited for the polymerization of

**Table 1.** Results of initial investigations of the ADMET polymerization of **M1**.

Catalyst (%) <sup>a</sup>	T (°C)	$M_n$ / PDI <sup>b</sup>
C1 (1%)	80	6,700 / 1.75
C2 (1 %)	80	21,300 / 2.33
C3 (1%)	80	6,000 / 1.77

<sup>a</sup> mol % relative to diene, <sup>b</sup> GPC data.

**M1** and used this condition for all further polymerizations. The  $^1\text{H-NMR}$  spectra of the monomer **M1** and the polymer **P1** are shown in Figure 1. Terminal olefin signals can clearly be observed at 4.93 and 5.73 ppm in the monomer spectrum. After ADMET polymerization, only an internal olefin signal centered at 5.4 ppm is observed, and no end group signals can be seen confirming the high molecular weight of the polymer. All other signals and relative integrals essentially remain unchanged indicating that **P1** has the depicted structure and no side reactions occurred.

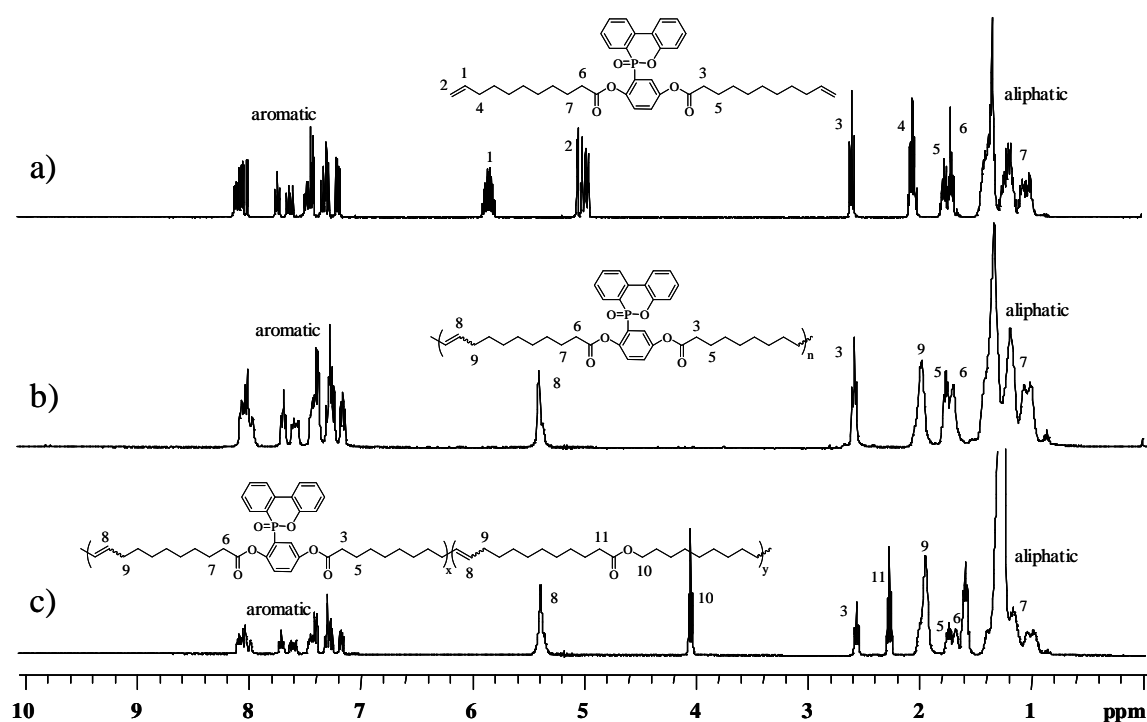
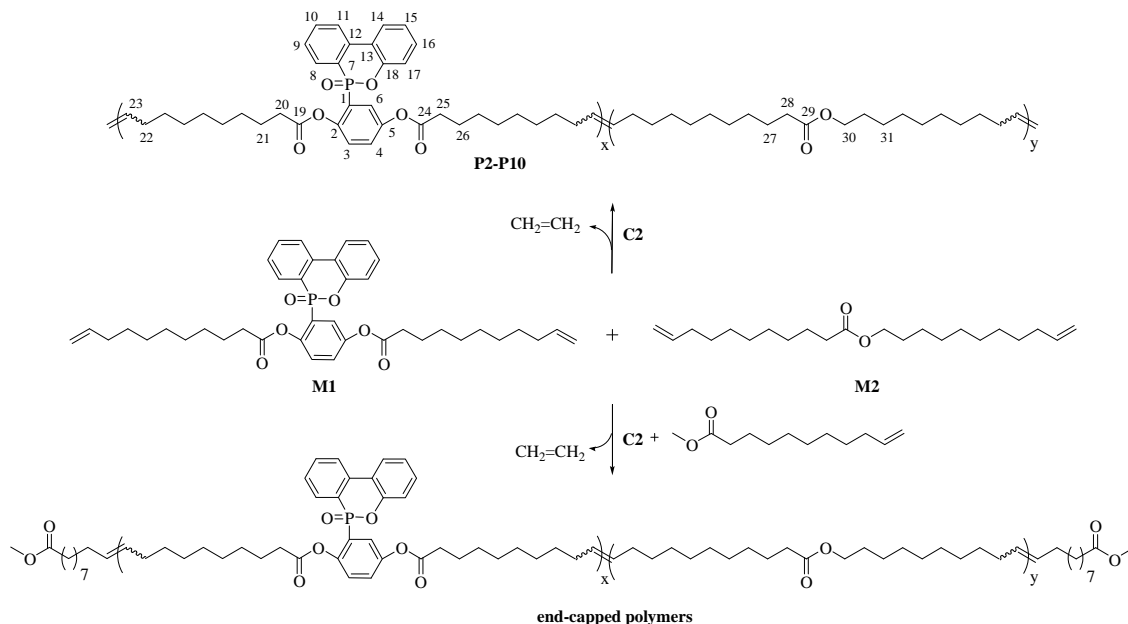


**Figure 1.**  $^1\text{H}$  NMR spectra of **M1** (a), **P1** (b) and **P7**(c).

Once demonstrated that the ADMET polymerization of the phosphorus-containing monomer **M1** can be carried out with **C2** to afford quite high molecular weight polymers, our next aim was to control the phosphorus content in the polymers regarding their flame retardant properties. **P1** has 4.72 wt% of phosphorus, but it is well known that percentages of 2-3 wt% of phosphorus are enough to infer flame retardant properties to polymers.<sup>12</sup> In order to lower the phosphorus content, and, at the same time, increase the renewable content of the final polymers, we decided to copolymerize **M1** with undecylenyl undecenoate (**M2**) (Scheme 2), an  $\alpha,\omega$ -diene that is 100 % renewable.<sup>21</sup> The ADMET copolymerizations were carried out at 80 °C using the

metathesis catalyst **C2**. The copolymerizations were run at different **M1/M2** molar ratios to study the effect of the copolymer on the molecular weight. The results are summarized in Table 2.



**Scheme 2.** Synthesis of phosphorus-containing renewable copolymers and copolymer telechelics via ADMET polymerization.

The most surprising effect is observed when a 9/1 (**M1/M2**) ratio is used. The molecular weight was increased twofold compared to the **M1** homopolymer. One possible explanation is that adding a little amount of **M2**, which is liquid at room temperature, provides higher homogeneity to the reaction mixture by acting as a solvent. However, this effect is not observed at higher **M2** contents and the molecular weights decrease for the other **M1/M2** ratios. Moreover, the addition of higher amounts of **M1** causes a non-homogeneous molecular weight distribution in the final polymers. The GPC curves of the polymers with intermediate **M1/M2** ratios show a bimodal molecular weight distribution (Figure 2), probably due to a lack of miscibility of both monomers when mixed in similar amounts. An increase of the reaction temperature should help to increase the miscibility of both components, but it could also affect the stability of the metathesis catalyst. Therefore, copolymerizations were also carried out at 100 °C since **C2** is also active at higher temperatures. Table 3 shows the results of the

**Table 2.** Analytic results of M1/M2 copolymers prepared at 80 °C.

Sample (M1 / M2) <sup>a</sup>	% P <sup>b</sup>	M <sub>n</sub> <sup>c</sup>	PDI <sup>c</sup>	T <sub>g</sub> (°C) <sup>d</sup> / T <sub>m</sub> (°C) <sup>d</sup>
P1 (10 / 0)	4.72	21,300	2.33	7.9 / -
P2 (9 / 1)	4.46	38,000	2.09	25.5 / -
P3 (8 / 2)	4.18	32,000	3.01	20.1 / -
P4 (7 / 3)	3.87	21,700	2.60	3.9 / -
P5 (6 / 4)	3.52	9,400	1.73	-29.3 / 9.4
P6 (5 / 5)	3.12	12,900	3.46	-16.6 / 23.7
P7 (4 / 6)	2.67	12,700	3.51	- / 27.7
P8 (3 / 7)	2.15	10,600	2.85	- / 35.2
P9 (2 / 8)	1.54	14,000	2.96	- / 41.7
P10 (1 / 9)	0.84	16,100	2.33	- / 47.7
P11 (0 / 10)	0.00	11,800	2.32	- / 54.6

<sup>a</sup> mol/mol ratio, <sup>b</sup> weight/weight percentages, <sup>c</sup> GPC data, <sup>d</sup> from DSC experiments.

100 °C ADMET copolymerization of **M1** and **M2** at different monomer ratios. Despite the resistance of **C2** to high temperatures, the molecular weights obtained for this copolymer series are lower compared to the copolymers obtained at 80 °C. This indicates that the catalyst loses activity at 100 °C. However, the increase of the temperature gave homogeneous copolymers at all **M1/M2** ratios (observed by GPC, Figure 2), thus solving the problem of the bimodal molecular weight distribution. As a representative example of this copolymer series, Figure 1 depicts the <sup>1</sup>H-NMR spectrum of the 80 °C 4/6 copolymer (**P7**). Also here, the terminal olefin signals are not observed confirming the high molecular weight of the copolymer.

The addition of a monofunctional monomer (chain stopper) to ADMET polymerizations not only permits to control the molecular weight of the polymers but also chain-end functionalized polymers can be obtained. This is a useful strategy allowing further modifications and the production of phase-separated materials such as ABA triblock copolymers or segmented block copolymers.<sup>1</sup> Moreover, when a functional group with easy to integrate <sup>1</sup>H-NMR signals is used in the end-capping, the

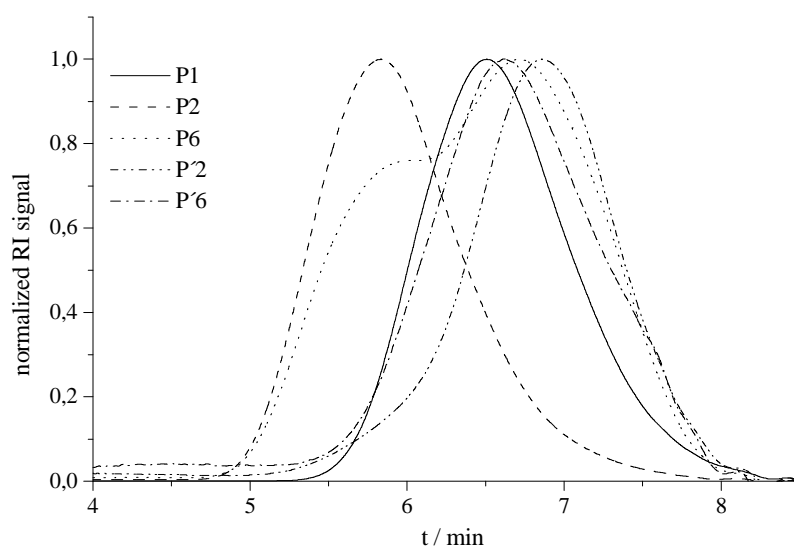


**Figure 2.** GPC traces of different copolymers.

**Table 3.** Analytic results of M1/M2 copolymers prepared at 100 °C.

Sample (M1 / M2) <sup>a</sup>	% P <sup>b</sup>	M <sub>n</sub> <sup>c</sup>	PDI <sup>c</sup>	T <sub>g</sub> (°C) <sup>d</sup> / T <sub>m</sub> (°C) <sup>d</sup>
P'1 (10 / 0)	4.72	6,300	2.38	1.4 / -
P'2 (9 / 1)	4.46	10,900	2.20	8.6 / -
P'3 (8 / 2)	4.18	14,000	2.50	14.7 / -
P'4 (7 / 3)	3.87	13,700	2.34	-2.2 / -
P'5 (6 / 4)	3.52	8,200	2.25	-19.2 / -
P'6 (5 / 5)	3.12	7,800	2.34	-16.2 / 22.2
P'7 (4 / 6)	2.67	10,500	2.66	- / 26.7
P'8 (3 / 7)	2.15	10,600	2.05	- / 34.0
P'9 (2 / 8)	1.54	11,100	1.98	- / 39.2
P'10 (1 / 9)	0.84	16,200	1.83	- / 45.6
P'11 (0 / 10)	0.00	17,800	2.10	- / 56.8

<sup>a</sup> mol/mol ratio, <sup>b</sup> weight/weight percentages, <sup>c</sup> GPC data, <sup>d</sup> from DSC experiments.



precise determination of the number of repeating units can be achieved. In this way, methyl 10-undecenoate was added as monofunctional chain stopper to selected ADMET polymerizations (Scheme 2). The analysis of the end-capped polymers by  $^1\text{H-NMR}$  spectroscopy allowed us to determine the ratio of the methoxy end-group signals with backbone signals. Thus we were able to accurately determine the DP and molecular weights of these telechelics. The obtained values for different copolymers are clearly higher than those calculated by GPC (Table 4). The molecular weight values obtained by GPC can be underestimated due to the difference of the hydrodynamic volume between the polymers synthesized and the PMMA standards used in the GPC calibration. For this reason, the actual molecular weights of the non-capped copolymers presented in Tables 2 and 3 are expected to be about twice as high as molecular weights obtained by GPC and presented in Tables 2 and 3.

The DSC traces of the copolymers synthesized at 80 °C are shown in Figure 3a and the data are collected in Table 2. The homopolymer **P1** shows a glass transition temperature ( $T_g$ ) at 7.9 °C. For **P2** (9/1 **M1/M2** ratio) this value is increased to 25.5 °C, but higher **M2** contents lower the  $T_g$ . This behavior can not only be attributed to variations of the molecular weight, but other factors such as the higher segmental mobility of **M2** must be taken into account. Moreover, at percentages of **M2** higher than

**Table 4.** Analytic data of copolymers prepared with methyl 10-undecenoate as a chainstopper. <sup>a</sup> mol/mol ratio.

M1 / M2 <sup>a</sup>	methyl 10-undecenoate (%)	T (°C)	$M_n^c$	$M_n$ ( $^1\text{H-NMR}$ )	PDI <sup>c</sup>
10 / 0	5	80	19,700	35,100	2.3
9 / 1	5	100	11,500	26,700	2.3
1 / 9	5	80	12,200	28,700	1.8
1 / 9	5	100	12,100	21,000	1.9

<sup>a</sup> mol/mol ratio, <sup>b</sup> mol % relative to diene, <sup>c</sup> GPC data.

40%, **M2** rich regions are able to arrange and crystallize and thus a  $T_m$  is also observed (**P5** and **P6**). For these semicrystalline materials both  $T_g$  and  $T_m$  increase as the **M2** content does. This behavior can be related to the physical crosslinking effect of

crystalline regions of increasing size and order. At percentages of **M2** higher than 50%, the crystalline fraction dominates and only a melting endotherm with maximum temperatures increasing from **P7** to **P11** is observed. The DSC traces of the polymers obtained at 100 °C (Figure 3b) show a similar behavior. However, the  $T_g$  values of the amorphous materials are slightly lower due to the lower molecular weights achieved. The semicrystalline materials show comparable  $T_m$  values as expected for a similar crystalline arrangement.

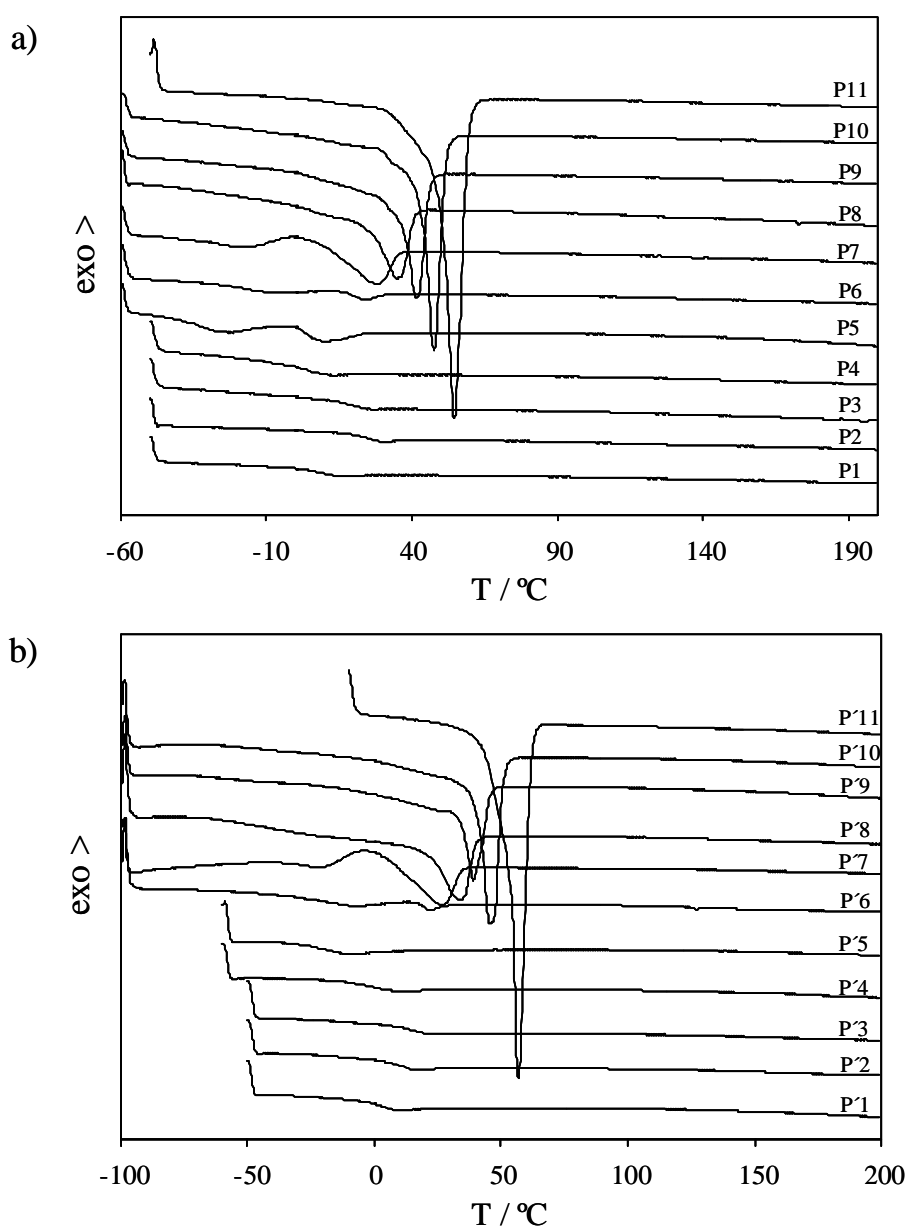


**Figure 3.** DSC traces of all investigated polymers prepared at 80°C (a) and 100°C (b).

The thermal stability of the copolymer series was studied by thermogravimetric analysis (TGA) in nitrogen and air atmospheres. The thermal stability of the copolymers obtained at 80 °C and 100 °C under nitrogen (Figure 4, data in tables 5 and 6) is similar in both series with 5% weight loss temperature ( $T_{5\%}$ ) between 290 and 390 °C for the 80 °C series and between 242 and 344 °C for the 100 °C series. The main maximum weight

**Table 5.** Thermal stability data and flame retardant characterization of copolymers prepared at 80 °C

Sample (M1 / M2) <sup>a</sup>	% P <sup>b</sup>	TGA (N <sub>2</sub> )			TGA (Air)			LOI
		T <sub>5% loss</sub> (°C)	T <sub>max</sub> (°C) <sup>c</sup>	Char <sub>800°C</sub> (%) <sup>b</sup>	T <sub>5% loss</sub> (°C)	T <sub>max</sub> (°C) <sup>c</sup>	Char <sub>800°C</sub> (%) <sup>b</sup>	
P1 (10 / 0)	4.72	317	327 / 464	9.3	317	441 / 550 / 746	8.4	22.8
P2 (9 / 1)	4.46	348	316 / 460	8.9	356	438 / 480 / 568 / 713	4.2	22.1
P3 (8 / 2)	4.18	390	460	8.8	356	452 / 595 / 705	5.2	22.4
P4 (7 / 3)	3.87	381	462	8.4	359	440 / 555	1.8	22.6
P5 (6 / 4)	3.52	290	232 / 332 / 464	7.8	310	427 / 461 / 533	1.4	22.7
P6 (5 / 5)	3.12	357	310 / 470	5.7	336	418 / 541 / 665 / 693	1.6	23.5
P7 (4 / 6)	2.67	353	465	4.9	330	343 / 460 / 544 / 680	1.1	22.1
P8 (3 / 7)	2.15	350	311 / 470	2.8	336	413 / 535 / 678	0.9	21.6
P9 (2 / 8)	1.54	356	314 / 438 / 466	1.8	338	421 / 460 / 548 / 619	0.5	21.3
P10 (1 / 9)	0.84	358	326 / 437 / 467	1.8	322	396 / 424 / 512	0.0	20.9
P11 (0 / 10)	0.00	378	433 / 462	0.0	330	421 / 509	0.0	19.0

<sup>a</sup> mol/mol ratio, <sup>b</sup> weight/weight percentages, <sup>c</sup> temperatures of maximum weight loss rate.

loss rates were found between 433 and 470 °C for the 80 °C series and between 422 and 469 °C for the 100 °C series. The typical bond energies of P-C, C-C, C-O and C-H bonds are 260, 349, 286 and 370 KJ/mol, respectively. This means that the thermal stability of a polymer should be lowered by addition of a phosphorus-containing comonomer. However, **M1** contains phosphorus as a pendant group and it has been demonstrated that the presence of phosphorus as a pendant group does not affect the thermal stability as it does when it is part of the main chain.<sup>28</sup> Moreover, Wang and Lin

reported the unusual high thermal stability of the P-O-C bond in a similar DOPO-derived polyester, which could be attributed to the three phenylene groups protection.<sup>29</sup> The thermal degradation of the pendant group leads to the formation of the phosphorus-containing char, which acts as a protective layer for the polymer surface. Therefore, the residues obtained at 800 °C increase as the phosphorus content does, reaching a maximum around 10% in both copolymer series. The TGA measurements in air atmosphere (Figure 5) show a main degradation step followed by a complex degradation process for both copolymer series.

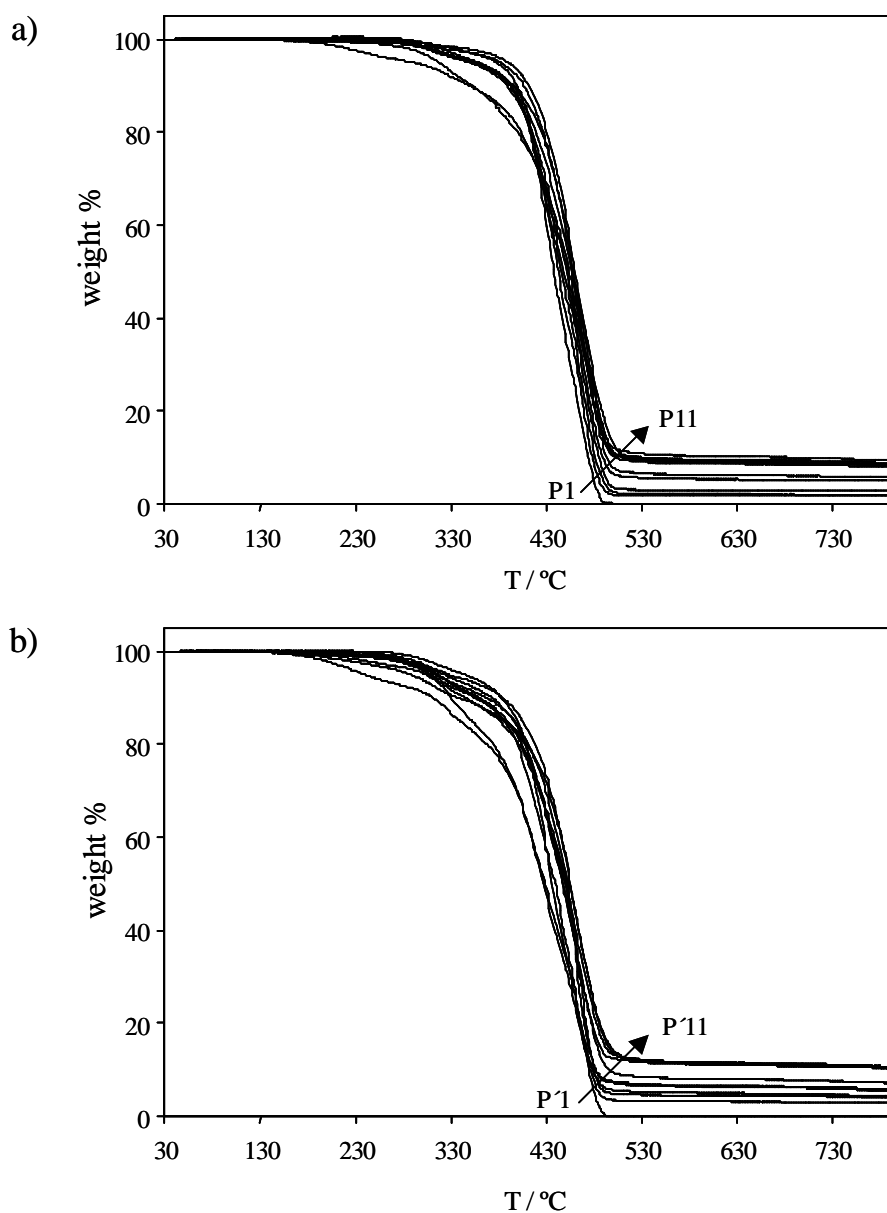


**Figure 4.** TGA measurements of copolymers obtained at 80 °C (a) and 100 °C (b) under nitrogen atmosphere.

In all samples, the weight loss rate is lowered around 500 °C by formation of an intermediate residue. The thermal behavior of the polymers at this temperature is representative of the polymer surface behavior under flame conditions. Thus, a high amount of char at 500 °C would mean a better protection of the non-burned polymer. The general tendency observed in both copolymer series is a direct relationship between

**Table 6.** Thermal stability data and flame retardant characterization of copolymers prepared at 100 °C

Sample (M1 / M2) <sup>a</sup>	% P <sup>b</sup>	TGA (N <sub>2</sub> )			TGA (Air)		
		T <sub>5% loss</sub> (°C)	T <sub>max</sub> (°C) <sup>c</sup>	Char <sub>800°C</sub> (%) <sup>b</sup>	T <sub>5% loss</sub> (°C)	T <sub>max</sub> (°C) <sup>c</sup>	Char <sub>800°C</sub> (%) <sup>b</sup>
P'1 (10 / 0)	4.72	288	310 / 460	10.4	297	410 / 543 / 656	4.7
P'2 (9 / 1)	4.46	307	316 / 456	10.3	302	409 / 445 / 529 / 692	3.1
P'3 (8 / 2)	4.18	328	308 / 460	10.3	320	424 / 528 / 714	4.6
P'4 (7 / 3)	3.87	315	316 / 457	10.5	310	406 / 456 / 531 / 668	2.7
P'5 (6 / 4)	3.52	310	311 / 462	7.0	306	425 / 540 / 624	0.7
P'6 (5 / 5)	3.12	314	314 / 466	5.7	310	417 / 442 / 519 / 617	1.1
P'7 (4 / 6)	2.67	322	431 / 468	5.4	308	392 / 465 / 523 / 586	1.5
P'8 (3 / 7)	2.15	316	325 / 422 / 454	4.2	308	400 / 448 / 544	1.4
P'9 (2 / 8)	1.54	242	229 / 327 / 427 / 463	4.0	291	413 / 464 / 531 / 593	1.1
P'10 (1 / 9)	0.84	304	330 / 424 / 464	2.8	290	360 / 430 / 453 / 525	0.1
P'11 (0 / 10)	0.00	344	431 / 469	0.0	344	425 / 506	0.0

<sup>a</sup> mol/mol ratio, <sup>b</sup> weight/weight percentages, <sup>c</sup> temperatures of maximum weight loss rate.

the phosphorus content and the amount of char formed at 500 °C. As a consequence, the subsequent oxidative degradation is retarded proportionally to the phosphorus content. Thus, the char residues found at 800 °C in air atmosphere range from 0.0 to 8.4 % in the 80 °C copolymer series and from 0.0 to 4.7 % in the 100 °C copolymer series. These observations clearly indicate the advantages of defined polymer libraries in polymer

science.<sup>30</sup> Here, the systematic variation of the phosphorous content allowed us a straightforward correlation of material properties with molecular characteristics.

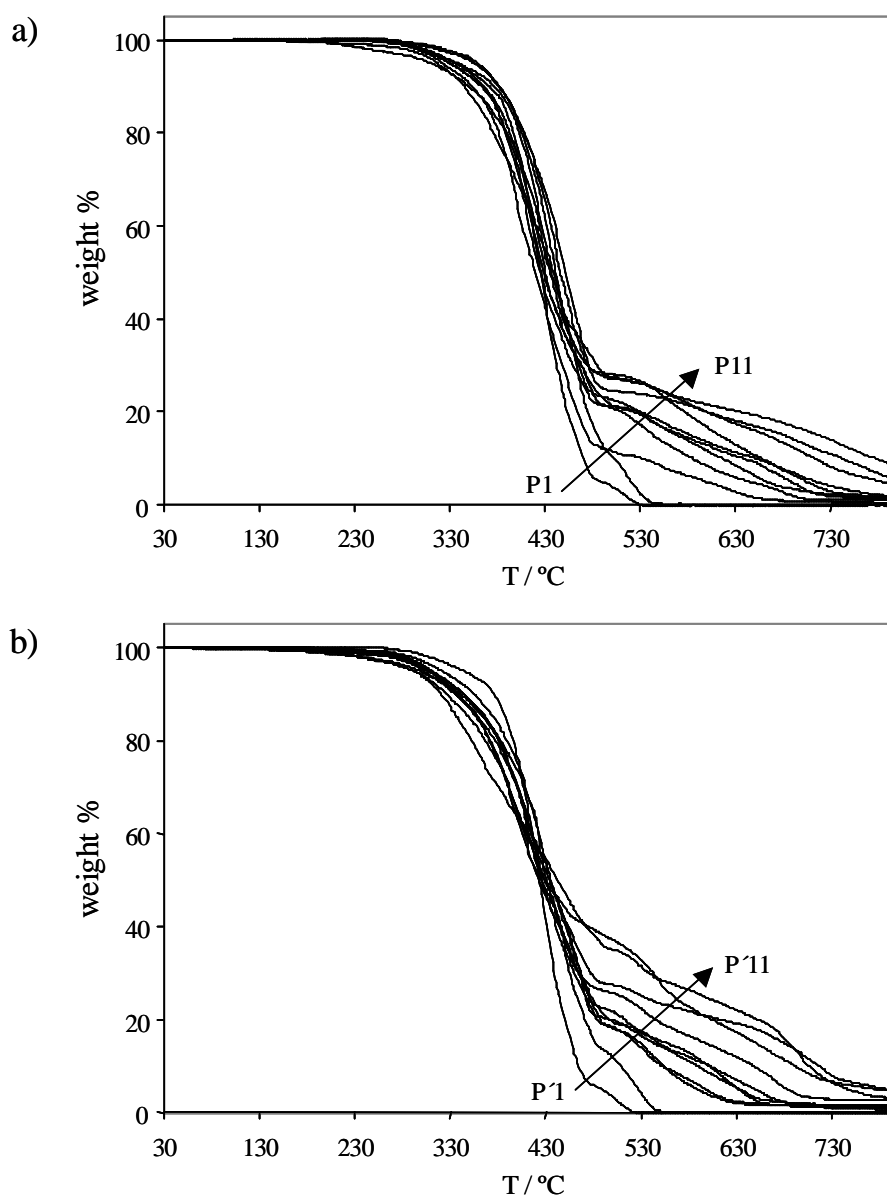


**Figure 5.** TGA measurements of copolymers obtained at 80 °C (a) and 100 °C (b) under air atmosphere.

The flame retardancy properties of the copolymer series synthesized at 80 °C were evaluated using the limiting oxygen index (LOI) test. The LOI is the minimum concentration of oxygen determined in a flowing mixture of oxygen and nitrogen that will just support the flaming combustion of a certain material. For the preparation of the samples, concentrated solutions of each polymer in THF were used to impregnate glass fiber probes (50 x 10 x 1 mm<sup>3</sup>). We used these probes instead of standard ones due to

the lack of consistence of the obtained polymers. The LOI values obtained are shown in Table 2. **P11** gave a LOI of 19.0, which indicates that it has not flame retardant properties. However, the introduction of **M1** as comonomer causes a clear and steady increase of the LOI with the increasing P content reaching a maximum value of 23.5 for a phosphorus content of 3.12 % (**P6**). Interestingly, higher phosphorus contents did not give an increase in the LOI values but a slight decrease from 23.5 (**P6**) to 22.1 (**P2**). It is known that low phosphorus contents are sufficient to infer flame retardant properties to polymers and that high contents do not usually give better results.<sup>31,32</sup> However, in this case a decrease in the LOI values is observed when the phosphorus content is increased. A possible explanation to this fact may be found in the thermal properties of the copolymers. As mentioned above, **P11** is crystalline with a melting point of 54.6 °C. The incorporation of increasing amounts of **M2** comonomer causes a gradual decrease of  $T_m$  until amorphous copolymers are obtained. In polymers, the amount of energy required to initiate combustion varies as a function of the physical characteristics of the material. During the heating of semi-crystalline thermoplastics, the polymer softens, melts and drips. As a consequence, depending on the heat-storage capacity and the enthalpy of fusion of the polymer, part of the energy involved in the combustion process is consumed.<sup>33</sup> For this reason, the LOI values found for the copolymers **P10-P6** could be affected not only by the presence of phosphorus, but also by its crystalline fraction. The polymers **P5-P1** are essentially amorphous and thus, no endothermic processes can be added to the effect of phosphorus resulting in lower LOI values.

## CONCLUSIONS

A phosphorus-containing  $\alpha,\omega$ -diene bearing two 10-undecenoic acid moieties has been homopolymerized via acyclic diene metathesis (ADMET) using Grubbs 2<sup>nd</sup> generation metathesis catalyst. This monomer was also copolymerized with undecylenyl undecenoate leading to a series of copolymers with different phosphorus contents. Moreover, the molecular weight of the prepared polyesters could be controlled by addition of methyl 10-undecenoate as chain stopper. The presence of phosphorus in the structure of the monomer did not affect the activity of the catalyst and high molecular weight polyesters could be obtained. The polymerizations were carried out at two different temperatures. When working at 80 °C, inhomogeneous molecular weight distributions were obtained for intermediate comonomer ratios. When the temperature

was increased to 100 °C the catalyst lost activity, as observed by somewhat lower molecular weights, but homogeneous molecular weight distributions were found in all polymers. LOI values up to 23.5 were obtained for the phosphorus-containing polyesters **P1-P10**. These values show an increase in the flame retardant properties of the polyesters compared to the phosphorous-free sample **P11**. Both studies monomers have a high percentage of renewable resources, in this case a castor oil derived platform chemical, and thus the studied polymers can be considered as renewable flame retardant materials.

The authors express their thanks to MCIN (Ministerio de Ciencia e Innovación (MAT2008-01412) for financial support for this work. MARM kindly acknowledges financial support from the German Federal Ministry of Food, Agriculture and Consumer Protection (represented by the Fachagentur Nachwachsende Rohstoffe; FKZ 22026905).

## REFERENCES

- <sup>1</sup> Schwendeman, J. E.; Church, A. C.; Wagener, K. B. *Adv Synth Catal* 2002, 344, 597-613
- <sup>2</sup> Schwab, P.; France, M. B.; Ziller, J. W.; Grubbs, R. H. *Angew Chem Int Ed* 1995, 34(18), 2039-2041
- <sup>3</sup> Schwab, P.; Grubbs, R. H.; Ziller, J. W. *J Am Chem Soc* 1996, 118(1), 100-110
- <sup>4</sup> Weskamp, T.; Schattenmann, W. C.; Spiegler, M.; Herrmann, W. A. *Angew Chem Int Ed* 1998, 37(18), 2490-2493
- <sup>5</sup> Scholl, M.; Ding, S.; Lee, C. W.; Grubbs, R. H. *Org Lett* 1999, 1(6), 953-956
- <sup>6</sup> Wagener, K. B.; Brzezinska, K.; Anderson, J. D.; Younkin, T. R.; Steppe, K.; DeBoer, W. *Macromolecules* 1997, 30(24), 7363-7369
- <sup>7</sup> Wolfe, P. S.; Wagener, K. B. *Macromolecules* 1999, 32(24), 7961-7967
- <sup>8</sup> Shultz, G. V.; Zakharov, L. N.; Tyler, D. R. *Macromolecules* 2008, 41(15), 5555-5558
- <sup>9</sup> Terada, K.; Berda, E. B.; Wagener, K. B.; Sanda, F.; Masuda, T. *Macromolecules* 2008, 41(16), 6041-6046
- <sup>10</sup> Irvine, D. J.; McCluskey, J. A.; Robinson, I. M. *Polym Deg Stab* 2000, 67(3), 383-396
- <sup>11</sup> Ebdon, J. R.; Jones, M. S. In *Concise Polymeric Materials Encyclopedia*; Salamone, J. C., Ed.; CRC Press, 1996; 2397-2411
- <sup>12</sup> Lu, S.; Hamerton, I. *Prog Polym Sci* 2002, 27(8), 1661-1712
- <sup>13</sup> Allcock, H. R.; Kellam, E. C.; Hofmann, M. A. *Macromolecules* 2001, 34(15), 5140-5146



- 
- <sup>14</sup> Allcock, H. R.; Kellam, E. C., *Macromolecules* 2002, 35(1), 40-47
- <sup>15</sup> Aizenshtein, E. M. *Fibre Chemistry* 2008, 39(5), 355-362
- <sup>16</sup> Meier, M. A. R.; Metzger, J. O.; Schubert, U. S. *Chem Soc Rev* 2007, 36, 1788–1802
- <sup>17</sup> Güner, F. S.; Yağcı, Y.; Erciyas, A. T. *Prog Polym Sci* 2006, 31, 633-670
- <sup>18</sup> Sharma, V.; Kundu, P. P. *Prog Polym Sci* 2006, 31, 983-1008
- <sup>19</sup> Sharma, V.; Kundu, P. P. *Prog Polym Sci* 2008, 33, 1199-1215
- <sup>20</sup> Çaylı, C.; Meier, M. A. R. *Eur. J Lipid Sci Technol* 2008, 110, 853-859
- <sup>21</sup> Rybak, A.; Meier, M. A. R. *ChemSusChem* 2008, 1, 542-547
- <sup>22</sup> Fokou, P. A.; Meier, M. A. R. *Macromol Rapid Commun* 2008, 29, 1620-1625
- <sup>23</sup> Montero de Espinosa, L.; Ronda, J. C.; Galià, M.; Cádiz, V. *J Polym Sci Part A: Polym Chem* 2008, 46(20), 6843-6850
- <sup>24</sup> Montero de Espinosa, L.; Ronda, J. C.; Galià, M.; Cádiz, V. *J Polym Sci Part A: Polym Chem* 2009, 47(4), 1159-1167
- <sup>25</sup> Montero de Espinosa, L.; Ronda, J. C.; Galià, M.; Cádiz, V. *J Polym Sci Part A: Polym Chem* 2009 *in Press*
- <sup>26</sup> Chin, W. K.; Hsao, M. D.; Tsai, W. C. *J Polym Sci Part A: Polym Chem* 1995, 33, 373.
- <sup>27</sup> Lligadas, G.; Ronda, J. C.; Galià, M.; Cádiz, V., *J Polym Sci Part A: Polym Chem* 2006, 44(19), 5630-5644
- <sup>28</sup> Chang, S. J.; Sheen, Y. C.; Chang, R. S.; Chang, F.C. *Polym Deg Stab* 1996, 54 (2-3), 365-371
- <sup>29</sup> Wang, C. S.; Lin, C. H. *Polymer* 1999, 40(3), 747-757
- <sup>30</sup> Webster, D. C.; Meier, M. A. R. *Adv Polym Sci* 2009, in press.
- <sup>31</sup> Ge, X.-G.; Wang, G.; Hu, Z.; Xiang, X.; Wang, J.-S.; Wang, D.-Y.; Liu, C. P.; Wang, Y.-Z. *J Polym Sci Part A: Polym Chem* 2008, 46(9), 2994-3006
- <sup>32</sup> Spontón, M.; Mercado, L. A.; Ronda, J. C.; Galià, M.; Cádiz, V. *Polym Deg Stab* 2008, 93(11), 2025-2031
- <sup>33</sup> Laoutid, F.; Bonnaud, L.; Alexandre, M.; Lopez-Cuesta, J.-M.; Dubois, Ph. *Mater Sci Eng* 2009, 63, 100-125



# Phosphorus-Containing Renewable Polyester-Polyols via ADMET Polymerization. Synthesis, Functionalization and Radical Cross-Linking.

Lucas Montero de Espinosa,<sup>1</sup> Michael A. R. Meier,<sup>2</sup> Juan C. Ronda,<sup>1</sup> Marina Galià,<sup>1</sup> Virginia Cádiz<sup>1</sup>

<sup>1</sup>Department of Analytical and Organic Chemistry, Rovira i Virgili University, Campus Sescelades, Marcel·lí Domingo s/n, 43007 Tarragona, Spain. <sup>2</sup>University of Potsdam, Institute of Chemistry, Laboratory of Sustainable Organic Synthesis, Karl-Liebknecht-Str. 24-25, 14476 Golm / Potsdam (Germany)

**ABSTRACT.** An  $\alpha,\omega$ -diene containing hydroxyl groups was prepared from plant oil derived platform chemicals. The acyclic diene metathesis copolymerization (ADMET) of this monomer with a phosphorus-containing  $\alpha,\omega$ -diene (DOPO II), also plant oil derived, afforded a series of phosphorus containing linear polyesters, which have been fully characterized. The backbone hydroxyls of these polyesters have been acrylated and radically polymerized to produce cross-linked polymers. The thermomechanical and mechanical properties, the thermal stability, and the flame retardancy of these phosphorus based thermosets have been studied. Moreover, methyl 10-undecenoate has been used as chain stopper in selected ADMET polymerizations in order to study the effect of the prepolymers molecular weights on the different properties of the final materials.

**Keywords:** polyester, renewable resources, ADMET, flame retardant, cross-linked polymer.

## INTRODUCTION

Recently, the use of plant oils as renewable feedstock for the development of designed polymeric materials has received particular attention due to environmental concerns.<sup>1</sup> The main components of vegetable oils are triglycerides, consisting of glycerol and fatty acids. The chemical modification of their structure enables the synthesis a wide variety

of monomers for the development of polymers with specific properties,<sup>2</sup> that are now being used in an increasing number of industrial applications.

Synthetic polymer materials are used in many areas and thus the fire hazards associated with the use of these materials are of great concern for both consumers and manufacturers.<sup>3</sup> Due to the composition of triglycerides, plant oil based polymers are flammable, just like many other currently used polymeric materials. The flammability of these materials is a shortcoming in some applications. Therefore, the use of flame retardants to reduce the combustibility of polymers is an important part of the development of plant oil based polymeric materials. In this way, the synthesis of flame-retardant polymers from bromoacrylated plant oil triglycerides was reported.<sup>4</sup> However, it is known that bromine-containing flame-retardant resins release hydrogen bromide during combustion, which is toxic and corrosive.<sup>5</sup> The concept of sustainable development requires fire retardant technologies to be developed that have a minimum impact on health and the environment throughout the life cycle of the fire-resistant material: starting from its synthesis, via fabrication, use, and recycling to its final disposal. Therefore, the search for new environmentally friendly flame-retardant polymeric materials is of large current interest. Phosphorus based polymers, for instance, are an effective and well established class of flame retardant materials.<sup>6</sup> They have a good flame retardant performance and are preferred to the widely applied halogenated flame retardants due to environmental and health reasons.<sup>7</sup>

Acyclic diene metathesis (ADMET) polymerization has proven to be a useful tool for the synthesis of polymers bearing a wide variety of functional groups.<sup>8,9</sup> The ADMET polymerization of  $\alpha,\omega$ -dienes affords strictly linear, unsaturated polymers through a step-growth polycondensation, which is driven by the release of ethylene. In a previous study,<sup>10</sup> we synthesized a series of phosphorus-containing linear polyesters through ADMET copolymerization of a phosphorus based  $\alpha,\omega$ -diene with different amounts of a castor oil derived diene. These polymers showed good flame retardancy and potential application as flame retardant coatings. However, the low  $T_g$  of these polymers can be a limiting factor for some applications. Taking into account the high functional group tolerance of the so called second generation Grubbs metathesis catalysts,<sup>11,12</sup> ADMET polymerization enables the introduction of functional groups that can act as cross-linking points for the development of thermosets with improved mechanical properties.<sup>13</sup> This work thus deals with the synthesis of plant oil based linear polyesters containing phosphorus and alcohol functionalities via ADMET. Further

cross-linking of these polymers has been achieved through acrylation of the hydroxyl groups and subsequent radical polymerization affording flame retardant resins. The thermal and flame retardant properties of the obtained materials are reported within this contribution.

## EXPERIMENTAL SECTION

### Materials

All chemicals were used as received unless otherwise specified. 10-undecenoic acid, 1,3-dichloro-2-propanol, ethyl vinyl ether and dicumyl peroxide were purchased from Aldrich. Potassium carbonate and tetrabutylammonium hydrogen sulfate were purchased from Fluka, anhydrous magnesium sulfate and hydrochloric acid were purchased from Scharlab. Benzylidene-*bis*(tricyclohexylphosphine)dichlororuthenium (C1, Grubbs catalyst 1<sup>st</sup> generation), benzylidene[1,3-*bis*(2,4,6-trimethylphenyl)-2-imidazolidinylidene]dichloro(tricyclohexylphosphine)ruthenium (C2, Grubbs catalyst 2<sup>nd</sup> generation) and [1,3-*Bis*-(2,4,6-trimethylphenyl)-2-imidazolidinylidene]dichloro(*o*-isopropoxyphenylmethylene)ruthenium (C3, Hoveyda-Grubbs catalyst 2<sup>nd</sup> generation) were purchased from Aldrich. Hexane, ethyl acetate and methanol were purchased from Scharlab. Tetrahydrofuran CHROMASOLV<sup>®</sup> Plus (HPLC) was purchased from Aldrich. Triethylamine (Aldrich) was dried by distillation over CaH<sub>2</sub> and acryloyl chloride (Aldrich) was distilled under vacuum before use. Dimethylformamide and dichloromethane (Scharlab) were dried over P<sub>2</sub>O<sub>5</sub> and distilled immediately before use. Toluene was distilled from sodium/benzophenone. Thin layer chromatography (TLC) was performed on silica gel TLC-cards (60 F<sub>254</sub>, Merck). Compounds were visualized by spraying with sulphuric acid/anisaldehyde ethanol solution and heating at 200 °C. For column chromatography, silica gel 60 A.C.C. 40-63 μm (SDS) was used. Methyl 10-undecenoate was prepared by esterification with methanol from corresponding 10-undecenoic acid according to standard procedures. 10-[2',5'-Bis(10-undecenoyloxy)phenyl]-9,10-dihydro-9-oxa-10-phosphaphenanthrene-10-oxide (DOPO-II) was synthesized according to a previously published procedure.<sup>14</sup>

**Synthesis of 1,3- and 1,2-di-10-undecenoylglycerol mixture (M1).** 10-undecenoic acid (7.14 g, 38.7 mmol), potassium carbonate (5.36 g, 38.7 mmol) and tetrabutylammonium hydrogen sulfate (0.26 g, 0.77 mmol) were mixed in a dry 250 mL

two-necked flask under argon. The potassium carbonate was grinded and kept at 100 °C for 24 h prior to use. Anhydrous dimethylformamide (60 mL) and anhydrous toluene (60 mL) were added. The mixture was heated to reflux and stirred for 20 min. 1,3-dichloro-2-propanol (1.85 mL, 19.4 mmol) was then added with vigorous stirring and the reaction was monitored with TLC (hexane/ethyl acetate 5/1). After completion of the reaction (approximately 4 h), the mixture was allowed to cool down under a constant flow of argon. The reaction mixture was diluted with toluene, washed twice with water, twice with HCl (5%) and once with brine. The organic layer was dried over MgSO<sub>4</sub> and the solvent was removed under reduced pressure. The 1,3- and 1,2-di-10-undecenoylglycerol mixture (**M1**) was obtained in 55 % yield after column chromatography with hexane/ethyl acetate 6/1.

FTIR (cm<sup>-1</sup>): 3475 (O-H), 3077 (=C-H), 1735 (C=O), 1638 (C=C), 1163 (C-O).

<sup>1</sup>H NMR (CDCl<sub>3</sub>, TMS, δ in ppm): 5.83-5.73 (m, CH<sub>2</sub>=CH), 5.09-5.04 (m, CH-O of 1,2 isomer), 5.00-4.89 (m, CH<sub>2</sub>=CH), 4.30 (dd, *J* = 12.00, 4.40 Hz, CH<sub>2</sub>-CO of 1,2 isomer), 4.24-4.03 (m, O-CH<sub>2</sub>-CHOH-CH<sub>2</sub>-O of 1,3 isomer and CH<sub>2</sub>-CO of 1,2 isomer), 3.70 (d, *J* = 5.20 Hz, CH<sub>2</sub>-OH of 1,2 isomer), 2.65 (broad, OH), 2.33 (t, *J* = 7.60 Hz, CH<sub>2</sub>-COOCH<sub>2</sub>), 2.30 (t, *J* = 7.60 Hz, CH<sub>2</sub>-COOCH), 2.01 (q, *J* = 7.07 Hz, CH<sub>2</sub>-CH=CH<sub>2</sub>), 1.64-1.56 (m, CH<sub>2</sub>-CH<sub>2</sub>CO), 1.39-1.22 (m, CH<sub>2</sub>).

<sup>13</sup>C NMR (CDCl<sub>3</sub>, TMS, δ in ppm): 174.11 (COOR of 1,3 isomer), 173.98 (COOR of 1,2 isomer), 173.63 (COOR of 1,2 isomer), 139.32 (CH<sub>2</sub>=CH), 114.34 (CH<sub>2</sub>=CH), 72.23 (CH-O of 1,2 isomer), 68.43 (CH-OH of 1,3 isomer), 65.18 (CH<sub>2</sub>-O of 1,3 isomer), 62.23 (CH<sub>2</sub>-CO of 1,2 isomer), 61.60 (CH<sub>2</sub>-OH of 1,2 isomer), 34.43 (CH<sub>2</sub>-CO), 34.25 (CH<sub>2</sub>-CH=CH<sub>2</sub>), 33.95 (CH<sub>2</sub>-CO), 29.46 (CH<sub>2</sub>), 29.44 (CH<sub>2</sub>), 29.37 (CH<sub>2</sub>), 29.35 (CH<sub>2</sub>), 29.25 (CH<sub>2</sub>), 29.22 (CH<sub>2</sub>), 29.21 (CH<sub>2</sub>), 29.03 (CH<sub>2</sub>), 29.07 (CH<sub>2</sub>), 25.08 (CH<sub>2</sub>-CH<sub>2</sub>CO), 25.03 (CH<sub>2</sub>-CH<sub>2</sub>CO).

**ADMET polymerization of M1.** **M1** (3g, 7.07 mmol) and Hoveyda-Grubbs 2<sup>nd</sup> generation catalyst (22.1 mg, 0.035 mmol) were placed in a dry 10 mL round-bottom flask under nitrogen atmosphere. The mixture was stirred magnetically at 80 °C under a constant flow of nitrogen. After 12 h, the residue was dissolved in THF and the metathesis reaction was stopped by adding ethyl vinyl ether (500-fold excess to the catalyst) and stirring for 30 min at room temperature. **P1** was precipitated from methanol as a light brown sticky solid with 96% yield.

FTIR (cm<sup>-1</sup>): 3540 (O-H), 1742 (C=O), 1142 (C-O).

$^1\text{H}$  NMR ( $\text{CDCl}_3$ , TMS,  $\delta$  in ppm): 5.42-5.30 (m,  $\text{CH}=\text{CH}$ ), 5.10-5.05 (m,  $\text{CH}-\text{O}$  of 1,2 isomer), 4.31 (dd,  $J = 11.60$ , 4.40 Hz,  $\text{CH}_2-\text{CO}$  of 1,2 isomer), 4.24-4.04 (m,  $\text{O}-\text{CH}_2-\text{CHOH}-\text{CH}_2-\text{O}$  of 1,3 isomer and  $\text{CH}_2-\text{CO}$  of 1,2 isomer), 3.74-3.69 (m,  $\text{CH}_2-\text{OH}$  of 1,2 isomer), 2.65 (broad, OH), 2.35-2.29 (m,  $\text{CH}_2-\text{CO}$ ), 2.04-1.90 ( $\text{CH}_2-\text{CH}=\text{CH}$ ), 1.70-1.56 (m,  $\text{CH}_2-\text{CH}_2\text{CO}$ ), 1.38-1.21 (m,  $\text{CH}_2$ ).

$^{13}\text{C}$  NMR ( $\text{CDCl}_3$ , TMS,  $\delta$  in ppm): 174.14 (COOR), 173.65 (COOR), 131.00-129.50 ( $\text{CH}=\text{CH}$ ), 72.23 ( $\text{CH}-\text{O}$  of 1,2 isomer), 68.40 ( $\text{CH}-\text{OH}$  of 1,3 isomer), 65.19 ( $\text{CH}_2-\text{O}$  of 1,3 isomer), 62.24 ( $\text{CH}_2-\text{CO}$  of 1,2 isomer), 61.57 ( $\text{CH}_2-\text{OH}$  of 1,2 isomer), 34.44 ( $\text{CH}_2-\text{CO}$ ), 34.26 ( $\text{CH}_2-\text{CO}$ ), 32.76 ( $\text{CH}_2-\text{CH}=\text{CH}$ , *trans*), 29.77 ( $\text{CH}_2$ ), 29.62 ( $\text{CH}_2$ ), 29.41 ( $\text{CH}_2$ ), 29.28 ( $\text{CH}_2$ ), 29.14 ( $\text{CH}_2$ ), 28.91 ( $\text{CH}_2$ ), 28.76 ( $\text{CH}_2$ ), 27.35 ( $\text{CH}_2-\text{CH}=\text{CH}$ , *cis*), 25.04 ( $\text{CH}_2-\text{CH}_2\text{CO}$ ), 24.90 ( $\text{CH}_2-\text{CH}_2\text{CO}$ ).

**ADMET copolymerization of M1 and DOPO II (M2).** M1 and M2 were mixed (3 g scale) in the desired molar ratio (see table 1) in a dry 10 mL round-bottom flask under nitrogen atmosphere. If required, the respective amount of end-capper (methyl 10-undecenoate) was added. Grubbs 2<sup>nd</sup> generation catalyst (0.5 % mol related to dienes) was added and the mixture was stirred magnetically at 70 °C under a constant flow of nitrogen. After 12 h, the residue was dissolved in THF and the metathesis reaction was stopped by adding ethyl vinyl ether (500-fold excess to the catalyst) and stirring for 30 min at room temperature. **P2-P6** were precipitated from methanol with yields >95%. The spectroscopic data is essentially the same for all polymers.

FTIR ( $\text{cm}^{-1}$ ): 3450 (O-H), 1764 (C=O, Ar-COOR), 1735 (C=O, COOR), 1607, 1595, 1582 and 1560 (Ar C-C), 1165 (C-O), 1116 (P=O), 925 (P-O), 780 and 757 (Ar C-H).

$^1\text{H}$  NMR ( $\text{CDCl}_3$ , TMS,  $\delta$  in ppm, number assignments related to scheme 2): 8.07-7.94 (m,  $\text{H}_{8,14,6}$ ), 7.69 (t,  $J = 7.4$  Hz,  $\text{H}_9$ ), 7.57 (dd,  $J = 15.2$ , 7.6 Hz,  $\text{H}_{11}$ ), 7.45-7.36 (m,  $\text{H}_{10,16,4}$ ), 7.30-7.23 (m,  $\text{H}_{15,17}$ ), 7.14 (dd,  $J = 8.6$ , 6.6 Hz,  $\text{H}_3$ ), 5.43-5.31 (m,  $\text{CH}=\text{CH}$ ), 5.10-5.06 (m,  $\text{CH}-\text{O}$  of 1,2 isomer), 4.31 (dd,  $J = 11.60$ , 4.40 Hz,  $\text{CH}_2-\text{CO}$  of 1,2 isomer), 4.23-4.03 (m,  $\text{O}-\text{CH}_2-\text{CHOH}-\text{CH}_2-\text{O}$  of 1,3 isomer and  $\text{CH}_2-\text{CO}$  of 1,2 isomer), 3.71 (d,  $J = 4.4$  Hz,  $\text{CH}_2-\text{OH}$  of 1,2 isomer), 2.57 (t,  $J = 7.6$  Hz,  $\text{H}_{23}$ ), 2.35-2.29 (m,  $\text{CH}_2-\text{CO}$ ), 2.04-1.90 ( $\text{CH}_2-\text{CH}=\text{CH}$ ), 1.78-1.56 (m,  $\text{H}_{24,20}$  and  $\text{CH}_2-\text{CH}_2\text{CO}$ ), 1.44-0.92 (m,  $\text{H}_{21}$  and  $\text{CH}_2$ ).

$^{13}\text{C}$  NMR ( $\text{CDCl}_3$ , TMS,  $\delta$  in ppm, number assignments related to scheme 2): 173.91 (COOR of 1,3 isomer), 173.76 (COOR of 1,2 isomer), 173.46 (COOR of 1,2 isomer),

171.94 (C<sub>19</sub>), 170.85 (C<sub>22</sub>), 149.71 (C<sub>5</sub>), 149.22 (d, 9.15 Hz, C<sub>2</sub>), 147.82 (d, 16.80 Hz, C<sub>18</sub>), 135.09 (d, 5.33 Hz, C<sub>12</sub>), 133.28 (C<sub>9</sub>), 130.90 (C<sub>11</sub>), 130.73 (C<sub>16</sub>), 130.32 (CH=CH), 128.61 (d,  $J = 15.29$  Hz, C<sub>10</sub>), 128.31 (C<sub>4</sub>), 128.01 (d,  $J = 8.35$  Hz, C<sub>6</sub>), 124.30 (d,  $J = 134.30$  Hz, C<sub>7</sub>), 124.80-124.61 (C<sub>3</sub>, C<sub>14</sub>, C<sub>15</sub>), 123.21 (d,  $J = 9.87$  Hz, C<sub>8</sub>), 122.48 (d,  $J = 145.26$  Hz, C<sub>1</sub>), 121.02 (d,  $J = 11.47$  Hz, C<sub>13</sub>), 120.66 (d,  $J = 6.84$  Hz, C<sub>17</sub>), 72.04 (CH-O of 1,2 isomer), 67.91 (CH-OH of 1,3 isomer), 64.98 (CH<sub>2</sub>-O of 1,3 isomer), 62.28 (CH<sub>2</sub>-CO of 1,2 isomer), 61.16 (CH<sub>2</sub>-OH of 1,2 isomer), 34.26 (CH<sub>2</sub>-CO), 34.21 (C<sub>23</sub>), 34.08 (CH<sub>2</sub>-CO), 33.17 (C<sub>20</sub>), 32.59 (CH<sub>2</sub>-CH=CH, *trans*), 29.72 (CH<sub>2</sub>), 29.59 (CH<sub>2</sub>), 29.47 (CH<sub>2</sub>), 29.32 (CH<sub>2</sub>), 29.25 (CH<sub>2</sub>), 29.12 (CH<sub>2</sub>), 28.95 (CH<sub>2</sub>), 28.79 (CH<sub>2</sub>), 27.19 (CH<sub>2</sub>-CH=CH, *cis*), 24.86 (CH<sub>2</sub>-CH<sub>2</sub>CO, C<sub>24</sub>), 24.03 (C<sub>21</sub>). <sup>31</sup>P NMR (CDCl<sub>3</sub>, 162 MHz,  $\delta$  in ppm): 18.15.

**Acrylation of ADMET polymers P1-P6.** In a standard procedure, an anhydrous dichloromethane solution of an ADMET polymer (8 mL of DCM per g of polymer) was placed in a round-bottom flask under argon. The solution was cooled to 0 °C and acryloyl chloride (1.5 mol-fold excess to hydroxyl groups), followed by triethylamine (3 mol-fold excess to hydroxyl groups) were added. The reaction mixture was allowed to reach room temperature and vigorous stirring was maintained for 2 h. The residue was added dropwise to stirring methanol and the pure acrylated polymers (**AP1-AP6**) were obtained in yields between 60 and 96 % as a light brown sticky solid precipitate.

Spectroscopic data for **AP1**:

FTIR (cm<sup>-1</sup>): 1740 (C=O, COOR), 1637 (C=C, acrylate), 1173 (C-O), 808 (C=C-H).

<sup>1</sup>H NMR (CDCl<sub>3</sub>, TMS,  $\delta$  in ppm): 6.43 (dd,  $J = 17.2$ , 1.2 Hz, COCH=CH<sub>2</sub>), 6.41 (dd,  $J = 17.2$ , 1.2 Hz, COCH=CH<sub>2</sub>), 6.12 (dd,  $J = 17.2$ , 10.0 Hz, COCH=CH<sub>2</sub>), 6.11 (dd,  $J = 17.2$ , 10.0 Hz, COCH=CH<sub>2</sub>), 5.88 (dd,  $J = 10.0$ , 1.2 Hz, COCH=CH<sub>2</sub>), 5.87 (dd,  $J = 10.0$ , 1.2 Hz, COCH=CH<sub>2</sub>), 5.45-5.27 (m, CH=CH and CH-O of 1,2 isomer), 4.44-4.09 (m, O-CH<sub>2</sub>-CH-CH<sub>2</sub>-O of 1,3 isomer, CH<sub>2</sub>-CO of 1,2 isomer and CH<sub>2</sub>-O of 1,2 isomer), 2.34-2.28 (m, CH<sub>2</sub>-CO), 2.04-1.90 (m, CH<sub>2</sub>-CH=CH), 1.72-1.59 (m, CH<sub>2</sub>-CH<sub>2</sub>CO), 1.44-1.20 (CH<sub>2</sub>).

<sup>13</sup>C NMR (CDCl<sub>3</sub>, TMS,  $\delta$  in ppm): 173.50 (COOR), 165.31 (COOR acrylate), 132.06 (CH=CH<sub>2</sub> acrylate), 130.51 (CH=CH), 128.00 (CH=CH<sub>2</sub> acrylate), 69.47 (CH-OCOCH=CH<sub>2</sub>), 68.95 (CH-OCOR), 62.59 (CH<sub>2</sub>-OCOCH=CH<sub>2</sub>), 62.22 (CH<sub>2</sub>-OCOR),



34.19 ( $\text{CH}_2\text{-CO}$ ), 32.79 ( $\text{CH}_2\text{-CH=CH}$ , *trans*), 29.82-28.98 ( $\text{CH}_2$ ), 27.38 ( $\text{CH}_2\text{-CH=CH}$ , *cis*), 24.22 ( $\text{CH}_2\text{-CH}_2\text{CO}$ ).

Spectroscopic data for **AP2-AP6**:

FTIR ( $\text{cm}^{-1}$ ): 3066 (Ar C-H), 1764 (C=O, Ar COOR), 1736 (C=O, COOR), 1637 (C=C, acrylate), 1607, 1595, 1582 and 1560 (Ar C-C), 1180 (C-O), 1118 (P=O), 922 (P-O), 808 (C=C-H), 780 and 757 (Ar C-H).

$^1\text{H}$  NMR ( $\text{CDCl}_3$ , TMS,  $\delta$  in ppm, number assignments related to scheme 2): 8.07-7.95 (m,  $\text{H}_{8,14,6}$ ), 7.69 (t,  $J = 7.8$  Hz,  $\text{H}_9$ ), 7.60-7.55 (m,  $\text{H}_{11}$ ), 7.45-7.36 (m,  $\text{H}_{10,16,4}$ ), 7.30-7.23 (m,  $\text{H}_{15,17}$ ), 7.15 (dd,  $J = 8.6, 6.6$  Hz,  $\text{H}_3$ ), 6.43 (dd,  $J = 17.2, 1.2$  Hz,  $\text{COCH=CH}_2$ ), 6.41 (dd,  $J = 17.2, 1.2$  Hz,  $\text{COCH=CH}'_2$ ), 6.12 (dd,  $J = 17.2, 10.0$  Hz,  $\text{COCH=CH}_2$ ), 6.11 (dd,  $J = 17.2, 10.0$  Hz,  $\text{COCH}'=\text{CH}_2$ ), 5.88 (dd,  $J = 10.0, 1.2$  Hz,  $\text{COCH=CH}_2$ ), 5.87 (dd,  $J = 10.0, 1.2$  Hz,  $\text{COCH=CH}'_2$ ), 5.45-5.27 (m,  $\text{CH=CH}$  and  $\text{CH-O}$  of 1,2 isomer), 4.42-4.10 (m,  $\text{O-CH}_2\text{-CH-CH}_2\text{-O}$  of 1,3 isomer,  $\text{CH}_2\text{-CO}$  of 1,2 isomer and  $\text{CH}_2\text{-O}$  of 1,2 isomer), 2.57 (t,  $J = 7.6$  Hz,  $\text{H}_{23}$ ), 2.32-2.28 (m,  $\text{CH}_2\text{-CO}$ ), 2.04-1.90 ( $\text{CH}_2\text{-CH=CH}$ ), 1.78-1.54 (m,  $\text{H}_{24,20}$  and  $\text{CH}_2\text{-CH}_2\text{CO}$ ), 1.44-0.92 (m,  $\text{H}_{21}$  and  $\text{CH}_2$ ).

$^{13}\text{C}$  NMR ( $\text{CDCl}_3$ , TMS,  $\delta$  in ppm, number assignments related to scheme 2): 173.47 (COOR), 172.08 ( $\text{C}_{19}$ ), 171.03 ( $\text{C}_{22}$ ), 165.29 (COOR acrylate), 149.85 ( $\text{C}_5$ ), 149.45 (d, 9.20 Hz,  $\text{C}_2$ ), 147.97 (d, 16.80 Hz,  $\text{C}_{18}$ ), 135.24 ( $\text{C}_{12}$ ), 133.32 ( ), 132.02 ( $\text{CH=CH}_2$  acrylate), 131.03 ( $\text{C}_{11}$ ), 130.83 ( $\text{C}_{16}$ ), 130.48 ( $\text{CH=CH}$ ), 128.72 (d,  $J = 14.48$  Hz,  $\text{C}_{10}$ ), 128.37 ( $\text{C}_4$ ), 128.25 (d,  $J = 7.64$  Hz,  $\text{C}_6$ ), 127.96 ( $\text{CH=CH}_2$  acrylate), 124.72 (d,  $J = 135.00$  Hz,  $\text{C}_7$ ), 124.92-124.83 ( $\text{C}_3, \text{C}_{14}, \text{C}_{15}$ ), 123.31 (d,  $J = 9.86$  Hz,  $\text{C}_8$ ), 122.82 (d,  $J = 144.86$  Hz,  $\text{C}_1$ ), 121.23 (d,  $J = 11.47$  Hz,  $\text{C}_{13}$ ), 120.88 (d,  $J = 6.04$  Hz,  $\text{C}_{17}$ ), 69.45 ( $\text{CH-OCOCH=CH}_2$ ), 68.91 ( $\text{CH-OCOR}$ ), 62.57 ( $\text{CH}_2\text{-OCOCH=CH}_2$ ), 62.19 ( $\text{CH}_2\text{-OCOR}$ ), 34.39 ( $\text{CH}_2\text{-CO}$ ,  $\text{C}_{23}$ ), 34.18 ( $\text{CH}_2\text{-CO}$ ), 33.34 ( $\text{CH}_2\text{-CO}$ ,  $\text{C}_{20}$ ), 32.76 ( $\text{CH}_2\text{-CH=CH}$ , *trans*), 29.78-28.97 ( $\text{CH}_2$ ), 27.37 ( $\text{CH}_2\text{-CH=CH}$ , *cis*), 24.99 ( $\text{CH}_2\text{-CH}_2\text{CO}$ ,  $\text{C}_{24}$ ), 24.19 ( $\text{CH}_2\text{-CH}_2\text{CO}$ ,  $\text{C}_{21}$ ).

### Curing reactions and extraction of soluble parts

A dichloromethane solution (0.3 g/mL) of each acrylated polyester (**APs**) and dicumyl peroxide (2% mol related to acrylate groups) was cast on a glass plates of 7.5 x 2.5  $\text{cm}^2$ . The samples were heated to 40 °C for 2h in order to remove the solvent and then the temperature was raised to 150 °C at 1 °C/min and maintained for 12h. All samples were subjected to soxhlet extraction with previously distilled dichloromethane to determine

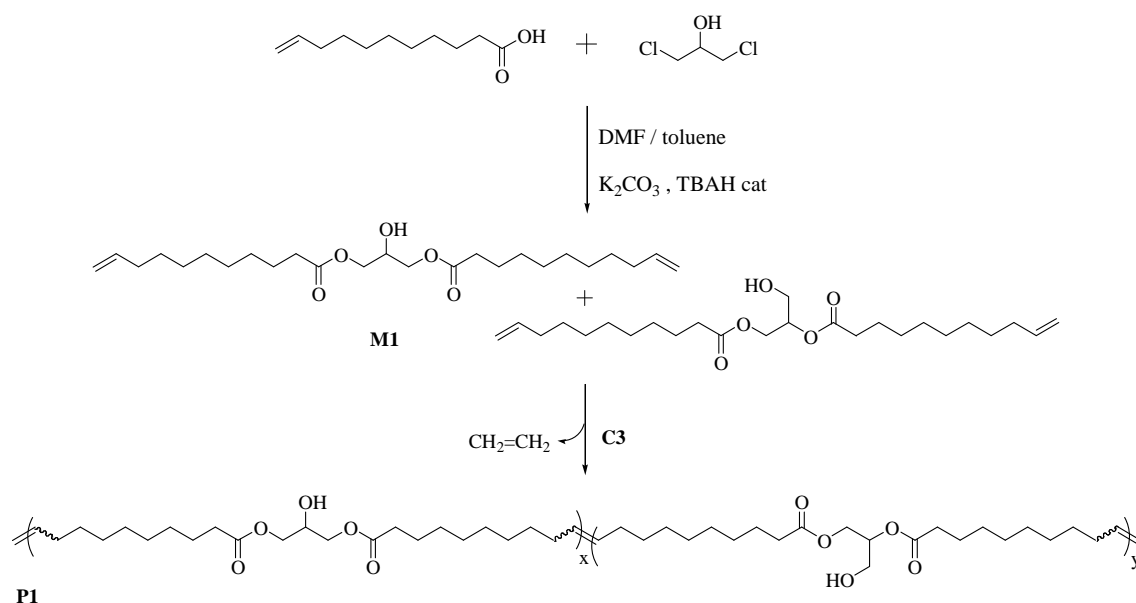
their soluble fractions. 0.5g of each sample were extracted with 125 mL of dichlorometane. Previously to extractions, the samples were grinded to maximize the extraction efficiency.

### Instrumentation

$^1\text{H}$  NMR 400 MHz and  $^{13}\text{C}$  NMR 100.6 MHz NMR spectra were obtained using a Varian Gemini 400 spectrometer with Fourier transform.  $\text{CDCl}_3$  was used as solvent and TMS as internal reference. Molecular weights were determined on a Shimadzu gel permeation chromatography (GPC) system equipped with a LC-20AD pump, RID-10A refractive index detector, SIL-20A autosampler, and a CTO-20A column oven set to 50 °C. A PLgel 5  $\mu\text{m}$  Mixed-D column from Polymerlabs in THF at a flow rate of 1 mL/min was used. Linear poly(methyl methacrylate) standards (Polymer Standards Service PPS, Germany, Mp 102-981.000 Da) were used for calibration. The IR analyses were performed on a FTIR-680PLUS spectrophotometer with a resolution of 4  $\text{cm}^{-1}$  in the transmittance mode. An attenuated-total-reflection accessory with thermal control and a diamond crystal was used to determine FTIR/ATR spectra. Calorimetric studies were carried out on a Mettler DSC822 differential scanning calorimeter using  $\text{N}_2$  as a purge gas (20 mL/min). Dynamic mechanical thermal analysis (DMTA) and tensile tests were performed using a TA DMA 2928 in the controlled force-Tension Film mode with a preload force of 0.1 N, an amplitude of 10  $\mu\text{m}$  and at a fixed frequency of 1 Hz in the -100 to 200 °C range and at a heating rate of 3 °C/min. Rectangular samples with dimensions 10 x 5 x 0.5  $\text{mm}^3$  were used. The tensile assays were performed by triplicate on rectangular samples (10 x 5 x 0.5  $\text{mm}^3$ ) measuring the strain while applying a ramp of 0.5 N/min at 30 °C. A preload force of 0.05 N and a soak time of 3 min were used. Thermal stability studies were carried out on a Mettler TGA/SDTA851e/LF/1100 with  $\text{N}_2$  as purge gas. The studies were performed in the 30-800 °C temperature range at a scan rate of 10°C/min. The limiting oxygen index (LOI) is the minimum concentration of oxygen determined in a flowing mixture of oxygen and nitrogen that will just support the flaming combustion of materials. LOI values were measured in vertical tests on a Stanton Redcroft instrument provided with an oxygen analyser. The dimensions of the polymer films were 100 x 5 x 0.5  $\text{mm}^3$ .

## RESULTS AND DISCUSSION

The versatility of ADMET polymerization enables the synthesis of linear polymers with functional groups that can be used as cross-linking points.<sup>13,15</sup> Taking into account the good flame retardant properties obtained in our previous work with DOPO II (**M2**) as phosphorus containing comonomer,<sup>10</sup> we decided to use it for the preparation of flame retardant thermosets. To introduce cross-linking points into the polymer backbone, a hydroxyl containing  $\alpha,\omega$ -diene (**M1**, scheme 1) was synthesized. **M1** and **M2** were copolymerized in different molar ratios via ADMET to give a series of linear polyesters with different phosphorus contents. The hydroxyl groups of these polyesters were then esterified with acryloyl chloride to introduce polymerizable groups, and finally, the resulting acrylated polyesters were cross-linked *via* radical polymerization to obtain a family of flame retardant thermosets.



**Scheme 1.** Synthesis of 1,3- and 1,2-di-10-undecenylglycerol mixture and ADMET polymerization in presence of Hoveyda-Grubbs 2<sup>nd</sup> generation catalyst.

For the synthesis of **M1**, 1,3-dichloro-2-propanol was reacted with two equivalents of 10-undecenoic acid in presence of potassium carbonate and tetrabutylammonium hydrogen sulfate (TBAH) as phase transfer catalyst (Scheme 1). It

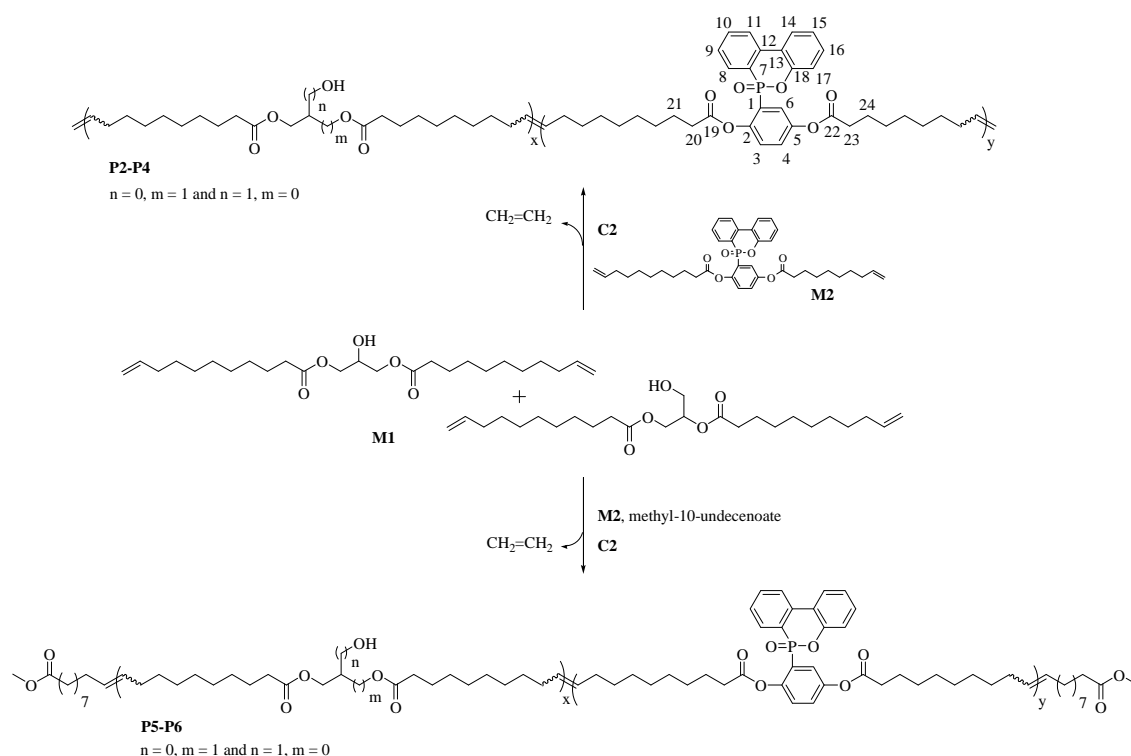
must be pointed out that 1,3-dichloro-2-propanol can be obtained directly from glycerol<sup>16</sup> and 10-undecenoic acid is obtained from castor oil pyrolysis, thus, both reagents can be plant oil derived and **M1** can be considered as 100% renewable. The <sup>1</sup>H-NMR analysis of the reaction mixture revealed the presence of 1,3-diundecenoylglycerol together with 1,2-diundecenoylglycerol and triundecenoylglycerol as byproducts. In the reaction conditions, glycidyl undecenoate is formed as intermediate (detected by <sup>1</sup>H-NMR), and eventually, the epoxide is opened by another undecenoic acid molecule, leading to a mixture of both diacylglycerols. The crude reaction mixture was subjected to column chromatography and the resulting mixture of 1,3- and 1,2-di-10-undecenoylglycerol (60:40, as determined by <sup>1</sup>H-NMR, see figure 1) was used in the ADMET polymerizations.

It is known that ADMET polymerizations can be carried out with heteroatom-containing dienes, if the heteroatom is not situated close to the double bonds.<sup>17</sup> In both **M1** and **M2**, the terminal olefins are nine carbon atoms spaced from the functional groups. Moreover, previous work in Wagener's group<sup>9</sup> proved the viability of ADMET polymerization of alcohol containing dienes using Grubbs 1<sup>st</sup> generation catalyst.

We first tested different metathesis catalysts in the polymerization of **M1**. The ADMET polymerizations were run in bulk while a continuous flow of nitrogen was passed through the reaction mixture in order to remove the ethylene, which is released during the metathesis reaction. When 1% mol Grubbs 1<sup>st</sup> generation catalyst (**C1**) was used, oligomerization and poor conversion (by GPC) at 80 °C after 24 h occurred, probably due to catalyst degradation in presence of the primary alcohol of 1,2-diundecenoylglycerol.<sup>18</sup> On the other hand, when 1% mol Grubbs (**C2**) and Hoveyda-Grubbs (**C3**) 2<sup>nd</sup> generation catalysts were used at 80 °C, THF insoluble products were obtained. Moreover, the polymerization products were not soluble in common organic solvents, suggesting that some kind of cross-linking reaction might have taken place. This poor solubility of hydroxyl functionalized ADMET polymers was also observed by Valenti et al., and the only proposed reason for this behavior was the high molecular weight of the investigated polymers.<sup>9</sup> However, when the catalyst load was lowered to 0.5% mol, THF soluble polymers were obtained at 80 °C with **C1** and **C2**. Similar results were found in the bulk copolymerization of **M1** and **M2** at 80 °C in 1:1 molar ratio. **C1** gave oligomerization, while **C2** and **C3** produced insoluble polymers with 1% mol catalyst. When the polymerizations were conducted at 70 °C with 0.5% mol of **C2**

and **C3**, soluble polymers were obtained with monomer conversions over 98% (by GPC).

On the basis of the results obtained in the initial experiments, we synthesized a series of polymers (**P1-P4**) with different **M1/M2** molar ratios (Scheme 2) with the aim of determining the effect of the phosphorus content on the properties of the ADMET polymers and the final materials. We also wanted to study the effect of the molecular weight of the ADMET polymers on the flame retardant properties of the cross-linked materials. For this purpose, we performed ADMET polymerizations with 10 and 20% of methyl 10-undecenoate as chain stopper for the highest phosphorus content (**P5** and **P6**, scheme 2). As reported previously, this procedure results in an efficient end-capping and reduction of the molecular weight.<sup>10,19</sup> Thus, six polyesters (**P1-P6**) with different **M1/M2** molar ratios were synthesized (see table 1).



**Scheme 2.** Synthesis of phosphorous containing polyesters via ADMET copolymerization with (bottom) and without (top) chain stopper.

Figure 1 shows the <sup>1</sup>H-NMR spectra of **M1** (as a mixture of isomers) (Fig. 1a), **P1** (Fig. 1b) and **P3** (Fig. 1c) as representative examples. The ADMET polymerizations could be confirmed by the disappearance of the terminal olefin signals at 5.8 and 4.9

ppm together with the appearance of a multiplet at 5.3 ppm in both **P1** and **P3**. Although not possible in all cases, the analysis of the integrations of the chain end olefins revealed a  $M_n$  of 24,600 Da for **P2** and 18,400 Da for **P3**. These values are significantly higher than the ones obtained by GPC (3,700 and 5,200 Da, respectively). However, there is no direct correlation between GPC and NMR  $M_n$  values due to the different **M1/M2** contents of **P2** and **P3**, which cause different hydrodynamic volumes. For **P1** and **P4**, the chain end signals were too small for reliable integration indicating that high molecular weight polymers were obtained. In the cases of **P5** and **P6**, the  $M_n$  could not be determined as the end-capping was not completely efficient and both terminal olefins and methyl ester signals were observed. Nevertheless, the objective of obtaining two polyesters with the same phosphorus content as **P4**, but lower molecular weights was achieved. Furthermore, these results indicate that high molecular weight hydroxyl-containing polyesters could be synthesized *via* ADMET polymerization.

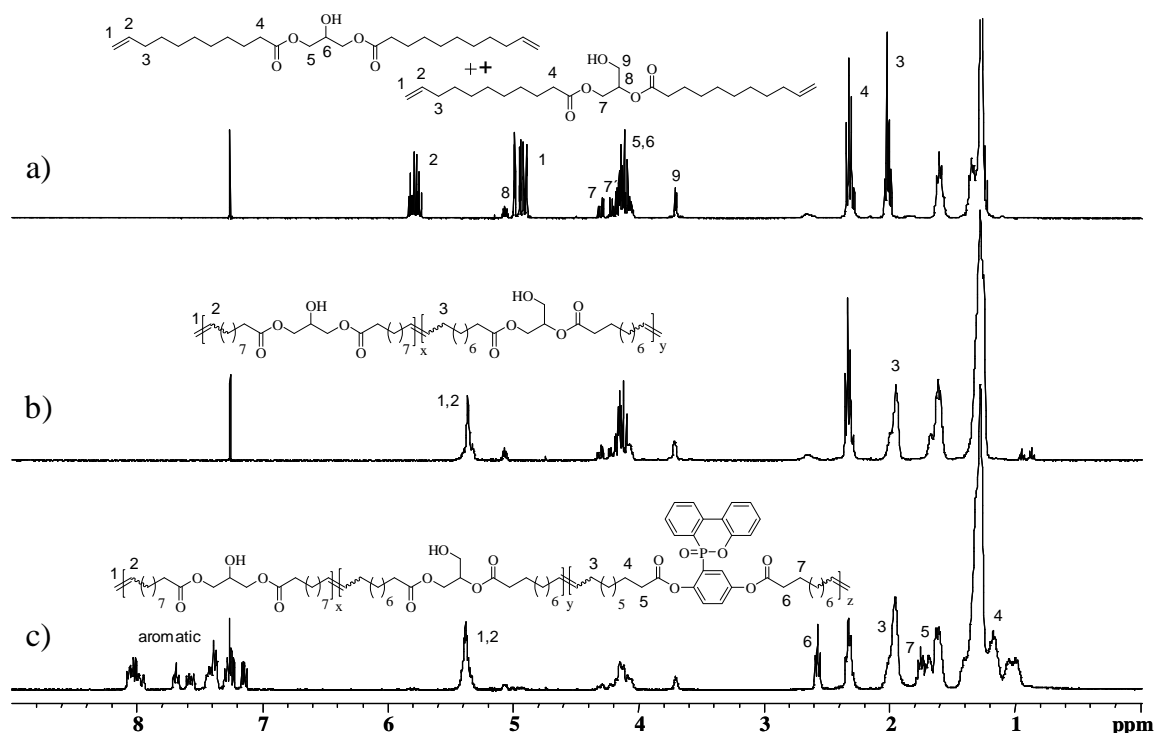


**Figure 1.**  $^1\text{H}$  NMR spectra of a) **M1** (mixture of isomers), b) **P1** and c) **P3**.

**Table 1.** GPC, <sup>1</sup>H-NMR and thermal characterization of the phosphorus-containing ADMET polyesters.

Polymer (M1 / M2) <sup>a</sup>	% P <sup>b</sup>	M <sub>n</sub> <sup>c</sup>	M <sub>n</sub> (NMR)	PDI <sup>c</sup>	T <sub>g</sub> (°C) <sup>d</sup> / T <sub>m</sub> (°C) <sup>d</sup>
P1 (10.0 / 0.0)	0.0	5,300	- <sup>d</sup>	2.18	-25.8 / 41.3
P2 (7.5 / 2.5)	1.6	3,700	24,600	2.20	-27.2 / 21.7
P3 (5.0 / 5.0)	2.9	5,200	18,400	2.56	-12.4
P4 (2.5 / 7.5)	3.9	7,300	- <sup>d</sup>	3.13	5.9
P5 (2.5 / 7.5)	3.9	4,400	-	2.32	-16.6
P6 (2.5 / 7.5)	3.9	3,900	-	2.04	-19.1

<sup>a</sup> mol/mol ratio, <sup>b</sup> weight/weight percentages, <sup>c</sup> GPC data,

<sup>d</sup> end group signals not detectable, <sup>e</sup> DSC data.

The thermal characterization of the ADMET polyesters was carried out with differential scanning calorimetry (DSC). The DSC traces stemming from the second heating run (20 °C/min) of **P1-P4** are shown in figure 2 and the data is collected in table 1. The thermal analysis of **P1** showed a glass transition (T<sub>g</sub>) at -25.8 °C and a melt followed by a cold crystallization and a second melt (T<sub>m</sub>) at 41.3 °C. However, observations with a polarizing microscope did not reveal two different melting processes when using different heating rates or annealing conditions. As **M2** is added as comonomer, polymer crystallization becomes more difficult due to the bulky aromatic core of **M2**. Moreover, the increase in the aromatic content causes restrictions in the segmental mobility and an increase in the T<sub>g</sub> occurs. The DSC trace of **P2**, with only a low content of **M2**, reveals a T<sub>g</sub> of -27.2 °C and just one T<sub>m</sub> of 21.7 °C. Finally, **P3** and **P4** show only glass transitions at -12.4 °C and 5.9 °C respectively. As previously mentioned, the addition of methyl 10-undecenoate as chain stopper in the synthesis of

**P4** affords lower molecular weights. As a result, the  $T_g$ s obtained for **P5** (-16.6 °C) and **P6** (-19.1 °C) are found below that of **P4**.

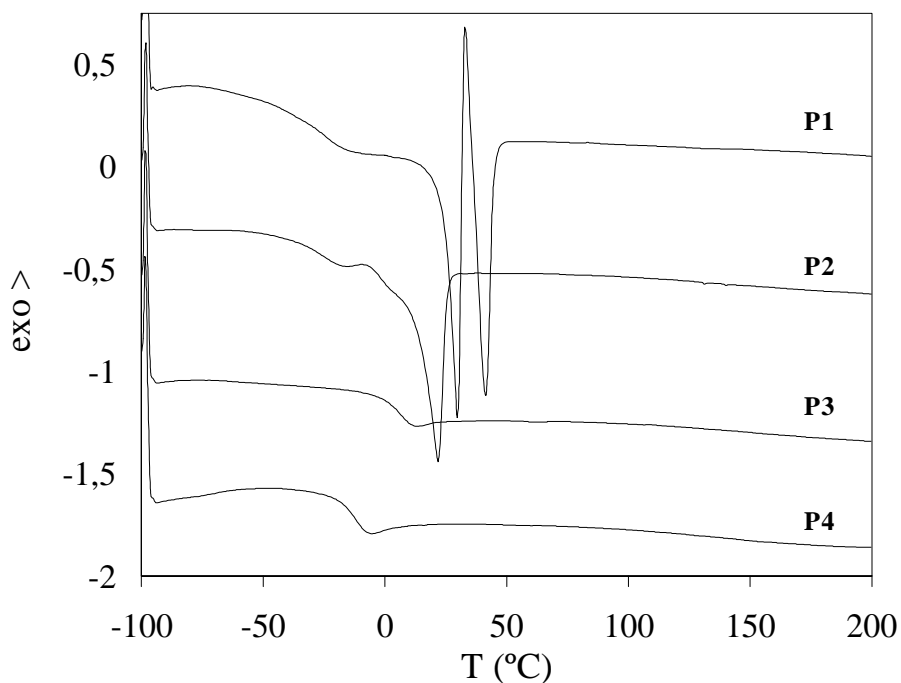


**Figure 2.** DSC traces of the phosphorus-containing ADMET polyesters **P1-P4**.

The thermal stability of the ADMET polyesters was studied by thermogravimetric analysis (TGA) under nitrogen and air atmospheres (data in table 2). Good thermal stability is observed for **P1-P6** under nitrogen (Fig 3a) with 5% weight loss around 310 °C. For **P1**, the main degradation step takes place at 430 °C but as **M2** is introduced, the thermal stability increases and a new degradation step appears around 460 °C. Moreover, an increase in the aromatic and phosphorus content carries an increase in the char obtained at 800 °C from **P1** (0.0%) to **P4** (8.8 %). The thermal stability and char obtained at 800 °C of **P5** and **P6** is lowered with respect to **P4** due to their lower molecular weight. A similar trend is observed in the thermal degradation behaviour under air (Fig 3b). 5% weight loss around 310 °C and two main degradation steps related with the **M1/M2** composition at 430 and 450 °C were observed under these conditions. Under air, the residues at 800 °C increase with the phosphorus content reaching a maximum value of 9.1% for **P4**.



**Table 2.** TGA results of the phosphorus-containing ADMET polyesters.

Polymer	% P <sup>a</sup>	TGA (N <sub>2</sub> )			TGA (Air)		
		T <sub>5% loss</sub> (°C)	T <sub>max</sub> (°C) <sup>b</sup>	Char <sub>800°C</sub> (%)	T <sub>5% loss</sub> (°C)	T <sub>max</sub> (°C) <sup>b</sup>	Char <sub>800°C</sub> (%)
P1	0.0	315	316 / 432	0.0	295	316 / 431 / 496	0.0
P2	1.6	297	307 / 413 / 465	6.0	296	306 / 413 / 457 / 653	0.0
P3	2.9	311	413 / 465	7.4	315	412 / 448 / 603	4.1
P4	3.9	313	462	8.8	324	452 / 577	9.1
P5	3.9	312	413 / 463	8.2	313	420 / 453 / 564	3.0
P6	3.9	309	413 / 465	7.9	312	393 / 453 / 564	2.2

<sup>a</sup> weight/weight percentages, <sup>b</sup> temperature of maximum weight loss rate.

In the next step, the hydroxyl functionalized polyesters **P1** to **P6** were reacted with acryloyl chloride in the presence of triethylamine (Scheme 3). The acrylated polyesters (**AP1** to **AP6**) were isolated by slow addition of the reaction mixture to methanol in yields between 60 and 96 %. Non quantitative yields were probably due to the increased solubility of the polyesters in methanol after acrylation of the hydroxyl groups, that led to partial fractionation. Two representative <sup>1</sup>H-NMR spectra are shown in figure 4, where the characteristic set of signals at 6.3, 6.1 and 5.7 ppm confirm the presence of the acrylate groups. Moreover, in the <sup>13</sup>C-NMR spectrum, the complete disappearance of the signals belonging to the non acrylated polymer **P3** and the appearance of the signals of **AP3** confirms full functionalization.

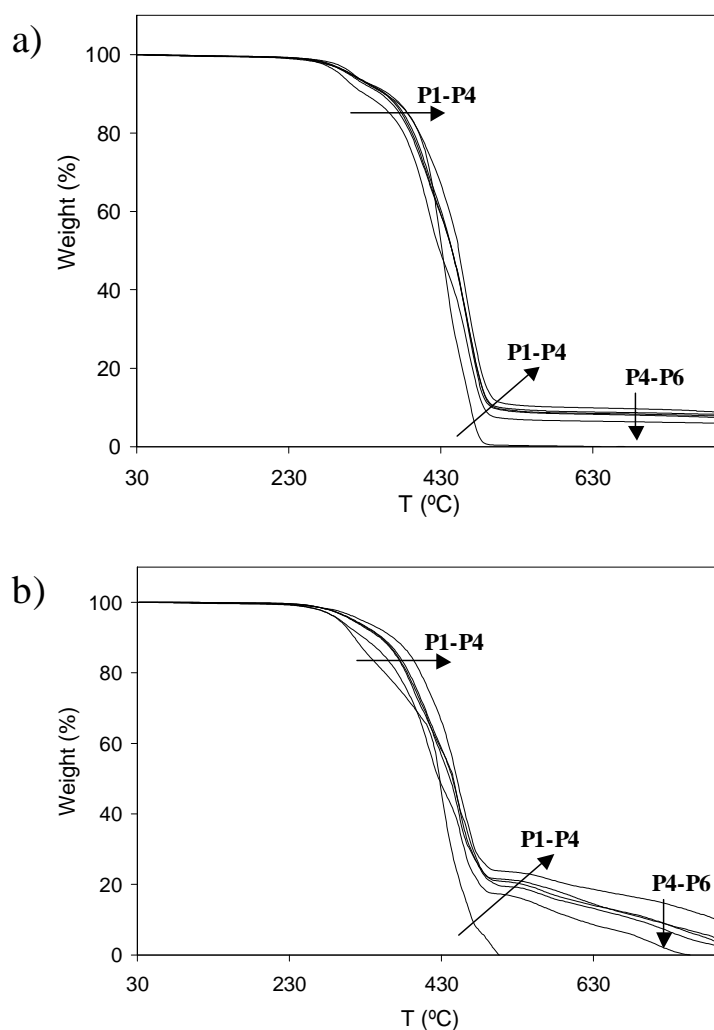
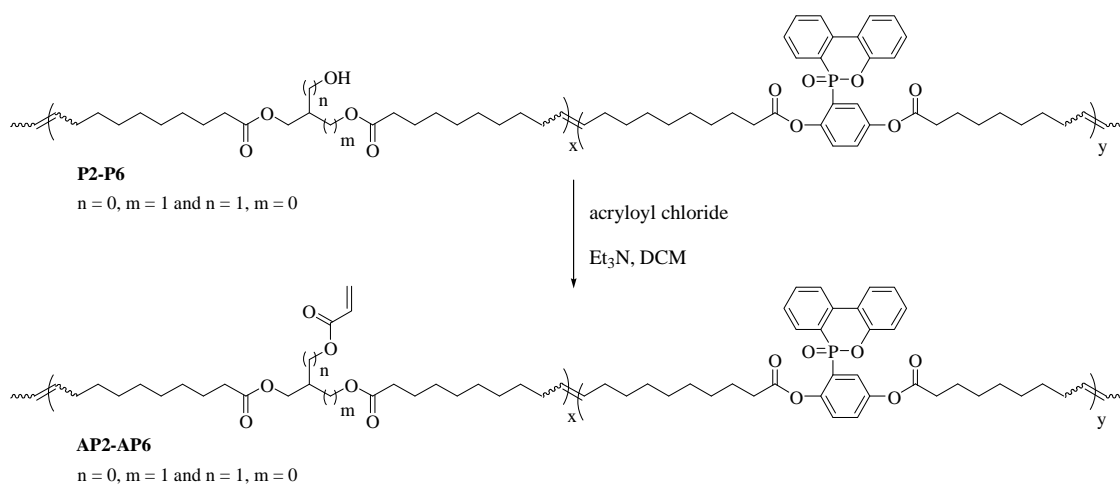


**Figure 3.** TGA measurements a) under nitrogen, and b) under air of the phosphorus-containing ADMET polyesters **P1-P6**.



**Scheme 3.** Synthesis of acrylated phosphorous-containing polyesters **AP1-AP6**.

Based on our previous experience in the cross-linking of acrylate derivatives,<sup>20,21</sup> dicumyl peroxide was chosen as radical initiator for the cross-linking reaction of the acrylated ADMET polyesters. DSC curing runs between **APs** and dicumyl peroxide (2% molar to acrylate groups) showed similar exotherms with onsets ca. 150 °C for all the acrylated polyesters. Once the curing conditions were established, **APs** and dicumyl

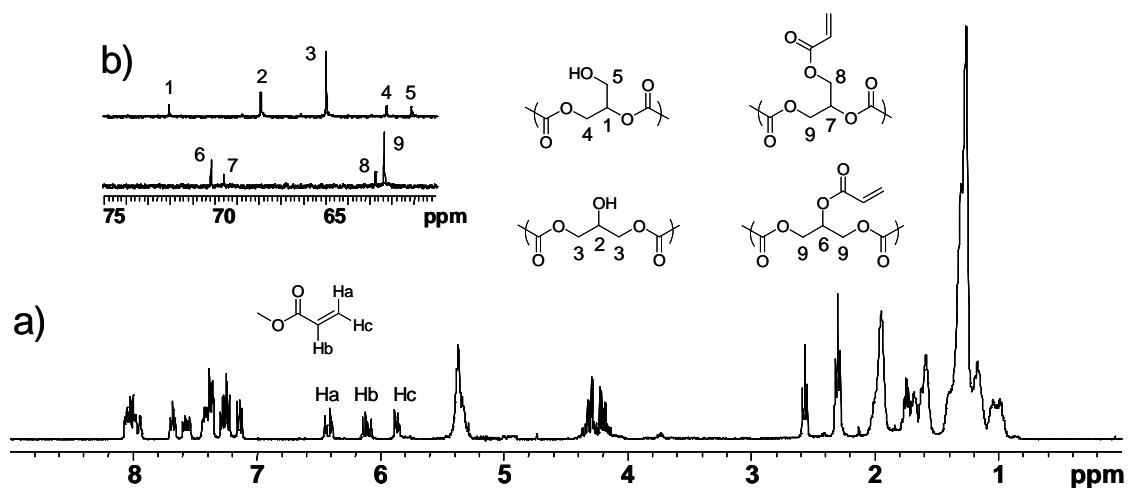
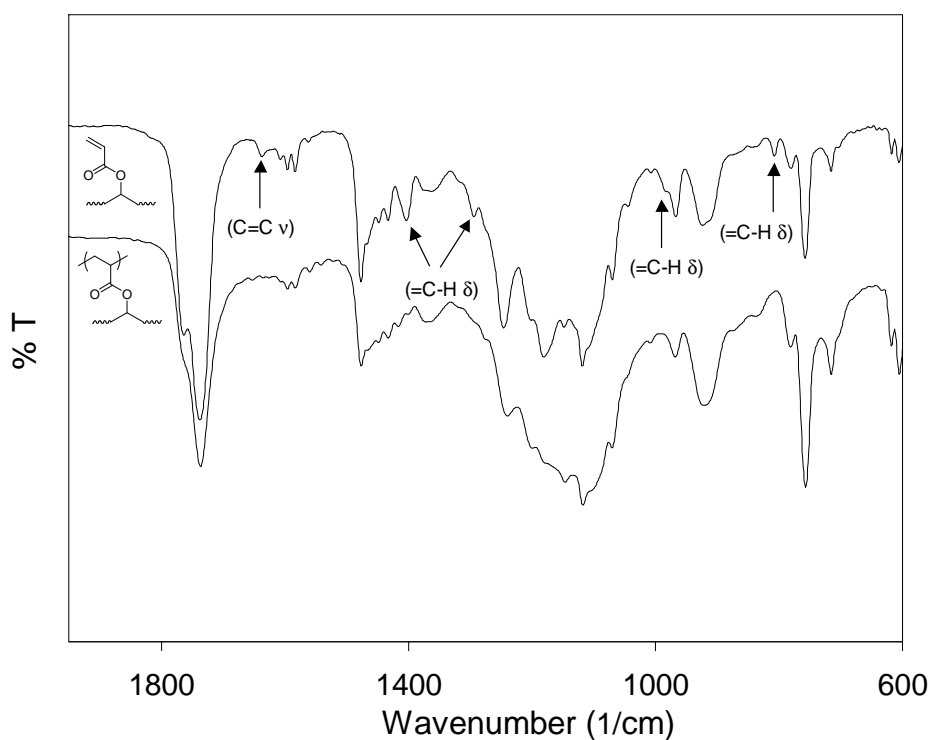


**Figure 4.** <sup>1</sup>H-NMR spectrum of **AP3** and enlargement of the 75-60 ppm region of <sup>13</sup>C-NMR spectra of **P3** and **AP3**.

peroxide (2% mol) were dissolved in dichloromethane (0.3 g/mL) and the resulting solution was cast on a glass plate. The samples were heated at 40 °C for 2h to remove the solvent and then the temperature was raised to 150 °C at 1 °C/min and maintained for 12h. The cured materials (samples **I** to **VI**), were obtained as light brown transparent films. The curing extent of the cross-linking reactions was studied with FTIR spectroscopy by following the disappearance of the acrylate group bands. Figure 5 shows the FTIR spectra of **AP3** and sample **III** as a representative example of the cross-linking reaction. The bands at 1637 cm<sup>-1</sup> (C=C stretching), 1403 and 1294 cm<sup>-1</sup> (=C-H in-plane deformation) and 983 and 808 cm<sup>-1</sup> (=C-H out-of-plane deformation) completely disappear confirming the polymerization of the acrylate groups. The reactivity of non-conjugated internal double bonds towards radical polymerization is very low,<sup>22,23</sup> thus, the double bonds of the polyester backbone were not expected to polymerize. This is confirmed in the ATR-FTIR spectrum after cross-linking by the presence of the band at 967 cm<sup>-1</sup>, which is associated to the C=C-H out-of-plane

deformation. The cross-link extent was also investigated by extracting the soluble fraction of samples **I-VI**. Sample **I** presents a soluble fraction of 0.9 %, that indicates a very high cross-linking degree. The soluble fractions increase as the **M2** content does reaching a value of 20.3 % for sample **IV** due to the decreasing number of cross-link points available in the linear prepolymers. The soluble fractions of samples **V** (16.8 %) and **VI** (17.7 %) are similar to that of sample **IV** showing that similar cross-linking degrees were achieved independently of the prepolymers molecular weights.

The soluble fractions were analyzed by  $^1\text{H}$  and  $^{31}\text{P}$ -NMR spectroscopy.  $^1\text{H}$ -NMR showed total reaction of the acrylate double bonds and the presence of a triplet ca. 2.4 ppm belonging to the methylene protons adjacent to the carbonyls of the polymerized acrylates. This clearly indicates that the soluble fractions are composed of low molecular weight polymers instead of non polymerized acrylates. However, the aromatic region showed little variations suggesting some change taking place in the DOPO moiety. This was further confirmed by examining the  $^{31}\text{P}$ -NMR spectra, where a new singlet at 32.6 ppm appeared together with DOPO signal (18.2 ppm). This new signal matches with the opened DOPO form, having a phosphinic acid functionality (hydrolysis of the P-O bond). Although the DOPO ring was closed throughout the synthesis of **M2**, ADMET polymerizations and acrylation reactions, it is known that a certain amount of hydrated DOPO can be found when using DOPO as a reagent, and dehydration at temperatures over 200 °C under vacuum are usually necessary prior to use.<sup>24</sup> It is thus possible that part of the pendant DOPO moieties were hydrated by long exposure of the samples to air. Since the DOPO P-O bond is cleaved in the early stages of thermal degradation (300 °C),<sup>25</sup> the flame retardant action of these materials will not be affected in any case and thus, the presence of the opened form of DOPO does not interfere with the aim of this study.



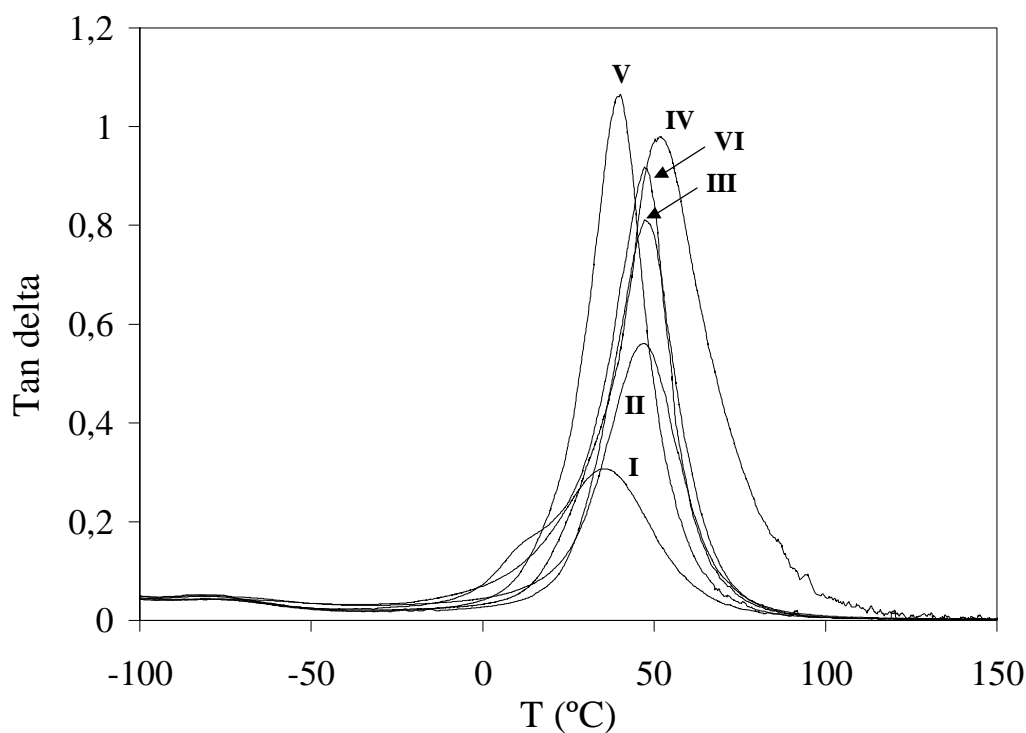
**Figure 5.** FTIR-ATR spectra of a) **AP3** and b) sample **III**. The absorption bands associated to the acrylate group are indicated.

Figure 6 shows the dynamic thermomechanical analysis of samples **I** to **VI** as the tan delta plots from  $-100$  to  $150$  °C. The main peak of the tan delta plots, that is the alpha relaxation, is related to the glass transition temperature. As expected, from sample **I** to sample **IV**, the maximum of the tan delta peak shifts to higher temperatures as **M2** content increases due to the increasing aromatic fraction. On the other hand, an increase in **M2** content means more space between acrylate groups, that is accompanied by a loss of crosslink density, and a decreased cross-link density is manifested by a smaller tan delta peak.<sup>26</sup> This fact is confirmed by the height of the tan delta peak, which increases from sample **I** to sample **IV**. The effect of the prepolymer molecular weight on the dynamic mechanical properties of the cross-linked materials is observed in samples **IV**, **V** and **VI**. The  $T_g$  value drops from sample **IV** to samples **V** and **VI** as a consequence of the lower molecular weights of **P5** and **P6** with respect to **P4**.

**Table 3.** Dynamic thermomechanical characterization, TGA results and LOI values of cross-linked polymers I-VI.

Sample	% P <sup>a</sup>	T <sub>g</sub> <sup>b</sup> (°C)	Soluble fraction (%) <sup>a</sup>	TGA (N <sub>2</sub> )			TGA (Air)			LOI
				T <sub>5% loss</sub> (°C)	T <sub>max</sub> (°C) <sup>c</sup>	Char <sub>800°C</sub> (%)	T <sub>5% loss</sub> (°C)	T <sub>max</sub> (°C) <sup>c</sup>	Char <sub>800°C</sub> (%)	
I	0.0	35.4	0.9	343	434	5.0	331	428	0.0	18.4
II	1.5	47.0	4.1	328	423 / 462	9.8	324	418 / 452 / 564	0.1	21.8
III	2.7	47.3	8.9	346	425 / 463	10.9	328	418 / 449 / 619	2.6	24.0
IV	3.8	52.2	20.3	358	463	11.2	337	449 / 592	7.6	25.7
V	3.8	40.0	16.8	344	425 / 462	10.7	325	419 / 449 / 609	4.8	21.9
VI	3.8	47.9	17.7	337	425 / 462	10.2	329	419 / 452 / 631	6.0	21.7

<sup>a</sup> Weight/weight percentages, <sup>b</sup> Maxima of the tan delta peak, <sup>d</sup> Temperatures of maximum weight loss rate.



**Figure 6.** Tan delta plots of the cross-linked polymers I-VI.

The thermal degradation behaviour of the cross-linked materials under nitrogen and air atmospheres is shown in figure 7 and the data is collected in table 3. Under nitrogen (Fig. 7a), all samples present good thermal stability with 5 % weight loss around 340 °C. From the maxima of weight loss rate it can be inferred that two general degradation mechanisms are taking place, which can be related to the prepolymer composition. Sample **I** contains the **M1** homopolymer and degrades in one single step with the maximum weight loss rate around 430 °C. As **M2** is added, a new maximum of weight loss rate appears around 460 °C, which becomes the main degradation step as the **M2** content increases. The char at 800 °C increases from sample **I** (5.0 %) to sample **IV** (11.2 %) as the phosphorus content does and slightly decreases for samples **V** and **VI** as a result of their lower crosslink density that causes a lower thermal stability. The thermal degradation behaviour under air atmosphere is presented in figure 7b. 5 % weight loss around 330 °C is observed for all samples followed by a main degradation process and an oxidative degradation step. Sample **I** presents a one-step degradation mechanism around 430 °C before the oxidative degradation. As explained above, the introduction of **M2** as comonomer increases the thermal stability and a second degradation step appears at a higher temperature (ca. 450 °C). For the **M2** containing samples, the degradation rate is retarded over 500 °C with formation of an intermediate char. The amount of char formed at these temperatures, that increases proportionally to the phosphorus content, indicates how efficiently the burning surface would protect the rest of the polymer under real fire conditions. Moreover, the char at 800 °C increases with the phosphorus content from sample **I** to sample **IV** and decreases for samples **V** and **VI** for the reasons explained above. These cross-linked systems show an increased thermal stability with onset degradation temperatures 30 °C above the non-cross-linked polymers, both under nitrogen and air atmospheres. The cross-linking retards the release of volatiles and favours char formation.

The mechanical properties of the cross-linked materials were investigated in tensile assays. The mechanical parameters obtained are collected in Table 4 and selected stress-strain curves of samples **I** to **VI** are compared in Figure 8. When examining the behaviour of samples **I** to **IV**, two different factors must be taken into account. There is an increase in the aromatic content that leads to an increase of the network rigidity, but at the same time there is a decrease in the cross-link density. Due to the combination of

both factors, the modulus decreases from sample **I** to sample **IV** as a result of the decreasing cross-link density, but as the same time, the tensile strength increases due to

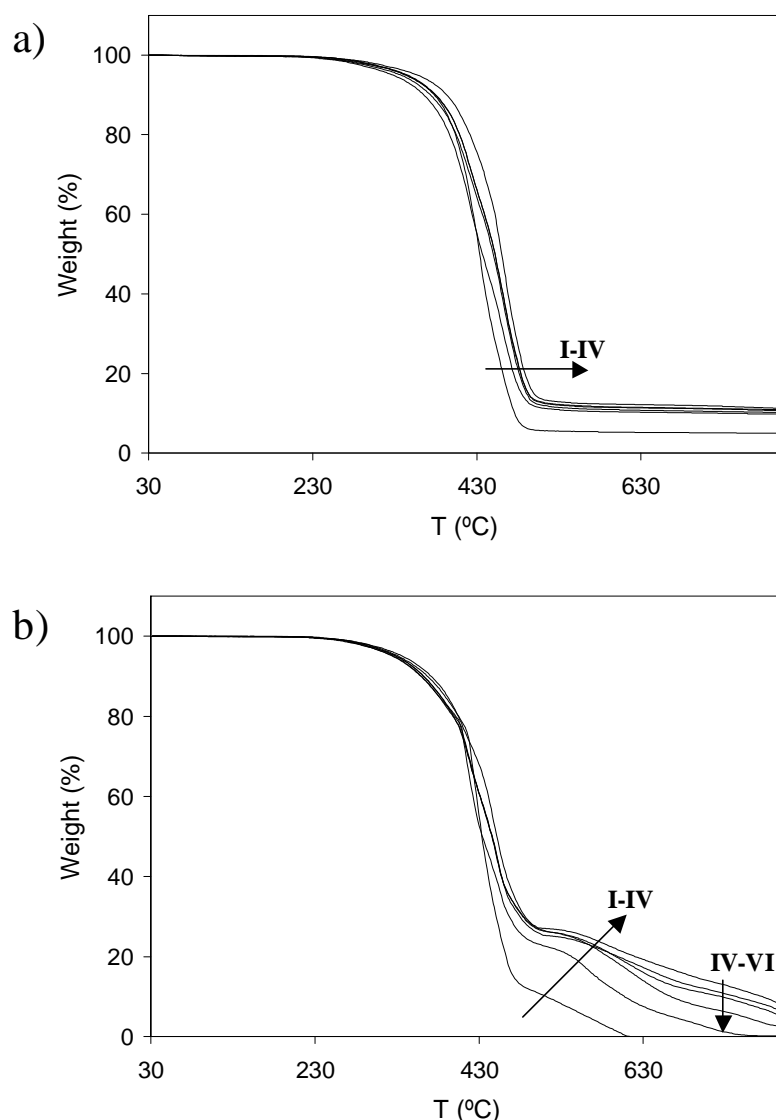


**Figure 7.** TGA measurements a) under nitrogen, and b) under air of the cross-linked polymers **I-VI**.

the increasing aromatic content. The decrease of cross-link density also determines the elongation at break, that increases from sample **I** to sample **IV** reaching a maximum value of 142 % for sample **IV**. However, the variation of these parameters is not completely linear; the modulus increases for sample **III**, suggesting a higher influence of the aromatic fraction on mechanical behaviour of this sample. Moreover, sample **IV** shows a decrease in tensile strength due to its lower cross-link density compared to samples **I-III**, that is confirmed by the differences in soluble fractions. The effect of the



prepolymer molecular weight on the mechanical properties is clearly observed when comparing the stress/strain curves of samples **IV** to **VI**. Although the aromatic content remains constant, the tensile strength and modulus decrease. Moreover, the elongation at break is reduced twofold.

The flame retardancy of the cross-linked materials was evaluated using the limiting oxygen index (LOI) vertical test with films of thickness between 0.4 and 0.5 mm. Table 3 contains the LOI values obtained for samples **I** to **VI**. The phosphorus-free

**Table 4.** Mechanical properties of the cross-linked polymers **I-VI**.

Sample	Modulus (MPa)	TS (MPa)	Elongation (%)
I	65.8	2.37	5
II	31.5	3.07	15
III	54.2	4.50	31
IV	16.8	2.16	142
V	10.3	1.46	64
VI	10.1	1.96	62

<sup>a</sup> Tensile strength, <sup>b</sup> Elongation at break.

sample **I** gave a LOI value of 18.4, a low index, which is related to its high aliphatic content. The LOI values clearly increase with the phosphorus content from sample **II** to sample **IV** reaching a value of 25.7 for the later. The effect of the prepolymer molecular weight at a constant phosphorus content on the flame retardancy can be observed by comparing samples **IV**, **V** and **VI**. The LOI value drops from 25.7 in sample **IV** to 21.9 and 21.7 in samples **V** and **VI** respectively. During combustion, the thermal scission of the polymer backbone leads to fragments of different sizes. In the case of low crosslink density, small volatile fragments are rapidly produced and released to the flame, thus feeding it. Since the prepolymer molecular weights decrease from sample **IV** to sample **VI**, the crosslink density also does and as a result lower LOI values are obtained. The effect of the crosslink density on the flame retardant properties is further confirmed when comparing the LOI values of samples **II** and **VI**. Despite its lower phosphorus

content (1.5%), sample **II** gave the same LOI than sample **VI** (3.8%). The molecular weights of **P2** and **P6** are similar; however, the higher hydroxyl content of **P2** is responsible for the higher cross-link density of sample **II**. As a result, a similar flame retardant behaviour is obtained for both samples.

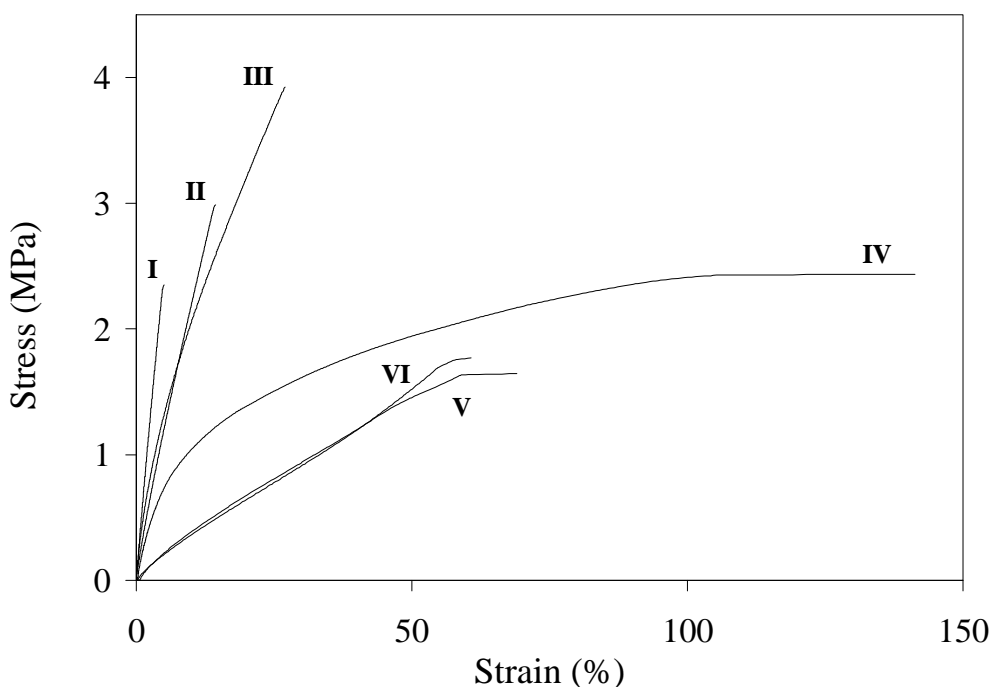


**Figure 8.** Stress/strain curves of the cross-linked polymers **I-VI**.

## CONCLUSIONS

A plant oil-based  $\alpha,\omega$ -diene containing hydroxyl groups (**M1**) has been successfully polymerized via acyclic diene metathesis (ADMET) polymerization with Hoveyda-Grubbs 2<sup>nd</sup> generation catalyst, reaching high molecular weights. This monomer has also been copolymerized with an  $\alpha,\omega$ -diene bearing a DOPO pendant group using Grubbs 2<sup>nd</sup> generation catalyst. In this way, phosphorus containing polyesters with molecular weights over 18,000 Da have been obtained. Moreover, while maintaining a constant phosphorus content, the molecular weight of the polyesters has been reduced using methyl 10-undecenoate as renewable chain stopper. The crystallinity of these polyesters decreased as the amount of DOPO-based comonomer (**M2**) was increased

and totally amorphous polymers were obtained for the higher **M2** contents. Extensive acrylation of the hydroxyl groups in the polyesters backbone followed by radical polymerization afforded thermosetting polymers with high cross-linking degrees. These plant oil-based thermosets show glass transition temperatures ranging from 35 to 52 °C, good thermal stability, and relatively good flame retardancy despite their high aliphatic (fatty acid) content.

- 
- <sup>1</sup> Güner, F. S.; Yagci, Y.; Erciyas, A. T. *Prog Polym Sci* 2006, 31, 633-670.
  - <sup>2</sup> Meier, M. A. R.; Metzger, J. O.; Schubert, U. S. *Chem Soc Rev* 2007, 36, 1788-1802.
  - <sup>3</sup> Irvine, D. J.; McCluskey, J. A.; Robinson, I. M., *Polym Deg Stab*, 2000, 67(3), 383-396.
  - <sup>4</sup> Eren, T; Küseföglu, S.H.; *J Appl Polym Sci* 2004, 91, 2700
  - <sup>5</sup> Purser, D. In *Fire Retardant Materials*; Horrocks A. R. and Price D., Eds.; CRC Press, 2001; 69-127.
  - <sup>6</sup> Jain, P; Choudary, V, Varma, I.K. *J Macromol Sci Polym Rev* 2002,42, 139
  - <sup>7</sup> Lu, S. Y.; Hamerton, I. *Prog Polym Sci* 2002, 27, 1661–1712.
  - <sup>8</sup> Baughman, T. W.; Wagener, K. B. *Adv Polym Sci* 2005, 176, 1-42.
  - <sup>9</sup> Valenti, D. J.; Wagener, K. B. *Macromolecules* 1998, 31 (9), 2764-2773
  - <sup>10</sup> Montero de Espinosa, L.; Ronda, J. C.; Galià, M.; Cádiz, V.; Meier, M. A. R. *J Polym Sci Part A: Polym Chem* 2009, 47, 5760-5771.
  - <sup>11</sup> Weskamp, T.; Schattenmann, W. C.; Spiegler, M.; Herrmann, W. A. *Angew Chem Int Ed* 1998, 37(18), 2490-2493
  - <sup>12</sup> Scholl, M.; Ding, S.; Lee, C. W.; Grubbs, R. H. *Org Lett* 1999, 1(6), 953-956
  - <sup>13</sup> Matloka, P. P.; Kean, Z.; Greenfield, M.; Wagener, K. B. *J Polym Sci Part A: Polym Chem* 2008, 46, 3992-4011
  - <sup>14</sup> Lligadas, G.; Ronda, J. C.; Galià, M.; Cádiz, V., *J Polym Sci Part A: Polym Chem* 2006, 44(19), 5630-5644
  - <sup>15</sup> Delgado, P. A.; Zuluaga, F.; Matloka, P.; Wagener, K. B. *J Polym Sci Part A: Polym Chem* 2009, 47, 5180-5183
  - <sup>16</sup> Zheng, Y.; Chen, X.; Shen, Y. *Chem Rev* 2008, 108, 5253–5277
  - <sup>17</sup> Wagener, K. B.; Brzezinska, K.; Anderson, J. D.; Younkin, T. R.; Steppe, K.; DeBoer, W. *Macromolecules* 1997, 30(24), 7363-7369
  - <sup>18</sup> Dinger, M. B.; Mol, J. C. *Organometallics* 2003, 22, 1089-1095
  - <sup>19</sup> Rybak, A.; Meier, M. A. R. *ChemSusChem* 2008, 1, 542-547

- 
- <sup>20</sup> Montero de Espinosa, L.; Ronda, J. C.; Galià, M.; Cádiz V. *J Polym Sci Part A: Polym Chem* 2009, 47, 1159-1167.
- <sup>21</sup> Montero de Espinosa, L.; Ronda, J. C.; Galià, M.; Cádiz V. *J Polym Sci Part A: Polym Chem* 2009, 47, 4051-4063.
- <sup>22</sup> Valverde, M.; Andjelkovic, D.; Kundu, P.P.; Larock, R. C. *J Appl Polym Sci* 2008, 107, 423–430.
- <sup>23</sup> Henna, P. H.; Andjelkovic, D. D.; Kundu, P. P.; Larock, R. C. *J Appl Polym Sci* 2007, 104, 979–985.
- <sup>24</sup> Liu, Y. L.; Wei, W. L.; Chen, W. Y. *Polym Int* 2003, 52, 1275–1279.
- <sup>25</sup> Wenjeng Guo, Wen-Tsuen Leu, Sheng-Huei Hsiao, Guey-Sheng Liou *Polymer Degradation and Stability* 91 (2006) 21-30
- <sup>26</sup> Sepe, M. P. In *Thermal Analysis of Polymers*; Rapra Review Reports 95; Rapra, 1995; p 28.

## GENERAL CONCLUSIONS

- High oleic sunflower oil has been used as renewable starting material for the synthesis of two monomers as precursors of plant oil-based cross-linked polymers.
- The photoperoxidation of high oleic sunflower oil with singlet oxygen has been used as an efficient reaction for the synthesis of functionalized triglyceride derivatives. In this reaction, high oleic sunflower oil and oxygen are the only reactants, making this transformation very attractive from an environmental point of view.
- A triglyceride derivative containing  $\alpha,\beta$ -unsaturated ketones has been synthesized and cross-linked *via* aza-Michael addition with an aromatic diamine. The high reactivity of this monomer and the properties of the final materials make this curing system a good alternative to the conventional plant oil-based epoxy-amine systems.
- The effects of the reaction conditions on the mentioned aza-Michael cross-linking reaction have been studied. High temperatures and the presence of a Lewis acid promote the formation of substituted quinolines as cross-link points. On the basis of these findings, new plant oil-based quinoline-containing thermosets have been synthesized.
- A triglyceride derivative containing allylic alcohol groups has been synthesized, acrylated, and cross-linked *via* radical polymerization. The extensive hydrogenation of this derivative, prior to acrylation and radical polymerisation, has led to an improvement of the thermal stability of the cross-linked polymers. In both cases, highly cross-linked thermosets have been obtained.
- High oleic sunflower oil and 10-undecenoic acid have been used as renewable starting materials for the synthesis of plant oil-based flame retardant polymers.

- A series of new high oleic sunflower oil-based monomers containing phosphine oxide and acrylate groups have been synthesized and cross-linked *via* radical polymerization. These cross-linked materials have shown improved thermal stability and flame retardancy. Phosphorus compounds have been found among the pyrolysis products in the gas-phase suggesting a gas-phase mechanism of flame inhibition. Finally, a thermal degradation mechanism has been proposed.
- Acyclic diene metathesis (ADMET) polymerization has been proven to be an efficient tool for the synthesis of phosphorus-containing plant oil-based linear polyesters.
- A series of new phosphorus-containing castor oil-derived polyesters have been synthesized *via* ADMET polymerization. Some of these linear polyesters have shown good flame retardant properties.
- A series of new castor oil-derived polyesters containing hydroxyl and phosphine oxide groups have been synthesized *via* ADMET polymerization. Acrylation of the backbone hydroxyls followed by radical polymerization has led to a family of flame retardant cross-linked polymers.

## APENDIXES

### Appendix A. List of abbreviations

$^1\text{H}$ , $^{13}\text{C}$ and $^{31}\text{P}$ -NMR	Proton, carbon and phosphorus nuclear magnetic resonance
ADMET	Acyclic diene metathesis
ASO	Acrylated high oleic sunflower oil
ASO[H]	Acrylated hydrogenated high oleic sunflower oil
BF <sub>3</sub> ·MEA	Boron trifluoride-ethylamine complex
CDPP	Chlorodiphenylphosphine
DCM	Dichloromethane
DCP	Dicumyl peroxide
DDM	4,4'-Diaminodiphenylmethane
DMTA	Dynamomechanical thermal analysis
DOPO	9,10-dihydro-9-oxa-10-phosphaphenanthrene-10-oxide
DSC	Differential scanning calorimetry
EDX	Energy-dispersive X-ray spectroscopy
EMO	Epoxidized methyl oleate
FR	Flame retardant
FTIR/ATR	Fourier transform infrared spectroscopy
gHSQC	Gradient-selected heteronuclear single quantum correlation
gCOSY	Gradient-selected correlation spectroscopy
GC/MS	Gas chromatography coupled with mass spectrometry
GPC	Gel permeation chromatography
hr-MAS NMR	High resolution magic angle spinning nuclear magnetic resonance
HSO	Hydrogenated high oleic sunflower oil
HSO[H]	Acrylated hydrogenated high oleic sunflower oil
LOI	Limiting oxygen index
$M_n$	Number average molecular weight
$M_w$	Weight average molecular weight

P-ASO	Tertiary phosphine oxide containing acrylated high oleic sunflower oil
PDI	Polydispersity index ( $M_w/M_n$ )
PETA	Pentaerithritol tetraacrylate
P-SO	Tertiary phosphine oxide containing high oleic sunflower oil
SEM	Scanning electron microscopy
SO	High oleic sunflower oil
$T_{5\% \text{ loss}}$	Temperature of 5 % weight loss
$T_g$	Glass transition temperature
TGA	Thermogravimetric analysis
THF	Tetrahydrofuran
TLC	Thin layer chromatography
$T_m$	Melting temperature
$T_{\text{max}}$	Temperature of maximum weight loss
TMS	Tetramethylsilane
TPP	Tetraphenylporphyrine
UV-vis	Ultraviolet-visible spectroscopy



## Appendix B. List of publications

A New Enone-Containing Triglyceride Derivative as Precursor of Thermosets from Renewable Resources.

Montero de Espinosa, L.; Ronda, J. C.; Galià, M.; Cádiz, V. *J Polym Sci Part A: Polym Chem* 2008, 46, 6843-6850.

Quinoline-Containing Networks from Enone and Aldehyde Triglyceride Derivatives.

Montero de Espinosa, L.; Ronda, J. C.; Galià, M.; Cádiz, V. Submitted to *J Polym Sci Part A: Polym Chem*.

A New Route To Acrylated Oils. Crosslinking And Properties Of Acrylated Triglycerides From High Oleic Sunflower Oil.

Montero de Espinosa, L.; Ronda, J. C.; Galià, M.; Cádiz V. *J Polym Sci Part A: Polym Chem* 2009, 47, 1159-1167.

A Straightforward Strategy For The Efficient Synthesis Of Acrylate And Phosphine Oxide-Containing Vegetable Oils And Their Crosslinked Materials

Montero de Espinosa, L.; Ronda, J. C.; Galià, M.; Cádiz, V. *J Polym Sci Part A: Polym Chem* 2009, 47, 4051-4063.

Fatty Acid Derived Phosphorus-Containing Polyesters Via Acyclic Diene Metathesis (ADMET) Polymerization

Montero de Espinosa, L.; Ronda, J. C.; Galià, M.; Cádiz, V.; Meier, M. A. R. *J Polym Sci Part A: Polym Chem* 2009, 47, 5760-5771.

Phosphorus-containing polyesters from plant oil derivatives via ADMET polymerization. Synthesis and radical crosslinking.

Montero de Espinosa, L.; Ronda, J. C.; Galià, M.; Cádiz, V. Submitted to *J Polym Sci Part A: Polym Chem*.

Chemometric resolution of NIR spectra data of a model aza-Michael reaction with a combination of local rank exploratory analysis and multivariate curve resolution-alternating least squares (MCR-ALS) method.

del Río, V.; Callao, M. P.; Larrechi, M. S.; Montero de Espinosa, L.; Ronda, J. C.; Cádiz, V. *Anal Chim Acta* 2009, 642, 148–154.

Vegetable oil-based thermosetting polymers.

Galià, M.; Montero de Espinosa, L.; Ronda, J. C.; Lligadas, G.; Cádiz, V. *Eur. J. Lipid Sci Technol* 2009, 111, DOI 10.1002/ejlt.200900096, in press.

## **Appendix C. Stages and meeting contributions**

### **Stages**

Three months stay (1<sup>st</sup> September - 1<sup>st</sup> December 2008) at the University of Applied Sciences Oldenburg / Ostfriesland / Wilhelmshaven, Faculty of Technology, Emden (Germany) under the supervision of Prof. Dr. Michael A. R. Meier.

Two weeks stay (July 2009) at the University of Applied Sciences Oldenburg / Ostfriesland / Wilhelmshaven, Faculty of Technology, Emden (Germany) under the supervision of Prof. Dr. Michael A. R. Meier.

### **Meeting contributions**

Flame Retardant Vegetable Oil-based Thermosetting Polymers.

L. Montero de Espinosa, J. C. Ronda, M. Galià, V. Cádiz.

Oral communication.

11th European Meeting on Fire Retardant Polymers, Bolton, Manchester (UK), 03-06 July, 2007.

Polímeros retardantes a la llama derivados de ésteres del ácido oléico modificados con óxidos de fosfina.

L. Montero de Espinosa, J. C. Ronda, M. Galià, V. Cádiz.

Oral communication.

X Reunión Del Grupo Especializado De Polímeros (RSEQ y RSEF), Sevilla (Spain), 16-20 September, 2007.

Vegetable oil-based thermosetting polymers.

V. Cádiz, L. Montero de Espinosa, J. C. Ronda, M. Galià.

Poster.

International Workshop On Biomacromolecules 2008, Stockholm (Sweden), 1-4 June, 2008.

Flame retardant polyesters from renewable resources *via* ADMET.

L. Montero de Espinosa, J. C. Ronda, V. Cádiz, M. A. R. Meier.

Poster.

2nd Workshop On Fats And Oils As Renewable Feedstock For The Chemical Industry,  
Emden (Germany), 22-24 March, 2009.

A new route to phosphorus-containing vegetable oils. Crosslinking and properties of  
phosphorus-containing acrylate triglycerides from high oleic sunflower oil.

L. Montero de Espinosa, J. C. Ronda, M. Galià, V. Cádiz.

Poster.

Frontiers In Polymer Science International Symposium, Mainz (Germany), 7-9 June,  
2009.

Synthesis of plant oil derived polyester-polyols *via* ADMET as precursors of flame  
retardant materials.

L. Montero de Espinosa, M. A. R. Meier, J. C. Ronda, V. Cádiz.

Poster.

XI Reunión Del Grupo Especializado De Polímeros (RSEQ y RSEF), Valladolid  
(Spain), 20-24 September, 2009.

Crosslinking of enone-containing triglycerides with aromatic amines.

L. Montero de Espinosa, J. C. Ronda, M. Galià, V. Cádiz.

Poster.

XI Reunión Del Grupo Especializado De Polímeros (RSEQ y RSEF), Valladolid  
(Spain), 20-24 September, 2009.